Targeting gene therapy to intraperitoneal ovarian carcinoma

Joanne Morrison

MA BM BCh MRCOG

Balliol College

University of Oxford

A thesis submitted for the degree of Doctor of Philosophy

to the Faculty of Clinical Medicine, University of Oxford.

Michaelmas Term 2006

Supervisors: Prof. L.W. Seymour and Prof. S. Kehoe

Targeting gene therapy to intraperitoneal ovarian carcinoma

Joanne Morrison

Balliol College, University of Oxford

A thesis submitted for the degree of Doctor of Philosophy to the Faculty of Clinical Medicine

University of Oxford, Michaelmas Term 2006

Abstract

Adenovirus gene therapy for intraperitoneal cancer is limited in clinical trials by inefficient tumour cell transduction and by development of peritoneal adhesions. Retargeting adenovirus to tumour-associated receptors, such as the epidermal growth factor receptor (EGFR), may reduce infection of non-target cells and simultaneously improve tumour cell transduction. Coating adenovirus with poly[N-(2-hydroxypropyl)methacrylamide] (pHPMA) ablates infection via normal pathways including the coxsackie adenovirus receptor (CAR); it was therefore hypothesised that linkage of EGFR-binding ligands to the polymer-coated virus (pcv) might retarget infection to cancer cells and elevate the therapeutic index.

EGF retained biological activity following linkage to pHPMA via its N-terminus, stimulating phosphorylation and internalisation of EGFR in A431 cells. To permit definitive study, human EGFR was expressed in a CAR-negative murine fibroblast cell line (A9), and significant levels of EGFR-mediated transduction were demonstrated selectively using the EGF-retargeted pcv. The EGFR internalisation pathway was therefore permissive for adenovirus transduction. EGFR-dependent transduction was also shown in human cancer cell lines, proportional to the level of EGFR expression. Transduction could be inhibited using anti EGFR antibody to block EGF binding. Specific activity of transduction for EGF-retargeted pcv was similar to unmodified virus, indicating efficient intracellular processing and transgene expression following EGFR-mediated uptake. Other EGFR ligands (transforming growth factor-α and an anti-EGFR-antibody, Cetuximab) also mediated pcv retargeting. This approach was used to target lytic 'virotherapy' using wild type adenovirus (Ad5WT) in a peritoneal xenograft model of human ovarian cancer. Anti-cancer activity of Ad5WT was retained following polymer coating and EGF-retargeting, defined by reduced tumour load and extended survival compared to controls, and adhesion formation was decreased compared with unmodified virus.

This is the first study to demonstrate a therapeutic advantage of polymer coating and retargeting adenovirus, promising an improved anti-cancer therapeutic index.

Acknowledgements

I am very fortunate to have the support and advice of both of my supervisors, Professor Sean Kehoe and Professor Leonard Seymour. I am particularly grateful for their encouragement, experienced advice and guidance during the course of this work.

I am indebted to my laboratory colleagues for their support, advice, patient teaching, humour and friendship. I have been privileged to be included as part of the wider lab 'family', despite being the token medic. In particular I would like to thank Dr Simon Briggs for his patient explanation and provision of all things chemical, Dr Robert Carlisle for his thoughtful advice and input into the scientific process and his insightful comments in preparation of this thesis, and Dr Kerry Fisher, for his inspirational ideas and novel directions. I am also grateful to Drs Mark Stevenson, Sarah Hale and Paul Farrow, Miriam Bazan-Peregrino, Victor Ramos-Perez, Ashley Hale, Sue Phipps, Fionnadh Carroll for their daily advice and support. I would also like to thank: Dr Nicky Green, of Hybrid Systems Ltd., for her balanced opinions and advice, training and assistance with the animal work; Dr Iain McNeish, of St Bartholomew's and The London School of Medicine, for donating the SKOV-luc cell line; and Dr Shaila Sarvana for independent histopathological review of liver samples.

I am ever grateful to my family and friends, and in particular my husband, Nick Alp, for his love, support, critical review and red pen-wielding during proof reading.

Finally, I would like to thank Macmillan Cancer Relief, Wellbeing of Women and the Oxfordshire Health Services Research Committee for giving me the opportunity to perform this work by funding laboratory consumables, university fees and my salary. Without their help I would be still slaving away on delivery suite and I am very appreciative of their support.

Table of contents

ABSTRACT 2

ACKNOWLEDGEMENTS 3

TABLE OF CONTENTS 4

LIST OF FIGURES 10

LIST OF TABLES 13

LIST OF ABBREVIATIONS 14

1 INTRODUCTION 18

1.1 Ovarian cancer 18

1.1.1 Presentation 20

1.1.2 Surgical management 20

1.1.3 Chemotherapy 22

1.1.4 Epidermal growth factor receptor as a target for ovarian cancer therapy 24

1.1.5 Gene therapy 26

1.1.6 Adenovirus gene therapy strategies in ovarian cancer 35

1.1.7 Adenovirus infection mechanisms 38

1.2 Aims and scope of the thesis 51

1.2.1 Hypotheses 51

1.2.2 Aims of the thesis 51

2 MATERIALS AND METHODS 53

2.1 General laboratory methods 53

2.1.1 Cell lines and culture 53

2.1.2 Generation of A9 cell lines stably transfected with EGFR plasmid 56

2.1.3 Protein Assay 57

2.1.4 MTS assay 57

2.1.5 Antibodies 58

2.1.6 Analysis of cell receptor status by flow cytometry 59

2.1.7 Analysis of cell receptor status by ELISA 60

2.1.8 Binding of EGF-polymer to EGFR positive cells 61

2.1.9 Internalisation of EGF receptors 62

2.1.10 Western blot 64

2.2 Virus techniques 67

2.2.1 Adenovirus vectors 67

2.2.2 Adenovirus propagation 67

2.2.3 Purification of adenovirus 68

2.2.4 Double Stranded DNA quantification to calculate number of viral particles 69

2.2.5 Quantification of infectious virus particles 70

2.2.6 Polymer coating virus 71

2.2.7 Purification of polymer coated adenovirus vectors 72

2.2.8 Viral transduction of cells *in vitro* 72

2.2.9 Quantitative polymerase chain reaction (Q-PCR) 73

2.2.10 Assessment of oncolytic activity of viruses 77

2.3 Animal techniques 77

2.3.1 Housing conditions 77

2.3.2 Diets 78

2.3.3 Generation of human ovarian cancer xenografts 78

2.3.4 Virus transduction studies 78

2.3.5 DNA extraction 78

2.3.6 Assessment of liver transaminase levels 79

2.3.7 Assessment of hepatic pathology 79

2.4 Statistical analysis 80

3 PRODUCTION OF EGFR-POSITIVE, CAR-NEGATIVE CELL LINE 81

3.1 Introduction 81

3.2 Methods and Results 81

3.2.1 EGFR containing plasmid 81

3.2.2 Determination of concentration of Geneticin (G418) required for plasmid-positive A9 cell selection 82

3.2.3 Transfection of A9 cells with EGFR plasmid 83

3.2.4 Effect of removing G418 from growth media on EGFR expression levels 85

3.2.5 Functionality of transfected EGFR 87

3.3 Discussion 94

4 *IN VITRO* ACTIVITY OF EGF- POLYMER CONJUGATE 96

4.1 Introduction 96

4.2 Methods and results 97

4.2.1 Binding of EGF-polymer to EGFR positive cells 97

4.2.2 EGF-polymer ability to stimulate EGFR tyrosine kinase activity 97

4.2.3 EGF-polymer co-localisation with EGFR in vesicles 100

4.2.4 EGF-polymer retargeting adenovirus to A9-EGFR clones 102

4.2.5 EGF-polymer retargeting in ovarian tumour cell lines 106

4.2.6 Effect of anti-CAR antibody on virus infection 112

4.2.7 Specific activity of EGF-pcv compared to unmodified virus 112

4.3 Discussion 114

5 RETARGETING POLYMER COATED ADENOVIRUS TO EGFR WITH ALTERNATIVE LIGANDS 117

5.1 Introduction 117

5.2 Methods and results 119

5.2.1 Production of Cetuximab retargeted polymer coated adenovirus 119

5.2.2 Cetuximab is able to prevent EGFR stimulation by its ligand 119

5.2.3 Cetuximab initiation of EGFR internalisation 121

5.2.4 Cetuximab retargeting of adenovirus infection 123

5.2.5 TGF-α polymer is able to retarget adenovirus transduction of EGFR positive cells 128

5.2.6 Mitogenic activity of polymer coated viruses 131

5.2.7 Stimulation of EGFR tyrosine kinase activity by EGFR retargeted adenovirus 135

5.3 Discussion 137

6 THERAPEUTIC EFFECT OF EGF-POLYMER COATING AN ONCOLYTIC ADENOVIRUS IN AN ANIMAL MODEL 140

6.1 Introduction 140

6.2 Methods and results 143

6.2.1 Effect of EGF-polymer on adenovirus organ transduction 143

6.2.2 Potency of oncolytic adenoviruses on a panel of ovarian tumour cell lines 146

6.2.3 Effect of coating with EGF-polymer on oncolytic effect of wild type adenovirus (Ad5WT) 150

6.2.4 Effect of adenovirus coating and re-targeting on anti-tumour activity 152

6.2.5 Calculation of tumour load by Q-PCR for human β-actin 157

6.2.6 Development of a bioluminescent i.p. tumour model to monitor tumour load *in vivo* 159

6.2.7 Determining the sample size required to adequately power a survival study of EGF-pcv Ad5WT 163

6.2.8 *In vivo* effect of EGF-polymer and Cetuximab-polymer coating of Ad5WT in a tumour load/survival experiment 164

6.3 Discussion 180

6.3.1 Use of EGF-polymer coating to improve therapeutic index 180

6.3.2 Use of bioluminescence to refine animal studies 180

6.3.3 Effect of polymer coating concentration on level of anti-tumour activity 182

7 GENERAL DISCUSSION AND CONCLUSIONS 184

7.1 Principal findings 185

7.1.1 Retargeting adenovirus with EGF-pHPMA *in vitro* 185

7.1.2 Retargeting adenovirus to EGFR with Cetuximab and TGF-α 188

7.1.3 *In vivo* effects of retargeting adenovirus to the EGFR 188

7.2 Limitations 192

7.3 Future work 193

7.4 Conclusions 197

8 REFERENCES 198

9 APPENDIX 218

9.1 Unmodified human TGF-α protein sequence 218

9.2 Human EGF protein sequence 218

9.3 Murine EGF protein sequence 218

9.4 Post-mortem findings from survival experiment 218

9.5 Publications arising from this work 225

9.5.1 Publications in peer-reviewed journals 225

9.5.2 Book chapters 225

9.5.3 Abstracts presented at scientific conferences 226

9.5.4 Paper submitted for publication 227

List of figures

Figure 1-1 Mechanism of normal adenovirus infection 40

Figure 1-2 Schematic of EGF-EGFR binding and action of Cetuximab 43

Figure 1-3 EGFR auto-phosphorylation and down-stream signalling 45

Figure 1-4 Diagrammatic representation of polymer binding to murine and human EGF 50

Figure 2-1 Conversion of the MTS reagent by viable cells 58

Figure 2-2 Conversion of luciferin to oxyluciferin by firefly luciferase 73

Figure 2-3 Q-PCR amplification plot of adenovirus standards 75

Figure 2-4 Standard curve of Q-PCR generated CT values of adenovirus standards 75

Figure 2-5 Standard curve obtained following Q-PCR of a serial dilution of pDRIVE-hβ-Actin-RU5' spiked into mouse tissue lysate 76

Figure 3-1 Diagrammatic representation of the pUSEampEGFR plasmid 82

Figure 3-2 Survival of A9 mouse fibroblasts with increasing concentration of Geneticin (G418) 83

Figure 3-3 Assessment of EGFR expression in transfected A9 clones 84

Figure 3-4 Assessment of EGFR expression in transfected A9 clones after 12 months of passage 85

Figure 3-5 Change in EGFR expression over time following G418 removal 86

Figure 3-6 Flow cytometry assessment of internalised EGFR following incubation with an EGF-Fluorescein conjugate 88

Figure 3-7 Cellular internalisation of EGFR following stimulation with EGF 90

Figure 3-8 Western blot of A9-EGFR clones stimulated with EGF and probed with an anti-pEGFR antibody 92

Figure 3-9 Down-stream signalling in clone A9-EGFR C10 following EGF stimulation 93

Figure 4-1 Flow cytometry assessment of EGF-polymer binding to EGFR positive and negative cell lines 98

Figure 4-2 EGF-polymer stimulation of EGFR phosphorylation 99

Figure 4-3 EGF-polymer co-localised with EGFR in vesicles following stimulation and time for internalisation 101

Figure 4-4	Retargeting adenovirus to A9-EGFR cells with EGF-polymer coating	103
Figure 4-5	An EGF-blocking antibody inhibits EGF-polymer retargeting	104
Figure 4-6	A9-CAR expression of EGFR and CAR by flow cytometry	105
Figure 4-7	EGFR and CAR status of cancer cell lines by flow cytometry	107
Figure 4-8	Number of EGFR per cell in various different cell lines	108
Figure 4-9	EGF-polymer retargets adenovirus to EGFR-positive cancer cells	110
Figure 4-10	Retargeted transgene expression is proportional to cellular EGFR levels	110
Figure 4-11	EGF-blocking antibody inhibits EGF-polymer retargeting in cancer cells	111
Figure 4-12	Blocking CAR-mediated virus uptake does not affect EGF-polymer coated adenovirus transgene expression	113
Figure 4-13	Specific activity of EGF-pcv *in vitro*	114
Figure 5-1	Cetuximab is able to inhibit EGF stimulated EGFR tyrosine kinase activity	120
Figure 5-2	Cetuximab stimulates EGFR internalisation	122
Figure 5-3	CAR and EGFR status of T24 and SW620 cell lines	124
Figure 5-4	Cetuximab and EGF-polymer bind to T24 cells but not SW620 cells	125
Figure 5-5	Cetuximab conjugation is able to retarget polymer-coated adenovirus to EGFR-positive cells	126
Figure 5-6	Blocking EGF-binding inhibits Cetuximab retargeted virus infection	127
Figure 5-7	Cetuximab-pcv has reduced activity after a freeze-thaw cycle, but transduction remains EGFR specific	129
Figure 5-8	TGF-α polymer is able to retarget adenovirus infection via the EGFR	130
Figure 5-9	Cell standard curves for MTS assay	133
Figure 5-10	Mitogenic effect of adenoviruses coated with retargeted polymers	134
Figure 5-11	Stimulation of EGFR tyrosine kinase activity by EGF & TGF-α retargeted adenovirus	136
Figure 5-12	Stimulation of EGFR tyrosine kinase activity with purified EGF-pcv	137
Figure 6-1	Transaminase levels at 24 hours in mice injected with adenovirus i.p.	144
Figure 6-2	Luciferase expression *in vivo* at different polymer coating concentrations	145
Figure 6-3	Oncolytic effect of conditionally replicating adenovirus	148
Figure 6-4	IC_{50} of conditionally replicating adenoviruses in ovarian cancer cells	149

Figure 6-5	Effect of EGF-polymer coating on oncolytic potential of wild type Ad5	151
Figure 6-6	Therapeutic effect of polymer coating and re-targeting wild type adenovirus	154
Figure 6-7	Adhesion score by i.p. adenovirus treatment groups	156
Figure 6-8	Standard curve of plasmid copy no. by Q-PCR vs. cell number	158
Figure 6-9	SKOV-luc cell luminescence is directly proportional to cell number	160
Figure 6-10	The IVIS 100 imaging system	161
Figure 6-11	Flux measurements over time for individual mice	162
Figure 6-12	Exponential increase in total mouse flux over time in mice implanted with SKOV-luc cells	163
Figure 6-13	Schematic of survival experiment design	165
Figure 6-14	Bioluminescence by group at 10 days post treatment	167
Figure 6-15	Composite bioluminescence images of mice 10 days post treatment	168
Figure 6-16	Bioluminescence by group at time intervals over 38 days post treatment	169
Figure 6-17	Survival curves for mice implanted with SKOV-luc	170
Figure 6-18	Relationship of mean group flux and median group survival	172
Figure 6-19	Mass of tumours removed at time of post-mortem examination	173
Figure 6-20	*In vivo* bioluminescence of homogenised SKOV-luc tumours	174
Figure 6-21	Post-mortem laparotomy images	176
Figure 6-22	Adhesion scores for the survival study	177
Figure 6-23	Hepatic histology findings	179

List of tables

Table 1-1	FIGO staging of epithelial ovarian cancer	18
Table 1-2	Histological subtypes of ovarian cancer	19
Table 1-3	Pros and cons of viral vectors for cancer gene therapy	34
Table 1-4	Enzyme-prodrug combinations for VDEPT strategies	37
Table 2-1	Cell culture details of primary and established cell lines	54
Table 2-2	Antibodies	58
Table 6-1	Interaction of adenovirus proteins with cell cycle control proteins	142
Table 6-2	Oncolytic viruses and their genetic modifications	147
Table 6-3	Adhesion scoring system	153
Table 6-4	Analysis of survival curves	170

List of abbreviations

A9-EGFR C10/C22	Murine fibroblast A9 cells stably transfected with human EGFR
AAV	Adeno-associated virus
Ad	Adenovirus
Ad5	Human adenovirus serotype 5
AdCMV-GFP $_{\Delta E1}$	Adenovirus encoding green fluorescence protein transgene
AdCMV-Luc $_{\Delta E1}$	Adenovirus encoding firefly luciferase transgene under control of the CMV promoter
CA125	Carcinoma antigen 125
CAR	Coxsackie adenovirus receptor
CB 1954	5-(aziridin-1-yl)- 2,4-dinitrobenzamide
CD	Cytosine deaminase
CHORUS	Chemotherapy or Up-front Surgery in ovarian cancer MRC trial
CMV	Human cytomegalovirus
DAB	3,3'Diaminobenzidine
DAPI	4',6-Diamidino-2-phenylindole
DLT	Dose limiting toxicity
DMEM	Dulbecco's modified Eagle's media
DMSO	Dimethyl sulphoxide
DNA	Deoxyribonucleic acid
DOPE	Dioleoylphosphatidylethanolamine
DOTAP	N-[1-(2,3-Dioleoyloxy)propyl]-N,N,N-trimethylammonium chloride
DPX	p-Xylene-bis(N-pyridinium bromide)

E. Coli	*Escherichia coli*
EDTA	Ethylenediamine tetra-acetic acid
EGF	Epidermal growth factor
EGF-pcv	Epidermal growth factor retargeted, pHPMA coated adenovirus
EGFR	Epidermal growth factor receptor
ELISA	Enzyme linked immunosorbent assay
EORTC	European Organisation for Research and Treatment of Cancer
FCS	Foetal calf serum
FIGO	International Federation of Gynaecological Oncology
G418	Geneticin
GFP	Green fluorescent protein (from *Aequorea Victoria*)
GOG	Gynecologic Oncology Group
HEPES	4-(2-Hydroxyethyl)piperazine-1-ethanesulfonic acid, N-(2-Hydroxyethyl)piperazine-N'-(2-ethanesulfonic acid)
HINGS	Heat inactivated goat serum
HIV	Human immunodeficiency virus
HRP	Horse radish peroxidase
hrs	Hours
HSV	Herpes simplex virus
i.p.	Intraperitoneal
i.v.	Intravenous
Ig	Immunoglobulin
IL-6	Interleukin 6
IMS	Industrial methylated spirit

l	Litre
mg	Milligram
min	Minute
ml	Millilitre
mm	Millimetre
mmol/l	Millimoles per litre
MOI	Multiplicity of infection
mol/l	Moles per litre
MRC	Medical Research Council
MTS	3-(4,5-dimethylthiazol-2-yl)-5-(3-carboxymethoxyphenyl)-2-(4-sulphophenyl)-2H-tetrazolium
MW	Molecular weight
ng	Nanogram
nm	Nanometre
NTR	*E.coli* nitroimidazole reductase (nitroreductase)
OD	Optical density
PBS	Phosphate buffered saline
PCR	Polymerase chain reaction
pcv	Polymer coated adenovirus
pfu	Plaque forming units
pHPMA	Poly[N-92-hydroxypropyl)methacrlyamide]
Q-PCR	Quantitative polymerase chain reaction
RLU	Relative light units
RNA	Ribonucleic acid

rpm	Revolutions per minute
RPMI	RPMI-1640 media
RT	Room temperature
s	Second
s.c.	Subcutaneous
SDS	Sodium dodecyl sulphate
SEM	Standard error of the mean
TBS	Tris buffered saline
TGF-α	Human transforming growth factor alpha
tk	Thymidine kinase
TMPEG	Tresylmonomethoxypolyethylene glycol
Tris HCl	Tris(hydroxymethyl)aminomethane hydrochloride
Triton X 100	4-(1,1,3,3-Tetramethylbutyl)phenyl-polyethylene glycol solution
v.p.	Viral particles
VDEPT	Virus directed enzyme-prodrug therapy
VZV	Varicella zoster virus
WT	Wild type
β-Gal	E. coli β-galactosidase
λ	Wavelength (in nm)
μ	micro
μg	Microgram
μl	Microlitre
μmol/l	Micromoles per litre

1 Introduction

1.1 Ovarian cancer

Ovarian cancer has an incidence of 6,500 cases per year in England and Wales, but is responsible for more deaths than the other gynaecological cancers combined, with a mortality rate of 4,000 per year (Quinn *et al.* 2001). The onset is often insidious; the symptoms are vague and may mimic other conditions. This leads to a delay in presentation and diagnosis, and currently three-quarters of women present once the disease has spread throughout the abdomen (stage III or IV – see Table 1-1) (Shepherd 1989) when the 5 year survival is 20-30% (Lambert *et al.* 2004). Epithelial ovarian cancer accounts for 90% of all ovarian cancers and typically presents in post-menopausal women, with a peak incidence at 63 years of age. This thesis will address epithelial ovarian cancer and not the rarer ovarian cancers (see Table 1-2), which are often responsive to chemotherapy, present at an earlier stage and pose less of a health burden than the epithelial tumours.

Table 1-1 FIGO staging of epithelial ovarian cancer

Stage	***Extent of disease***
Stage I	Limited to ovaries
a	one ovary
b	both ovaries
c	ruptured capsule, tumour on ovarian surface or positive peritoneal washings
Stage II	Limited to pelvis
a	uterus or tubes
b	other pelvis structures
c	positive peritoneal washings/ascites
Stage III	Limited to abdomen
a	microscopic metastases
b	macroscopic metastases <2 cm
c	macroscopic metastases >2 cm
Stage IV	Distant metastases outside abdominal cavity

Table 1-2 Histological subtypes of ovarian cancer

Classification	*Examples*
Epithelial	Serous cystadenocarcinoma
	Mucinous cystadenocarcinoma
	Endometrioid adenocarcinoma
	Clear cell
	Undifferentiated
Sex Cord-Stromal	
Granulosa-stromal cell tumours	Granulosa cell
	Thecoma
	Fibroma
Androblastomas	Sertoli cell
	Sertoli-Leydig cell
	Leydig cell
Germ cell	Dysgerminoma
Embryonic	Mature teratoma
	Immature teratoma
	Struma ovarii
	Carcinoid
Extra embryonic	Endodermal sinus tumour (yolk sac)
	Choriocarcinoma
Other	Lipoid cell tumour
	Sarcoma
	Small cell carcinoma
Metastatic tumour	
Gynaecological	Tubal
	Endometrial
	Cervical
Non-gynaecological	Breast
	Gastrointestinal (stomach/colon)
	Lymphoma
	Melanoma
	Carcinoid

1.1.1 Presentation

Symptoms of ovarian cancer may not be apparent until the disease has spread throughout the peritoneal cavity. In addition, the non-specific nature of symptoms means that 50% of women may be initially referred to a specialty other than gynaecology. The most common symptoms include: bloating; abdominal pain; unexpected weight loss or gain; bowel symptoms; urinary urgency or incontinence; dyspareunia; menstrual irregularity or post-menopausal bleeding; deep venous thrombosis; and dyspnoea. However, pre-diagnostic symptoms may have a longer duration than previously thought (Vine *et al.* 2003). Furthermore, according to this study, whereas individual symptoms commonly occurred in age-matched controls, it is the combination of unrelated symptoms that should cause suspicion and initiate appropriate referral.

Diagnosis relies on obtaining histological or cytological specimens. Ultrasound features may increase the suspicion of malignancy and can be combined with serum CA125 levels, a tumour marker increased in 80% of epithelial ovarian cancers, and the age of the woman into a risk of malignancy index (RMI) (Jacobs *et al.* 1990). This can aid appropriate referral to a specialist gynaecological oncologist for primary surgery, which has been shown to improve survival (Kehoe *et al.* 1994).

1.1.2 Surgical management

The current first step in primary management of ovarian cancer is a debulking laparotomy. Surgical objectives are to diagnose, stage and excise all macroscopic disease. Surgery normally includes a total hysterectomy, bilateral salpingo-oophorectomy, omentectomy, retroperitoneal lymph node dissection/sampling, and collection of peritoneal fluid for cytological examination. In younger women fertility preservation may be a concern, and so performing a pelvic clearance without first obtaining a histological diagnosis of carcinoma would be unwise. In addition, in this age group germ cell tumours are relatively common. These often respond well to chemotherapy and so fertility-sparing surgery may be appropriate.

In early stage disease (low grade FIGO stage Ia-Ib) (see Table 1-1) radical surgery in adequately staged women will provide a cure in most cases (Young *et al.* 1990). Adjuvant

chemotherapy will benefit some women with early stage disease (Trimbos *et al.* 2003), but the problem is accurately identifying which individuals these are, although advances in elucidating the genetic signatures of tumours may make this possible in the future (Bingham *et al.* 2001). Sub-group analysis of the two large randomised control trials of adjuvant chemotherapy in high risk early stage disease (ICON1 and ACTION), combined in the meta-analysis (Trimbos *et al.* 2003), highlighted the need for adequate surgical staging, since women with inadequate staging had greater benefit from chemotherapy, most likely indicating that they had unrecognised higher stage disease at presentation. In adequately staged patients it has been reported that there was no difference in survival between the two arms, although there were small numbers of events in this sub-group; these data were not included in the published version of ICON1 because of the concern over the small numbers upon which this sub-group analysis could be based (for a discussion of this see (Swart and Parmar 2005)). The conclusion of the ICON1 and ACTION meta-analysis was that there was a significant improvement in 5-year overall survival with platinum-based adjuvant chemotherapy (82% in the chemotherapy arm and 74% in the observation arm; hazard ratio (HR) = 0.67, 95% confidence interval (CI) = 0.50 to 0.90; P = 0.008). These two trials included patients with high-risk early-stage ovarian cancer (FIGO stage Ia and Ib with grade II or III tumour, all grades of FIGO stage Ic–IIa, and all clear cell carcinomas). A more recent study from the Gynecologic Oncology Group (GOG) did not demonstrate any improvement in survival for women with high risk early stage disease (grade 3 stage 1a-b, including high risk histology, e.g. clear cell, stage 1c and stage II) if they were given 6 cycles of carboplatin/paclitaxel, compared with those receiving only 3 cycles (Bell *et al.* 2006).

In advanced disease, where it is not possible to resect all macroscopic disease, the practice has been to perform debulking surgery and remove as much tumour as possible. The definition of optimal debulking has changed with improvements in anaesthetic care and surgical technique: currently the aim is to leave no macroscopic disease. Evidence in favour of this management comes from a retrospective study of 102 women, in whom there was improved survival if no tumour deposit remained which was greater than 1.6 cm in diameter (Griffiths 1975). A further small prospective study by the same group concluded that the surgical intervention was the cause of the improved outcome (Griffiths and Fuller 1978). Recently two randomized control

trials from the European Organisation for Research and Treatment of Cancer (EORTC) and the Medical Research Council (the CHORUS trial) have started to recruit, and aim to determine whether surgery is indeed beneficial to these women, or whether being able to achieve optimal debulking merely reflects a more favourable tumour biology (Kehoe and Wheeler 2003).

Evidence for interval debulking surgery in women with residual disease following primary surgery comes from two randomized control trials with conflicting results. In the EORTC trial women with stage IIb-IV ovarian cancer - with greater than 1 cm disease remaining following primary surgery were randomized to either interval debulking surgery or no further surgery if they showed some response to three cycles of cisplatin/cyclophosphamide chemotherapy (van der Burg *et al.* 1995). Women randomized to interval debulking surgery had an increased median survival of 6 months (P = 0.01). However, a second study from North America demonstrated no benefit from interval debulking surgery (Rose *et al.* 2004). In this study women received both paclitaxel and cisplatin and every woman was operated on by trained gynaecological oncologists, so the two studies may not be directly comparable.

1.1.3 Chemotherapy

1.1.3.1 Platinum agents

First-line chemotherapy management in ovarian cancer is based on the alkylating platinum agents: cisplatin and carboplatin. Cisplatin was first introduced in the 1970s and achieved response rates of up to 50% in relapsed disease. The cisplatin analogue, carboplatin, was then developed and responses in heavily pre-treated relapsed patients were demonstrated, but with less severe side effects. A Cochrane systematic review by the Advanced Ovarian Cancer Trialists Group (AOCTG) analysed individual patient data from 49 trials involving 8,763 women. This group compared combination non-platinum chemotherapy with the same combination including a platinum agent. They demonstrated improved survival for women receiving platinum agents (hazard ratio (HR) for survival 0.88, 95% CI 0.79-0.98) but with no significant difference between carboplatin and cisplatin (Chemotherapy in advanced ovarian cancer: an overview of randomised clinical trials. Advanced Ovarian Cancer Trialists Group 1991). Carboplatin is therefore the agent of choice, due to less severe toxic side effects.

1.1.3.2 Taxanes

Taxanes were initially derived from the bark of the Pacific yew (*Taxus brevifolia*). Paclitaxel was introduced in the 1980s, when responses in women with relapsed ovarian cancer were demonstrated. In the Gynecologic Oncology Group study (GOG 111) women with suboptimally debulked disease were randomized to receive cisplatin and paclitaxel versus cisplatin and cyclophosphamide (McGuire *et al.* 1996). An improved overall survival was demonstrated in the paclitaxel arm (38 vs. 24 months; $P < 0.001$). These findings were confirmed in the OV10 study from the European/Canadian Intergroup (Piccart *et al.* 2003).

Paclitaxel was then compared as a single agent against paclitaxel/cisplatin and cisplatin in the three arm GOG 132 study (Muggia *et al.* 2000). Paclitaxel alone was not as effective as in combination with cisplatin. In addition, there was no difference in overall survival between the cisplatin and paclitaxel/cisplatin arms (30.2 vs. 26.0 months; not significant), which was in contradiction to the GOG 111 study, although there was a large number of patients who crossed over and received paclitaxel.

The International Collaborative Ovarian Neoplasm Group (ICON3) trial was the largest trial to examine the role of paclitaxel (Paclitaxel plus carboplatin versus standard chemotherapy with either single-agent carboplatin or cyclophosphamide, doxorubicin, and cisplatin in women with ovarian cancer: the ICON3 randomised trial 2002). In that study 2,074 women were randomized to carboplatin or CAP (carboplatin/cyclophosphamide/doxorubicin) versus carboplatin/paclitaxel. There were no differences in terms of survival between the groups, although the taxane arm experienced more adverse effects.

A meta-analysis of GOG 111, OV10, GOG 132 and ICON3 was complicated by heterogeneity between the treatments in the study arms, but found a non-significant trend towards improved survival for a platinum/paclitaxel combination (HR for survival 0.82, 95% CI 0.66-1.02) (Sandercock *et al.* 2002). The National Institute for Clinical Excellence (NICE), the government medical advisory group in the UK, has recommended that a platinum agent should be obligatory

first-line treatment in ovarian cancer, with paclitaxel use left up to the individual patient and doctor.

Other chemotherapeutic agents have been evaluated in a large international study (GOG 182/ICON5) to assess their effect on survival in first-line chemotherapy. This five-arm study combined topotecan, gemcitabine and PEGylated liposomal doxorubicin (Caelyx) with carboplatin/paclitaxel. Recruitment has now completed and follow up for survival data is awaited. A preliminary report of the data suggests that there is no benefit to the addition of a third chemotherapeutic agent to the platinum-paclitaxel regimen in terms of progression-free survival, although overall 5-year survival data is awaited (Bookman 2006).

Current first line management for advanced ovarian cancer therefore consists of primary debulking surgery, followed by platinum-based chemotherapy, plus or minus the addition of a taxane. However, in women presenting with advanced disease treatment is essentially palliative; despite the advances in conventional chemotherapy and small improvements in median survival, there has been little change to the five-year survival for stage III-IV disease over the past 20-30 years and it remains a disease that is controlled for a period rather than cured in most cases. Conventional chemotherapeutic agents were developed to have activity on all rapidly dividing cells, hence the common side effects of hair loss, bone marrow suppression and mucositis. Increasing knowledge of the genetic basis for cancer has lead to the development of novel reagents, which target cancer-specific pathways. It is hoped that these reagents will spare normal cells and reduce the toxic side effects of chemotherapy, in addition to having an enhanced therapeutic effect.

1.1.4 Epidermal growth factor receptor as a target for ovarian cancer therapy

1.1.4.1 Epidermal growth factor receptor and cancer aetiology

The epidermal growth factor receptor family, a subclass of the receptor tyrosine kinase superfamily, consists of four members: EGFR (ErbB1/HER1); HER2/neu (ErbB2); HER3

(ErbB3); and HER4 (ErbB4). All of these receptors are made up of an extra-cellular ligand-binding domain, a single membrane-spanning region, and a cytoplasmic tyrosine kinase domain. They were first implicated in cancer aetiology when it was discovered that the oncogenic avian erythroblastosis retrovirus encoded a mutated version of EGFR (Downward *et al.* 1984). Abnormal EGFR activation has been demonstrated in ovarian cancer, is associated with a poorer prognosis (Nicholson *et al.* 2001), and can happen through a variety of mechanisms. EGFR mutation occurs in some ovarian cancers (Moscatello *et al.* 1995); the most common EGFR mutation is in the extra-cellular region and been shown to result in ligand independent activation in glioblastomas (Ekstrand *et al.* 1992). Over-expression of EGFR is common (Bartlett *et al.* 1996; Slamon *et al.* 1989), but alone does not result in constitutive activity, unlike HER2/neu. Receptor activation is therefore by formation of an autocrine loop, with increased production of receptor ligand by the tumour cells (Bandera *et al.* 2003).

1.1.4.2 Epidermal growth factor directed treatments

1.1.4.2.1 Tyrosine kinase inhibitors

Tyrosine kinases, such as members of the EGFR family, are enzymes that phosphorylate target proteins and are central to cell regulation, being involved in apoptosis regulation, cell cycle progression, immune responses, differentiation and development, and are often dysregulated in cancer (Blume-Jensen and Hunter 2001). Thus, tyrosine kinases are attractive targets for cancer-targeted therapies. Gefitinib (Iressa/ZD1839) is a small molecule which specifically inhibits EGFR tyrosine kinase activity, preventing signal transduction (Moulder *et al.* 2001). Pre-clinical studies have shown anti-tumour activity, and the orally active agent was well tolerated in a phase I clinical trial in a range of tumour types, including ovarian (Baselga *et al.* 2002). Phase II or III data on the efficacy of iressa in ovarian cancer have yet to be published.

Erlotinib (Tarceva/OSI-774) is another EGFR tyrosine kinase inhibitor, which has been through phase I and II clinical trials. Results from a recent phase II trial suggest that Elotinib may have activity in ovarian carcinoma (Gordon *et al.* 2005). Thirty-four patients with EGFR-positive recurrent, refractory ovarian cancer, who had failed therapy with a platinum agent (+/- a taxane), were given single agent erlotinib. Two patients (6%) demonstrated a partial response and

another 44% had stable disease on treatment, suggesting that single agent erlotinib may have some activity in relapsed ovarian cancer. The major side effects of treatment were development of a skin rash (68%) and diarrhoea (38%), so although responses were modest, the treatment was well tolerated. Interestingly, patients who developed a skin rash had a significant increase in median survival compared to those who did not have this side effect.

1.1.4.2.2 Monoclonal antibodies

HER2/neu is a member of the EGFR family and over-expression is related to poor outcome in breast cancer. A monoclonal antibody, Trastuzumab (Herceptin) has been developed that binds to HER2/neu, down-regulates HER2/neu expression and down-stream signalling and, due to its humanised Fc portion, is able to stimulate antibody-dependent cellular toxicity (Baselga *et al.* 2001; Cooley *et al.* 1999) . In women with recurrent ovarian cancer treated with Herceptin, a 7.3% response rate was demonstrated, with no significant toxicity (Bookman *et al.* 2003).

IMC-C225 (Cetuximab/Erbitux) is a humanised mouse monoclonal antibody against EGFR (HER1/ErbB1) which has shown activity in combination with topotecan in pre-clinical studies (Ciardiello *et al.* 1999; Goldstein *et al.* 1995). It has been approved for the treatment of advanced-stage colorectal carcinoma (EGFR-positive) and is undergoing clinical trials for other solid tumours, including ovarian carcinoma. The mechanism of action is partly by inhibition of ligand (EGF) binding, thereby preventing pro-mitotic down-stream signalling by EGFR, in addition to antibody-dependent cellular toxicity.

It is possible to engineer bispecific antibodies; each antigen binding arm has a different target. HEA125xOKT3 has antigen-binding sites against Ep-CAM, an antigen over-expressed on epithelial tumours, and CD3, the T lymphocyte antigen. This reagent is able to direct tumour associated lymphocytes to lyse tumour cells and had a beneficial effect on ascites production and CA125 levels in all 10 women in a phase I clinical trial (Marme *et al.* 2002).

1.1.5 Gene therapy

Advances in molecular medicine have revealed some of the common mutations that are central to development of the malignant phenotype, for example mutations of p53 and the

retinoblastoma protein gene (Rb) pathway; these mutations provide potential targets for genetic therapy. The majority of gene therapy trials world-wide have been in cancer therapy. Central to all gene therapy is the requirement to deliver and then express the genetic payload.

Nucleic acids, normally in the more stable DNA form, can be delivered as plasmids, either as naked DNA or complexed with polycationic proteins or lipids. These condense the DNA and, in the case of cationic lipids such as N-[1-(2,3-Dioleoyloxy)propyl]-N,N,N-trimethylammonium methylsulphate (DOTAP), can fuse directly with lipid membranes. DOTAP is widely used to transfect cells *in vitro*. Since DOTAP cannot traffic DNA to the nucleus, it can only be used to transfect dividing cells, when the nuclear membrane is broken down during pro-metaphase, unless cytoplasmic transcription and translation can be achieved. Even *in vitro*, transfection is relatively inefficient and so more reliable and powerful vectors are required *in vivo*.

1.1.5.1 Viral vectors

Viruses have evolved over millennia to be able to enter cells and hijack the cellular mechanisms to express the viral genes, often at high levels. Several viruses have been developed for use as vectors. The perfect viral vector for cancer therapy would be: easy to generate; able to efficiently infect a variety of cell types; able to carry large transgenes; non-toxic to normal cells; infect dividing and non-dividing tumour cells; express the transgene at high levels and continue to express the transgene over time; maintain the inserted gene without mutations; and avoid unwanted host immune responses. Unfortunately such an ideal viral vector does not exist, and each of the five commonly used viral vectors has its own advantages and disadvantages (for summary see Table 1-1).

1.1.5.1.1 Adenovirus

Adenoviruses (Ad) are double-stranded DNA viruses with 36-40 kb genomes. The viral capsid is a non-enveloped icosahedron, made of 240 hexon and 12 penton molecules. The penton molecules have fibres, which, in the most common human group C adenoviruses, Ad2 and Ad5 (and most extensively studied as gene therapy vectors), interact with the cellular Coxsackie-adenovirus receptor (CAR) and lead to cell infection. Other adenoviruses interact with different primary receptors, e.g. group B adenovirus Ad3 binds to CD46, which is expressed in many

human tissues (Sirena *et al.* 2004). Adenoviruses have several features that make them attractive vectors for cancer gene therapy: they are easy to produce in high titres; they are able to infect a wide variety of cell types and are found in a large number of different species; they have low pathogenicity; adenoviral DNA is relatively easy to manipulate using recombinant DNA techniques and once inserted the transgene does not undergo a high rate of mutation; a relatively large amount of foreign DNA can be inserted into first-generation adenoviral genomes (7.5 kb), although with development of third generation 'gut-less' viruses, this can be much greater (see below).

However, adenoviruses also have several important disadvantages. Adenoviruses are highly immunogenic. Almost all adults will have been exposed to adenovirus in the past, and have adenovirus specific antibodies in both blood and ascitic fluid (Stallwood *et al.* 2000), of which 55% of anti-adenoviral antibodies will be neutralising (Chirmule *et al.* 1999). Neutralising antibodies are thought to be directed against the knob and fibre domains of the viral capsid. Administration of adenovirus for gene therapy can therefore provoke a large immune response. This has three main implications. First, adenovirus will be neutralised by the pre-existing antibodies and reduce the efficacy of cell infection. Infection will also stimulate further B cell clones specific for adenoviral antigens, and so subsequent administration of adenovirus will produce an even greater neutralising antibody response. Second, adenoviral proteins will be presented in conjunction with human leukocyte antigen (HLA) on the surface of infected cells. This HLA-viral peptide complex is a target for cytotoxic T lymphocytes (CTL), which destroy the infected cell, and so limit transgene expression. However, it is worth noting that CTL responses may also be beneficial in some circumstances, especially in cancer, as the cancer cell can be destroyed by the immune response as well as the gene therapy strategy. Third, some individuals are able to launch a massive inflammatory response to high doses of adenovirus, and this has caused the death of one individual from disseminated intravascular coagulation, acute respiratory distress and multi-organ failure (Assessment of adenoviral vector safety and toxicity: report of the National Institutes of Health Recombinant DNA Advisory Committee 2002). The inflammatory response to adenovirus is therefore a major obstacle to its use as a viral vector.

Genetic engineering of adenovirus has helped to reduce the cell mediated immune response. Initially replication incompetent adenoviruses were produced by deleting the early genes E1 and E3. E1 gene products are necessary for virus replication. E3 gene products were deleted to increase transgene capacity, but were subsequently found to have immune-modulatory functions (e.g. gp19K down-regulates MHC class I expression and inhibits tapasin, so preventing presentation of viral peptides and cell lysis by CTL, and 14.7K protects cells from TNFα and Fas-mediated cytolysis). However, despite their lack of replication, these viruses still expressed a number of viral proteins, which in the absence of key E3 gene peptides are readily presented to CTL in the context of MHC class I, thus limiting transgene expression. By deleting other viral genes (e.g. E2 and E4) a reduced cell mediated immune response was generated, thereby improving transgene expression (Lusky *et al.* 1998; O'Neal *et al.* 1998).

Recently 'gut-less' adenoviruses have been developed which can package up to 32 kb of foreign DNA (Amalfitano *et al.* 1998; Balague *et al.* 2000). These viruses retain the sequences required for their genome to be packaged into virions. However, as there are no viral genes left in the genome, virus production depends on a helper cell that encodes the viral genes necessary to make and package the viral particles. This system produces replication-incompetent viral particles that can produce large human gene products (e.g. human factor VIII). The other advantage is that, because no viral genes are expressed, the cell mediated immune response is much reduced. However, the viral particles will still be neutralised by antibodies, and can cause further sensitization to adenovirus.

Adenoviral vectors transfer the transgene to the target cell nucleus, but do not integrate their DNA into the host cell genome. Transgene expression is therefore temporary, but in cancer gene therapy this is not an adverse characteristic, as the aim is to kill the target cell. One important benefit of adenovirus when used to treat cancer is that it is able to infect both replicating and non-replicating cells. In any solid tumour, only a proportion of the tumour cells will be replicating at any time, so in order to infect a significant proportion of the tumour, a vector that can infect both replicating and non-replicating cells is essential.

1.1.5.1.2 Adeno-associated virus

Adeno-associated viruses are single-stranded parvoviruses. They have a 4.7kb genome, which encodes four proteins required for viral replication and three structural proteins. These sequences are flanked by inverted terminal repeat sequences that are necessary for viral replication, packaging and host cell integration (Hauswirth *et al.* 2000). Wild-type adeno-associated viruses exist in a latent form, either integrated within the host genome (in the q-arm of chromosome 19 in humans), or in an extra-chromosomal state (Dutheil *et al.* 2000). For adeno-associated viral replication the infected cell must be co-infected with a helper virus e.g. adenovirus or herpes simplex virus.

Recombinant adeno-associated viruses can be produced by replacing all of the viral encoding genes and leaving just the inverted terminal repeat sequences. Nevertheless, the amount of foreign DNA that can be inserted is relatively small (up to 5kb). This can be increased by splitting the transgene between two adeno-associated viruses and co-infecting cells, but the packaging capacity still remains limited (Yan *et al.* 2000). Another disadvantage of recombinant adeno-associated viruses is that they are difficult to produce in large quantity, because they require special packaging cell lines that encode the parvoviral and adenoviral genes needed for replication (Liu *et al.* 1999).

However, there are a number of advantages of adeno-associated virus, especially if stable gene expression is required. Adeno-associated virus is non-pathogenic in the wild-type form and no associated disease has been described. More significantly, adeno-associated virus does not induce a strong inflammatory response in the host, unlike adenovirus. This lack of immune response extends to the foreign transgene. A recombinant adeno-associated virus expressing an *E.coli*-derived β-galactosidase expressed for prolonged periods of time without a cell-mediated immune response in immune competent mice (Fisher *et al.* 1997). In contrast, the same transgene in an adenoviral vector induced strong CTL responses to transgene peptides, which eliminated β-galactosidase expressing cells previously transduced by adeno-associated virus (Jooss *et al.* 1998). Thirty percent of adults have neutralising antibodies to adeno-associated virus, compared to 60% against adenovirus (Chirmule *et al.* 1999). Although the

relative lack of humoral immunity against adeno-associated virus is a major benefit, as this allows the virus to avoid neutralising antibodies, and so remain available for infecting the target cells, a CTL response against a selectively transduced cell is of potential benefit in cancer treatment. Indeed, immunostimulatory genes have been transduced into cancer cells in an attempt to generate a specific anti-cancer immune response (Descamps *et al.* 1996).

1.1.5.1.3 Onco-retroviruses

Retroviruses have a genome of two identical single stranded RNA molecules and convert their genome into DNA using reverse transcriptase. There are seven groups of retrovirus. Five groups have oncogenic potential, are therefore called onco-retroviruses, and include the Moloney murine leukaemia virus, Rous sarcoma virus, and bovine leukaemia virus-human T cell leukaemia virus. The other two groups are the lentiviruses (e.g. human immunodeficiency virus (HIV)) and spumaviruses (e.g. foamy virus). Retroviruses have a relatively complicated life cycle, because of the need to convert their RNA genome into DNA. The virus binds to cell receptors, is internalised, and the RNA is reverse transcribed to DNA. The DNA is then transferred to the nucleus. Here the DNA integrates into the host genome and DNA is converted into RNA, for both the new RNA viral genomes and for protein production from mRNA. The RNA is transferred to the cytoplasm where proteins are produced, and RNA with the correct sequences (the packaging signal Ψ adjacent to a long terminal repeat (LTR)) is packaged into virions. The retroviral genome has three coding domains: gag, which encodes the matrix, capsid and nucleoproteins; pol, which encodes the enzymes necessary for integrating the RNA into the host genome; and env, which encodes the envelope glycoprotein. The cell tropism can be changed by modifying the envelope glycoprotein, e.g. to the G protein of vesicular stomatitis virus, which allows infectivity of a broad range of cells.

Most early onco-retroviral vectors were based on the Moloney murine leukaemia virus and were the first viral vectors to be used in clinical trials. Many early trials focused on introducing a therapeutic gene into individuals with a single gene mutation, e.g. X-linked severe combined immunodeficiency (SCID), and the aim was therefore for stable gene expression over a long time period, which is unnecessary for anti-cancer strategies that aim to kill transduced cells. One study has aimed to correct the genetic deficiency in children with SCID (Cavazzana-Calvo

et al. 2000), however, three of the eleven children treated have subsequently developed leukaemia. This is thought to be because the retrovirus integrated into a specific oncogene (LMO2), activating its expression, which seems to be a preferential integration site (Hacein-Bey-Abina *et al.* 2003). Interestingly, no cases of leukaemia have yet been observed in a parallel clinical trial of SCID gene therapy, which uses a gibbon-ape-leukaemia-virus pseudotyped gammaretroviral vector (Gaspar *et al.* 2004).

Another disadvantage of onco-retroviruses is that they require breakdown of the nuclear envelope during mitosis for their DNA to be transferred to the host cell nucleus. They can therefore only infect replicating cells. Even in an aggressive tumour, only a proportion of cells will be in mitosis at any time, and so this will limit their effectiveness in cancer therapy.

One possible advantage of retroviral vectors is that they produce a limited immune response compared to adenovirus. However, retroviral vectors can be neutralised *in vivo* by antibodies to mouse antigens, derived from the mouse producer cells, in which the viruses are produced. Human packaging cells have therefore been developed, but antibodies are still induced against the viral envelope proteins, which can limit infectivity.

1.1.5.1.4 Lentiviruses

Lentiviruses, e.g. HIV and equine infective anaemia virus (EIAV), are retroviruses and have an RNA genome. They preferentially infect replicating cells, but are able to cross an intact nuclear membrane to integrate within a non-dividing cell, due to the pre-initiation complex (PIC) that allows their cDNA to be actively transported through nuclear pores (Dvorin and Malim 2003). They can therefore infect and stably transduce non-dividing and terminally differentiated cells, such as neurons, which has led to their development in treatments for conditions such as Parkinson's disease and motor neuron disease (Blomer *et al.* 1997). Lentiviruses are currently difficult to produce to high titres. In addition, as reverse transcriptase has no proof-reading ability, this results in a high rate of transgene mutation, which if it resulted in inactivation of the anti-cancer transgene, would cause selection of the mutant tumour clone.

1.1.5.1.5 Herpes simplex virus

The herpes simplex virus is a large, complex virus, in contrast to the other common viral vectors. It has a double-stranded DNA genome of 152 kb and is able to persist as a latent infection within neurons. The neuron-specific latency-activated promoter to control transgene expression can be used for prolonged transgene expression (Palmer *et al.* 2000). Because of its large genome it is able to accept large transgenes, e.g. 30 kb. It is able to infect non-dividing cells and has a natural tropism for neuronal cells. All of these factors make it an attractive vector for neural diseases and gliomas. Replication-incompetent mutants can be produced by deleting most of the early genes, which prevents the virus lysing the infected cell, but reduces the expression of the transgene (Samaniego *et al.* 1998). Infection of cells involves numerous viral proteins, and so targeting treatment to specific cell types is difficult. However, a selectively replication-competent herpes simplex virus has been created which replicates in and lyses dividing cells (Yoon *et al.* 1998).

For ovarian cancer therapy adenovirus is the preferred viral vector (for summary see Table 1-3). This is because only short-term gene expression is required, as the aim is to rapidly kill infected cells, adenovirus is relatively easy to produce, it is easy to genetically engineer for introduction of therapeutic transgenes and has low pathogenicity.

Table 1-3 Pros and cons of viral vectors for cancer gene therapy

	Advantages	Disadvantages
Adenovirus	Low pathogenicity	Immune response
	Easy to produce to high titres	Infect wide range of cell types
	Easy to manipulate genetically	
	Direct oncolytic effect	
	Infect wide range of cell types	
	Large transgene capacity	
	Able to infect non-replicating cells	
	Low rate of mutation	
Adeno-associated virus	Non-pathogenic	Small transgene capacity
	Low inflammatory response	Need helper virus for productive infection
	Able to infect non-replicating cells	Difficult to produce to high titre
Onco-retroviruses	Limited inflammatory response to virus	Only infect replicating cells
		Oncogenic potential
		Immune response to packaging cell components
		Difficult to produce to high titre
Lentiviruses	Can infect non-replicating cells	Difficult to produce to high titre
	Limited inflammatory response to virus	High rate of transgene mutation
		Immune response to packaging cell components
Herpes simplex virus	Able to infect non-replicating cells	Infect wide range of cell types
	Oncolytic replication cycle	
	Very large transgene capacity	
	Infect wide range of cell types	

1.1.6 Adenovirus gene therapy strategies in ovarian cancer

To date most gene therapy for ovarian cancer has employed modified adenoviruses to deliver therapeutic DNA and there are several strategies through which DNA may mediate a therapeutic effect.

1.1.6.1 Tumour suppressor gene replacement therapy

The tumour suppressor gene p53 is commonly mutated or deleted in cancers. It has a central role in regulating the G1-S phase check-point and determines whether the cell is able to replicate, differentiate or die; mutations in p53 are associated with chemotherapeutic resistance in ovarian cancer (Buttitta *et al.* 1997). Replacement of wild-type p53 had anti-tumour activity *in vitro* and in nude mice models (Fujiwara *et al.* 1994). Adenovirus p53 replacement was relatively well tolerated in phase I clinical trials. However, promising preclinical results were not replicated in intraperitoneal clinical trials (Zeimet and Marth 2003), partly because many ovarian cancers down-regulate expression of the Coxsackie-adenovirus receptor (CAR), the major adenovirus type 5 cellular receptor (Bergelson *et al.* 1997; Khuu *et al.* 1999; Zeimet *et al.* 2002), and partly because most patients have neutralising antibodies to adenovirus (Stallwood *et al.* 2000). The multicentre phase III p53-replacement study of Schering Plough was halted ostensibly because of formation of adhesions, but also due to inefficient tumour infection and phagocytic scavenging (Stephen Chang and Jo-Ann Horowitz, personal communication). Unfortunately, the results of this trial have never been published.

1.1.6.2 Virus directed enzyme-prodrug therapy (VDEPT)

One potential strategy to improve tumour killing, without infecting every target cell, is to modify the virus so that it produces an enzyme within cancer cells. This enzyme then converts an inactive prodrug into a chemotherapeutic agent within the cancer cell: this strategy is termed virus directed enzyme-prodrug therapy (VDEPT). One advantage of this approach is the bystander effect; the chemotherapeutic agent is able to kill neighbouring non-infected cells; this is dependent on the activated prodrug being able to pass from cell to cell. In some cases satisfactory tumour cell killing can be achieved when only 10% of cells express the suicide enzyme (Djeha *et al.* 2000). Several enzyme/prodrug combinations have been developed, for

example: the herpes simplex virus enzyme, thymidine kinase, is able to convert gancyclovir into a toxic metabolite that inhibits DNA production, so killing replicating cells (Alvarez *et al.* 2000) (see Table 1-4).

1.1.6.3 Oncolytic adenovirus therapy

Another mechanism for viruses to kill cells is by a lytic infection cycle; the virus infects the cell, replicates and then lyses the cell in order to release the new virions. The virus induces the cell into S phase to enhance viral gene expression and replication, which is why many viruses have oncogenic potential. Adenovirus achieves this by inactivating p53 and the Rb gene product (pRb) with the E1B (55K gene product) and E1A gene products respectively. ONYX-015 is a modified adenovirus with an E1B deletion. This was intended to restrict virus replication to cells without wild-type p53, thus limiting virotherapy to cancer cells. ONYX-015 was well tolerated in phase I clinical trials (Vasey *et al.* 2002). However, it is now believed that the E1B-55K gene product is required for late viral RNA nuclear export, as some tumour cells which lack p53 mutations are still able to support ONYX-015 replication (O'Shea *et al.* 2004). These data also suggest that tumours have an alternative RNA export mechanism that is absent or inhibited in non-tumour cells.

Table 1-4 Enzyme-prodrug combinations for VDEPT strategies

Enzyme	*Origin of transgene*	*Prodrug*	*Activated product*	*References*
Carboxyl esterase	Rabbit (liver)	Irinotecan (CPT-11)	SN 38	(Wierdl *et al.* 2001)
Carboxypeptidase A	Human (pancreatic)	Methotrexate-alpha-phenylalanine (MTX-Phe) Methotrexate-alpha-(1-naphthyl)alanine (MTX-naphthylAla)	Methotrexate	(Hamstra and Rehemtulla 1999)
Carboxypeptidase G2 (CPG2)	Bacterial *E.coli*	para-N-bis (2-chloroethyl) aminobenzoylglutamic acid 4-[(2-chloroethyl)(2-mesyloxyethyl)amino]benzoyl-L-glutamic acid (CMDA)	benzoic acid mustard N,N-(2-chloroethyl)(2-mesyloxyethyl)aminobenzoic acid (CMBA)	(Stribbling *et al.* 2000)
Cytochrome P450	Rabbit, rat (liver)	Cyclophosphamide 4-ipomeanol (4-IM) 2-aminoanthracene (2-AA) Acetaminophen	Toxic metabolites (Alkylating agents) N-acetly-benzoquinone-imine	(Mohr *et al.* 2000) (Chen *et al.* 1997)
Cytosine deaminase	Bacterial *E. coli*, yeast	5-Fluorocytosine	5-Fluorouracil	(Block *et al.* 2000)
D-amino-acid oxidase	Yeast	D-Alanine	Hydrogen peroxide	(Stegman *et al.* 1998)
Deoxycytidine kinase	Human	Cytosine arabinoside (Ara-C)	Cytosine arabinoside monophosphate	(Manome *et al.* 1996)
DT-diaphorase	Human, rat	Indoloquinone 3-hydroxy-5-aziridinyl-1-methyl-(1H-indole-4,7-dione)-propenol (E09)	Reduced forms	(Misra *et al.* 2002)
Nitroreductase	Bacterial *E. coli*	5-(aziridin-1-yl)-2,4-dinitrobenzamide (CB1954)	5-(aziridin-1-yl)- 4-N-acetoxy-2-nitrobenzamide	(McNeish *et al.* 1998)
purine nucleoside phosphorylase (PNP)	Bacterial *E.coli*	9-(2-deoxy-beta-D-ribofuranosyl)-6-methylpurine (MeP-dR) 9-beta-D-arabinofuranosyl-2-fluoroadenine (F-araA)	methyl purine (MeP) 2-fluoroadenine (F-Ade)	(Parker *et al.* 1997)
Thymidine kinase	Viral HSV, VZV	Gancyclovir Acyclovir	Monophosphate nucleotide analogues	(Huber *et al.* 1991) (Moolten and Wells 1990)
Thymidine phosphorylase	Human leucocytes	5'-deoxy-5-fluorouridine (5'DFUR)	5-Fluorouracil	(Denning and Pitts 1997)
β-Galactosidase	Bacterial *E. coli*	Anthracycline prodrugs	Anthracyclines	(Farquhar *et al.* 2002)
β-Glucuronidase	Human	glucuronide prodrug HMR 1826	Doxocycline	(Weyel *et al.* 2000)
β-Lactamase	Bacterial *Enterobacter cloacae*	7-(4-carboxybutanamido)cephalosporin mustard (CCM)	cephalosporin nitrogen mustard	(Vrudhula *et al.* 1993) (Kerr *et al.* 1998)

1.1.7 Adenovirus infection mechanisms

Adenovirus gene therapy can be used for a variety of virus and gene therapy strategies. However, promising preclinical results have not been replicated in intraperitoneal clinical trials (see section 1.1.6.1). For adenovirus gene therapy to be effective in clinical practice it is necessary to improve tumour transduction, resist antibody neutralisation and ideally to decrease transduction or uptake by non-tumour cells. Inability to effectively deliver gene therapy is the critical limiting factor to the success of cancer gene therapy in patients with ovarian cancer. Understanding normal adenovirus infection is important to discovering how this can be manipulated for therapeutic effect.

1.1.7.1 Adenovirus cell entry

Adenoviruses can be classified into 6 subgroups or species (A-F). Adenovirus serotypes 2 and 5 belong to group C and are the most commonly used serotypes in gene therapy. The initial step of cell infection is mediated by the attachment of the terminal knob domain of the adenovirus fibre protein to the cellular Coxsackie adenovirus receptor (CAR) (Bergelson *et al.* 1997). This is a trans-membrane protein, although studies have shown that the intracellular and transmembrane sections are not required for virus internalisation (Wang and Bergelson 1999), and it therefore functions primarily as a high affinity anchor. Subsequent to virus attachment to the cell surface, the arginine-glycine-aspartate (RGD) sequence of the penton base binds to cellular co-receptors, the $\alpha_v\beta_{3/5}$ integrin receptors (Wickham *et al.* 1993). Binding to $\alpha_v\beta_{3/5}$ integrin induces a conformational change in the integrin receptor, which stimulates a down-stream signalling cascade involving several tyrosine kinases. This triggers clathrin-mediated endocytosis, as demonstrated by electron microscopy studies and inhibition of adenovirus uptake in cells expressing the dominant negative clathrin hub eps15 (Meier *et al.* 2002). Clathrin-mediated endocytosis involves the internalisation of receptors and their bound ligands via coated pits on the plasma membrane. They are formed by cytosolic coat proteins, including clathrin, which assemble at the inner leaf of the plasma membrane and distort the surface into pits. These pits then invaginate and are pinched off by the action of another protein, dynamin, to form clathrin-coated vesicles, which then fuse with early endosomes. Adenovirus is also able to infect cells by triggering macropinocytosis, which is stimulated following α_v integrin binding

during clathrin-mediated endocytosis. Macropinocytosis is a major endocytosis mechanism of epithelial cells and is stimulated by binding of ligands to receptors, such as EGFR. Ligand binding initiates formation of large endosomes by fusion of pseudopodia at ruffled membranes. Macropinocytosis removes large membrane domains in order to down-regulate receptors, is also involved in cell migration and can be hijacked by Salmonella to mediate infection. Following adenovirus infection, unlike EGF-triggered endocytosis, adenovirus-containing endosomes are disrupted rapidly after internalisation, releasing the endosomal contents into the cytosol.

Following cell binding of adenovirus, the penton fibres are released at the cell surface (Martin-Fernandez *et al.* 2004). However this process is not required for endocytosis and, together with data regarding CAR intracellular domains, suggests that CAR and adenovirus fibres mediate cell attachment and are not otherwise involved in the virus internalisation process. In addition, fibre release is not required for adenovirus endosomal escape, since blocking protein kinase C (PKC), a down-stream signalling target of EGFR and α_v integrins, does inhibit endosomal escape, even following fibre release (Nakano *et al.* 2000). Two independent studies have demonstrated that CAR is expressed at low levels in primary ovarian cancers (Khuu *et al.* 1999; Zeimet *et al.* 2002). CAR expression is reduced in more advanced stage disease, and in addition, α_v integrins are down-regulated in primary ovarian tumours (Zeimet *et al.* 2002), probably explaining why primary ovarian tumours and cell lines are relatively difficult to transduce with adenovirus.

1.1.7.2 Endosomal escape

Of the virus that binds to the cell surface 80% is internalised and 40% of the virus that binds to the cell releases its DNA into the nucleus (Greber *et al.* 1993). Very little virus, around 5% of that which enters the cell, is routed to the lysosomal compartment for destruction, suggesting that the endosomal escape mechanism is highly efficient. This study also demonstrated that the fibre proteins and the pentonal bases were shed in a two stage process. Following endocytosis the internal capsid protein VI is degraded and protein VIII dissociates from the remaining virion. More recent data suggest that protein VI, which is located beneath the peri-pentonal hexons, is

involved in endosomal escape (Wiethoff *et al.* 2005). Following internalisation, the endosome is acidified by activation of proton pumps and an acid-induced conformational change in the capsid occurs; peri-pentonal hexons, pentonal base, protein IIIa and protein VI dissociate from the capsid (Greber *et al.* 1993). Heat dissociated capsids were able to disrupt liposomes, but not if protein VI had been depleted by immunoprecipitation (Wiethoff *et al.* 2005). Modelling of protein VI found it to contain a highly conserved sequence that forms an amphipathic α-helix; recombinant truncated forms of protein VI, which contained this sequence, were able to disrupt liposomes independent of pH. Recombinant forms of protein VI with deletions in the α-helix were unable to disrupt liposomes. The proposed model suggested that protein VI, released by a partial disruption of the adenovirus capsid in an acidic environment, may associate with and disrupt the endosomal membrane in a manner similar to influenza haemaglutinin, rather than form a pore structure like the complement membrane attack complex.

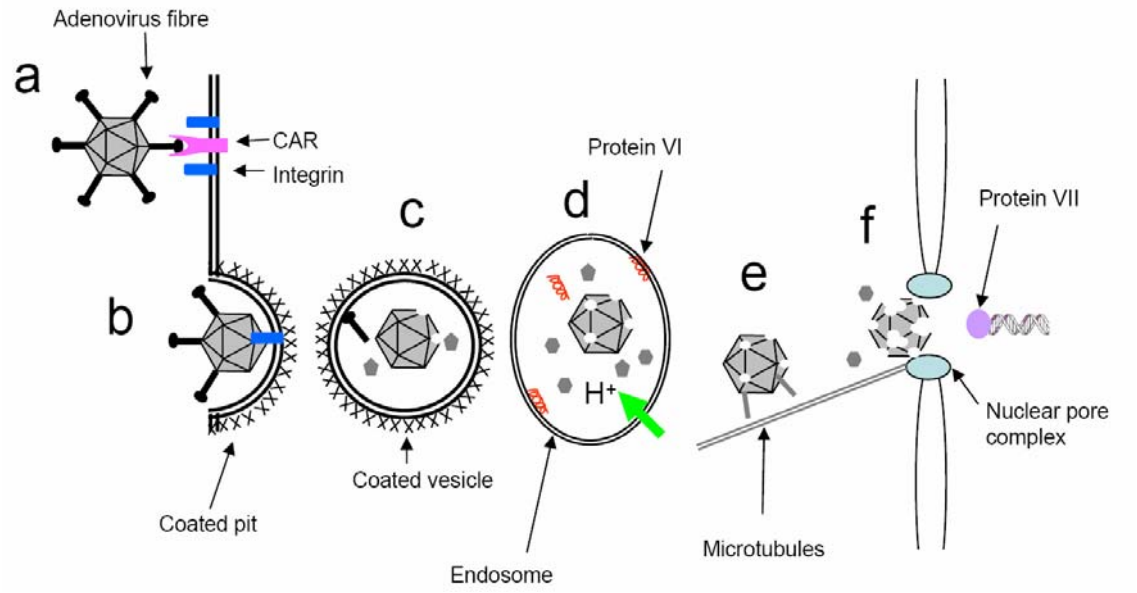


Figure 1-1 Mechanism of normal adenovirus infection

(a) Ad5 binds to the Coxsackie adenovirus receptor at the cell surface via the terminal knob of the fibre protein. The secondary receptors, $\alpha_v\beta_{3/5}$ integrins, bind to the penton base and mediate internalisation, stimulating formation of a clathrin coated pit (b). At this stage the penton fibre proteins are lost from the capsid. The clathrin coated pit becomes an early endosome, which is acidified by proton pumps (c). At this stage peri-pentonal hexon proteins are lost from the capsid and protein VI dissociates from the capsid mediating endosomal escape (d). Adenovirus attaches to microtubules (e) and is transported to the microtubule organising centre, where it then binds to the nuclear pore complex and capsid disassembly, with release of the viral genome and associated protein VII occurs (f). Adapted from (Greber *et al.* 1997; Greber *et al.* 1993; Wiethoff *et al.* 2005)

1.1.7.3 Nuclear trafficking and entry

Microtubules are cytoskeletal proteins that are involved with separating chromosomes during mitosis and organisation of the cytoplasm. Agents such as paclitaxel produce their anti-mitotic effect by disrupting microtubule organisation. Microtubules are organised with one end near the cell periphery and another at the microtubule organising centre (MTOC), which is located next to the nucleus. Experiments with fluorescence-labelled adenovirus and microtubule-disrupting agents have demonstrated that adenovirus can attach to microtubules and traffic to the nucleus, once released from the endosome (Giannakakou *et al.* 2002; Suomalainen *et al.* 1999). In enucleated cells adenovirus becomes concentrated at the MTOC, suggesting that a nuclear factor is necessary for detachment from the MTOC (Bailey *et al.* 2003).

The nuclear membrane is a double-layered membrane which has openings, or pores, controlled by macromolecules, which form the nuclear pore complex (NPC), linking the inner and outer membranes. Adenovirus capsids attach to the NPC and this attachment is required for final capsid disassembly and release of DNA (Greber *et al.* 1997); blocking attachment with a NPC-binding antibody prevented capsid disassembly and nuclear import of viral DNA. Depletion of NPC calcium did not prevent attachment of adenovirus to the NPC and capsid disassembly, but did prevent nuclear uptake, suggesting this was an active process. Subsequently it was shown that antibodies against CAN/Nup214, a fibrillar element of the NPC, inhibited adenovirus-NPC binding (Trotman *et al.* 2001). It was also demonstrated that the nuclear protein histone H1 bound to the virus capsid once it had attached to the NPC; capsid disassembly and nuclear uptake of viral DNA could be prevented by microinjection of anti-histone H1 antibodies to the nucleus. Histone H1 bound to residues on hexon proteins.

1.1.7.4 Retargeting adenovirus infection via EGFR

In designing a retargeting strategy, it would appear rational to retarget to a tumour up-regulated or specific receptor that internalises into an endosome. This would increase tumour specificity of treatment and subject adenovirus to acidification once internalised, hopefully allowing sufficient capsid disruption for protein VI dissociation and endosomal escape. More than 60%

of ovarian cancers over-express the epidermal growth factor receptor (EGFR or ErbB1), which is associated with the malignant phenotype (Alper *et al.* 2001). EGFR biology has been extensively studied and represents the classic example of receptor-mediated endocytosis.

The EGFR is a heavily glycosylated transmembrane protein that has four extracellular domains (L1, L2, CR1 and CR2), a transmembrane domain, and a cytoplasmic kinase domain and carboxyl-terminal domain, containing tyrosine residues, which are phosphorylated and mediate signal transduction. On binding of ligand, either epidermal growth factor (EGF) or transforming growth factor-α (TGF-α), EGFR dimerisation and tyrosine kinase activity is stimulated (Brown *et al.* 1994). In the absence of ligand, receptors can still dimerise, but tyrosine kinase activity is suppressed (Zhu *et al.* 2003); deletions within the extracellular domain can cause constitutive activation of the receptor, suggesting that the extracellular domains repress kinase activity in the absence of receptor binding (Huang *et al.* 1997). EGF and TGF-α bind to EGFR via both ligand-binding domains, L1 and L2, as shown by x-ray crystallography (Garrett *et al.* 2003; Ogiso *et al.* 2002). Ligand-binding stabilises the EGFR in an extended form, exposing residues in CR1 and CR2 that are involved in dimerisation (see Figure 1-2). The x-ray crystal structure of the anti-EGFR antibody, Cetuximab, suggest that it binds to one of the ligand-binding regions, sterically inhibiting EGF binding, preventing activation of tyrosine kinase activity and EGFR extension; residues required for dimerisation remain concealed as EGFR is stuck in a tethered position (Li *et al.* 2005).

The EGFR internalises via clathrin-coated pits, which fuse with early endosomes. Tyrosine phosphorylation is not required for EGFR internalisation, although the rate of internalisation is accelerated following ligand-binding, leading to receptor down-regulation. Receptor-mediated endocytosis involves a similar pathway to that of adenovirus internalisation; dynamin, Rab5 and phosphatidylinositol 3-kinase (PIK3) are required at an early stage in both events.

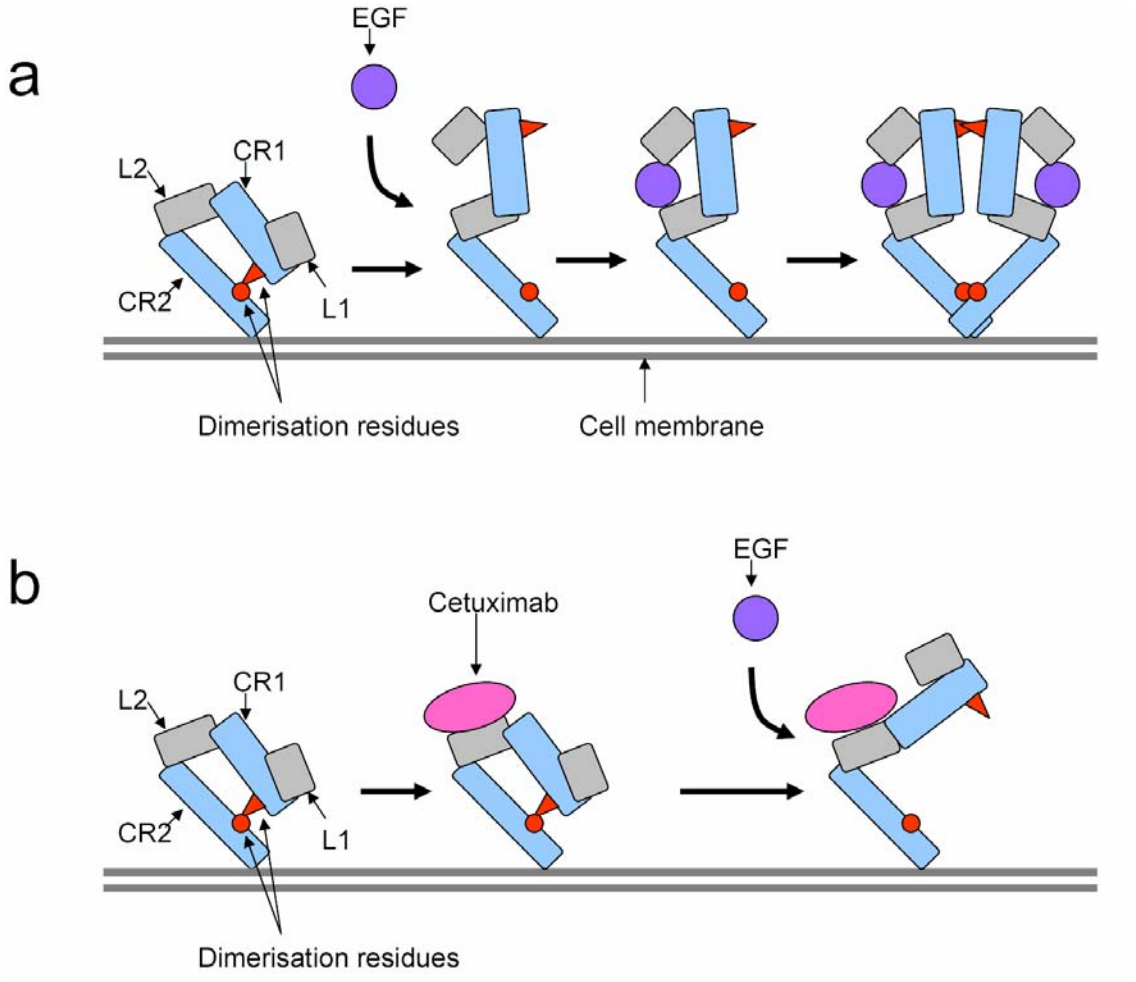


Figure 1-2 Schematic of EGF-EGFR binding and action of Cetuximab

(a) EGFR exists in both a tethered and extended form. In its tethered form the dimerisation residues (red) are shielded. In the extended form EGF (purple) binds to sites on L1 and L2 (grey) and stabilises the extended form, revealing the dimerisation residues and aiding dimerisation. (b) Cetuximab (pink) binds to a site on L2, preventing EGF binding and extension of EGFR, so that tyrosine kinase activity and dimerisation are inhibited. Adapted from (Li *et al.* 2005).

Following ligand-binding, tyrosine kinase activity is stimulated, leading to phosphorylation of tyrosine residues on EGFR itself (auto-phosphorylation) and other proteins (trans-phosphorylation); the phosphorylated tyrosine residues on EGFR act as docking sites for several proteins and enzymes (see Figure 1-3). This triggers down-stream signalling cascades and both positive and negative feedback loops (for full details of EGFR pathway map see (Oda *et al.* 2005)). EGFR signal transduction has been extensively investigated and is one of the best understood signalling systems. Down-stream signalling has been mapped using computer modelling systems in an attempt to unravel the interactions of the many pathways that are triggered following EGFR activation (Oda *et al.* 2005). A standardised notation system has also been devised to clarify diagrammatic depictions of such complex systems (Kohn *et al.* 2006). Stimulated signal transduction pathways include Src homology 2 domain containing transforming protein (Shc), which activates c-Src, an intracellular kinase, which leads on to stimulation of cell growth, via activation of c-Myc, and inhibition of apoptosis via CL-2-antagonist of cell death inhibition. Endocytosis and routing of EGF-bound EGFR to the lysosome for degradation is mediated by activation (via phosphorylation of tyrosine residues) of Casitas B-lineage lymphoma proto-oncogene (Cbl). Cbl has ubiquitin ligase activity and tags EGFR with ubiquitin at several sites. Cbl also interacts with CIN85 and Endophilin, a regulatory component of clathrin-coated pits, to form a complex, which accelerates endocytosis of ligand-bound EGFR, via the ubiquitin-binding protein Eps15 (for a review see (Bache *et al.* 2004)). This ubiquitination is required for EGFR down-regulation following receptor binding and internalisation into endosomes (see below). Fusion of the clathrin-coated vesicle with the early endosome requires the activity of the small GTPase, Rab5 (Chen and Wang 2001), which when activated recruits effector molecules, including Radaptin-5 and the phosphoinositide-binding coiled-coil protein, EEA1, to mediate membrane fusion of vesicle and endosome (reviewed in (Zerial and McBride 2001)).

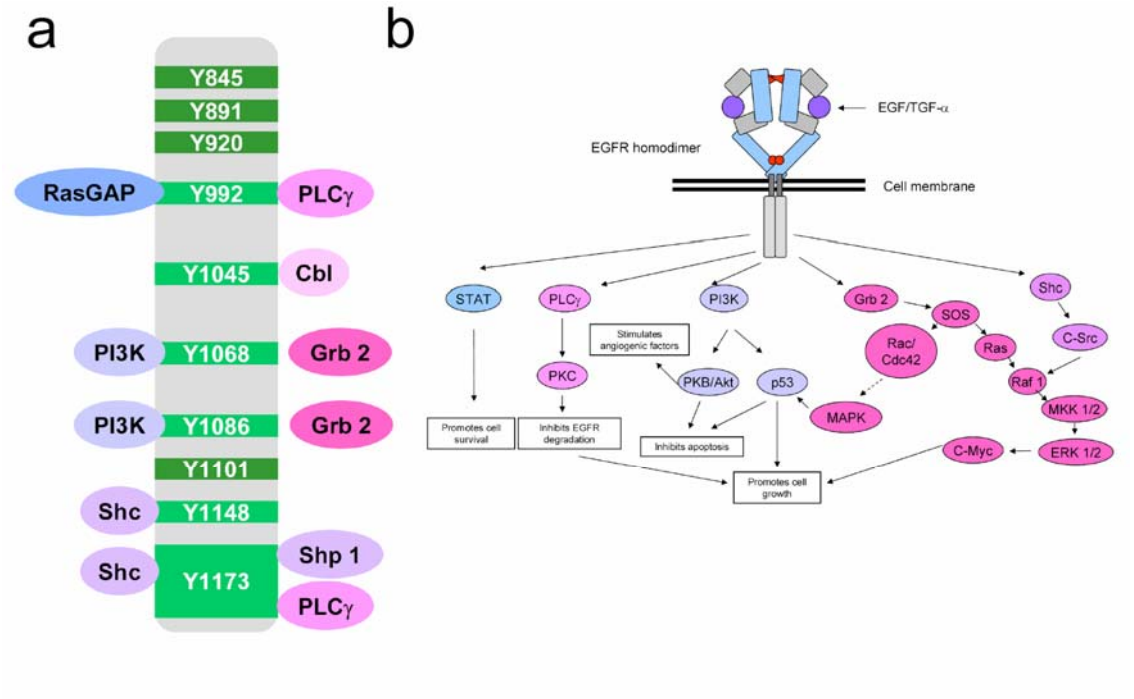


Figure 1-3 EGFR auto-phosphorylation and down-stream signalling

Following ligand binding, EGFR dimerise and tyrosine kinase activity is stimulated, leading to phosphorylation of tyrosine residues of the intracellular domain of EGFR (a). These residues, (shown in green) act as docking sites for proteins, which are activated by EGFR kinase activity and this triggers signal transduction pathways, a simplified version of which is demonstrated in (b). Atk, v-akt murine thymoma viral oncogene homolog; Cbl, Casitas B-lineage lymphoma proto-oncogene; C-Myc, v-myc myelocytomatosis viral oncogene homolog; C-Src, v-src sarcoma viral oncogene homolog; ERK 1/2, extracellular signal-regulated kinase; Grb 2, growth factor receptor-bound protein; MAPK, mitogen-activated protein kinase; MKK 1/2, MAPK kinase 1 and 2; p53, p53 gene product; PI3K, phosphotidylinositol-3-kinase; PKB, protein kinase B ; PKC, protein kinase C; PLCγ, phospholipase C gamma; Rac/cdc42, cell division cycle 42, ; Raf 1, v-raf-1 murine leukaemia viral oncogene homolog ; Ras, rat sarcoma viral oncogene homolog; RasGAP, Ras GTPase-activating protein; Shc, Src homology 2 domain containing transforming protein; Shp 1, Shp-2 tyrosine phosphatase; SOS, son of sevenless homolog; STAT, signal transducer and activator of transcription. Adapted from (Oda *et al.* 2005)

TGF-α and EGF only share 35% sequence homology (see appendix 9.1 and 9.2). However, analysis of their cysteine residues, disulphide binding and structure suggest that they have similar three-dimensional structure; human TGF-α and EGF and murine EGF all have two small anti-parallel β-sheets (Montelione *et al.* 1989). Purified recombinant human TGF-α, human and murine EGF have similar binding affinities (Lax *et al.* 1988; Massague 1983) although other data suggest that human TGF-α may have a 55% lower binding affinity for EGFR than human EGF (Winkler *et al.* 1986). This was unexpected, since TGF-α has greater potency and prolonged activity *in vitro* and *in vivo* than EGF in several different assay systems. In addition, a

monoclonal antibody was developed that would selectively inhibit TGF-α but not EGF binding, suggesting that, despite TGF-α and EGF competitively inhibiting EGFR-binding, they may not bind to the same receptor epitope (Winkler *et al.* 1989). Generation of recombinant chimeras of TGF-α and EGF demonstrated that the linear C-terminal regions of the ligands bound to different epitopes of EGFR (Lenferink *et al.* 1998). However, as binding affinities are similar, these data do not explain the differential effect of TGF-α and EGF *in vitro* and *in vivo*.

Analysis of events following receptor binding demonstrated that TGF-α and EGF have different fates, which exert an effect on the fate of the receptor to which they have bound (Ebner and Derynck 1991). TGF-α dissociated from EGFR at a much higher pH and this resulted in re-cycling to the cell surface of both the ligand and the receptor. In contrast, EGF had much greater affinity for EGFR at lower pH and remained bound to the receptor. Thus, the fate of internalised EGFR depends on whether it binds to a ligand and to which ligand it is bound; this has been demonstrated by several groups (Maeda *et al.* 2002). Unoccupied receptors largely re-cycle back to the cell membrane. However, those bound to EGF are preferentially routed to the lysosome for degradation (Carter and Sorkin 1998; Herbst *et al.* 1994). Hence, autocrine activation of cells by TGF-α is a potent growth stimulant, since both receptor and ligand are rapidly released back to the cell surface and are then available for re-stimulation (Martinez-Arca *et al.* 2005), whereas binding of EGF to EGFR results in receptor down-regulation. It is not clear whether these observations will have any impact on adenovirus retargeting, as normally the adenovirus is able to escape the endosomal compartment soon after internalisation and so may not be influenced by which ligand it is retargeted with.

1.1.7.4.1 Retargeting adenovirus with bispecific biological adapters

As the internalisation pathways of EGFR and adenovirus share many components and, in addition, EGFR is frequently up-regulated in cancer, it would seem to be an excellent candidate receptor for retargeting adenovirus infection.

EGF conjugated with poly-L-lysine has been used to increase uptake of DNA (Cristiano and Roth 1996; Deshpande *et al.* 1996) into EGFR positive cell lines, demonstrating that EGF-

conjugates can be internalised along with the EGFR. EGFR retargeting of DNA has similarly been achieved via other members of the EGFR family; peptides that bind to HER2/3 and HER2/4 heterodimers were complexed with penton base proteins, which interact with integrins, and conjugated to poly-L-lysine. Addition of penton base proteins increased the efficacy of DNA uptake (Medina-Kauwe *et al.* 2001).

Adenovirus has been retargeted to EGFR positive cells using adapter molecules. Efficient retargeting of adenovirus to squamous cell carcinoma cells was achieved by addition of a bispecific antibody; one arm of the antibody which bound to EGFR and the other which bound to the adenovirus fibre knob domain (Blackwell *et al.* 1999). They demonstrated that neither monoclonal antibodies to the fibre knob domain nor the EGFR alone were able to successfully retarget adenovirus infection to EGFR-positive cells. However, when adenovirus was pre-incubated with a bispecific anti-fibre-EGFR antibody, levels of transgene expression were 6-fold higher than unmodified adenovirus in a range of EGFR-positive cancer cell lines. Transgene expression could be inhibited by pre-incubating cells with the anti-EGFR antibody, but not by pre-incubation with free adenovirus fibre knob protein, unlike unmodified adenovirus. The same group went on to use their bispecific anti-fibre-EGFR antibody to retarget genetically-modified replication-competent adenovirus. This adenovirus had a mutation in the fibre knob to insert the integrin-binding RGD motif, which had previously been shown to retarget adenovirus infection to α_v integrin (Dmitriev *et al.* 1998). The group utilised spheroids, three-dimensional tumour models derived from primary gliomas tumours, to demonstrate the effect of retargeting replication competent adenovirus (Grill *et al.* 2001). The input virus was pre-incubated with the EGFR-fibre bispecific antibody, although progeny adenoviruses produced in the spheroid would not be retargeted. There was a significant increase in penetration of transgene expression throughout the spheroid, compared to RGD-retargeted adenovirus that had not been additionally retargeted with the EGFR-fibre antibody.

Bispecific adapter molecules can also be made from combinations of antibodies and alternative receptor ligands or combinations of receptor ligands and proteins other than antibodies. A fusion protein combining an anti-fibre antibody and human EGF was able to mediate transgene

expression in EGFR-receptor positive cells; transgene expression could be out-competed by incubating with excess free EGF (Watkins *et al.* 1997). Another group demonstrated that a fusion protein consisting of the extracellular portion of CAR and EGF was able to retarget adenovirus transduction when pre-incubated with EGFR-positive cells to levels approximately 10-fold greater than unmodified adenovirus (Dmitriev *et al.* 2000). Using ^{3}H-labelled adenovirus, they were able to demonstrate EGF-mediated binding to EGFR-positive cells in a competitive binding assay.

1.1.7.4.2 Genetic retargeting to EGFR

Bispecific adapter molecules only retarget the adenovirus that is initially delivered, the 'input virus'. Many adenovirus anti-cancer strategies involve replicating adenovirus and any virus produced by replication *in situ* would not be retargeted. Adenovirus can therefore be genetically engineered to produce its own bispecific adapter molecule. Adenovirus was successfully retargeted to EGFR by encoding a secreted CAR-EGF fusion molecule, which was produced by the virus in infected cells (Hemminki *et al.* 2001). The fusion molecule was not secreted by EGFR-positive cells, but it was secreted by EGFR-negative cells, suggesting that binding occurred intracellularly or immediately after release at the cell surface. Secretion of the adapter molecule enabled retargeting of adenovirus to EGFR-positive cells and improved tumour killing if co-delivered with an oncolytic adenovirus, which did not encode the adapter molecule. However, genetic engineering of the adapter molecule into the conditionally replicating oncolytic adenovirus reduced efficiency of replication and cell killing and so compromised the clinical utility of this approach (Hemminki *et al.* 2003). Furthermore, although adapter molecules partially inhibit CAR-mediated uptake, the level of knockdown of infection via conventional pathways is relatively low and does not offer protection from neutralising factors within the blood, such as human red blood cells (Lyons *et al.* 2006), antibodies and complement.

1.1.7.4.3 Polymer coating strategies

Polymers, based on polyethylene glycol (PEG) and poly[N-(2-hydroxypropyl)methacrylamide] (pHPMA) have been used to sterically stabilize liposomal-delivered small molecules to improve pharmacokinetics (Allen 1994). PEGylation of doxorubicin improves the therapeutic ratio in the treatment of ovarian cancer by reducing cardiotoxicity (D'Agostino *et al.* 2003; Working *et al.*

1999). PEG has also been conjugated to anti-EGFR antibodies for radioimmunoscintigraphy (Wen *et al.* 2001).

PEG was coupled to adenovirus by coating with a polycationic lipid GL-67 and adding dioleoylphosphatidylethanolamine-PEG (DOPE-PEG) (Chillon *et al.* 1998). GL-67/DOPE-PEG was able to partially shield adenovirus from binding of neutralising antibodies *in vitro*, but did not significantly reduce neutralisation *in vivo*. PEGylation of the adenovirus capsid can be also be achieved with reactive PEG polymers, e.g. tresylmonomethoxypolyethylene glycol (TMPEG), that are able to react with lysine residues on capsid proteins (O'Riordan *et al.* 1999). This produced a polymer coat on the virus, which gave partial protection from neutralising antibodies both *in vitro* and *in vivo*. Targeting peptides could then be coupled to PEG to allow retargeting of infection (Romanczuk *et al.* 1999). Recent studies demonstrated that PEGylated adenovirus stimulated reduced inflammatory responses compared to unmodified adenovirus delivered *in vivo* (Croyle *et al.* 2001; De Geest *et al.* 2005; Mok *et al.* 2005).

Co-polymers based on N-(2-hydroxypropyl)methacrylamide (pHPMA) have been used to deliver doxorubicin in clinical trials (Thomson *et al.* 1999). The Seymour group has developed reactive pHPMA co-polymers to covalently coat the surface of the adenovirus capsid, shielding receptor-binding epitopes and providing steric protection from cells and antibodies. Incorporation of targeting ligands, basic fibroblast growth factor (bFGF) and vascular endothelial growth factor (VEGF) on to the polymer-coated virus produced CAR-independent transduction of cells bearing appropriate receptors (Fisher *et al.* 2001). *In vivo* polymer coating adenovirus reduced hepatic gene expression by at least 100-fold, in addition to inhibiting liver toxicity, as demonstrated by serum transaminases (Green *et al.* 2004). Adenovirus is normally rapidly cleared from the circulation by Kupffer cells in the liver. Polymer coating of adenovirus was able to improve plasma circulation time; the virus particle dose detected at 30 min by quantitative polymerase chain reaction (Q-PCR) increased from 5% to 50% of the input virus. Polymer coating is therefore potentially a powerful tool to selectively target and increase bioavailability of adenovirus in cancer therapy.

Murine EGF (EGF), unlike human EGF, has a single non-essential amino-group at the N-terminus. Previous retargeting strategies using pHPMA have coated the virus with polymer, and then modified remaining active groups with the ligand, e.g. bFGF (Fisher *et al.* 2001). A more reproducible method for retargeting pHPMA coated viruses was achieved by synthesizing the reactive co-polymer-ligand conjugate prior to virus coating. This can only be achieved using ligands, such as murine EGF, that contain a unique reactive group. Human EGF has two lysine residues, one within the C-terminus receptor binding site (see appendix 9.2) and is likely to become cross-linked or sterically hindered by the polymer, thereby losing reactivity (Figure 1-4). HPLC analysis of the conjugate shows that >90% of the EGF is conjugated to the polymer following initial purification (Dr S. Briggs, unpublished data).

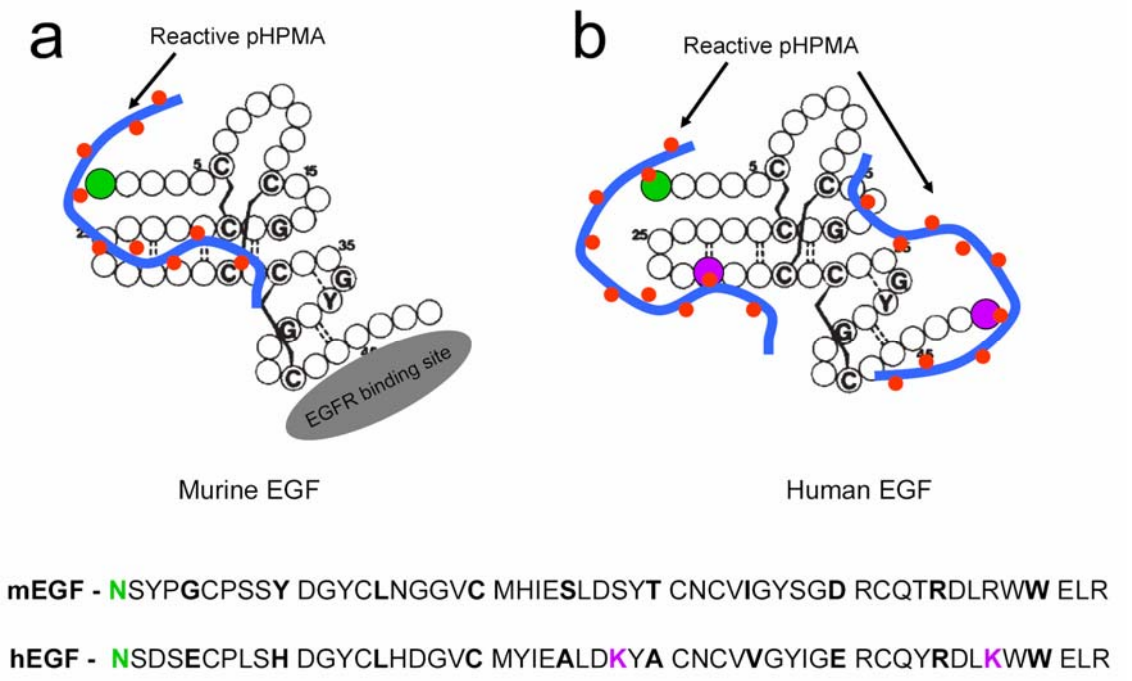


Figure 1-4 Diagrammatic representation of polymer covalent interaction with murine and human EGF

Reactive pHPMA (blue with red reactive side chains) binds by aminolysis to free amino groups, either at the N-terminus (green) or on lysine side chains (purple). In the murine EGF (a), only the N-terminus is available for binding. However, the human EGF (b) has two additional groups available for binding, in the form of lysine residues. Critically, one is found at the C-terminus receptor-binding site, and polymer therefore inhibits human EGF by blocking residues required for EGFR binding.

In summary, previous adenovirus retargeting work suggests that EGFR is an appropriate target for adenovirus infection. Polymer coating with pHPMA successfully detargets normal adenovirus infection and demonstrates reduced toxicity in animal models. Combination of pHPMA coating and EGF retargeting therefore has great potential for a variety of anti-cancer gene therapy strategies and offers excellent flexibility for delivery of different adenovirus payloads.

1.2 Aims and scope of the thesis

1.2.1 Hypotheses

It is already known that polymer coating of adenovirus with reactive HPMA co-polymers can block CAR-mediated uptake and that covalent linkage of ligands to the polymer coating can restore transduction. I hypothesised that conjugation of EGF to pcv would enable EGFR-mediated transduction and provide relatively selective infection of tumour cells, including ovarian cancer cells. This over-arching hypothesis can be considered as several specific hypotheses.

1. Murine EGF, which contains no lysine residues, can be conjugated to reactive HPMA selectively via its N-terminal amino group and retain biological activity.
2. This EGF-pHPMA reactive conjugate can be used to coat adenovirus and inhibit normal pathways of infection.
3. EGF retargeted pHPMA coated adenovirus will enter cells via EGFR binding and mediate virus transgene expression.
4. EGFR-mediated infection pathway can be used to deliver lytic viruses that will replicate within the cell and mediate cancer virotherapy.

1.2.2 Aims of the thesis

To address the above hypotheses, it is necessary to engineer an EGFR-positive, CAR-negative cell line with which to investigate EGF-polymer retargeting in the absence of background, CAR-mediated infection. This, in conjunction with an existing CAR-positive cell line, based on the same parental cell line, will be utilised to determine the effect of EGFR and CAR blockade on

retargeted transgene expression. The effect of EGF-retargeting will then be examined *in vitro* in a range of ovarian cancer cell lines, and *in vivo* using ovarian tumour xenografts in nude mice.

2 Materials and Methods

2.1 General laboratory methods

2.1.1 Cell lines and culture

2.1.1.1 Cell culture techniques

2.1.1.1.1 Cell Passage

Unless otherwise specified, serum-positive growth media was high glucose Dulbecco's modified Eagle's Media (DMEM) containing 2 mmol/l glutamine (PAA Laboratories), supplemented with 1% penicillin-streptomycin solution (10,000 units/ml penicillin and 10 mg/ml streptomycin, (Sigma, UK), 1% sodium pyruvate (GIBCO) and 10% FCS (PAA Laboratories). Cells were maintained at 37°C, 5% CO_2 in a humidity controlled incubator. Cells were handled using sterile techniques in a class II laminar flow cabinet. Cells were passaged twice weekly once they had attained 80-90% confluence in 75 cm^2 flasks (Corning Inc, USA). Serum-positive media was removed and cells were washed with PBS (PAA Laboratories). Trypsin-EDTA solution (3 ml, Sigma) was added to the flask incubated at 37°C, 5% CO_2 for 2-15 min, carefully observing when cells had become detached from the flask. Serum-positive media was added to make up to 10 ml and cells split into a new 75 cm^2 cell culture flask, containing 12 ml of fresh serum-positive growth media. Details of cell lines and their specific normal growth media are shown in Table 2-1.

Table 2-1 Cell culture details of primary and established cell lines

Cell Line	*Description*	*Normal Growth Media*	*Split*	*Reference/ Acknowledgement*
HEK293	Human embryonic kidney cells transformed with the Ad5 E1 region	DMEM 10% FCS 1% penicillin/streptomycin 1% sodium pyruvate 2 mmol/l glutamine	1:10	(Graham *et al.* 1977)
A2780	Human ovarian epithelial carcinoma cells	DMEM 10% FCS 1% penicillin/streptomycin 1% sodium pyruvate 2 mmol/l glutamine	1:5	(Hamilton *et al.* 1984)
A431	Human vulval epidermoid carcinoma	DMEM 10% FCS 1% penicillin/streptomycin 1% sodium pyruvate 2 mmol/l glutamine	1:5	(Giard *et al.* 1973)
A549	Human lung carcinoma cells	DMEM 10% FCS 1% penicillin/streptomycin 1% sodium pyruvate 2 mmol/l glutamine	1:10	European Collection of Animal Cell Cultures (ECACC) (Giard *et al.* 1973)
A9	Murine fibroblasts	DMEM 10% FCS 1% penicillin/streptomycin 1% sodium pyruvate 2 mmol/l glutamine	1:20	Gift from Professor R. Newbold (Mayr and Freimuth 1997)
A9-CAR	Murine fibroblasts transformed with human chromosome 21 (express CAR)	DMEM 10% FCS 1% penicillin/streptomycin 1% sodium pyruvate 2 mmol/l glutamine 800 μg/ml G418	1:10	Gift from Professor R. Newbold
A9-EGFR C10	Murine fibroblasts stably transfected with a human EGFR plasmid	DMEM 10% FCS 1% penicillin/streptomycin 1% sodium pyruvate 2 mmol/l glutamine 800 μg/ml G418	1:10	See Chapter 3
A9-EGFR C22	Murine fibroblasts stably transfected with a human EGFR plasmid	DMEM 10% FCS 1% penicillin/streptomycin 1% sodium pyruvate 2 mmol/l glutamine 800 μg/ml G418	1:10	See Chapter 3

Cell Line	*Description*	*Normal Growth Media*	*Split*	*Reference/ Acknowledgement*
IGROV-1	Human ovarian epithelial carcinoma cells	DMEM 10% FCS 1% penicillin/streptomycin 1% sodium pyruvate 2 mmol/l glutamine	1:5	(Benard *et al.* 1985)
K562	Human monocytic leukaemia	RPMI 1640 10% FCS 2 mmol/l glutamine	1:10	ECACC
OVCAR-3	Human ovarian epithelial carcinoma cells	RPMI 1640 10% FCS 1% penicillin/streptomycin 1 μg/ml bovine insulin 2 mmol/l glutamine	1:5	(Hamilton *et al.* 1983)
SKOV3	Human ovarian epithelial carcinoma cells	DMEM 10% FCS 1% penicillin/streptomycin 1% sodium pyruvate 2 mmol/l glutamine	1:5	(Fogh 1975)
SKOV-luc	SKOV-3-ip cells stably transfected with firefly luciferase	DMEM 20% FCS 1% penicillin/streptomycin 1% sodium pyruvate 2 mmol/l glutamine G418 500 μg/ml	1:3	Gift from Dr Iain McNeish, Cancer Research UK Molecular Oncology Unit, Charterhouse Square LONDON
SW620	Human colorectal carcinoma cell line	DMEM 10% FCS 1% penicillin/streptomycin 1% sodium pyruvate 2 mmol/l glutamine	1:10	ECACC (Fogh *et al.* 1977)
T24	Human bladder transitional cell carcinoma cell line	RPMI 10% FCS 1% penicillin/streptomycin	1:10	ECACC (O'Toole *et al.* 1972)

2.1.1.1.2 Storage of cell lines

Cells were passaged on the day prior to freezing, so that cells were approximately 75% confluent and in active growth phase. Serum-positive growth media was removed and the cells were washed with 10 ml of PBS. Trypsin-EDTA (3 ml) was added to a 75 cm^2 flask and incubated at 37°C, 5% CO_2 for 2-10 min, until the cells were observed to round-up and detach from the flask. Serum-positive media (27 ml) was then added to neutralise the trypsin, and the cell solution was spun at 1,000 rpm for 5 min. The resulting cell pellet was re-suspended in freezing solution (10% dimethyl sulphoxide (DMSO), 90% FCS) and 1 ml aliquots placed in a cryovial (Corning). Cells were incubated on ice for 2 hours and then stored in the −80°C freezer. Unfortunately, there was no facility for long-term storage of cell lines in liquid nitrogen or in a −150°C freezer available to the group, which would have been more ideal.

In order to resuscitate frozen cells, the cryovial was warmed in a water bath at 37°C until the solution was molten. The molten cells were then transferred to a 30 ml sterile centrifuge tube (Starsted, USA) and 15 ml of warm serum-positive growth media added slowly, a drop at a time. Another 10 ml of serum-positive growth media was then added more quickly drop-wise. The cell suspension was spun at 1,000 rpm for 5 min, the supernatant removed, and the cell pellet resuspended in 5 ml of serum-positive growth media, before being transferred to a 25 cm^2 flask (Starsted). Twenty-four hours later, the growth media was changed for fresh media, and the cells passaged to a 75 cm^2 flask when they were 90% confluent.

2.1.2 Generation of A9 cell lines stably transfected with EGFR plasmid

A9 cells (3 x 10^5 cells/well) were seeded into 6 well plates (Corning) in 2 ml of normal growth media. Twenty-four hours later normal growth media was removed, cells were washed with 500 μl of PBS and 600 μl serum-free DMEM (transfection media) was added to each well. Cells were transfected with 2.5 μg of plasmid pUSEampEGFR complexed with DOTAP (1 mg/ml; Sigma) (5:1 mass/mass ratio of DOTAP to DNA) in HEPES buffer, at a final concentration of 10 mmol/l, for 4 hours at 37°C, 5% CO_2. After 4 hours, serum negative DMEM was replaced with 2

ml normal growth media and cells incubated for a further 20 hours. Cells were washed with 500 μl of PBS, trypsinised (200 μl trypsin added and incubated for up to 5 min at 37°C), split 50- and 100-fold and re-plated in 6 well pates with 2 ml normal growth media, supplemented with 800 μg/ml G418. G418 containing media was replenished every 4-5 days.

2.1.3 Protein Assay

The Advanced Protein Assay was used to measure the concentration of total protein in cell lysate samples for western blots and luciferase assays. The Advanced Protein Assay Reagent (Cytoskeleton, Inc, USA) was diluted 1:5 with distilled water. A dilutional series of bovine serum albumin (Sigma) in 1x lysis buffer (Promega) was produced. Cell lysate (5 μl) from each sample and standards in duplicate were added to wells of a clear 96 well flat-bottomed plate (Corning). For a negative control, 5 μl of 1x lysis buffer was added to 3 wells. To each well 250 μl of diluted Advanced Protein Assay Reagent was added, plates incubated at room temperature for 1 min, prior to analysis of the green-blue colour change, which was performed in a Wallac 1420 Victor^2 multilabel counter (PerkinElmer Life and Analytical Sciences Inc, USA) at 595 nm. The mean absorbance of the negative controls (lysis buffer only) was subtracted from each unknown sample and the concentration of protein calculated by extrapolating sample-blank OD values from a standard curve, using Excel software (Microsoft, USA).

2.1.4 MTS assay

The MTS assay is a colourimetric assay for determining the number of viable cells in a cytotoxicity assay (Promega). MTS is a tetrazolium compound [3-(4,5-dimethylthiazol-2-yl)-5-(3-carboxymethoxyphenyl)-2-(4-sulphophenyl)-2H-tetrazolium] which is reduced in viable cells to a coloured formazan product (Figure 2-1).

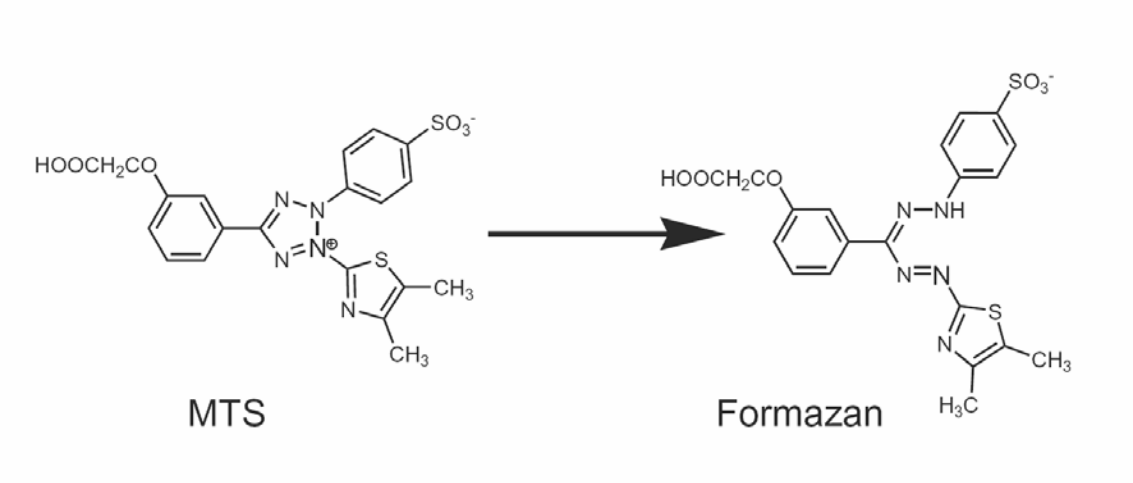


Figure 2-1 Conversion of the MTS reagent by viable cells

MTS reagent was thawed to room temperature and 20 μl added to each well of a 48 well flat-bottomed plate (Nunc) containing cells in 300 μl of culture media. The plate was incubated at 37°C, 5% CO_2. The plate was then analysed in a Wallac 1420 Victor^2 multilabel counter (PerkinElmer Life and Analytical Sciences) at 490 nm at time points between 15 min and 2 hours (depending on cell line). The negative control was generated by adding 20 μl MTS reagent to 300 μl serum-positive media, without cells. All experiments were performed in triplicate in order to calculate the mean percentage cell survival and SEM.

2.1.5 Antibodies

Antibodies used in experiments are detailed in Table 2-2. Cetuximab, a humanized anti-EGFR antibody (see section 1.1.4.2.2), was a generously donated by Merck.

Table 2-2 Antibodies

Antibody	*Species*	*Company*	*Catalogue number*
Anti- β-actin	Rabbit	Sigma	A5060
Anti-CA125	Mouse monoclonal	Vector, UK	NCL-L-CA125
Anti-Coxsackie adenovirus receptor (CAR)	Mouse monoclonal	Gift from Dr. V. Mautner, University of Birmingham, UK	n/a
Anti-Cytokeratin 7	Mouse monoclonal	Vector, UK	NCL-L-CK7-OVTL

Antibody	*Species*	*Company*	*Catalogue number*
Anti-EGFR	Mouse monoclonal	Santa Cruz, USA	sc-120
Anti-EGFR	Goat	Santa Cruz, USA	sc-03-G
Anti-EGFR	Mouse	Calbiochem	GR01L
Anti-EMA	Mouse monoclonal	Vector, UK	NCL-L-EMA
Anti-goat HRP conjugate	Goat	Vector	PI-9500
Anti-human IgG (FC portion)	Mouse	DakoCytomation	M0828
Anti-mouse R-PE conjugate	Goat	DakoCytomation	R0480
Anti-PCNA	Mouse monoclonal	Abcam	ab29
Anti-pEGFR (Tyr)	Goat polyclonal	Santa Cruz, USA	sc-16802
Anti-pTyr 100	Mouse	New England Biolabs	9411
Anti-rabbit IgG	Goat	Abcam	ab6721-1
Biotinylated anti-human secondary antibody	Goat	Vector	BA-3000
Biotinylated anti-mouse/rabbit secondary antibody	Horse	Vector, UK	Part of kit AK-5200
IgG isotype control	Mouse monoclonal	Cambridge Biosciences	0107-01
Anti-F4-80	Rat monoclonal	Serotec	MCA-497R
Anti-NIMP-14	Rat monoclonal	Abcam	ab2557-50
IgG 2b isotype control	Rat monoclonal	Abcam	ab185360-500
Biotinylated anti-rat IgG (mouse adsorbed)	Rabbit	Vector	BA-4001

2.1.6 Analysis of cell receptor status by flow cytometry

Serum-positive growth media was removed from cells in 25-125 cm^2 cell culture flasks. Cells were washed with PBS before 2-5 ml of DMEM containing 10% heat-inactivated (56°C for 30 min) goat serum (10% HINGS) (Sigma) was added to each flask. Cells were detached from the

flask surface by careful scraping and pipetting the resulting solution vigorously to break up cell clumps. The cell solution was centrifuged at 1,500 rpm for 3 min at 4°C, the pellet re-suspended in 10% HINGS and 50 μl of cell solution was added to each well of a 96 well v-bottomed plate (Bibby Sterilin Ltd, UK). The primary antibody was prepared by diluting to 2x the final concentration with 10% HINGS and 50 μl primary antibody was added to experimental wells, with appropriate negative and isotype antibody controls. The plate was incubated for 40 min at 4°C with gentle agitation. The plate was spun at 200 rpm for 5 min at 4°C, supernatant removed and cells re-suspended in 100 μl of 10% HINGS and the wash step repeated once more. The secondary antibody was diluted in 10% HINGS and 100 μl used to resuspend cells following the second wash. The plate was incubated for a further 40 min in the dark at 4°C with gentle agitation. Three wash steps were performed and following the third wash, cells were resuspended in 50 μl 10% HINGS and fixed with 50 μl 4% paraformaldehyde. The plate was stored at 4°C in the dark until analysis by flow cytometry using a FACSCalibur machine (BD Biosciences) at 585 nm (minimum 1 x 10^4 cells analysed).

2.1.7 Analysis of cell receptor status by ELISA

A commercial ELISA (DakoCytomation) has been produced to measure EGFR, which has been shed from the cell surface in serum or cell culture fluid. This assay is used clinically to select patients for treatments with anti-EGFR antibodies. Cells were trypsinized from 75 cm^2 tissue culture flasks, and counted. Cells of each type (2 x 10^6) were then plated onto 10 cm diameter tissue culture petri-dishes (Corning) and allowed to recover EGFR status over 4 hours. Plates were then scraped to detach cells, which were then spun at 1,000 rpm for 5 min, before being resuspended in 1 ml of resuspension buffer (50 mmol/l Tris HCl, 5 mmol/l EDTA, pH 7.4) and transferred to a 1.5 ml eppendorf tube. Extraction agent (200 μl) (1 mol/l KCl, 6% Zwittergent 3-14 detergent, Merck Biosciences) was then added to each sample and incubated on ice, with occasional vortexing, for 30 min. Samples were then spun at 13,000 rpm at 4°C for 5 min and the supernatant collected. A protein assay was performed on a 10-fold dilution of cell extract (see section 2.1.3). Dilutions (0-100 fold) of cell extracts were made using the sample diluent provided with the ELISA kit. Samples and kit were allowed to equilibrate to room temperature. Aliquots of samples and known EGFR standards (100 μl) were added in duplicate to wells of the

ELISA plate, sealed in a plastic bag and incubated at 37°C for 90 min. Wells were washed six times with 300 μl of 1x plate wash. Working conjugate was prepared as per manufacturer's instructions and 100 μl added to each well, except for the substrate blank well. The plate was sealed in plastic and incubated at room temperature for 30 min. Wells were washed six times with 300 μl of 1x plate wash. Working substrate was prepared as per manufacturer's instructions and 100 μl added to each well, including the substrate blank. The plate was sealed in plastic and incubated at room temperature for 60 min. Stop solution (100 μl) was added to each well and the plate read in a Wallac 1420 Victor^2 multilabel counter at 595 nm. A standard curve was generated using Prism3 software and unknown values calculated by extrapolation of sample OD from the standard curve. From the sample dilution, the concentration of EGFR in the sample was calculated. The number of EGFR molecules in the sample was then calculated using Avogadro's number and the molecular weight of shed EGFR (110 kDa). Hence, the number of EGFR per cell could be determined, given there were 2 x 10^6 cells in the sample.

2.1.8 Binding of EGF-polymer to EGFR positive cells

Cells were grown until ~90% confluent in 25 cm^2 tissue culture flasks. Adherent cells were detached from the flask surface by carefully scraping the base of the flask with a cell scraper and pipetting the resulting solution vigorously to break up cell clumps. The cell solution was centrifuged at 1,500 rpm for 3 min at 4°C and the pellet resuspended in 10% HINGS. Cell solution (50 μl) was added to each well of a 96 well v-bottomed plate. Cells were incubated with EGF-polymer to which free reactive groups had been conjugated to biotin. A biotin-only polymer was used as a negative control. Polymer at a concentration of 50 μg/ml and incubated with cells at 4°C for 40 min with gentle agitation. Cells were washed twice to remove free EGF-polymer and incubated with avidin-Texas red (diluted 1:100, Vector) at 4°C for 40 minutes with gentle agitation. Cells were washed three times, fixed with 50 μl 4% paraformaldehyde and analysed by flow cytometry at 585 nm (minimum 1 x 10^4 cells).

2.1.9 Internalisation of EGF receptors

2.1.9.1 Flow cytometry

Cells were grown in 25 cm^2 tissue culture flasks until 90% confluent. Cell lines requiring G418 selection pressure had G418-positive media replaced with G418-negative media 20-24 hours prior to the experiment. All cells were serum-starved for >4 hours prior to the experiment. Cells were washed with 5 ml ice cold PBS and detached by scraping cells in 5 ml ice cold 0.1% BSA DMEM. Cells were spun at 1,000 rpm for 5 min at 4°C and the cell pellet resuspended in ice cold 0.1% BSA DMEM at 2 x 10^7 cells/ml. Aliquots (50 μl) were plated in a 96 well v-bottomed plate. Cells were pre-incubated with monensin to a final concentration of 50 μmol/l for 30 min at 4°C. EGF-Fluorescein (50 μl) (Molecular Probes) at a concentration of 1 μg/ml in 0.1% BSA DMEM was added to experimental wells, and 50μl of 0.1% BSA DMEM added to control wells. Cells were incubated for 45 min on ice, washed three times with 100 μl ice cold PBS, spun at 200 rpm for 5 min at 4°C, resuspended in 200 μl 0.1% BSA DMEM, and incubated for 30 min at 37°C, 5% CO_2. Cells were then transferred to falcon tubes (BD Biosciences) and placed immediately on ice before analysis by flow cytometry at 530 nm.

2.1.9.2 Fluorescence microscopy (1)

Cells were plated out at a density of 2 x 10^3 to 4 x 10^4 in 200 μl normal growth media in 8 well glass or plastic chamber cell culture slides (Nunc) before being cultured for 48-72 hours. Cell lines requiring G418 selection pressure had G418-positive media replaced with G418-negative media 20-24 hours prior to the experiment. Slides were placed on ice and washed with 200 μl ice cold PBS. EGF-Fluorescein conjugate (100 μl), in DMEM with 0.1% bovine serum albumin (BSA), was added at a concentration of 0.5 μg/ml. Control slides had a 100-fold excess of non-labelled EGF added to compete with labelled-EGF binding as a negative control. Slides were incubated at 4°C for 45 min before being washed 5 times with 200 μl ice cold PBS. At this point the control slide and the slide for 0 min were fixed with 100 μl 4% paraformaldehyde in ice cold PBS and incubated at room temperature for 20 min. Other slides were incubated for 2, 10, 20 and 45 min at 37°C, 5% CO_2 prior to fixing. Slides were mounted with Vectashield with DAPI

and viewed with a Axiovert fluorescence microscope (Zeiss) using a x63 oil immersion lens and photomicrographs taken with a Cybershot 3.3 Megapixels digital camera (Sony).

2.1.9.3 Fluorescence microscopy (2)

Cells were plated out at a density of 2 x 10^3 to 4 x 10^4 in 200 μl normal growth media in 8 well glass or plastic chamber cell culture slides (Nunc) before being cultured for 48-72 hours. Cell lines requiring G418 selection pressure had G418-positive media replaced with G418-negative media 20-24 hours prior to the experiment. All cells were serum-starved for 2-4 hours prior to the experiment. Slides were placed on ice and washed with 200 μl ice cold PBS. Ice cold 0.1% BSA DMEM (100 μl) was added to each chamber. EGF (Sigma) was added to experimental chambers to a concentration of 200 ng/ml. Slides were incubated on ice for 60-90 min, washed three times with 100 μl ice cold PBS, before 200 μl 0.1% BSA DMEM was added to each well and incubated at 37°C, 5% CO_2 for 30 min prior to fixing with 2% paraformaldehyde in PBS. Slides were then left at 4°C overnight prior to antibody labelling.

Cells were permeablised with 100 μl 0.1% Triton x-100 for 5 min at 4°C, then blocked with 1% blocking serum in PBS for 1 hour at room temperature in a humidified chamber. Blocking serum was removed and replaced with 100 μl of the first primary antibody (rabbit anti-EEA-1 (Abcam) diluted 1:250 or rat anti-LAMP-2 (Abcam) diluted 1:200) and incubated at room temperature for 1 hour. Antibody was removed and cells washed three times with PBS. Cells were incubated with 100 μl secondary antibody (anti-mouse biotinylated antibody (Vector) diluted 1:200 for the EEA-1 primary and anti-rat Alexa 594 (Molecular Probes) diluted 1:100 for the LAMP-2 primary for 45 min at room temperature. Antibody was removed and cells washed three times with PBS. Blocking serum was added to the LAMP-2 wells and 100 μl avidin D-Texas red (Vector, diluted 1:100 in 0.1 mol/l sodium bicarbonate, 0.15 mol/l sodium chloride, pH 8.5 buffer) was added to the EEA-1 wells prior to incubation for 45 min at room temperature. Cells were washed three times with 100 μl PBS and incubated with blocking buffer for 1 hour at room temperature. Cells were then labelled with mouse anti-EGFR antibody (diluted 1:100, Santa Cruz) for 1 hour at room temperature, washed three times with 100 μl PBS, and incubated with the second secondary antibody, (horse anti-mouse fluorescein, diluted 1:100) for 45 min at room

temperature. Cells were washed three times with PBS and mounted in Vectashield hardest with DAPI and TO-PRO-3 (Molecular Probes). Photomicrographs were taken using a confocal microscope (Nikon Optiphot-2 upright microscope, fitted with a 60x oil immersion objective; Bio-Rad MRC1024 with Krypton/Argon lasers, giving lines at 488nm (for FITC), 568nm (for TRITC, Texas Red) and 647nm (for Cy5, To-Pro-3). Images were processed using LaserSharp 2000 image processing software (Biorad).

2.1.10 Western blot

2.1.10.1 Separating gel

Deionised water	4.85 ml
1.5 mol/l Tris HCl pH 8.8	2.5 ml
10% SDS	100 μl
Acrylamide	2.5 ml
10% Ammonium persulphate	100 μl
TEMED	20 μl

2.1.10.2 Stacking gel

Deionised water	6.1 ml
0.5 mol/l Tris HCl pH 6.8	2.5 ml
10% SDS	100 μl
Acrylamide	1.33 ml
10% Ammonium persulphate	100 μl
TEMED	20 μl

2.1.10.3 Electrode buffer (5x)

Tris base	9.9 g
Glycine	43.2 g
SDS	3.0 g
Deionised water	600 ml

Make to pH 8.3. Dilute 1 in 5 with deionised water before use

2.1.10.4 Sample loading buffer

Deionised water	3.8 ml
0.5 mol/l Tris HCl pH 6.8	1.0 ml
Glycerol	0.8 ml
10% SDS	1.6 ml
β-mercaptoethanol	0.4 ml
1% Bromophenol blue	0.4 ml

2.1.10.5 Transfer buffer

Tris base 25mmol/l	3.129 g
Deionised water	800 ml
Glycine	14.4 g
Methanol	200 ml
Make to pH 8.3	

2.1.10.6 Sample and gel preparation

Cells (2 x 10^5) were added to wells of a 6 well plate (Corning) and cultured overnight in 10% FCS DMEM. Cell lines requiring G418 selection pressure had G418-positive media replaced with G418-negative media 20-24 hours prior to the experiment. All cells were serum-starved for >4 hours prior to the experiment. Cells were washed with PBS and incubated with 200 μl 0.1% BSA DMEM containing EGF at 100 nmol/l (positive control) or without EGF (negative control) at 37°C, 5% CO_2 for up to 30 min. Media was removed, cells washed with PBS and then 100 μl of 1x cell lysis buffer (Promega) containing Complete® protease inhibitors (Roche Diagnostics) added. Plates were frozen for at least 30 min at −80°C, thawed, then were scraped to detach cell membranes and the cell lysate stored at –20°C. Protein content of each sample was calculated using the protein assay (see section 2.1.3) and the volume required to provide 20 μg of protein was loaded onto a 7.5% SDS gel (see sections 2.1.10.1 and 2.1.10.2) with sample loading buffer containing β-mercaptoethanol (see section 2.1.10.4) to make each sample up to a volume of 25 μl (approx 3x volume of buffer to sample). Samples were loaded into wells of the

gel, including a lane for the kaleidoscope pre-stained standards (Bio-rad) and run at 120 V for 1-2 hours.

2.1.10.7 Nitrocellulose transfer

The nitrocellulose membrane, filter papers and fibre pads were pre-soaked in transfer buffer (see section 2.1.10.5). Gels were removed from their glass plates, rinsed in transfer buffer and assembled as part of a blotting sandwich in the following order: fibre pad; filter paper; gel; nitrocellulose membrane; filter paper; and fibre pad whilst immersed in transfer buffer to exclude air bubbles. The 'sandwich' was placed in the transfer cassette and blotted overnight at 30V, 4°C.

2.1.10.8 Western blot development

The nitrocellulose membrane was removed from the transfer cassette and blocked in 20 ml 5% non-fat milk PBS solution at room temperature for 1½ hours. The membrane was washed in PBS/0.1% Tween and incubated with a 1:1,000 dilution of goat anti-pEGFR antibody (Santa Cruz), made up in 5% non-fat milk/PBS, with gentle agitation at room temperature for 1½ hours. The membrane was washed three times for 5 min with PBS/0.1% Tween. The membrane was then incubated with a 1:500 dilution of anti-goat HRP antibody (Vector), made up in 5% non-fat milk/PBS, with gentle agitation at room temperature for 1½ hours. The membrane was washed three times for 5 min with PBS/0.1% Tween and developed for 5 min with 3-4 ml Lumiglo® (Insight Biotechnology Ltd) before imaging for 10-20 min. Some membranes were cut in two in order to simultaneously probe for pEGFR and control for loading by probing for β-actin. The β-actin portion of the nitrocellulose membrane was incubated with rabbit anti β-actin antibody (Sigma 1:2,000 dilution) and Goat polyclonal anti-rabbit antibody conjugated to horseradish peroxidase (Abcam 1:1,000), conditions as above.

2.2 Virus techniques

2.2.1 Adenovirus vectors

AdCMV-GFP$_{\Delta E1}$ and AdCMV-Luc$_{\Delta E1}$ are replication incompetent serotype 5 adenovirus (Ad5), which express enhanced green fluorescent protein or firefly luciferase reporter genes respectively, under the control of the cytomegalovirus (CMV) immediate early promoter in the deleted E1 region. There were kindly supplied by Dr V. Mautner and Dr P. Searle (CRUK Institute for Cancer Studies, University of Birmingham, UK). E1-deleted viruses were propagated in HEK293 cells, which are stably transduced with the E1 region, thus supplying E1 gene products in *trans*. Wild type adenovirus serotype 5 (Ad5WT) was also donated by Dr Mautner.

A variety of conditionally-replication competent adenoviruses, engineered to replicate specifically within cancer cells and all based on Ad5, were used in this thesis (see section 6.2.2 and Table 6-2 for further details). ONYX-015 (Heise *et al.* 1997) and ONYX-017 (Jounaidi and Waxman 2004) have deletions in the E1B region, and were kindly donated by Dr V. Mautner and Dr Yuqiao Shen (West Coast Biologicals, San Francisco, California) respectively. Adenovirus *dl*922-947 has a deletion in the E1A region (Heise *et al.* 2000) and was generously donated by Dr Gunnel Hallden (St Bartholomew's Hospital and the London School of Medicine). EHE2F has the E1A and E1B regions under the control of oestrogen and hypoxia response elements (Hernandez-Alcoceba *et al.* 2002) and was a gift from Dr Ruben Hernandez-Alcoceba (Gene Therapy Unit, Centre for Applied Medical Research, Pamplona, Spain). All of the conditionally-replication competent adenoviruses were propagated in HEK293 cells, as described below.

2.2.2 Adenovirus propagation

Adenovirus vectors were propagated in HEK293 cells. Adenovirus seed stock was incubated with subconfluent cells (80-90%) in 175 cm^2 tissue culture flasks in 4 ml of low serum media (DMEM 2% FCS, 1% glutamine, 1% penicillin/streptomycin) at a multiplicity of infection (MOI) of one plaque forming unit per cell. Adenovirus was incubated with cells for 90 min at 37°C, 5%

CO_2. At this stage a further 36 ml of low serum media was added without removing the original inoculum. Cells were incubated at 37°C, 5% CO_2 for 3-4 days until extensive cytopathic effect was visualised.

Cells were trypsinised and centrifuged in 250 ml centrifuge tubes (Corning) at 290 g for 10 min at 4°C. The supernatant was discarded, the cell pellet resuspended in 1 ml of low serum media and the cells lysed by three cycles of rapid freeze/thaw (-70°C/37°C) to release virions. Cells were centrifuged to remove the cell debris and the supernatant stored at -70°C as crude virus stock prior to purification.

2.2.3 Purification of adenovirus

Adenovirus was purified from contaminating cell, virus and serum proteins using density banding to separate intact virus particles from empty or incomplete capsids.

N-butanol (Sigma) was added to the crude virus stock to a final concentration of 1% (volume/volume) and incubated on ice for 1 hour in order to dissociate lipid membranes. Following this virus was isolated by centrifugation (290 g for 10 min at 4°C) and the supernatant layered onto glycerol/caesium chloride gradients. The gradient consisted off 2 ml caesium chloride (BDH) (ρ = 1.45) in 10 mmol/l Tris pH 7.9 at the bottom, followed by 3 ml caesium chloride (ρ = 1.32) in 10 mmol/l Tris pH 7.9, and then 2 ml 40% glycerol (volume/volume) with 10 mmol/l Tris pH 7.9 at the top. Crude virus stock (~5-7 ml) was carefully layered on top of the glycerol and the tubes (Beckman) centrifuged (Beckman ultracentrifuge with SW40Ti rotor) for 90 min at 25,000 rpm, 4°C.

Purified virus was seen as an opalescent band at ρ = 1.345 and was collected by puncturing the tube just below the band with a syringe and hypodermic needle (21G Terumo) and carefully withdrawing the band. This was then dialysed against PBS containing 10% glycerol (volume/volume), 50 mmol/l HEPES, 0.1 g/l $MgCl_2$ and 0.1 g/l $CaCl_2$ overnight at 4°C, using a 10 kDa dialysis cassette (Pierce). Following single purification the dialysed virus was treated with benzonase (125 units/ml) (Novagen) for 30 min at room temperature, to degrade

contaminating DNA in the sample. Virus was then re-purified on glycerol/caesium chloride gradients and dialysed against PBS (containing 10% glycerol (volume/volume), 50 mmol/l HEPES, 0.1 g/l $MgCl_2$, 0.1 g/l $CaCl_2$, pH 7.8) overnight at 4°C as described above. Highly purified virus was aliquoted and stored at -70°C. Density purified adenovirus was used for all experiments.

2.2.4 Double Stranded DNA quantification to calculate number of viral particles

The asymmetrical monomethine cyanine dye PicoGreen® (Molecular Probes Inc, USA) is a fluorescent nucleic acid stain that binds to double stranded DNA (Singer *et al.* 1997). It may be used to determine the number of viral particles of adenovirus, if the virus has been prepared with benzonase to remove free viral DNA. Viral samples were incubated at 56^{o}C for 30 min to inactivate the virus before aliquots were diluted 10- and 100-fold. Virus dilutions (15 μl) were added to 255 μl of 1x TE buffer and 30 μl of 1x TE/0.5% Sodium Dodecyl Sulphate (SDS) and incubated for 5 min at room temperature to disrupt the viral particles. Lambda DNA was made into a logarithmic dilutional series to create a standard curve, from which the amount of DNA in the unknown viral samples could be calculated. All samples were performed in triplicate to generate a mean and SEM.

For each DNA standard or unknown sample 100 μl was placed in wells of a 96 well black plate (Corning). PicoGreen® reagent (200x) was diluted 200-fold with TE buffer and 100 μl of diluted reagent was added to each sample. The plate was incubated at room temperature for 2-3 min and then read in a Wallac 1420 Victor^2 multilabel counter, using the 'Fluorescein (485 nm/535 nm, 1.0s)' analysis. A standard curve was generated from the DNA standards and the amount of DNA in the unknown samples calculated using Prism3 software. The number of viral particles in the sample was then calculated from the amount of DNA, assuming 1 μg/ml of DNA is equivalent to 2.7 x 10^{10} viral particles (Mittereder *et al.* 1996).

2.2.5 Quantification of infectious virus particles

2.2.5.1 Plaque assay method

HEK293 cells were (5 x 10^5/well) seeded into 6 well plates (Corning) in 2 ml of serum-positive media (see Table 2-1) prior to overnight incubation at 37°C, 5% CO_2. Duplicate serial dilutions of each virus were prepared (10^{-2}, 10^{-4}, 10^{-6}. 10^{-7}, 10^{-8}, 10^{-9}, 10^{-10}, 10^{-11}, 10^{-12}, 10^{-13}) in 2 ml aliquots of low-serum media. Cells were washed with PBS and 1 ml of virus solutions applied to wells in duplicate (triplicate at higher dilutions). Cells were incubated at 37°C, 5% CO_2 for 2 hours. Low melting point agar (1.4% made up in dH_2O and autoclaved) was kept at 42°C in a water bath. This was mixed with 2x low-serum DMEM (at 37°C) and 4 ml immediately added to cells after virus media was removed following the 2 hour incubation. Plates were left in the hood for 10 min to set and then incubated at 37°C, 5% CO_2 for 10 days, feeding plates with fresh 1.4% agar/ 2x low-serum DMEM mix every 4 days. After 10 days plates were read using an inverted microscope (Axiovert 25, Zeiss), number of plaques counted per plate and the number of plaque forming units/ml (pfu/ml) of the original virus aliquot calculated.

For example, there were 2, 1 and 1 plaques observed in the wells of virus diluted by 10^{-12} and no plaques in wells of virus diluted 10^{-13}.

$$\text{Virus titre} = ((2 + 1 + 1)/3) \times 10^{12}$$

$$\text{Virus titre (pfu/ml)} = 1.3 \times 10^{12}$$

2.2.5.2 Tissue culture infectious dose 50 ($TCID_{50}$) method

HEK293 cells (1 x 10^4) were seeded into each well of a 96 well flat-bottomed plate (Starsted Inc, USA) in 200 μl of serum-positive media (see Table 2-1) prior to overnight incubation at 37°C, 5% CO_2. Serum-positive media was removed and cells washed with PBS. Duplicate serial dilutions of each virus were prepared (10^{-2}, 10^{-4}, 10^{-6}. 10^{-7}, 10^{-8}, 10^{-9}, 10^{-10}, 10^{-11}, 10^{-12}, 10^{-13}) in low-serum media and 100 μl aliquots of each dilution of virus and a non-virus control was added to 10 wells of the 96-well plate. Plates were incubated for 10 days at 37°C, 5% CO_2 with additional low-serum media added to wells on days 4 and 7 to feed cells. After 10 days plates were read using an inverted microscope (Axiovert 25, Zeiss). The number of wells per virus

dilution that had evidence of cytopathic effect (CPE) was recorded and the ratio of wells affected by CPE per dilution determined. The $TCID_{50}$ was calculated using the KÄRBER statistical method (see Equation 2-1).

Equation 2-1 Calculation of $TCID_{50}$ and plaque forming units

$$\text{Virus titre } (TCID_{50}/ml) = 10^{\,1 + d\,(S - 0.5)}$$

$$d = \log 10 \text{ of the dilution}$$

$$S = \text{the sum of the ratios (starting from a 10-fold dilution)}$$

Virus titre as measured by $TCID_{50}$ is 0.7 Log higher than by plaque assay and so to transform $TCID_{50}$/ml into pfu/ml:

$$\text{Virus titre } (pfu/ml) = 10^{\,(1 + d\,(S - 0.5)) - 0.7}$$

For example, Ad5WT gave a 100% CPE at all dilutions less than 10^{-11} dilution, 80% CPE at 10^{-11} dilution, 50% CPE at 10^{-12} dilution and 20% % CPE at 10^{-12} dilution.

$$S = (1+1+1+1+1+1+1+1+1+1+ 0.8 + 0.5 + 0.2) - 0.5$$

$$\therefore S = 11.3$$

$$\text{Virus titre } (TCID_{50}/ 100\ \mu l) = 10^{\,1 + 1\,(11.3 - 0.5)}$$

$$\text{Virus titre } (TCID_{50}/ 100\ \mu l) = 10^{\,11.8}$$

$$\text{Virus titre } (TCID_{50}/ml) = 10^{\,12.8}$$

$$\text{Virus titre } (pfu/ml) = 10^{\,(12.8- 0.7)}$$

$$\therefore \text{ Virus titre } (pfu/ml) = 1.3 \times 10^{12}$$

2.2.6 Polymer coating virus

Polymers based on pHPMA-TT were dissolved in sterile distilled water at 100 mg/ml and diluted with sterile distilled water to give final polymer concentrations of 20 mg/ml, 10 mg/ml and 5 mg/ml when added to virus. Virus stock in 40 μl storage buffer (50 mmol/l HEPES, pH 7.8, 0.1 g/L Ca and $MgCl_2$, 10% Glycerol) (Fisher *et al.* 2001) was added to 10 μl polymer and incubated at room temperature for 40 min. Virus was then transferred onto ice and incubated at 4°C overnight, prior to purification (see section 2.2.7), PicoGreen analysis for virus particle number (see section 2.2.4), and transduction of target cells (see section 2.2.8).

2.2.7 Purification of polymer coated adenovirus vectors

S400 microspin columns (Amersham Biosciences, UK) were briefly vortexed, placed in 1.5 ml eppendorfs, and the column spun in a spin-out centrifuge at 2,600 rpm for 1 min. The eluate was discarded, the column transferred to a fresh eppendorf tube, and 50 μl of virus placed on the column. The column was spun at 2,600 rpm for 2 min and the eluted virus analysed by PicoGreen assay (see section 2.2.4) before being stored at −80°C.

2.2.8 Viral transduction of cells *in vitro*

Cells (1 x 10^4) were seeded into each well of a 96 well flat-bottomed plate (Starsted Inc, USA) in 200 μl of serum-positive media (see Table 2-1) prior to overnight incubation at 37°C, 5% CO_2. Next day, cells were washed with PBS and infected with adenovirus at a known multiplicity of infection (MOI) of viral particles (v.p.) per cell (see section 2.2.4). Virus was diluted in low-serum media (DMEM with 2% FCS) to appropriate concentration and added to each well (25-100 μl). All experiments were performed in triplicate. Cells and virus were incubated at 37°C, 5% CO_2 for 90 min. After this time virus media was removed, cells were rinsed with 200 μl PBS, and 200 μl serum-positive media was added to each well and incubated at 37°C, 5% CO_2 for 24-48 hours.

2.2.8.1 Measurement of firefly luciferase expression in transduced cells

Following transduction with adenovirus encoding the luciferase transgene under the control of the CMV promoter (AdCMV-Luc$_{\Delta E1}$), cells were incubated for 24-48 hours (at 37°C, 5% CO_2), serum-positive media was removed and cells were washed with PBS. Luciferase expression was analysed using the Luciferase Assay System (Promega, UK). Lysis buffer (100 μl) was added to each well and the plate was incubated at −80°C until frozen (~30 min). Plates were allowed to thaw to room temperature. Cell lysate (25 μl) was added to a luminometer tube and placed in a luminometer (Berthold Technologies, Germany). Following insertion of the luminometer tube, the luminometer injected luciferase assay substrate (100 μl) (Beetle luciferin), which was converted to the luminescent product, oxyluciferin, using ATP·Mg^{2+} as a co-substrate (see Figure 2-2). Luminescence was detected over 10 seconds with a 2 second delay. Cells

which had not been transduced with AdCMV-Luc $_{\Delta E1}$ were used as a negative control to determine background luminescence.

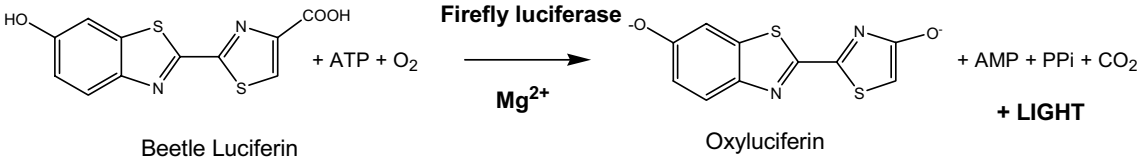


Figure 2-2 Conversion of luciferin to oxyluciferin by firefly luciferase

All experiments were performed in triplicate in order to generate the mean and SEM and the results were calibrated for protein concentration (see section 2.1.3) to generate relative light units per milligram of protein (RLU/mg).

2.2.9 Quantitative polymerase chain reaction (Q-PCR)

Q-PCR was used to detect the presence of adenovirus DNA in extracted DNA samples using ABI 5700 Sequence Detection System and software. DNA was extracted from 50 μl aliquots of cell lysate or 200 μl of tissue lysate, diluted to 300 mg/ml in 1x Promega lysis buffer, using the GeneElute genomic mammalian DNA miniprep kit (Sigma). Amplification of an 84 base pair fragment of adenovirus fibre gene was carried out using the following primers and probe (Sigma Genoysis):

Forward 5' TGG CTG TTA AAG GCA GTT TGG 3'

Reverse 5' GCA CTC CAT TTT CGT CAA ATC TT 3'

Probe 5' TCC AAT ATC TGG AAC AGT TCA AAG TGC TCA TCT 3'

The probe was labelled with the FAM fluorophore at the 5' end and the TAMRA quencher at the 3' end. Reactions were carried out in a total volume of 25 μl in Abgene Q-PCR master mix containing primers at 1 μmol/l and probe at 0.1 μmol/l, with 5 μl aliquots of standards and unknowns and 0.5 μl of 1:50 diluted Rox to minimize background fluorescence. All equipment and non-DNA containing components were UV irradiated for 15 min prior to reactions and the plates were set up in a sterile environment that was adenovirus-free. Thermocycling parameters were optimized as 2 min at 50°C, 15 min at 95°C, followed by 40 cycles of 95°C (30

s) and 60°C (2 min) (example of an amplification plot shown in Figure 2-3). Data analysis was performed with the ABI software and test samples compared to samples with known adenovirus content based on PicoGreen analysis (example of a Q-PCR standard curve shown in Figure 2-4). Standards were generated by spiking serial dilutions of known virus amounts into appropriate cell or tissue lysate, and performing DNA extraction as above, to control for DNA extraction and effect of lysate.

Quantification of number of human tumour cells was also performed by Q-PCR. Primers and probe were designed based on the promoter sequence of the human β-actin gene:

Forward 5' CGG CCA ACG CCA AAA C 3'
Reverse 5' TCC CCT CCT CCC TTT GCG AAA A 3'
Probe 5' CTC CCT CCT CCT CTT CCT CAA TCT CGC 3'

The probe was labelled with the FAM fluorophore at the 5' end and the TAMRA quencher at the 3' end. Reactions were carried out in a total volume of 25 μl in ABgene Q-PCR master mix containing primers at 1 μmol/l and probe at 0.1 μmol/l, with 5 μl aliquots of standards and unknowns and 0.5 μl of 1:50 diluted Rox to minimize background fluorescence.

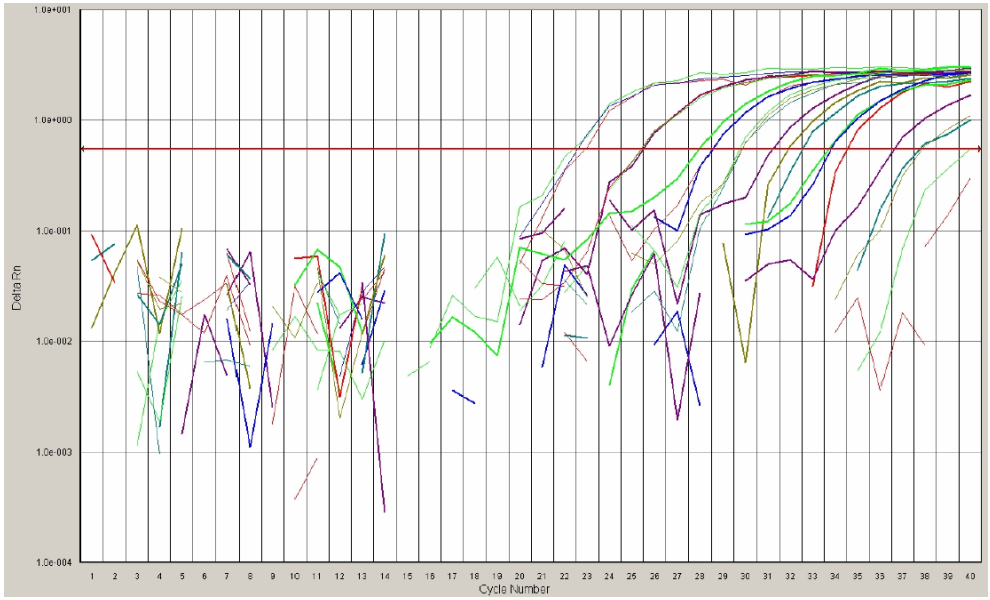


Figure 2-3 Q-PCR amplification plot of adenovirus standards

Known amounts of adenovirus were spiked into 50 μl aliquots of A431 cell lysate, DNA extracted and 5 μl aliquots (in triplicate) run in a Q-PCR reaction (see section 2.2.9). A threshold line was drawn across the amplification plots during the exponential growth phase of all samples to record the cycle number for each sample at that threshold (CT).

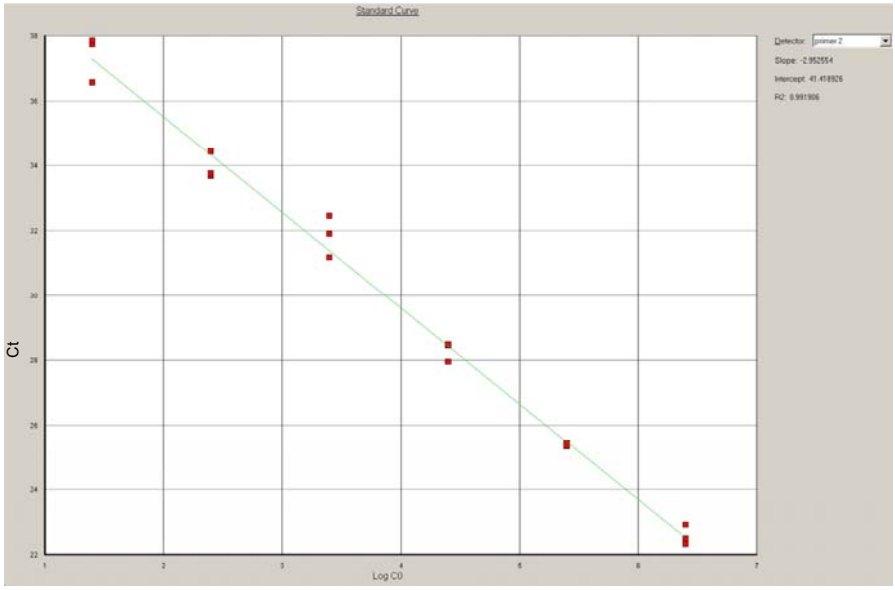


Figure 2-4 Standard curve of Q-PCR generated CT values of adenovirus standards

CT values were plotted against Log[adenovirus] of standards to generate a standard using ABI software.

Thermocycling parameters were optimized as 2 min at 50°C, 15 min at 95°C, followed by 40 cycles of 95°C (30 s) and 60°C (2 min). Data analysis was performed with the ABI software and test samples compared to samples with known standards generated using a plasmid encoding the human β-actin promoter sequence, pDRIVE-hβ-Actin-RU5' (Autogen bioclear) spiked into mouse tissue lysate, prior to DNA extraction as above (Figure 2-5). From plasmid size and concentration of DNA in the plasmid preparation measured by absorbance at 280 nm, the number of plasmid copies in the top standard was 6.825 x 10^5 in 5 μl. For samples, mouse tumours were homogenized in 1x Promega lysis buffer to a concentration of 300 mg/ml and DNA extracted as previously described. A dilutional series of SKOV-3 cell DNA was also prepared in mouse tissue lysate, to allow conversion of plasmid copy number into an approximation of cell count in tumour samples.

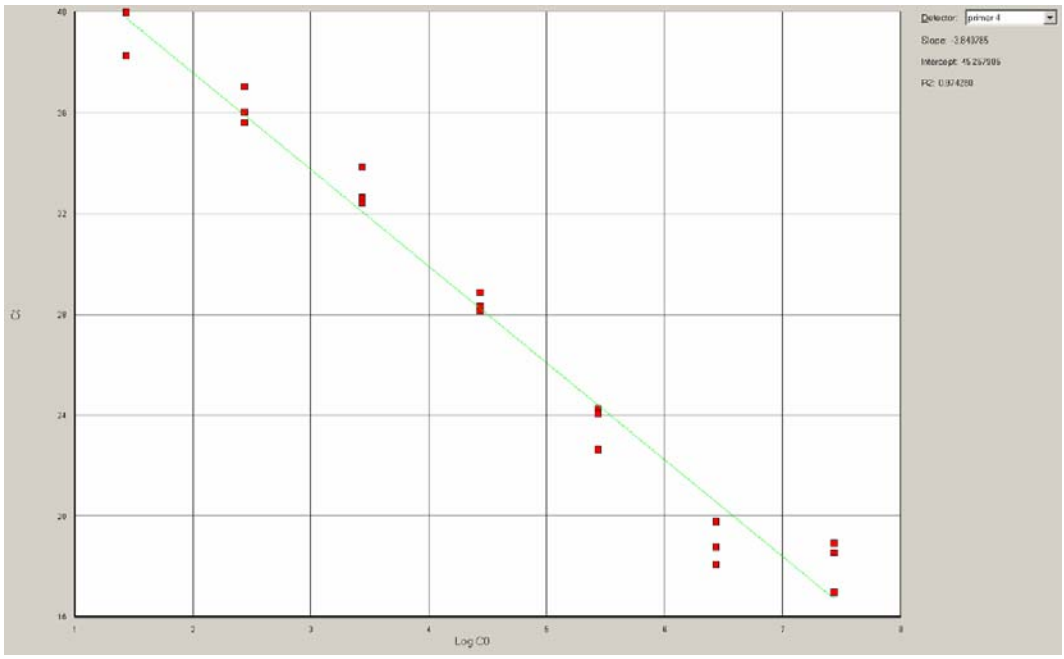


Figure 2-5 Standard curve obtained following Q-PCR of a serial dilution of pDRIVE-hβ-Actin-RU5' spiked into mouse tissue lysate

2.2.10 Assessment of oncolytic activity of viruses

Cells (1 x 10^4) were seeded into each well of a 96 well flat-bottomed plate in 100 μl of serum-positive media (see Table 2-1) prior to overnight incubation at 37°C, 5% CO_2. Next day, cells were washed with PBS and infected with adenovirus at range of multiplicity of infection (MOI) of plaque forming units (pfu) per cell (see section 2.2.4). Virus was diluted in low-serum media (DMEM with 2% FCS) to appropriate concentration and added to each well (100 μl). All experiments were performed in triplicate. Cells and virus were incubated at 37°C, 5% CO_2 for 90 min. After this time virus media was removed, cells were rinsed with 200 μl PBS, and 100 μl low-serum media was added to each well and incubated at 37°C, 5% CO_2 for 6 days. Cells were fed by topping up with fresh low-serum media every 2-3 days. After six days cell viability was assessed by the MTS assay (section 2.1.4) and percentage survival compared to non-infected control cells calculated, after removal of background levels from wells with media alone. Sigmoid dose-response curves were generated using GraphPad Prism 4 software in order to calculate the IC_{50} values: the number of pfu required to reduce cell numbers to 50% of the control.

2.3 Animal techniques

All studies involving laboratory animals were conducted in accordance with the UK Home Office Animals (Scientific Procedures) Act 1986, under Project Licence PPL 40/2262 and Personal licence PIL 30/6746.

Female nude mice, between 6-9 weeks of age, were used for all experiments, except where specifically indicated in the text.

2.3.1 Housing conditions

Mice were housed in temperature and humidity-controlled conditions (20-22°C) at Biomedical Services, John Radcliffe Hospital, Oxford. Mice were given free access to sterile tap water and formulated diets, housed in environmentally-enriched individually ventilated cages with no more than 6 mice per cage, and exposed to a 12-hour light-dark cycle.

2.3.2 Diets

Mice were fed freely on irradiated formulated rat and mouse diet (B&K Universal, Aldbrough, UK). The composition of this diet in g/kg was: cereal products 769.5, Hipro soya 140, animal proteins 50, soya oil 8, vitamin and mineral mix 32.5.

2.3.3 Generation of human ovarian cancer xenografts

SKOV cells were grown in 175 cm^2 tissue culture flasks, trypsinised and resuspended in PBS to a concentration of 2 x 10^7 cells/ml. Female nude mice aged 6-9 weeks were injected i.p. with 1 x 10^7 SKOV cells (0.5 ml) using a 25G needle. Tumours cells were allowed to establish (4-6 weeks) until mice developed palpable masses and/or small amounts of ascites. For survival studies, humane end points were established and refined. Any mouse showing signs of reduced movement, hunching, poor condition, weight loss, jaundice, ascites formation, anaemia or large tumour masses was euthanized by a Schedule 1 approved method.

2.3.4 Virus transduction studies

Adenovirus (AdCMV-Luc $_{\Delta E1}$ 5 x 10^{10} v.p.) was injected i.p. to tumour bearing mice. Twenty-four hours later mice were harvested, blood taken for determination of liver function (alanine transaminase and aspartate transaminase) and the following organs collected by careful dissection: tumours; peritoneal wall; diaphragm; liver; spleen; ovaries/uterus/bladder; kidneys; heart; and lungs. Organs were homogenised using a motorised homogeniser (IKA ultratorax T18, Fisher) in Promega lysis buffer (300 mg tissue/ml of lysis buffer). Using a wide bore pipette tip, 25 μl aliquots were analysed in a luminometer with automatic injection of 25 μl of beetle luciferin (see section 2.2.8.1). Luminescence was detected over 10 seconds with a 2 second delay. All samples were performed in triplicate to generate the mean and SEM.

2.3.5 DNA extraction

DNA was extracted from murine organs to enable determination of virus content by quantitative polymerase chain reaction (Q-PCR). Organs were homogenised using a motorised homogeniser (IKA ultratorax T18, Fisher) in Promega lysis buffer (300 mg tissue/ml of lysis buffer). DNA was extracted from a 200 μl aliquot of tissue lysate using the Qiagen QIAmp DNA

mini kit according to manufacturer's instructions. The purified DNA was eluted from the Qiagen column in 200 μl of elution buffer and 5 μl aliquots were used in each Q-PCR reaction (in triplicate).

2.3.6 Assessment of liver transaminase levels

Mice were injected i.p. with adenovirus (AdCMV-Luc$_{\Delta E1}$ 5 x 10^{10} v.p.) which was either unmodified or coated with polymer or EGF-polymer. Twenty-four hours after virus injection, mice were harvested and blood taken by cardiac puncture (~ 1ml). Serum was separated from blood samples (spun 10 min, 13,000 rpm in a microcentrifuge) and 10 μl aliquots added to 90 μl water in a microcuvette (Fisher). Infinity™ AST or ALT reagent (Thermo) (1 ml) was added to the diluted serum immediately before analysis, and absorbance at 340 nm read on a spectrophotometer. Activity in units per litre (U/l) was then calculated from absorption, allowing for sample dilution.

2.3.7 Assessment of hepatic pathology

At post-mortem examination murine livers were removed, fixed in 4% formaldehyde/PBS and embedded in paraffin prior to sectioning (7 μm). Sections were de-waxed and re-hydrated by immersing slides in a slide rack through a series of staining dishes as follows:

Histoclear (RA Lamb, UK)	3 min
Histoclear	3 min
99% Industrial methylated spirit (IMS)	1 min
99% IMS	1 min
99% IMS	1 min
95% IMS	1 min
Running tap water	1 min

Slides were immersed in haematoxylin (Vector) for 10 min and rinsed in running tap water to 'blue' for 1 min. Slides were counter-stained for 4 min in eosin (Vector) and rinsed in running tap water for 30 seconds. Slides were dehydrated by reversing the re-hydration protocol and

mounted with DPX. Slides were examined and scored for degree of liver pathology by an independent histopathologist (Dr S. Survana), who was blinded to the treatment groups and the nature of the experiment.

2.4 Statistical analysis

GraphPad Prism3 or Prism4 software was used to calculate mean and standard deviation (SD) or standard error of the mean (SEM) for experiments performed in triplicate. Numerical data were log transformed, to normalise data and produce similar variances between data sets, and analysed by analysis of variance (ANOVA) (two-tailed). Post-hoc analyses were performed using Bonferroni's (allowing for comparison between selected groups) or Dunnett's corrections (comparison of several groups to a control group) where appropriate, to reduce the probability of a type I error (rejecting the null hypothesis when it is true), which is otherwise a risk when performing multiple comparisons. Bonferroni's approach multiplies each individual P-value by the number of tests carried out, so generating an adjusted P-value. Non-parametric data were analysed by the Kruskal-Wallis method (an extension of the Wilcoxon rank sum test) and is the non-parametric equivalent of ANOVA, with Dunn's correction for multiple analyses (a non-parametric post-hoc test to limit type I errors, if multiple groups are analysed) where appropriate. Categorical data were analysed by Chi-square analysis following generation of contingency tables. Survival data were analysed using GraphPad Prism4 software by Kaplan-Meier analysis.

3 Production of EGFR-positive, CAR-negative cell line

3.1 Introduction

Previous work has demonstrated that coating adenovirus with reactive pHPMA was able to prevent most CAR-mediated binding (Fisher *et al.* 2001). However, as CAR-mediated uptake is not completely ablated, a low level of EGFR-mediated uptake could be masked by the residual CAR-mediated uptake. Therefore, I aimed to produce a CAR-negative EGFR-positive cell line with which to investigate EGFR-mediated uptake in the absence of CAR. The murine fibroblast cell line A9, does not express CAR or EGFR, and so provides an attractive tool to investigate EGF-retargeting of adenoviral transduction, by generating stably transfected cells lines that express EGFR, but not CAR. A CAR-positive A9 cell line has already been produced (Mayr and Freimuth 1997) and can therefore be used for comparison.

The specific aims of this piece of work were therefore:

- To transfect murine A9 fibroblasts with a plasmid encoding human EGFR and select clones stably expressing EGFR;
- To determine whether the transfected EGFR was functional and could provide an appropriate target for assessment of adenovirus retargeting.

3.2 Methods and Results

3.2.1 EGFR containing plasmid

Plasmid pUSEampEGFR (Upstate, NY, USA) encodes the gene for human EGFR under the control of a CMV promoter. It also encodes the neomycin/Geneticin (Neo) resistance gene, which enables antibiotic selection of transfected cells (see Figure 3-1).

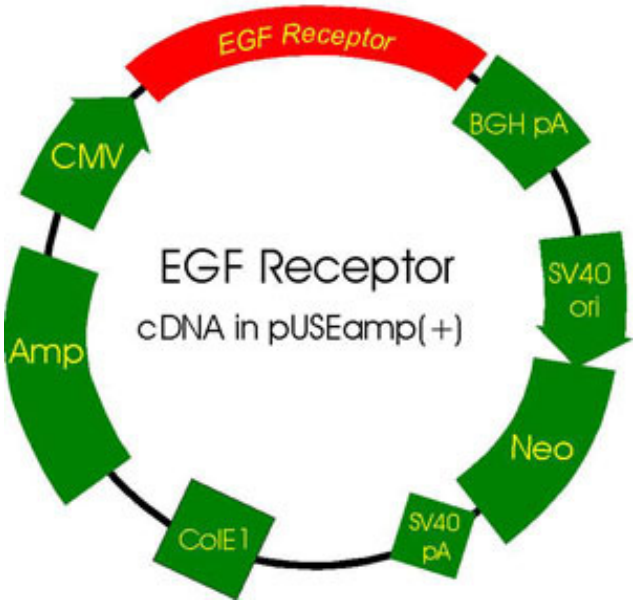


Figure 3-1 Diagrammatic representation of the pUSEampEGFR plasmid [1]

3.2.2 Determination of concentration of Geneticin (G418) required for plasmid-positive A9 cell selection

In order to determine the concentration of G418 (GIBCO) required to positively select transfected A9 cells, cells were grown in media containing increasing concentrations of G418. A9 cells were initially cultured in normal growth media (see section 2.1.1.1) for 48 hours. Subsequently, media were removed and replaced with media containing increasing concentrations of G418 (0 to 1,200 μg/ml). Cells were incubated for 96 hours before an MTS assay (see section 2.1.4) was performed to assess cell viability. A G418 concentration of 800 μg/ml resulted in less than 2% cell viability (see Figure 3-2).

[1] Plasmid diagram courtesy of Upstate, NY

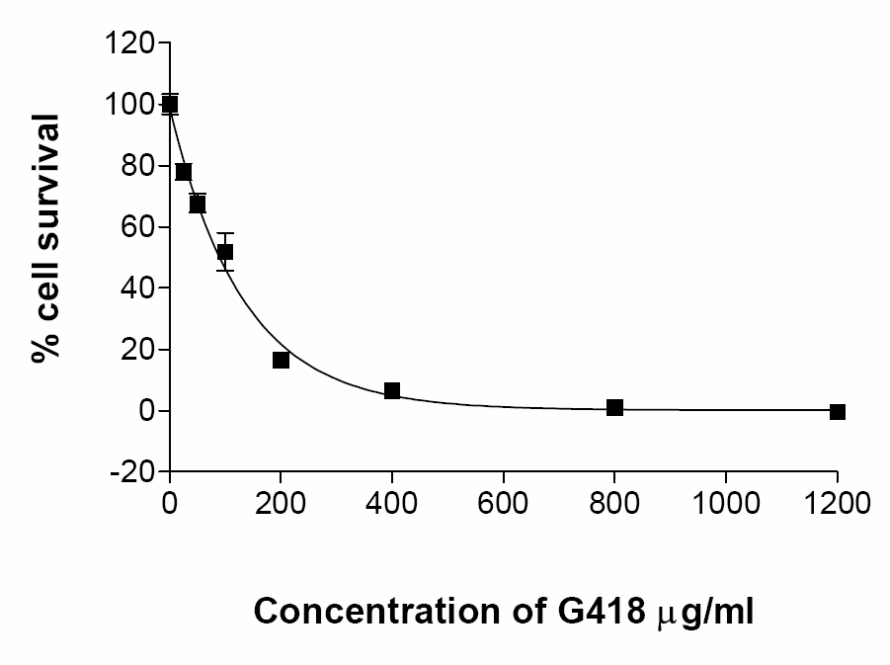


Figure 3-2 Survival of A9 mouse fibroblasts with increasing concentration of Geneticin (G418)

A9 cells (5 x 10^3 cells per well) were seeded in a 48 well plate in serum-positive growth media. After 24 hours, increasing concentrations of G418 were added to wells in triplicate. Cells were cultured for a further 96 hours before performing an MTS assay. 0% survival was achieved at a G418 concentration of 800 μg/ml. Mean results are shown with error bars +/- SEM for samples in triplicate.

3.2.3 Transfection of A9 cells with EGFR plasmid

A9 cells (3 x 10^5 cells/well) were transfected with DOTAP based lipoplexes containing plasmid pUSEampEGFR (see section 2.1.2) and transfected cells selected with G418 containing media. Colonies (100-200 cell size) were selected using glass cloning cylinders (Sigma). The cells were passaged in G418-containing growth media until there were sufficient cells to be grown in 25 cm^2 tissue culture flasks (Starsted Inc, USA); this typically took 5-6 passages (4-5 weeks). At this stage cell clones were examined for EGFR status by flow cytometry (see section 2.1.6) by labelling with a mouse anti-EGFR antibody (with appropriate isotype control) and a goat anti-mouse secondary antibody labelled with RPE (Figure 3-3).

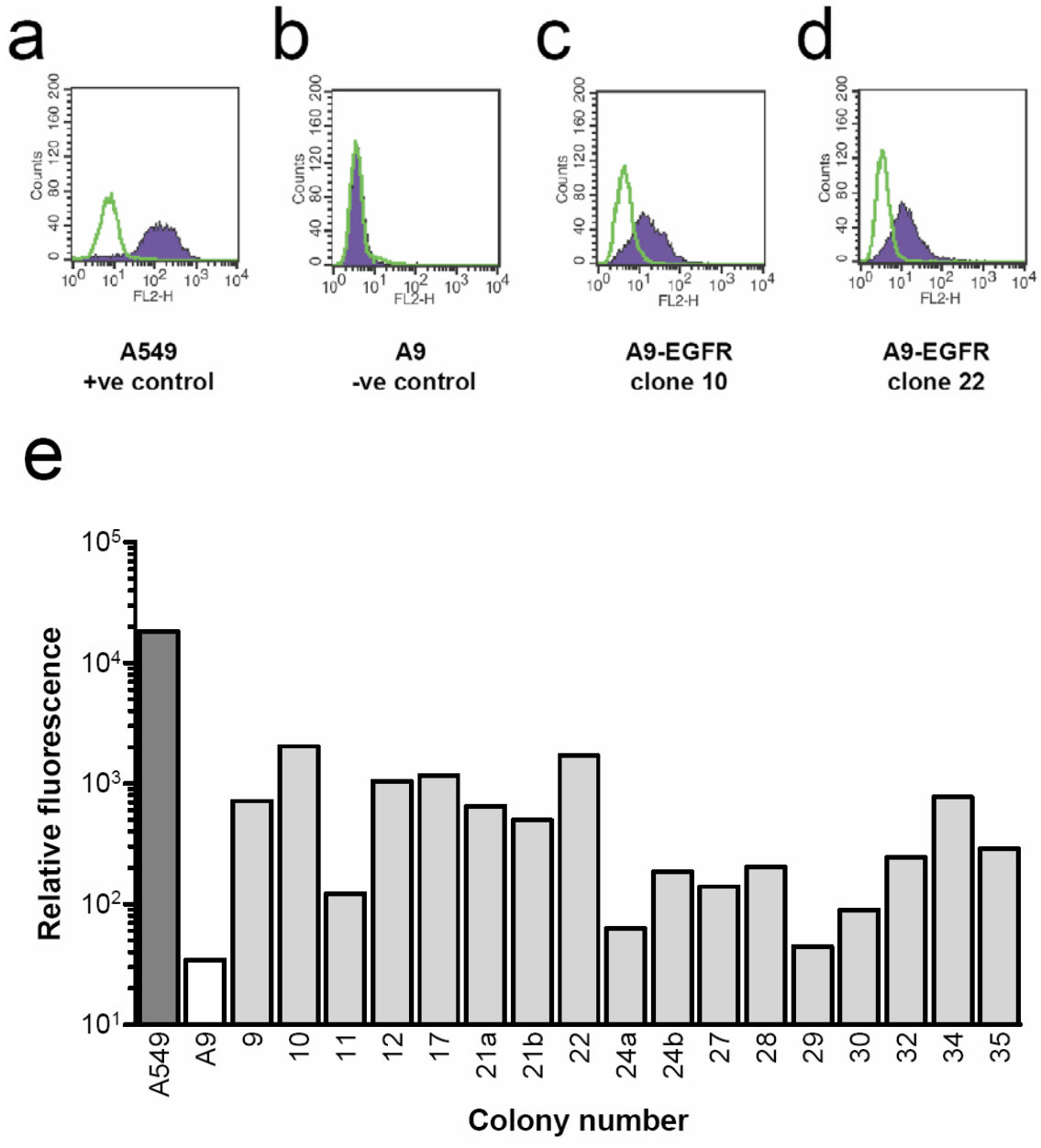


Figure 3-3 Assessment of EGFR expression in transfected A9 clones

A9 cells were transfected with pUSEampEGFR and colonies selected from cells grown in media containing 800 μg/ml G418. Colonies were passaged until they could be grown in 25 cm^2 culture flasks. At this stage cells were screened for presence of EGFR by dual staining with mouse anti-EGFR antibody and goat anti-mouse antibody, conjugated to RPE, and analysed by flow cytometry at 585 nm. Results for anti-EGFR antibody samples are shown as a purple shaded histogram, with the isotype antibody negative control as an unfilled green histogram: (a) A549 cells (positive control); (b) A9 cells (negative control); (c) A9-EGFR transfected colony C10; (d) A9-EGFR transfected colony C22; (e) relative fluorescence (% positive cells x GMean of positive population) of positive cells in each colony: A549 positive control (dark grey bar); A9 negative control (white bar). The results for A9-EGFR colonies C10 and C22 are representative of experiments performed at regular intervals to confirm stable EGFR expression over a twelve month period (see Figure 3-4).

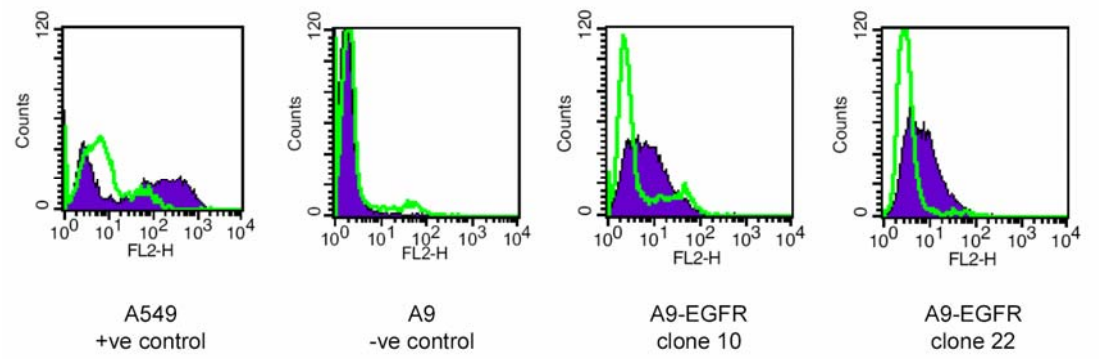


Figure 3-4 Assessment of EGFR expression in transfected A9 clones after 12 months of passage

A9-EGFR clones were passaged for 12 months in the continuous presence of G418 selection (800 μg/ml). A9-EGFR clones 10 and 22 were regularly screened for presence of EGFR by dual staining with mouse anti-EGFR antibody and goat anti-mouse antibody, conjugated to RPE, and analysed by flow cytometry at 585 nm. Results for anti-EGFR antibody samples are shown as a purple shaded histogram, with the isotype antibody negative control as an unfilled green histogram: (a) A549 cells (positive control); (b) A9 cells (negative control); (c) A9-EGFR transfected colony C10; (d) A9-EGFR transfected colony C22. These data were obtained 12 months after the initial infection, demonstrating that the clone maintained a low but relatively stable expression of EGFR over this time period.

3.2.4 Effect of removing G418 from growth media on EGFR expression levels

It was noted that the level of EGFR expression was low if cells were maintained in media containing G418 at 800μg/ml immediately prior to assessment of EGFR status. G418 is an aminoglycoside, and acts by binding to ribosomes, thereby inhibiting protein synthesis. The EGFR plasmid includes the neomycin resistance gene that encodes an enzyme, which modifies the aminoglycoside, reducing ribosomal binding and limiting drug toxicity. However, even with the neomycin resistance gene overall protein production might be affected. Removal of selective pressure has been shown to result in silencing of CMV promoter driven transgenes by DNA methylation (Gram *et al.* 1998); hence there might be an optimal time to withdraw G418 to produce maximal EGFR levels.

Flasks (25cm^2) of A9-EGFR clones C10 and C22 were grown with G418-containing media, which was replaced with normal growth media at different time points prior to analysis of EGFR

levels (see section 2.1.6). Results (Figure 3-5) suggest that G418 does inhibit EGFR production, and removal of G418 leads to a burst in EGFR levels. EGFR levels then fall, presumably due to reduced receptor production, and internalisation and degradation of existing receptors. Thus, the optimum time for removing G418 prior to experiments, which require high EGFR levels, would be between 5.5 and 24 hours. Since EGFR levels were relatively stable between 8-24 hours, this period of G418 withdrawal was chosen for subsequent experiments. Absence of G418 may also be necessary in experiments where reporter transgene expression is a surrogate for cellular uptake of adenovirus is, as these data suggest that the reporter transgene would also be suppressed by high concentrations of G418, and 24-hour withdrawal would avoid this effect.

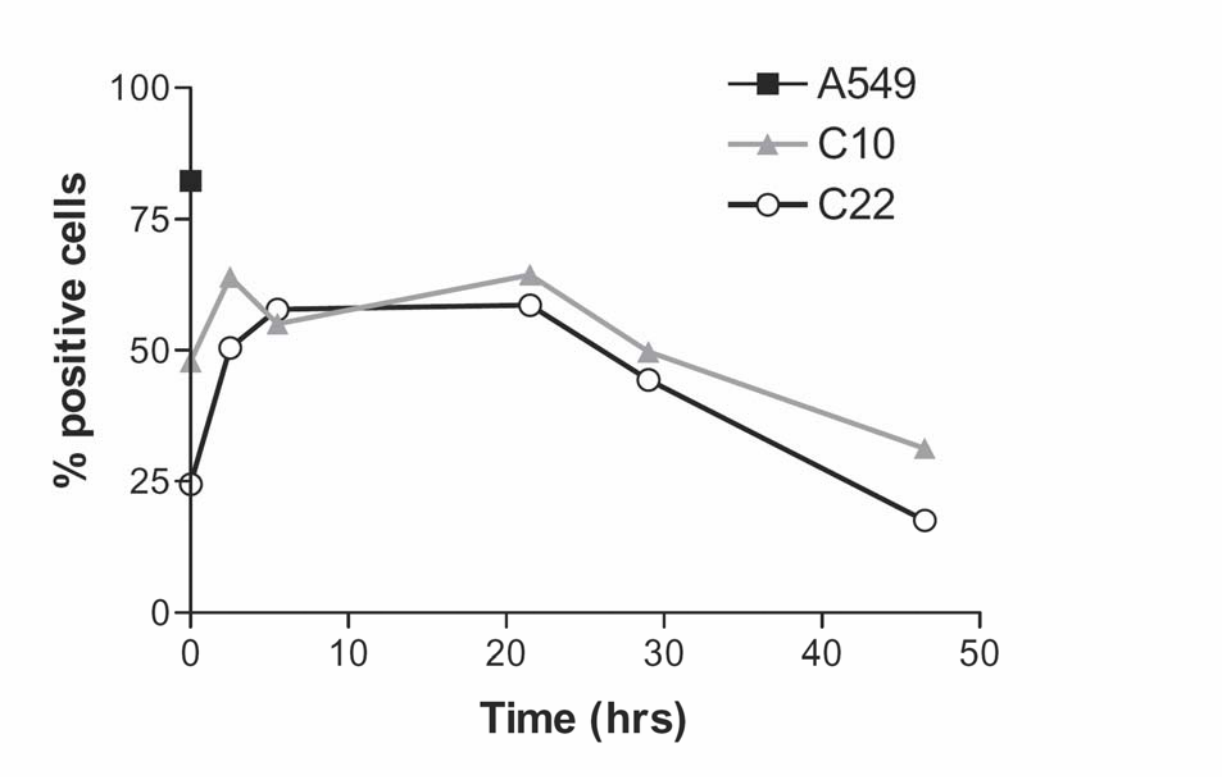


Figure 3-5 Change in EGFR expression over time following G418 removal

A9 clones stably transfected with pUSEampEGFR were grown in 25cm^2 flasks and normal growth media containing G418 at a concentration of 800 μg/ml. Media were removed and replaced with G418-free normal growth media at various time points prior to analysis of EGFR levels by flow cytometry at 585 nm. The graph demonstrates % of positive A9-EGFR C10 clones (light grey triangles) and A9-EGFR C22 clones (open circles). 2 x 10^4 cells were counted in each sample.

3.2.5 Functionality of transfected EGFR

3.2.5.1 Assessment of EGFR internalisation by flow cytometry

During adenovirus infection the fibre knob of adenovirus binds to the Coxsackie-adenovirus receptor, the penton base and integrins on the cell surface interact, leading to adenovirus internalisation and transfer to an early endosome (Meier and Greber 2004). EGFR internalises via endosomes once bound to its ligand, EGF, and is therefore an attractive alternative adenovirus receptor for experimental studies. EGF remains bound to the receptor, and the receptor and ligand are transferred to early then late endosomes, before being degraded in lysosomes (Wada *et al.* 1992).

A9-EGFR transfected clones were assessed for their ability to internalise bound EGF by flow cytometry (see section 2.1.9.1). Using fluorescein labelled EGF, fluorescein fluorescence is quenched as pH falls from 7 to 5 (Yamashiro and Maxfield 1987). A fall in fluorescence might therefore indicate EGF-fluorescein internalisation into acidified endosomes. Monensin, a monovalent ion-selective ionophore, inhibits endosomal acidification by integrating into endosomal membranes and facilitating the transmembrane exchange of sodium ions for protons (Mollenhauer *et al.* 1990). Monensin therefore provides a non-quenched control to evaluate the total amount of EGF-fluorescein entering cells. A549 cells had higher levels of fluorescence following treatment with monensin (see Figure 3-6), probably representing EGF-fluorescein that had entered acidified intracellular compartments. A9-EGFR clones C10 and C22 also showed slightly greater fluorescence following administration of monensin. This suggests that the receptors are internalised following EGF binding in the A9-EGFR clone 10, since the change in fluorescence was consistently positive, following addition of monensin, although as EGFR expression on the A9-EGFR clones is very low, the absolute change in fluorescence with and without monensin is slight.

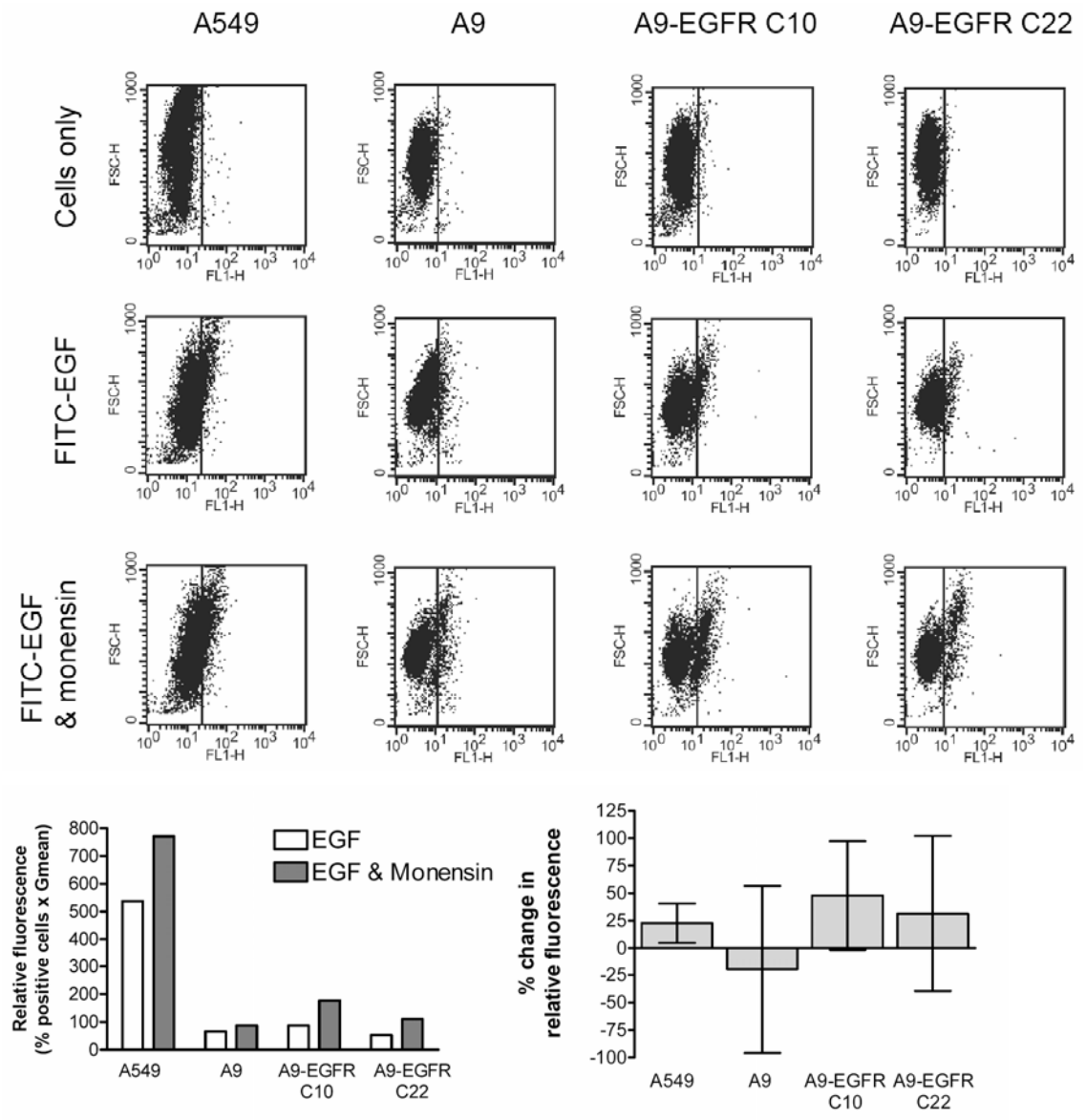


Figure 3-6 Flow cytometry assessment of internalised EGFR following incubation with an EGF-Fluorescein conjugate

Cells were grown in 25 cm^2 flasks until ~90% confluent, with G418 omitted 24 hours prior to the experiment. Cells were washed in ice cold PBS, scraped to detach, spun at 1,000 rpm for 5 min at 4°C to pellet and resuspended in 0.1% BSA in DMEM. Aliquots (50 μl) of cell suspension were transferred to a 96 well v-bottomed plate. Cells were pre-incubated with monensin, to a final concentration of 50 μmol/l, or an ethanol control for 30 min at 4°C. Fluorescein-labelled EGF was then added to the wells to a final concentration of 0.5 μg/ml. Cells were incubated at 4°C for 45 min, washed twice with PBS, and incubated at 37°C for 30 min. Cells were immediately put on ice and analysed by flow cytometry at 530 nm. 1 x 10^4 cells were counted per sample. These results are representative of three independent experiments. Mean percentage change in relative fluorescence was obtained from the results of three independent experiments. There was a large inter-experimental variation in level of EGF-labelling of EGFR positive control cells (10-40%), making comparison between days difficult. Bars represent mean values and error bars +/- SD.

In addition, although a similar pattern was achieved on repeated testing, it was difficult to combine results obtained on different days, as the level of labelling with EGF-FITC of the A549 EGFR-positive control cells was variable (10-40% positive) although intra-experimental results showed little intra-experimental variation in similar labelling experiments performed in triplicate (data not shown) and so the combined data are not statistically significant. This experiment was not performed in triplicate because of concerns that cell fluorescence could change during the time taken to performed large numbers of measurements by flow cytometry, since the cells could not be fixed following the 30 min incubation at 37°C. Cells could not be fixed, e.g. with paraformaldehyde solution, because this would have removed the effect of endosome acidification and hence negated the effect of adding monensin to experimental wells.

3.2.5.2 Assessment of EGFR internalisation by immunocytochemistry

EGFR internalisation following binding to its ligand, EGF, can be demonstrated by immunocytochemistry (Haigler *et al.* 1978). A9-EGFR clones were stimulated with EGF to allow EGFR internalisation (see section 2.1.9.2). Cells were fixed and labelled for EGFR (photomicrographs taken with a confocal microscope, Figure 3-7). In the A549 EGFR -positive control cells there were higher levels of EGFR expression compared with the A9-EGFR clones, which have much lower EGFR levels. A549 cells were used as an EGFR-positive control, as levels of EGFR expression were more similar to the A9-EGFR clones, compared with A431 cells, which have several orders of magnitude greater EGFR expression (see Figure 4-8). In the EGFR-positive cell lines the pattern of EGFR expression becomes more punctated and moves away from the cell membrane, becoming more perinuclear, compared with the more generalised staining in the unstimulated cells. In this early experiment, it had not been appreciated that the confocal microscope (located in another department) did not have a laser capable of visualising DAPI-stained nuclei, so that cells were located using fluorescence microscopy and then imaged using laser confocal microscopy, on the same microscope. In future experiments, the nuclear counterstain, TO-PRO-3, was added to Vectashield in order to visualise the nuclei with the far red wavelengths. In addition, the cells in this experiment were not serum starved, and so there is a relatively high background level of intracellular punctate

staining of EGFR, which was reduced in subsequent experiments by introducing a period of serum-starvation.

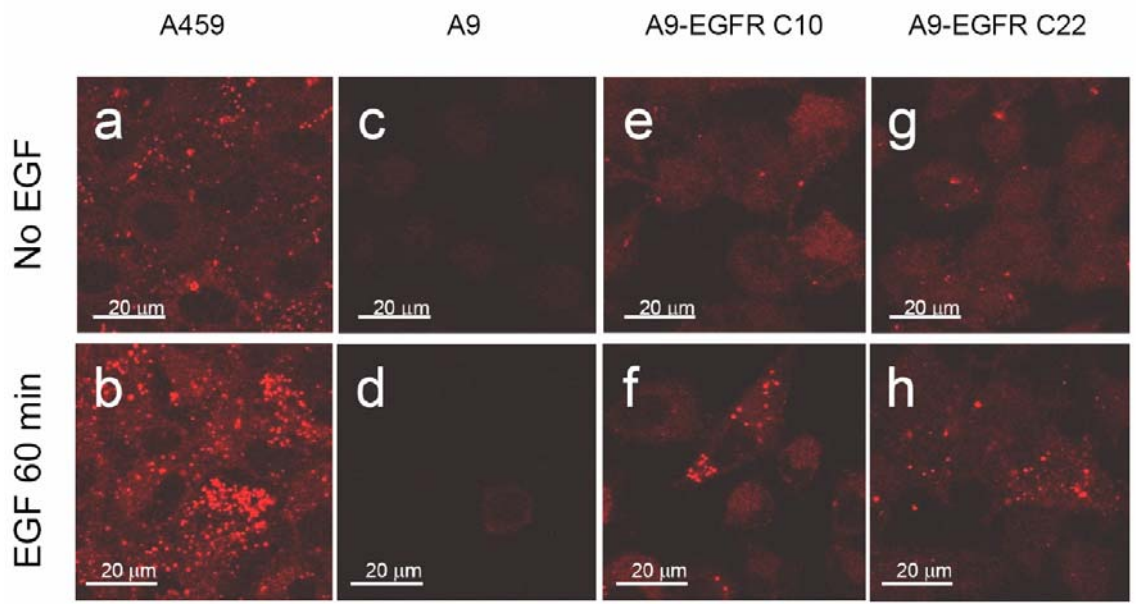


Figure 3-7 Cellular internalisation of EGFR following stimulation with EGF

Cells were suspended in normal growth media containing G418 (800 µg/ml) in an 8-well chamber slide (2 x 10^4 cells per well) and incubated at 37°C in 5% CO_2 for 48 hrs. Serum was then replaced with G418-free normal growth media and incubated for 24 hrs. Cells were incubated with EGF at 200ng/ml on ice for 60 min. Cells were washed x3 and incubated at 37°C in 5% CO_2 for 60 min. Cells were fixed with 4% paraformaldehyde and blocked with horse serum. Cells were stained using anti-EGFR (60 min RT), a biotinylated secondary anti-mouse antibody (30 min RT), a streptavidin/biotin/alkaline phosphatase complex (30 min RT) and the Vector red substrate (30 min RT). Cells were then mounted in Vectorshield hardset with DAPI. Photomicrographs were taken using a confocal microscope (Nikon Optiphot-2 upright microscope, fitted with a 60x oil immersion objective; Bio-Rad MRC1024 with Krypton/Argon lasers. Images were processed using LaserSharp 2000 image processing software (30% power, 2.0 iris, 1393 gain, 0.0 offset). Images (a), (c), (e) and (g) show cells incubated without EGF, images (b), (d), (f) and (h) show cells incubated with EGF. (a) and (b) A549 cells (positive control); (c) and (d) A9 cells (negative control – EGFR-negative); (e) and (f) A9-EGFR clone C10; and (g) and (h) A9-EGFR clone C22. Internalisation of EGFR in A9-EGFR clones was observed in at least three independent experiments.

3.2.5.3 Assessment of EGF-mediated EGFR phosphorylation in A9-EGFR clones

The EGFR is a transmembrane receptor that dimerises upon binding to its ligand, EGF. This dimerisation activates the tyrosine kinase activity of the intracellular portion of EGFR, leading to autophosphorylation of tyrosine residues (Schlessinger and Ullrich 1992). Signal transduction is then mediated through binding of signalling proteins to the phosphotyrosine (p-Tyr) residues. It was not known whether receptor stimulation and phosphorylation would be a necessary step in EGF-retargeted virus infection. Hence, I now sought to determine whether EGFR in the A9-EGFR clones was still capable of undergoing auto-phosphorylation on ligand binding.

Cells were prepared and stimulated with EGF as described in section 2.1.10.6. A protein assay was performed (section 2.1.3) and equal amounts of protein from each sample loaded onto a 7.5% SDS/polyacrylamide gel. The gel was blotted onto a nitrocellulose membrane overnight, and then probed with a goat anti-pEGFR antibody, followed by an anti-goat horseradish peroxidase-conjugated (HRP) secondary antibody. The HRP was detected using luminescence imaging (Lumiglo® reagent). Results (Figure 3-8) show positive bands of 170 kDa in the positive control cell line A549, with the intensity increasing up to 30 min incubation. No bands were seen in the A9 negative control cell line or the A9-EGFR clones. It is possible that no bands were seen because the expression of EGFR in A9-EGFR clones is below the threshold of detection for this method. Unfortunately, there are no loading controls available for this experiment, since after stripping the first labelling antibody from the nitrocellulose blot, prior to re-probing with a loading control antibody (β-actin), there were no visible bands, despite multiple attempts with this technique.

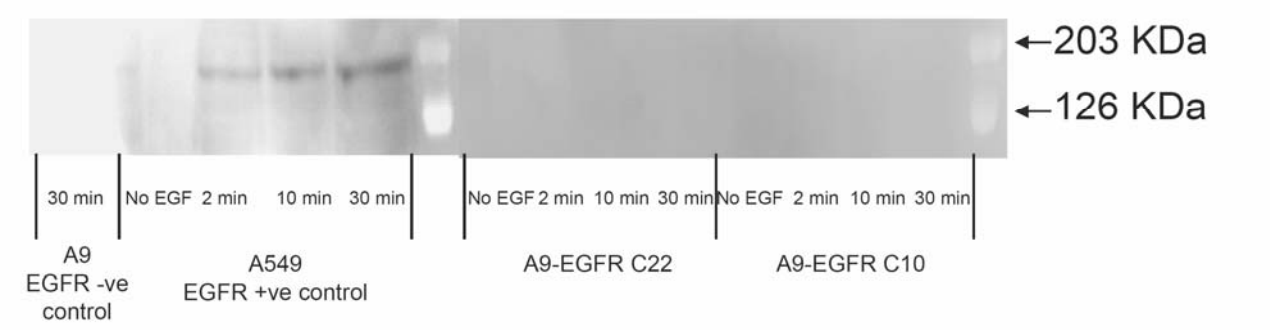


Figure 3-8 Western blot of A9-EGFR clones stimulated with EGF and probed with an anti-pEGFR antibody

Cells (5 x 10^5 per well) were plated out in 6 well plates in G418-free normal growth media overnight. Cells were then serum-starved for 4 hours. Cells were stimulated with 100 nmol/l EGF for up to 30 min at 37°C in 5% CO_2. Cells were lysed with Promega lysis buffer and a protein assay performed on the cell lysate. Equal amounts of protein (20 μg) from each sample were loaded onto a 7.5% SDS/polyacrylamide gel and run at 100 V for 1-2 hours. The gel was blotted overnight onto nitrocellulose membrane and probed with anti-pEGFR antibody and an anti-goat-HRP secondary. The blot was developed with Lumiglo® and visualised in a gel imaging system. Results are representative of at least three independent experiments.

3.2.5.4 Assessment of down-stream phosphorylation in A9-EGFR clones

Since phosphorylation of EGFR was not demonstrated for the A9-EGFR clones, down-stream signalling was investigated, as this may be amplified compared to the initial signal and several phosphorylated proteins might give a detectable signal. Cells were prepared and stimulated with EGF as above (section 2.1.10.6). Equal quantities of protein were loaded onto a 7.5% SDS/polyacrylamide gel. The gel was blotted onto a nitrocellulose membrane overnight and then probed with a polyclonal mouse antibody p-Tyr antibody conjugated to HRP. This antibody binds to any phosphorylated tyrosine residues, not just those on EGFR. In Figure 3-9 an additional band at ~35-36 kDa can be clearly visualised in A549 and A9-EGFR C10 cells stimulated with EGF for 30 min. A 35-36 kDa phosphorylated cytosolic protein was previously described following EGFR stimulation (De *et al.* 1986; Fava and Cohen 1984; Kwok and Yip 1987), and has been identified as a subunit of p60 c-src, which has a major role in the down-stream tyrosine kinase signal transduction cascade (Soric and Gordon 1986). This was a preliminary attempt at Western blotting for EGFR, and cells were not scraped to detach cell membranes; in addition a relatively weak cell lysis buffer was used (Promega). It is therefore likely that membrane bound proteins were under-represented in this experiment, perhaps explaining the lack of a 170 kDa band for pEGFR in any of the samples.

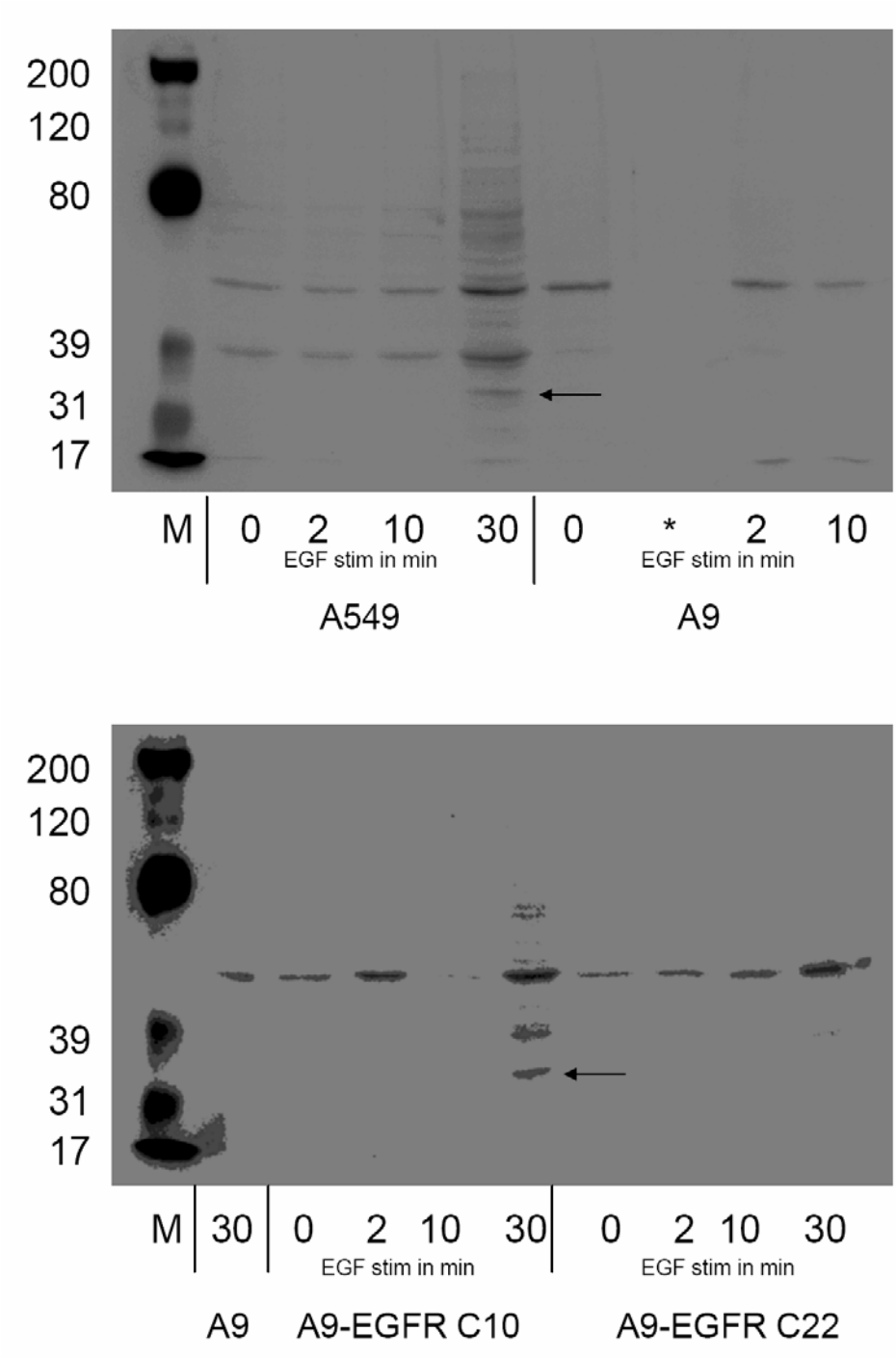


Figure 3-9 Down-stream signalling in clone A9-EGFR C10 following EGF stimulation

Cells (5 x 10^5 per well) were plated out in 6 well plates in G418-free normal growth media overnight. Cells were stimulated with 100 nmol/l EGF for up to 30 min at 37°C, 5% CO_2. Cells were lysed with Promega lysis buffer and a protein assay performed on the cell lysate. Equal amounts of protein from each sample (20 µl) were loaded onto a 7.5% SDS/polyacrylamide gel and run at 100 V for 1-2 hours. The gel was blotted overnight onto nitrocellulose membrane and probed with anti-pTyr 100-HRP antibody. The blot was developed with Lumiglo® and visualised in a gel imaging system. M = markers, 0-30 = time in min for EGF stimulation, * = blank lane. Gels were run, blotted and labelled together. Alpha imager settings: exposure 10 min; aperture fully open; sensitivity normal/high resolution. 35 kDa band visible in A549 and A9-EGFR C10 at 30 min after EGF stimulation – highlighted with arrows.

3.3 Discussion

EGFR positive A9 clones were generated by transfection with the plasmid pUSEampEGFR. Following G418 selection, 36 clones were grown until they could be analysed for EGFR expression by flow cytometry. The two most positive clones, A9-EGFR C10 and A9-EGFR-C22 were passaged for over six months, with regular analysis by flow cytometry for EGFR expression. These two clones maintained a low but relatively stable level of EGFR expression over this time, and continued to express EGFR following storage at −80°C.

A9 cells expressing engineered EGFR were tested for EGF-mediated internalisation. Following incubation with EGF-FITC, A9-EGFR cells had greater levels of fluorescence with the addition of monensin, suggesting that EGF-FITC was otherwise quenched in the acidic environment of early endosomes. This would indicate that EGFR in these cells might be able to internalise on ligand binding. Immunocytochemistry for EGFR in cells stimulated with EGF demonstrated a difference in the cellular distribution of EGFR compared to non-stimulated cells, although levels of EGFR in A9-EGFR clones were very low. Staining of EGFR was initially diffuse on the cell surface prior to stimulation, but became more punctate in pattern and peri-nuclear in localisation following addition of EGF and incubation at 37°C. This change would have been clearer had the cells been serum-starved prior to the experiment and had a nuclear-counterstain visible using the confocal microscope been employed, as in subsequent experiments (see Chapter 4).

Autophosphorylation of transfected EGFR could not be demonstrated by Western blotting, probably because the level of EGFR was below the level of detection for this assay. In addition, improved labelling of low-level phosphorylated proteins may have been achieved using an alternative block to milk. I have recently learned that bovine serum albumin (BSA) is commonly used as an alternative block in western blots for phosphorylated proteins , since BSA avoids over-blocking of relevant proteins. However, there was some evidence of down-stream signalling stimulated by EGF in the A9-EGFR clone C10 at 30 min, which was also observed in the EGFR-positive A549 cell line control.

The observation that levels of EGFR, expressed under the control of a CMV promoter, fell once the selection pressure of G418 had been withdrawn has been noted previously. It is thought to be due to silencing of viral and bacterial promoters by the mechanism of DNA methylation, since it has been shown that this can be reversed by using agents which block DNA methylation (Gram *et al.* 1998). Because of this, long-term gene therapy regimens often utilise human promoters, which gives additional benefits of regulating gene expression to more physiological levels.

These data demonstrate that I was able to produce a stably transfected cell line which expressed EGFR in the absence of CAR. Taken together, data were suggestive that the EGFR was able to internalise into endosomes and that there was some evidence of down-stream signalling following EGF stimulation in the A9-EGFR C10 clone. The A9-EGFR clones C10 and C22 are therefore potentially useful as a model for assessing whether EGF-polymer is able to retarget adenovirus specifically via the EGFR, without interference from the Coxsackie adenovirus receptor, which is the normal receptor for group C adenoviruses.

It can be seen that there was some difficulty in producing a stably transfected cell line that expressed high levels of CAR. An alternative strategy would have been to use a lentivirus to achieve a cell line stably expressing EGFR. However, since positive cell lines had been produced, I decided to use them to determine whether the low levels of EGFR could mediate EGF-retargeted adenovirus transduction.

4 *In vitro* activity of EGF- polymer conjugate

4.1 Introduction

CAR-mediated uptake of adenovirus can be successfully ablated by pHPMA coating. Coated adenovirus can then be retargeted by linkage of receptor ligands, such as bFGF which react with remaining reactive groups following virus coating (Fisher *et al.* 2001). However, bFGF is positively charged, able to bind to a variety of cationic proteins, and does not selectively retarget to a cellular receptor. Ideally, for cancer selective or specific targeting a receptor, which is up-regulated or only expressed on cancer cells, would be a better target. EGFR expression is up-regulated in a number of epithelial cancers, including ovarian cancer. Unfortunately, human EGF (hEGF) has two lysine residues, one within the receptor binding site, and was found to be not biologically active once bound to the polymer (Dr Shibani Nicum, D.Phil thesis, University of Oxford) (see Figure 1-4). However, murine EGF has only one reactive amino group at the N-terminal, and is able to bind to human EGFR, albeit with lower affinity than hEGF (mEGF affinity for human EGFR $K_d = 2.7 \times 10^{-10}$ mol/l; hEGF affinity for human EGFR $K_d = 1.9 \times 10^{-10}$ mol/l) (Connolly and Rose 1987). Whereas simple addition of bFGF to coated viruses resulted in covalent linkage of bFGF and efficient virus retargeting, this method did not succeed for murine EGF. Pre-conjugation with polymer, prior to adenovirus coating, was found to be difficult, as the murine EGF demonstrated poor stability in non-aqueous solvents, essential for preserving polymer reactivity to allow subsequent coating of virus. A technique for solubilising murine EGF in DMSO prior to pHPMA pre-conjugation was subsequently developed (Dr Simon Briggs, University of Oxford) producing a well-defined murine EGF-pHPMA product which could be purified to remove free murine EGF. This was shown to have an average of 1.8 murine EGF molecules per pHPMA molecule. This murine EGF-pHPMA was used in the investigations described in this thesis and will be referred to as EGF-polymer. All EGF is murine, unless otherwise stated.

The aims of the studies described in this chapter were therefore to:

- Investigate binding of EGF-polymer to EGFR-positive cells;

- Determine whether EGF conjugated to polymer retained biological activity;
- Investigate retargeting of EGF-polymer coated adenovirus to the EGFR-positive, CAR negative cells, engineered as previously described, and in human cancer cell lines.

4.2 Methods and results

4.2.1 Binding of EGF-polymer to EGFR positive cells

Initial studies determined whether EGF conjugated to polymer was able to bind specifically to EGFR-positive cells. Biotin was used to label EGF-polymer by reacting it with reactive sites on the polymer side chains (polymer chemistry by Dr Simon Briggs) (Figure 4-1a). A negative control, EGF-free, polymer was also biotinylated. SKOV-3 cells (EGFR positive) and K562 cells (EGFR negative) were incubated with EGF-biotin-polymer or the biotin-polymer control and polymer-binding to cells analysed by flow cytometry using an avidin-Texas red label (see section 2.1.7). Figure 4-1 demonstrates that EGF-biotin-polymer was able to bind to EGFR-positive SKOV-3 cells, but not EGFR-negative K562 cells, thus demonstrating that EGF-polymer binding to cells is dependent on the EGF and is not a non-specific polymer effect.

4.2.2 EGF-polymer ability to stimulate EGFR tyrosine kinase activity

To determine whether EGF, once conjugated to polymer, still had biological activity EGF-polymer conjugate was incubated with serum-starved EGFR-positive cells and cell lysates were examined by western blotting for evidence of phosphorylated EGFR (pEGFR) (see section 2.1.10). Figure 4-2a shows a western blot of A431 cells, stimulated with 300 ng/ml EGF (positive control) and dilutions of EGF-polymer conjugate. Using Image J software (National Institute of Health) band density was measured and pEGFR values adjusted for β-actin loading (Figure 4-2b). pEGFR values were used to generate an EGF-polymer conjugate standard curve. The equivalent EGF-polymer conjugate concentration for the 300 ng/ml EGF band (β-actin adjusted) was then extrapolated from the EGF-polymer conjugate standard curve using Prism3 software. EGF at a concentration of 300 ng/ml gave an equivalent band density to approximately 3,000 ng/ml of EGF-polymer conjugate.

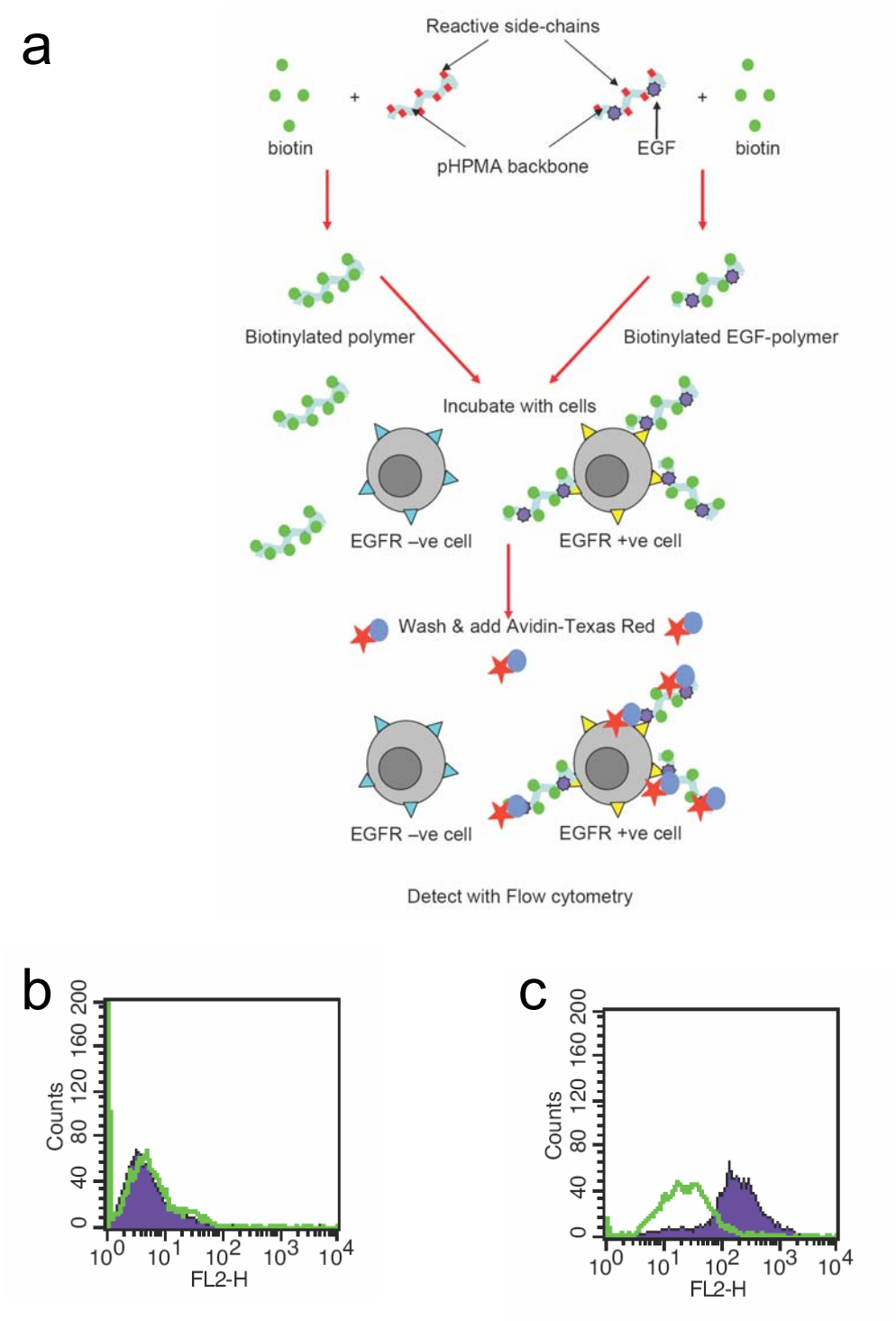
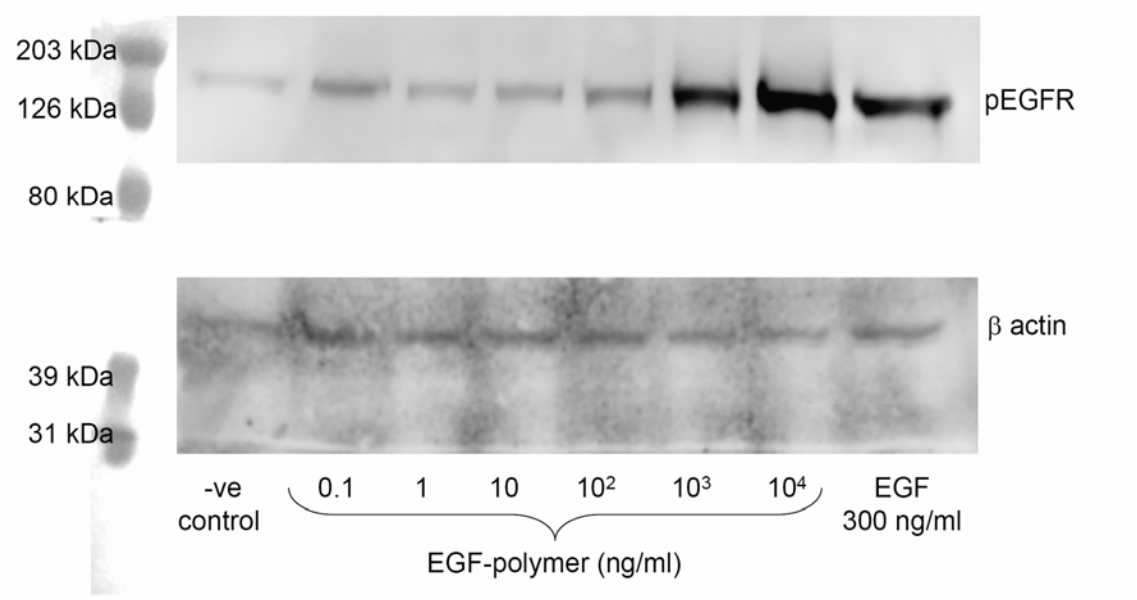


Figure 4-1 Flow cytometry assessment of EGF-polymer binding to EGFR positive and negative cell lines

Biotin was bound to EGF-conjugated polymer via the unreacted side chains (a). An EGF-free biotin-polymer control was also produced. EGF-biotin-polymer and biotin-polymer was incubated with EGFR-negative K562 cells (b) and EGFR-positive SKOV-3 cells (c) on ice for 40 min. Cells were washed and incubated with avidin-Texas red for 40 min on ice. Cells were washed, fixed with 2% paraformaldehyde and analysed by flow cytometry at 585 nm. Green histograms indicate biotin-polymer binding; the purple shaped histograms indicate the EGF-biotin polymer binding. 1 x 10^4 cells were counted per sample.

a



b

EGF-pc ng/ml	density reading pEGFR	density reading β–actin	results adjusted for β-actin loading	extrapolated [EGF-pc] (ng/ml)
0	6,500	3,700	1.8	
0	3,800	3,800	1.0	
1	3,200	3,400	0.9	
10	3,900	3,700	1.1	
100	5,000	3,900	1.3	
1,000	8,300	3,300	2.5	
10,000	12,600	2,500	5.0	
EGF control (300 ng/ml)	9,400	3,000	3.1	3,000

Figure 4-2 EGF-polymer stimulation of EGFR phosphorylation

(a) Cells (5 x 10^5) were plated out in 6 well plates and incubated overnight in normal growth media. They were then serum-starved overnight prior to stimulation with EGF (300 ng/ml) or EGF-polymer diluted in 0.1% BSA in DMEM. Cells were lysed, a protein assay performed and equal amounts of protein (20 μg) loaded onto a 7.5% SDS gel. The gel was blotted onto nitrocellulose overnight, labelled with a goat anti-pEGFR primary antibody and an anti-goat-HRP conjugated secondary antibody (top panel), or rabbit anti-β-actin and anti-rabbit-HRP conjugated secondary antibody (bottom panel), and developed with Lumiglo. Results are representative of at least three independent experiments. (b) Gel images were analysed using the National Institute of Health (NIH) Image J software to calculate density of pEGFR and β-actin bands. pEGFR values were adjusted for loading using the β-actin values and equivalent concentration of EGF-polymer conjugate required to give a similar density to 300 ng/ml EGF calculated from a standard curve using GraphPad Prism3 software.

The MW of EGF is 6.045 kDa. The MW of the average polymer molecule is 96 kDa. Amino acid analysis of EGF-polymer demonstrates an average of 1.8-2 EGF molecules per polymer (data from Dr S. Briggs). Therefore, approximately 10% of the mass of EGF-polymer conjugate is due to EGF. Thus, a 300 ng/ml solution of EGF contains a similar amount of EGF to a 3,000 ng/ml EGF-polymer conjugate solution (EGF contributes 10% of polymer weight). As EGF at 300 ng/ml gave an equivalent band density to approximately 3,000 ng/ml of EGF-polymer conjugate, this suggests that EGF, once conjugated to the polymer, retains its ability to stimulate EGFR phosphorylation.

4.2.3 EGF-polymer co-localisation with EGFR in vesicles

The next step was to investigate whether EGF-polymer was able to stimulate internalisation of EGFR in a similar manner to EGF, to determine whether EGF still retained this biological activity once it was conjugated to polymer. The biotinylated EGF-polymer conjugate was used to stimulate serum-starved A431 cells. After 60 min cells were fixed with 4% paraformaldehyde and cells were then labelled with an FITC-conjugated anti-EGFR antibody and Texas-red avidin (to label biotinylated EGF-polymer conjugates) (for methods see section 2.1.9.3).

Figure 4-3 demonstrates that EGF-polymer conjugate (shown in red) internalised and in addition was able to stimulate EGFR (shown in green) internalisation whereas the negative control cells retained EGFR at the cell membrane. Indeed, EGF-polymer conjugate co-localised with EGFR where the merged fluorescence is shown in yellow, suggesting that EGF-polymer conjugate internalised into endosomes.

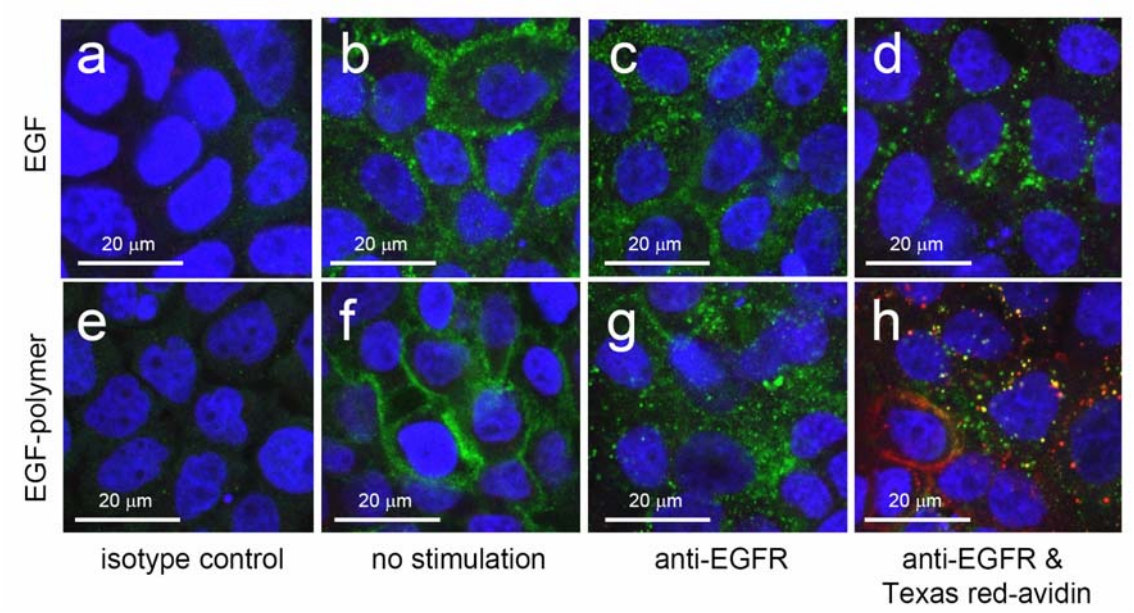


Figure 4-3 EGF-polymer co-localised with EGFR in vesicles following stimulation and time for internalisation

A431 Cells (2 x 10^5 cells/well) were grown on glass chamber slides for 24 hours in normal growth media. Cells were serum-starved for 4 hours. Cells were incubated with EGF at 100 ng/ml or biotinylated EGF-polymer conjugate at 200 ng/ml on ice for 60 min, then incubated at 37°C, 5% CO_2 for 60 min prior to fixing cells with 4% paraformaldehyde. Cells were labelled for EGFR using a mouse anti-EGFR primary antibody and a Fluorescein conjugated anti-mouse secondary antibody and mounted in Vectashield with DAPI containing 2 μmol/l TO-PRO-3 for nuclear counter-staining. Panels show EGFR in green, EGF-polymer conjugate in red and nuclei counterstained in blue. EGFR-EGF-polymer conjugate co-localisation is seen where the merged fluorescence is yellow. (a & e) Primary antibody isotype control; (b & f) no EGF or EGF-polymer stimulation (negative control); (c & d) EGF incubation for 60 min; (g & h) EGF-polymer incubation for 60 min. Following EGFR labelling, cells in panels d & h were incubated with Texas-red avidin to label biotinylated EGF-polymer. Photomicrographs were taken using a confocal microscope (Nikon Optiphot-2 upright microscope, fitted with a 60x oil immersion objective; Bio-Rad MRC1024 with Krypton/Argon lasers (Laser settings. Green: power 30%; iris 1.4; gain 1258; Kalman 2; accumulate x 2. Red: power 30%; iris 2.0; gain 1436; Kalman 2; accumulate x 4. Far red: power 30%; iris 2.0; gain 1182; Kalman 2; accumulate x 2).

4.2.4 EGF-polymer retargeting adenovirus to A9-EGFR clones

4.2.4.1 EGF-polymer retargeting of CAR-negative, EGFR positive cells

EGF-polymer coated AdCMV-Luc$_{\Delta E1}$ (see section 2.2.4-2.2.8.1) was assessed to determine whether it was able to transduce EGFR-positive, CAR-negative cells (see Chapter 3). Transduction of CAR-negative, EGFR-positive cells would demonstrate that EGF-retargeting was truly CAR independent. Figure 4-4 shows that EGF-polymer coating was able to significantly increase levels of transgene expression in A9-EGFR clones (b & c) compared with normal adenovirus or polymer coated virus alone. EGF-polymer coating did not increase levels of transgene expression in control A9 cells not expressing EGFR (a).

4.2.4.2 EGF-mediated retargeting can be blocked with an anti-EGFR antibody

Anti-EGFR antibody (Calbiochem GR01L) binds to EGFR, preventing EGF binding and EGFR stimulation (Kawamoto *et al.* 1983). This antibody was pre-incubated with target cells to determine whether luciferase transgene expression could be inhibited by blocking EGF-polymer binding. The cell line, A9-chromosome 21 (A9-CAR), is derived from the murine fibroblast cell line A9 and has been stably transfected with the human chromosome 21 to express high levels of CAR (gift from Professor R. Newbold) (see Figure 4-6). A9-CAR cells were used as a control. Figure 4-5 shows that anti-EGFR antibody significantly reduced EGF-polymer coated virus mediated transgene expression in EGFR-positive A9 clones (a & b), but not in CAR-positive, EGFR-negative A9-CAR cells (c). The EGF-blocking antibody had no effect on transgene expression from polymer–coated virus that had not been retargeted with EGF. These data indicate that EGF-polymer was able to significantly inhibit CAR-mediated adenovirus transduction and selectively retarget adenovirus infection via the EGFR receptor.

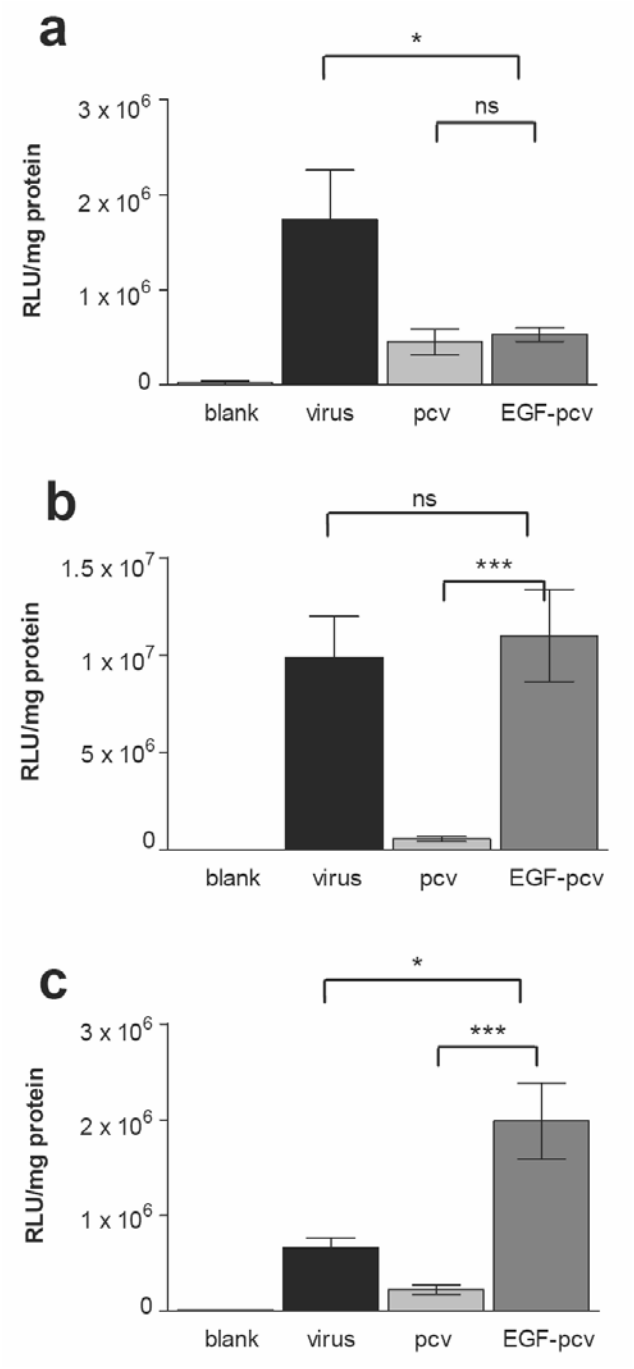


Figure 4-4 Retargeting adenovirus to A9-EGFR cells with EGF-polymer coating

Cells (1 x 10^4/well) were seeded into 96 well plates with G418 omitted from media for 24 hours. Virus was coated with polymer overnight at 5 mg/ml, purified on S400 spin columns, and particle number calculated from a PicoGreen analysis. Cells were incubated with either unmodified virus, polymer coated virus or EGF-polymer coated virus, at a MOI of 1,000 v.p./cell, in low serum media for 90 min. Cells were then washed and normal growth media, without G418 added and cells incubated for 48 hours. Cells were then lysed and assayed for luciferase transgene expression. Cells only are represented with white bars, uncoated virus with black bars, polymer coated virus with light grey bars and EGF-polymer coated virus with dark grey bars. (a) A9 cells, (b) A9-EGFR C10 cells, and (c) A9-EGFR C22 cells. Results are representative of at least three independent experiments with samples performed in triplicate. Error bars are +/- SEM and P values were calculated from log transformed data by ANOVA with Bonferroni's correction for multiple analyses. ns = not significant, * = $P < 0.05$, and *** = $P < 0.001$.

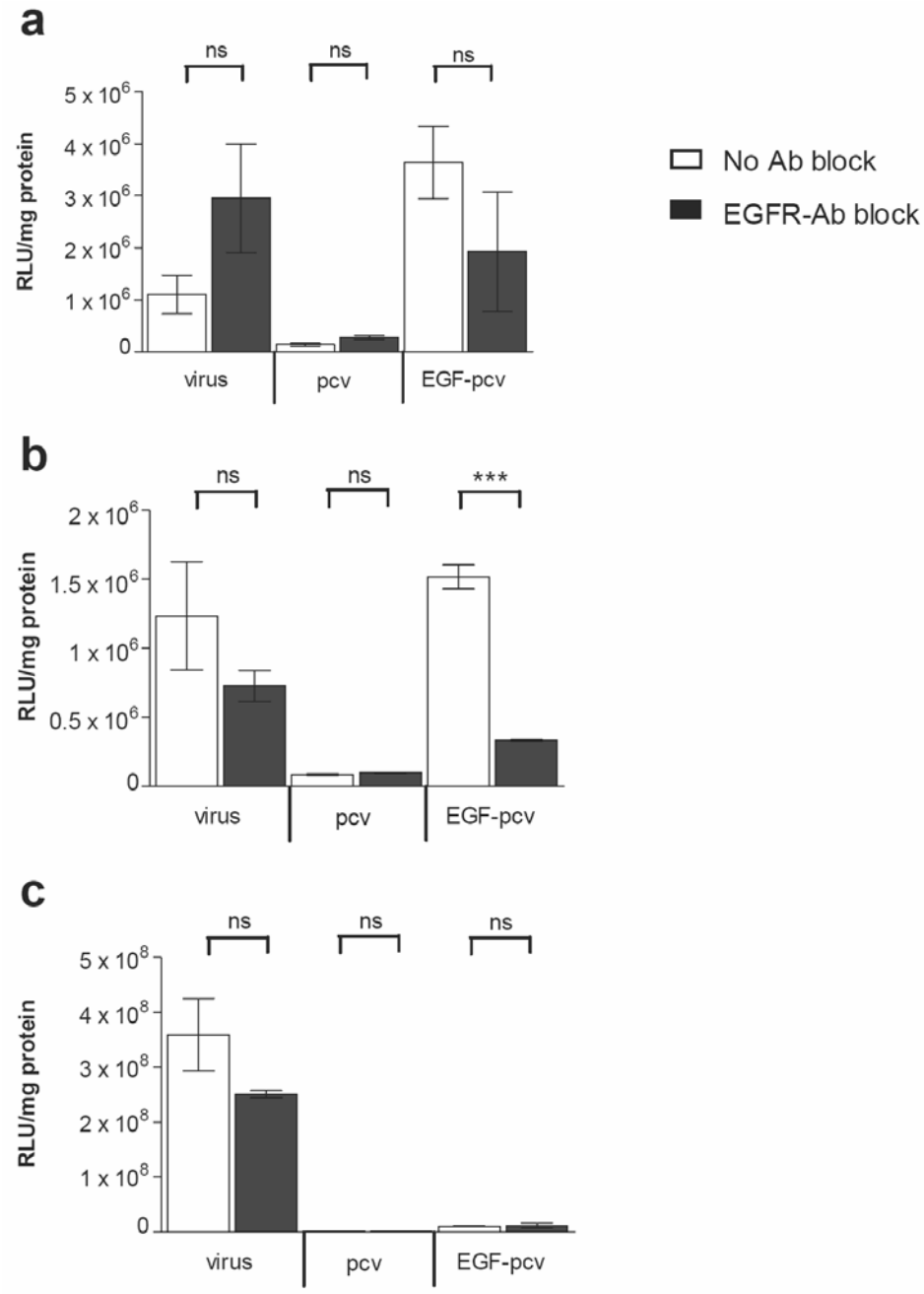


Figure 4-5 An EGF-blocking antibody inhibits EGF-polymer retargeting

Cells (1 x 10^4/well) were seeded into 96 well plates with G418 omitted from media for 24 hours. Virus was coated polymer overnight at 5 mg/ml, purified on S400 spin columns, and particle number calculated from a PicoGreen analysis. Cells were pre-incubated with EGFR-blocking antibody (10 μg/ml) for 40 min prior to addition of either unmodified virus, polymer coated virus or EGF-polymer coated virus, at a MOI of 1,000 v.p./cell in low serum media, and incubated at 37°C in 5% CO_2 for a further 90 min. Cells were then washed, normal growth media added (without G418) and cells incubated for 48 hours. Cells were then lysed and assayed for luciferase transgene expression. Figures show values for media control pre-incubation in white bars, and EGF-blocking antibody in dark grey bars: (a) A9-EGFR C10 cells; (b) A9-EGFR C22 cells; and (c) A9-CAR cells. All experiments were performed in triplicate. Error bars are +/- SEM and P values were calculated from log transformed data by ANOVA with Bonferroni's correction for multiple analyses. ns = not significant, and *** = $P < 0.001$.

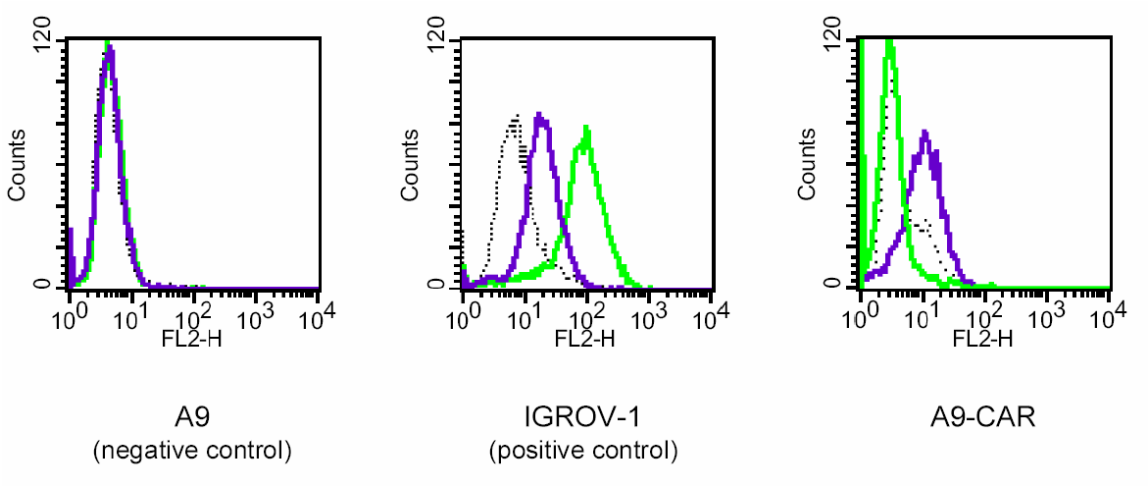


Figure 4-6 A9-CAR expression of EGFR and CAR by flow cytometry

Cells were grown in 25 cm^2 cell culture flasks until 90% confluent then scraped in 10% HINGS to detach. Cells were pelleted and resuspended in 10% HINGS in 96 well v-bottomed plates. Cells were labelled with primary antibody at 4°C for 40 min, washed x2 and labelled with secondary antibody for 40 min at 4°C. Cells were washed x3 and fixed with 4% paraformaldehyde then analysed using a FACSCalibur machine for fluorescence at 585 nm. Isotype antibody-labelled cells are represented with a black dotted histogram, anti-EGFR labelled cells with a green histogram, and CAR labelled cells with a purple histogram. 1 x 10^4 cells were counted per sample. A9 cells are a CAR and EGFR negative control, whereas IGROV-1 cells are positive for both CAR and EGFR.

4.2.5 EGF-polymer retargeting in ovarian tumour cell lines

4.2.5.1 EGFR levels in ovarian cancer cell lines

Flow cytometry was used to evaluate relative levels of EGFR and CAR on ovarian cancer cell lines using a mouse monoclonal anti-EGFR antibody, a mouse anti-CAR antibody, and a goat anti-mouse secondary antibody conjugated to RPE (see 2.1.6). Labelling of four different ovarian cancer cell lines (and the vulval epidermoid cancer cell line A431) with anti-CAR, anti-EGFR and isotype controls (Figure 4-7) demonstrated that A431 cells have the highest, and A2780 the lowest, levels of EGFR expression, whereas SKOV-3, IGROV-1 and OVCAR-3 have similar intermediate levels of EGFR. Furthermore, IGROV-1 cells also have moderately high levels of CAR expression, whereas the other cell lines had low CAR expression levels.

Flow cytometry was only able to give a qualitative level of EGFR expression, and so a commercial ELISA kit (see section 2.1.7) was used to quantify precisely the number of EGFR per cell in a variety of ovarian cancer cell lines (IGROV-1; OVCAR-3: SKOV-3: A2780), the A9-EGFR clones C10 and C22, and A431 cells. The concentration of EGFR in each sample was extrapolated from a standard curve and the number of EGFR per cell calculated (Figure 4-8). The ELISA data demonstrated a similar pattern of results to the flow cytometry data. A431 cells had very high levels of EGFR expression at 600,000 receptors per cell. Intermediate levels of EGFR expression were found in SKOV-3, IGROV-1 and OVCAR-3, equating to 60,000-90,000 receptor molecules per cell. A2780 had low levels of EGFR: ~3,500 per cell. A9-EGFR clones also had low levels of EGFR: ~2,000-3,000 per cell for A9-EGFR C22 and ~ 1,000 per cell for A9-EGFR C10. These data support the conclusion that the failure to demonstrate EGFR tyrosine kinase activity in the A9-EGFR clones by western blotting was due to the very low levels of cellular EGFR (see Figure 3-8).

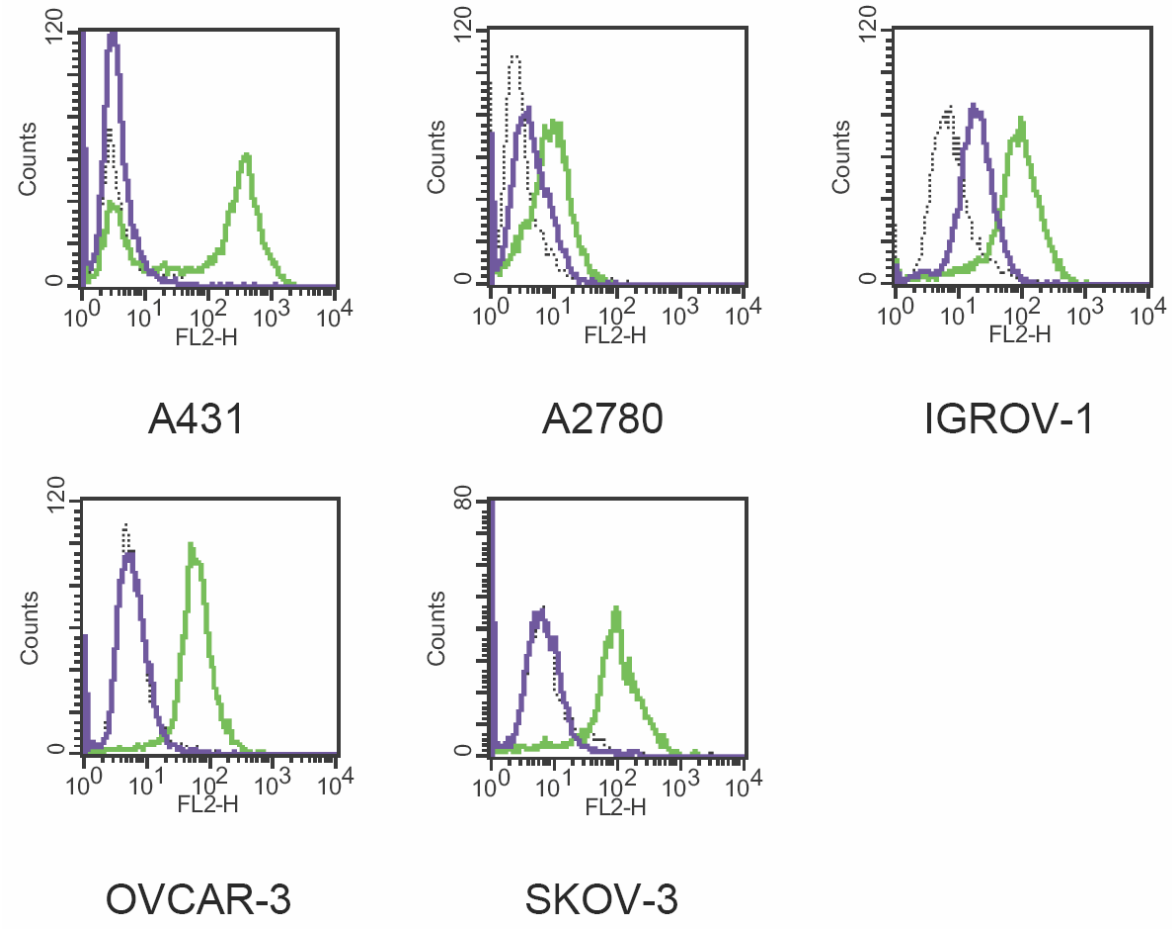


Figure 4-7 EGFR and CAR status of cancer cell lines by flow cytometry

Cells were grown in 25 cm^2 cell culture flasks until 90% confluent then scraped, pelleted and incubated in rotating polypropylene tubes with DMEM media containing Hepes at 37°C for 4 hours to allow recovery of EGFR expression. Cells were washed and resuspended in 10% HINGS in 96 well v-bottomed plates. Cells were labelled with primary antibody at 4°C for 40 min, washed x2 and labelled with secondary antibody for 40 min at 4°C. Cells were washed x3 and fixed with 4% paraformaldehyde then analysed using a FACSCalibur machine for fluorescence at 585 nm. Isotype antibody-labelled cells are represented with a black dotted histogram, anti-EGFR labelled cells with a green histogram and CAR labelled cells with a purple histogram.

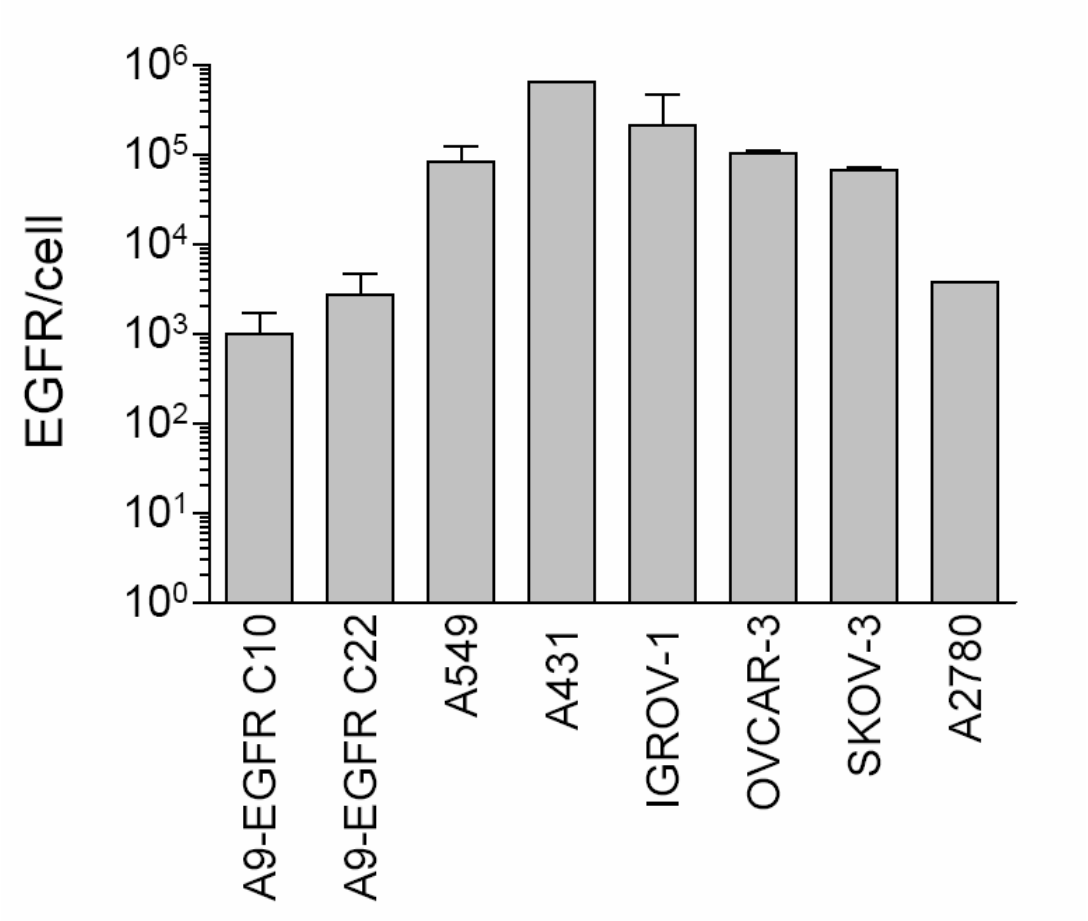


Figure 4-8 Number of EGFR per cell in various different cell lines

Cells (2 x 10^6 per cell line) were counted and allowed to recover EGFR expression following trypsinisation in 75 cm^2 tissue culture flasks. Cells were then scraped, pelleted and cell pellets lysed. Two different dilutions of each cell lysate in duplicate were used in a commercially available ELISA for estimating concentrations of soluble EGFR in patient serum. Standard concentrations of EGFR in duplicate were used to generate a standard curve. The concentration of EGFR in each sample was extrapolated from the standard curve using Prism 3 software and the number of EGFR per cell calculated. Results are the combination of two independent experiments (both performed in duplicate at two separate dilutions). Error bars represent SD (and are also present for A431 and A2780 cell lines).

4.2.5.2 EGF-polymer retargeting to EGFR-positive human ovarian tumour cells

Retargeting of EGF-polymer coated adenovirus was tested on a panel of human ovarian cancer cell lines (and A431) in order to determine whether levels of retargeting were proportional to cellular EGFR levels and whether they were quantitatively significant in the presence of CAR. A luciferase reporter gene expression assay demonstrated that EGF-polymer could successfully retarget adenovirus to all of the EGFR-positive cancer cell lines (Figure 4-9). Pre-incubation with an anti-EGFR blocking antibody (GR01L) was able to inhibit EGFR-mediated virus transduction in both A431 and SKOV-3 cells (Figure 4-11). A negative control isotype antibody did not inhibit EGF-polymer coated virus transgene expression (data not shown).

Luciferase transgene expression from EGF-polymer coated adenovirus was compared with cellular EGFR levels calculated by ELISA (see Figure 4-8). Figure 4-10 demonstrates that there was a linear relationship between transgene expression and number of EGFR per cell. The only outlier was the cell line IGROV-1, which also had relatively high CAR levels. The unexpectedly high transgene expression in IGROV-1 therefore may represent some uptake mediated by CAR. However, the polymer concentration used for adenovirus coating in this experiment was only 5 mg/ml, at which CAR mediated uptake is not completely inhibited (>90% inhibited)7. If the results for IGROV-1 cells are omitted from the analysis, the degree of fit (r^2) is greater than 0.99.

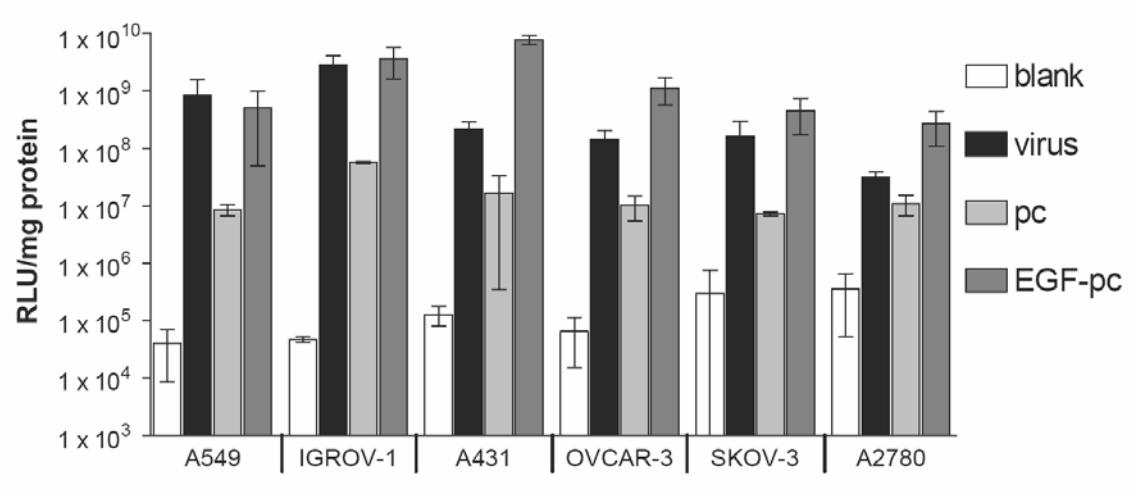


Figure 4-9 EGF-polymer retargets adenovirus to EGFR-positive cancer cells

Cells (1 x 10^4/well) were seeded into 96 well plates. Virus was coated with 5 mg/ml of polymer overnight, purified on S400 spin columns, and particle number calculated from a PicoGreen analysis. Cells were incubated at 37°C in 5% CO_2 for 90 min with either unmodified virus, polymer coated virus or EGF-polymer coated virus, at a MOI of 300 v.p./cell, in low serum media. Cells were then washed, normal growth media added and cells incubated for 48 hours. Cells were then lysed and assayed for luciferase transgene expression. Figures show values for cells only in white bars, uncoated virus in black bars polymer coated virus in light grey bars and EGF-polymer coated virus in dark grey bars; cell lines are as indicated on the x axis. Results are representative of at least two independent experiments performed in triplicate. Error bars are +/- SEM.

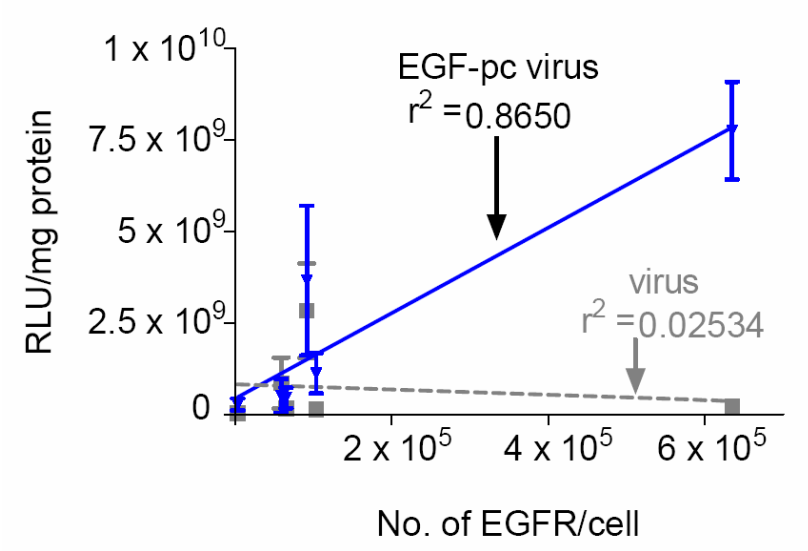


Figure 4-10 Retargeted transgene expression is proportional to cellular EGFR levels

Cells (1 x 10^4/well) were seeded into 96 well plates. Virus was coated with 5 mg/ml of polymer overnight, purified on S400 spin columns, and particle number calculated from a PicoGreen analysis. Cells were incubated at 37°C in 5% CO_2 for 90 min with unmodified adenovirus or EGF-polymer coated virus at a MOI of 300 v.p./cell in low serum media. Cells were then washed, normal growth media added and cells incubated for 48 hours. Cells were lysed and assayed for luciferase transgene expression. Results were plotted against cellular EGFR levels, calculated from a commercial ELISA kit (see Figure 4-8). Error bars represent SEM of wells performed in triplicate. Results are representative of at least two independent experiments.

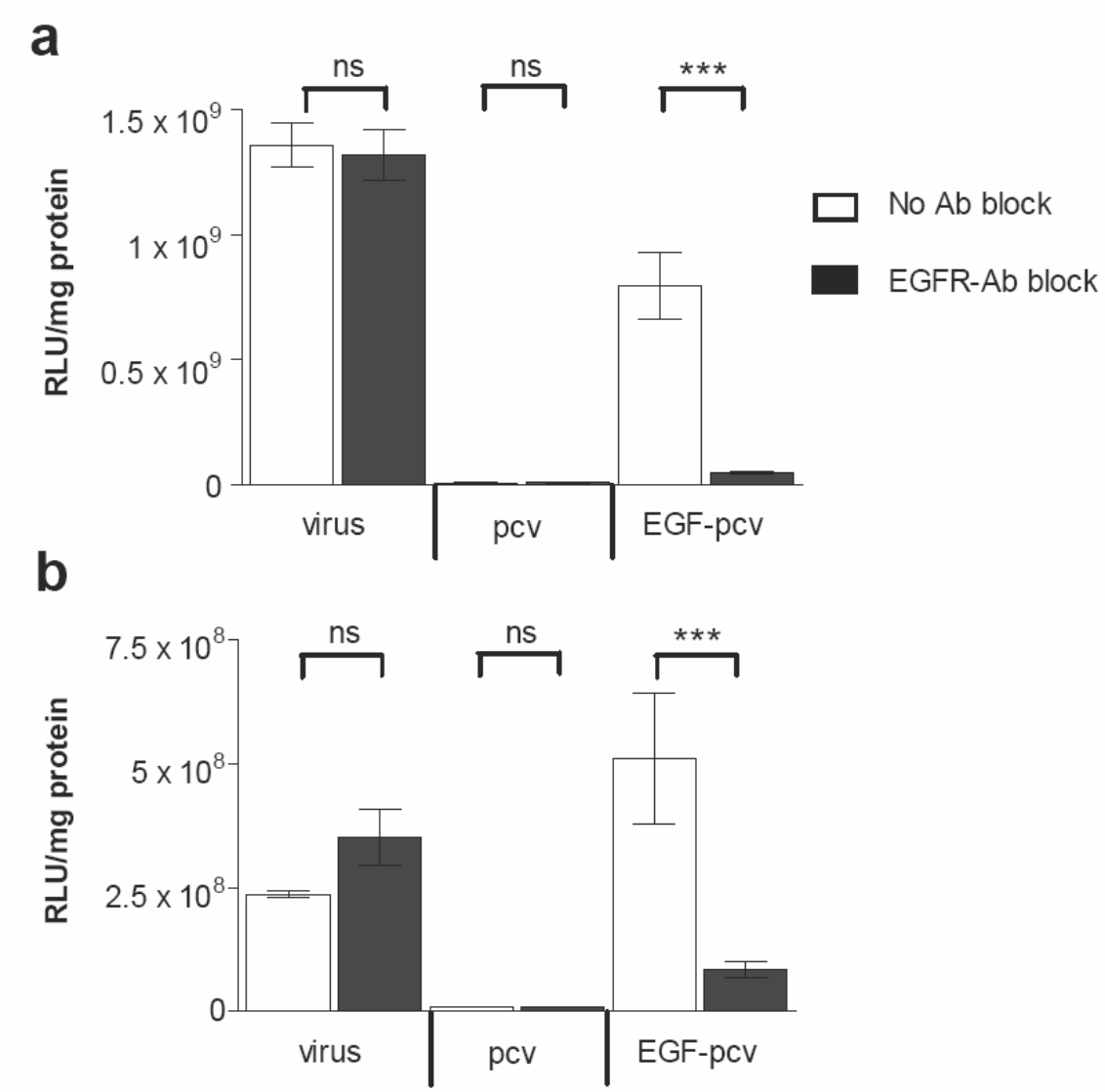


Figure 4-11 EGF-blocking antibody inhibits EGF-polymer retargeting in cancer cells

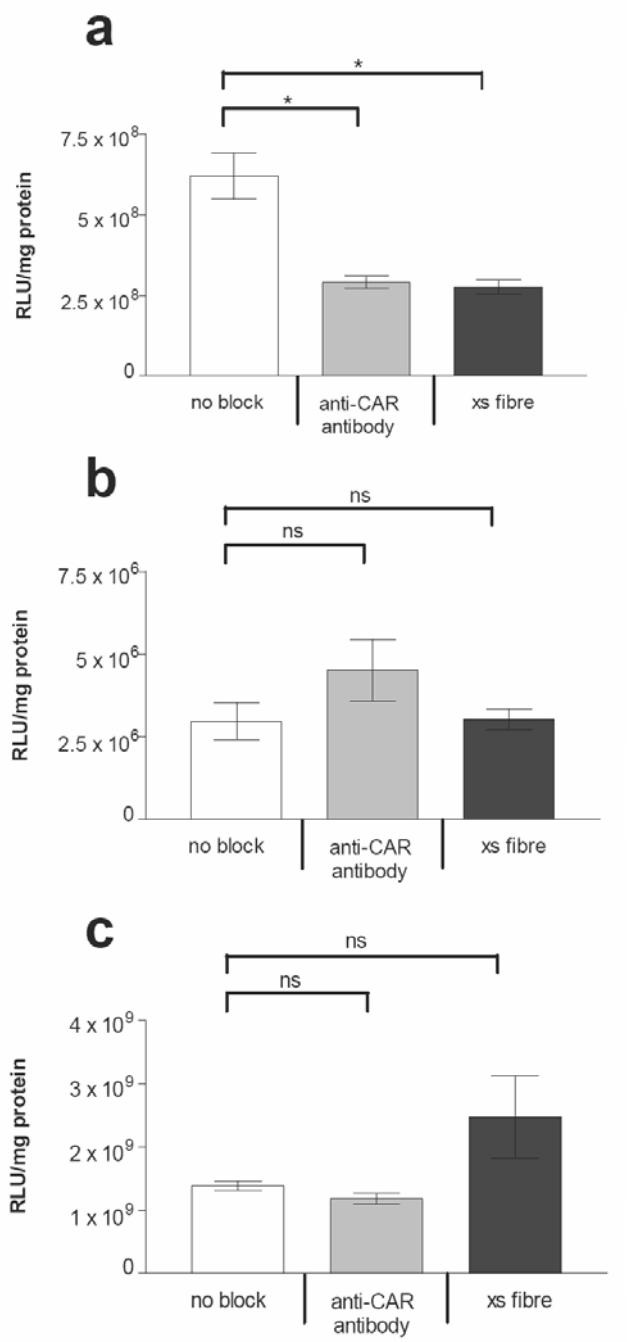
Cells (1 x 10^4/well) were seeded into 96 well plates for 24 hours. Virus was coated with 5 mg/ml of polymer overnight, purified on S400 spin columns, and particle number calculated from a PicoGreen analysis. Cells were pre-incubated with an EGF-blocking antibody or low serum media for 40 min. Either unmodified virus, polymer coated virus or EGF-polymer coated virus, at a MOI of 1,000 v.p./cell in low serum media, was added without removing antibody and incubated for 90 min. Cells were then washed, normal growth media added and cells incubated for 48 hours. Cells were then lysed and assayed for luciferase transgene expression. Figures show values for media control pre-incubation in white bars, and EGF-blocking antibody in dark grey bars; (a) A431 cells; and (b) SKOV-3 cells. Results are representative of two independent experiments performed in triplicate. Error bars are +/- SEM and P values were calculated from log transformed data by ANOVA with Bonferroni's correction for multiple analyses. ns = not significant, and *** = $P < 0.001$.

4.2.6 Effect of anti-CAR antibody on virus infection

It is possible to knock-down adenovirus infection using an anti-CAR antibody that inhibits adenovirus fibre knob binding. Alternatively, excess free fibre knob protein, isolated from by-products of virus production, can also inhibit adenovirus infection by competitively binding with CAR. Adenovirus 5 fibre knob was a gift from Dr V. Mautner. Both anti-CAR antibody and excess fibre knob were able to significantly knock-down transgene expression from unmodified virus but did not significantly inhibit polymer coated or EGF-polymer coated adenovirus transgene expression (Figure 4-12). A negative control isotype antibody did not inhibit unmodified virus transgene expression (data not shown).

4.2.7 Specific activity of EGF-pcv compared to unmodified virus

The specific activity (luciferase activity per virus particle) was compared to determine whether EGF-pcv retained activity, or whether the similar levels of luciferase activity seen in EGFR positive cells compared to unmodified virus was due to improved cell uptake of less active virus. This would indicate whether internalising via EGFR was a suitably permissive pathway and what effect different coating concentrations had on virus activity. A transduction assay was performed with AdCMV-Luc$_{\Delta E1}$ coated with polymer and EGF-polymer at 10 mg/ml and 20 mg/ml for 40 min at room temperature and then left overnight on ice. A431 cells were transduced with virus (as described in section 2.2.8) and cells incubated for 24 hrs. Cells were washed and lysed. Aliquots were used in a luciferase assay (25 μl) (section 2.2.8.1), protein assay (5 μl) (section 2.1.3) and Q-PCR for measurement of virus particle number (50 μl) (section 2.2.9). Luciferase expression and virus particle number were calculated per mg protein for comparison. Figure 4-13 demonstrates that unmodified virus and EGF-pcv coated at 10 mg/ml did not have significantly different activity per virus particle. Coating at a higher concentration of polymer reduced the specific activity, due to a reduction in luciferase expression per virus particle. This may be because at a higher coating concentration more lysine residues are modified, which may reach a point where there is a critical blockade of peri-pentonal hexons, which are required for binding at the nuclear pore complex (Greber *et al.* 1997). Another possibility is that over-modification prevents virus uncoating once internalised, so inhibiting escape from the endosomal compartment.



Unmodified adenovirus

Polymer coated adenovirus

EGF-polymer coated adenovirus

Figure 4-12 Blocking CAR-mediated virus uptake does not affect EGF-polymer coated adenovirus transgene expression

A431 cells ($1x10^4$/well) were seeded into 96 well plates. Virus was coated with 5 mg/ml of polymer overnight, purified on S400 spin columns, and particle number calculated from a PicoGreen analysis. Cells were pre-incubated at 37°C in 5% CO_2 for 40 min with anti-CAR antibody or excess adenovirus fibre knob protein. Adenovirus, polymer-coated virus, or EGF-polymer coated virus at a MOI of 1,000 v.p./cell in low serum media were added to wells and incubated for a further 90 min. Cells were then washed, normal growth media added and cells incubated for 48 hours. Cells were lysed and assayed for luciferase transgene expression. Results for (a) uncoated virus, (b) polymer coated virus, and (c) EGF-polymer coated virus are shown; virus/coated virus in white bars, anti-CAR antibody in light grey bars, and excess adenovirus fibre knob in dark grey bars. Results are representative of at least two independent experiments performed in triplicate; error bars are +/- SEM and P values were calculated with Prism3 software from log transformed data by ANOVA with Bonferroni's correction for multiple analyses. ns = not significant, * = $P < 0.05$, ** = $P < 0.01$ and *** = $P < 0.001$.

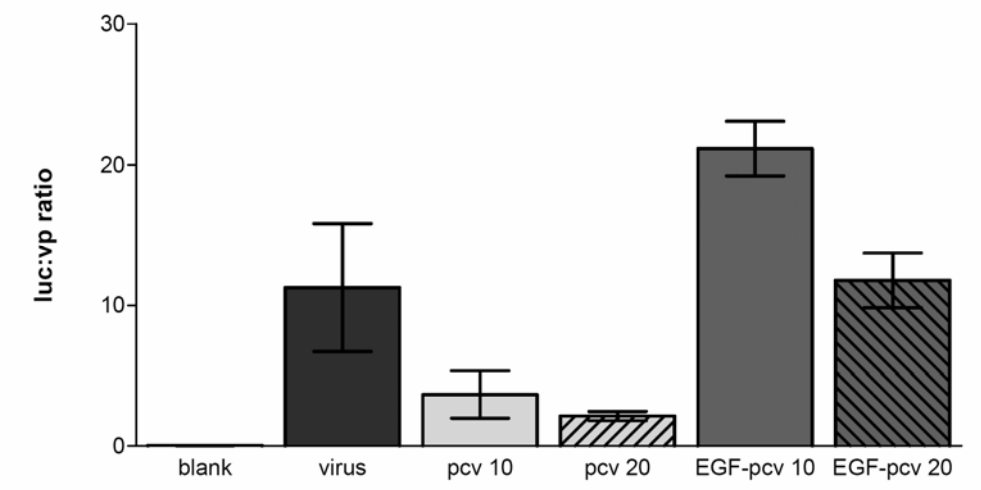


Figure 4-13 Specific activity of EGF-pcv *in vitro*

A431 cells (1 x 10^4) were infected with AdCMV-Luc $_{\Delta E1}$ coated overnight with polymer at different concentrations (pcv 10 and EGF-pcv 10 = 10 mg/ml; pcv 20 and EGF-pcv 20 = 20 mg/ml). Virus was incubated with cells for 90 min, cells washed and after 24 hrs cells were lysed and cell lysate analysed for luciferase expression and viral particles (by Q-PCR). Data shown are representative of at least three independent experiments.

4.3 Discussion

These data support the hypothesis that EGF-polymer is able to successfully retarget adenovirus infection and transgene expression via the EGFR, whilst inhibiting CAR-mediated virus uptake. EGF-polymer was able to mediate adenovirus transgene expression in A9-EGFR cells in the absence of CAR. Levels of transgene expression generated were significantly above those of unmodified virus in one of the A9-EGFR clones. This effect could be inhibited by an EGF-blocking antibody, and similar results were demonstrated in a panel of EGFR-positive ovarian and A431 cancer cell lines, with transgene expression levels roughly proportional to the EGFR level of the cell line.

Importantly, there appeared to be proportionally very little contribution to EGF-pcv transduction by CAR-mediated uptake in A431 cells, since blocking CAR, with either an antibody or excess free adenovirus fibre, had no significant effect on EGF-pcv transduction, in contrast to transduction by unmodified virus. Furthermore, the specific transgene expression activity of each EGF-pcv particle associated with the cell after a 90 min incubation, was similar to that of

unmodified virus, suggesting that internalisation via the EGFR enabled the virus to enter a viable route for efficient infection and transduction.

Retargeting of adenovirus gene therapy has previously been achieved using bispecific single chain antibodies, with dual specificity for adenoviral fibre knob and EGFR (Grill *et al.* 2001), or a secretory fusion molecule comprised of the CAR extra-cellular domain and EGF (Hemminki *et al.* 2001). A bispecific antibody for adenovirus fibre knob-EGFR enhanced transgene expression by approximately ten-fold in head and neck squamous cell carcinomas that had little CAR expression (Blackwell *et al.* 1999). Retargeted-transduction could be blocked by anti-EGFR antibodies, but not anti-CAR antibodies. Other studies have demonstrated that a fusion protein comprised of the soluble form of truncated CAR and EGF was able to retarget transgene expression of a luciferase-expressing adenovirus (Dmitriev *et al.* 2000). In pancreatic carcinoma cell lines transgene expression from retargeted adenovirus was up to five times that of non-retargeted virus; these cell lines have very low CAR levels (Wesseling *et al.* 2001). These data support the findings of this chapter, since other groups have demonstrated that virus transduction can be mediated through alternative receptors. However, specific activity of virus (number of particles:luciferase expression) was not demonstrated in these studies.

There are several important advantages to the polymer-coating strategy for adenovirus retargeting. First, as the interaction between virus, polymer and ligand is a covalent reaction, there is no 'off-rate', unlike antibody or ligand receptor interactions, which depend on electrostatic forces. This should ensure that a more stable product is produced, which would be important for clinical applications.

Second, polymer coating acts across the virus capsid and so shields not only the fibre-knob, which is the normal CAR ligand, but also the integrin-binding domains on the penton-base and the fibre shaft, which mediates binding via heparin-sulphate proteoglycans (Dr S. Hale – D.Phil. thesis, University of Oxford). Indeed, binding via mechanisms other than the adenovirus fibre knob-CAR interaction may in fact be more important *in vivo*, than *in vitro*. Recently published data suggest that residues on the fibre shaft bind to vitamin K dependent coagulation factors

and activated complement cascade components, and it is this interaction that enhances liver transduction *in vivo* (Parker *et al.* 2006; Shayakhmetov *et al.* 2005b). This may explain why retargeting strategies involving the fibre knob alone, as with the bispecific adapter molecules, are ineffective at preventing liver transduction *in vivo* (reviewed in (Nicklin *et al.* 2005)). However, one important limitation of these data is that they are performed in murine models; adenovirus distribution in the blood is markedly different to humans, due to the lack of erythrocyte binding (Lyons *et al.* 2006).

A third advantage of the polymer coating strategy is that it affords a level of protection from neutralising antibody binding (Fisher *et al.* 2001). Studies have demonstrated that the majority of neutralising antibodies generated are anti-hexon antibodies and bind to residues which are involved with up-take through the nuclear pore complex, rather than at the level of cell uptake (Sumida *et al.* 2005; Varghese *et al.* 2004). Thus, modification of the fibre knob alone is unlikely to significantly avoid antibody neutralisation of adenovirus.

In summary, taken together the data in this chapter strongly suggest that EGF-polymer retains biological activity and is able to retarget via the EGFR in vitro. Given the differences observed *in vitro* and *in vivo* with other retargeting strategies, the next step is to determine the effect of retargeting in an *in vivo* model of human ovarian cancer.

5 Retargeting polymer coated adenovirus to EGFR with alternative ligands

5.1 Introduction

In the experiments described in the previous chapter, murine EGF polymer conjugate was used to retarget adenovirus. However, since it differs from human EGF, it may induce antibody formation against murine EGF, and hence lead to neutralisation of the EGF-polymer coated adenovirus. Transforming growth factor-alpha (TGF-α) is a 5.5 kDa polypeptide containing 50 amino acids in its mature form (see appendix 9.1). It is a natural human ligand for EGFR with 55% of the receptor binding affinity of human EGF, induces tyrosine kinase activity, receptor dimerisation and internalisation. However, EGF and TGF-α have different pH-dependent receptor/ligand dissociations (Ebner and Derynck 1991). TGF- α has lower binding affinity than EGF at pH 6.0, which is the pH in the early endosome, and hence dissociates more rapidly following internalisation (Maeda *et al.* 2002). This may have implications for adenovirus retargeting. However, murine EGF is more similar to TGF- α in its binding affinity than human EGF, and so the difference may not actually be so great. Another attractive feature of TGF- α is that, unlike human EGF, it has only one lysine residue (see appendix 9.1), which is not located within the EGFR binding domain, and so its biological activity may not be adversely affected by polymer conjugation, which involves covalent modification of reactive amino groups. Nevertheless, the TGF-α used in this study was engineered to remove the lysine residue, so leaving only the N-terminal amine group for modification and was generously donated by Berlex, USA. Other modifications were also made to enable correct folding when produced in bacteria and details of the exact protein sequence have not yet been made available to us.

EGF stimulates cell growth and therefore has a mitogenic effect on tumours. Hence, there is the potential that EGF-polymer coated adenovirus may stimulate tumour growth, rather than inhibit it. There is, however, data to suggest that many tumours become non-EGF dependent in terms of growth activity, either because they have an autocrine loop, generating their own

localised EGF, or because the EGFR mutates and has constitutive activity (Massoglia *et al.* 1990; Morishige *et al.* 1991). Indeed, the related Her2/neu member of the EGFR family has no recognised ligand and develops tyrosine kinase activity on forming dimers, which occurs more frequently in cells over-expressing Her2/neu (Worthylake *et al.* 1999).

Cetuximab is a humanised monoclonal antibody that has been developed for therapeutic use and has been introduced for treatment of some human cancers (Raben *et al.* 2005; Vanhoefer *et al.* 2004). Cetuximab binds to the EGFR and is able to inhibit EGF binding (Goldstein *et al.* 1995) (see Figure 1-2) thus mediating part of the anti-tumour effect. In addition, the humanised Fc portion encourages antibody dependent cell killing, which may also be responsible for the therapeutic effect in patients, although not in murine models. Cetuximab was therefore an attractive candidate for adenovirus gene therapy retargeting ligand and may have a dual therapeutic effect.

Unpublished data from the Curiel group suggested that EGFR tyrosine kinase activity might not be necessary for retargeted virus internalisation (personal communication). This group made stably transfected cell lines expression truncated EGFR, which lacked tyrosine kinase activity. Utilising hybrid EGF-anti-CAR antibody adaptors, they were still able to produce adenovirus transgene expression in cells expressing truncated EGFR. Thus, even without EGFR stimulation, Cetuximab may still be able to re-target polymer coated adenovirus infection.

The aims of this chapter were therefore:

- To determine whether TGF-α, pre-conjugated to reactive pHPMA co-polymers, was able to retarget adenovirus transduction;
- To conjugate Cetuximab to reactive groups on polymer coated adenovirus in a two-step process and determine whether adenovirus could be retargeted to the EGFR;
- To assess the stimulatory effect of EGF-pcv and TGF-α-pcv on EGFR-positive cells and determine whether this translated into a significant mitogenic effect.

5.2 Methods and results

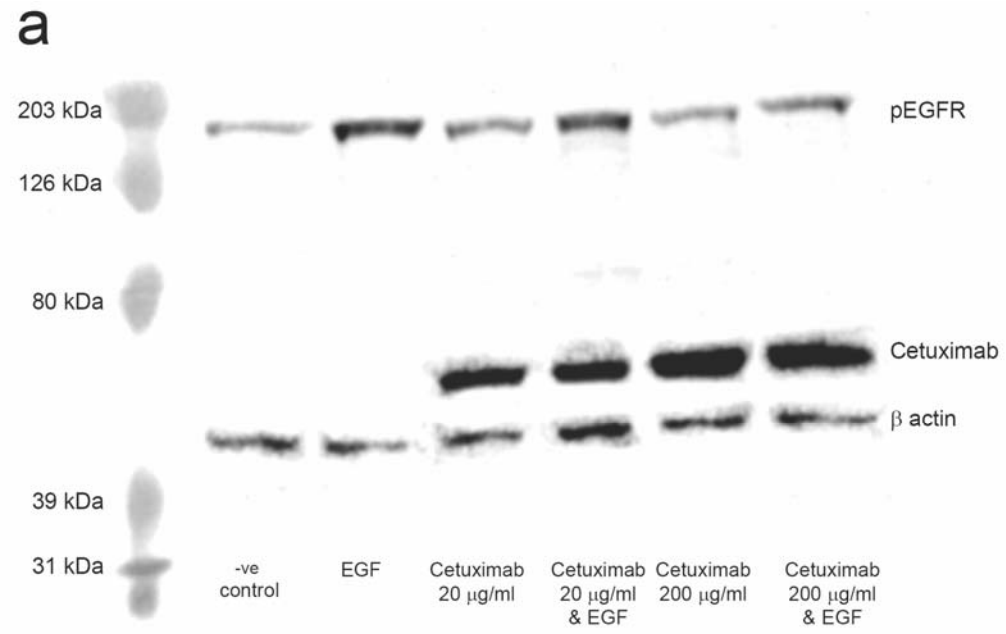
5.2.1 Production of Cetuximab retargeted polymer coated adenovirus

Unlike EGF-polymer coating, where EGF had been pre-conjugated to the polymer, Cetuximab retargeted polymer coated adenovirus was produced using a two stage coating method. First, adenovirus was coated with reactive polymer at 20 mg/ml. Excess free polymer was removed after 40 min by passing through a S400 spin column (see section 2.2.7) and Cetuximab was added to the polymer coated virus mix. This was incubated overnight on ice to allow free reactive groups on the virus-bound polymer to react with amino groups on the Cetuximab. Free Cetuximab could then be removed by a further spin column purification, although this resulted in inefficient virus recovery. As dilutions of virus for experiments would reduce free Cetuximab to negligible levels, which were unlikely to out-compete virus binding, Cetuximab purification was omitted. Virus titres were calculated using dsDNA quantification (see section 2.2.4).

5.2.2 Cetuximab is able to prevent EGFR stimulation by its ligand

Cetuximab (kindly donated by Merck) was investigated to explore whether it was indeed able to inhibit EGFR phosphorylation. A431 cells were pre-incubated with Cetuximab at 2 μg/ml, 20 μg/ml and 200 μg/ml at 37°C for 30 min. Cells were then exposed to EGF (100 nmol/l) for 30 min at 37°C. Cell lysates were prepared and examined by Western blotting (see section 2.1.9). Nitrocellulose membranes were divided prior to pEGFR labelling and the lower molecular weight half of the membrane blotted for β-actin as a loading control. Figure 5-1 demonstrates the results of the Western blot. Despite serum-starving for four hours there was a degree of background pEGFR, perhaps due to autocrine EGF or TGF-α activity. This was then used to adjust experimental levels of pEGFR. The results show that there was some increase in tyrosine kinase activity following Cetuximab pre-incubation, even without subsequent stimulation with EGF. However, cells pre-incubated with Cetuximab and then stimulated with EGF had a much reduced pEGFR level, suggesting that Cetuximab was able to block EGF stimulation. This effect appeared to be dose dependent (minimal inhibition was observed following pre-incubation with 2 μg/ml Cetuximab - data not shown).

a



b

	pEGFR band density	β-actin band density	adjusted pEGFR density
negative control	2,700	6,450	0.0
EGF positive control	7,400	4,300	108.6
Cetuximab 20 μg/ml	4,100	7,400	18.8
Cetuximab 20 μg/ml & EGF	7,750	12,400	40.6
Cetuximab 200 μg/ml	4,050	9,600	13.9
Cetuximab 200 μg/ml & EGF	4,300	11,450	14.1

c

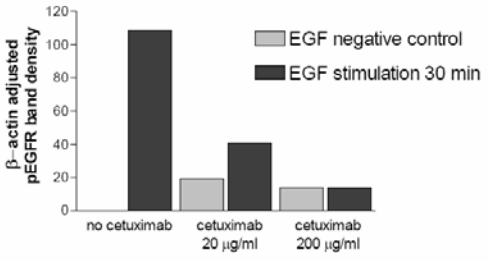


Figure 5-1 Cetuximab is able to inhibit EGF stimulated EGFR tyrosine kinase activity

(a) A431 cells (2 x 10^5) were plated out in 6 well plates and incubated for 72 hours in normal growth media. They were then serum-starved for 4 hours prior to pre-incubation for 30 min with Cetuximab or negative control and subsequent stimulation with EGF (100 nmol/l) diluted in 0.1% BSA in DMEM. Cells were lysed, a protein assay performed and equal amounts of protein (20 μg) loaded onto a 7.5% SDS gel. The gel was blotted onto nitrocellulose overnight, labelled with a goat anti-pEGFR primary antibody and an anti-goat-HRP conjugated secondary antibody (band at 170 kDa), or rabbit anti-β-actin and anti-rabbit-HRP conjugated secondary antibody (bands at 42 kDa), and developed with Lumiglo®. Results are representative of at least three independent experiments. (b) Gel images were analysed using the National Institute of Health (NIH) Image J software to calculate density of pEGFR and β-actin bands. pEGFR values were adjusted for loading using the β-actin values and background pEGFR in the negative control. (c) Values for β-actin and background adjusted values were plotted, with EGF stimulated bars shown in black and non-stimulated cells shown in grey.

5.2.3 Cetuximab initiation of EGFR internalisation

On binding EGF, EGFR dimerise and internalise. Cetuximab was known to bind to EGFR and block EGF binding. However, it was not known whether part of this effect was due to stimulating EGFR internalisation, therefore down-regulating EGFR levels and reducing the effect of EGF stimulation. For retargeting of adenovirus, it was assumed that internalisation via the receptor would be necessary. The next step was therefore to determine whether EGFR did internalise following incubation with Cetuximab. A431 cells were incubated with Cetuximab or EGF with appropriate negative controls. After 60 min cells were fixed and immunocytochemistry used to label EGFR (see section 2.1.9.3). Figure 5-2 demonstrates that Cetuximab was able to stimulate EGFR internalisation. This suggests that part of the mechanism of action of Cetuximab blocking is due to causing EGFR to internalise and be degraded in the lysosomes, hence down-regulating cellular EGFR levels and therefore reducing the response to EGF, in addition to direct receptor competition.

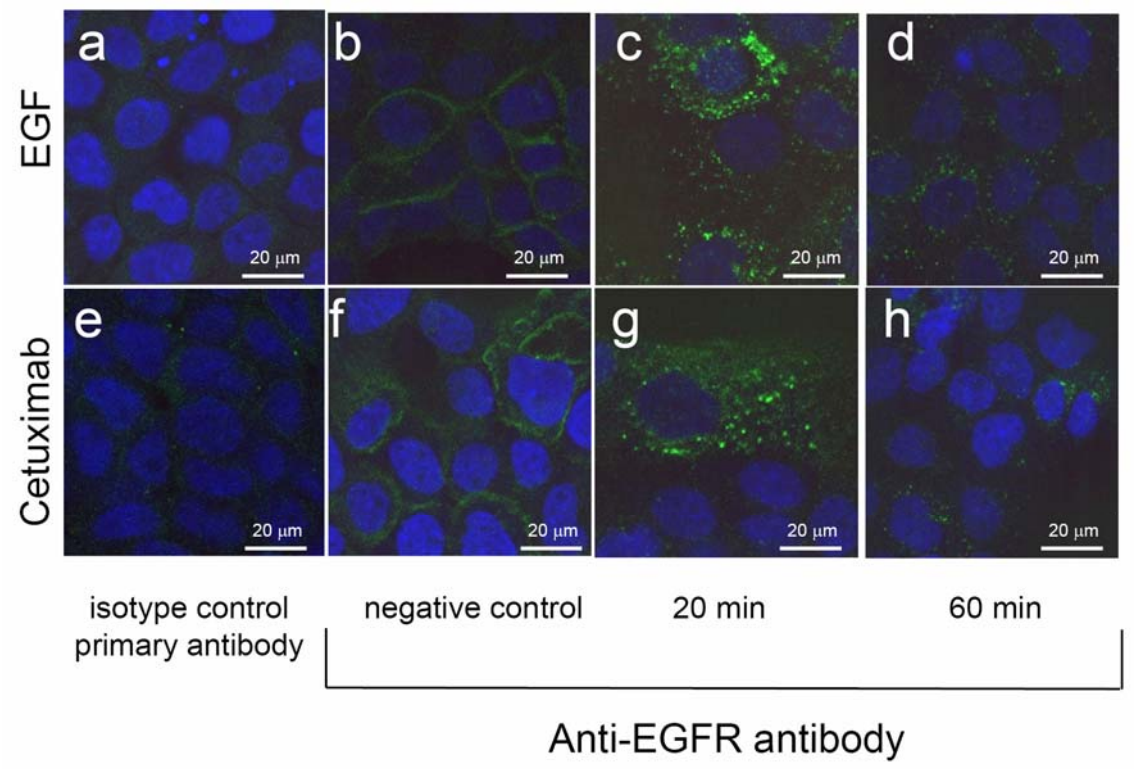


Figure 5-2 Cetuximab stimulates EGFR internalisation

A431 Cells (5 x 10^4 cells/well) were grown on glass chamber slides for 24 hours in normal growth media. Cells were serum-starved overnight. Cells were incubated with EGF at 100 ng/ml or Cetuximab at 10 μg/ml on ice for 60 min, then incubated at 37°C, 5% CO_2 for 20-60 min prior to fixing cells with 4% paraformaldehyde. Cells were labelled for EGFR using a mouse anti-EGFR primary antibody and mounted in Vectashield containing 2 μmol/l TO-PRO-3 for nuclear counter-staining. Panels show EGFR in green and nuclei counter-stained in blue. (a & e) Primary antibody isotype control; (b & f) no EGF or Cetuximab stimulation (negative control); (c & d) EGF incubation for 20 & 60 min; (g & h) Cetuximab incubation for 20 & 60 min. Photomicrographs were taken using a confocal microscope (Nikon Optiphot-2 upright microscope, fitted with a 60x oil immersion objective; Bio-Rad MRC1024 with Krypton/Argon lasers (Laser settings. Green: power 30%; iris 1.4; gain 1258; Kalman 2; accumulate x 2. Far red: power 30%; iris 2.0; gain 1182; Kalman 2; accumulate x 2). Differences in nuclear counter-staining are due to inconsistent staining with TO-PRO-3, not changes in laser settings.

5.2.4 Cetuximab retargeting of adenovirus infection

Because of the low levels of EGFR expression of the A9-EGFR clones, I decided to use commercially available cell lines to determine EGFR specificity, instead of the A9-EGFR cell lines, especially since the equivalent A9-CAR cell line had high levels of CAR expression. The T24 cell line is derived from a bladder epithelial cancer and is EGFR positive and CAR negative. SW620 cells are a colorectal carcinoma cell line that express CAR, but are EGFR negative. Cellular receptor expression was confirmed using antibody labelling and flow cytometry (see section 2.1.6). K562 cells were used as a double CAR/EGFR negative control and IGROV-1 cells as a double CAR/EGFR positive control. Figure 5-3 demonstrates that SW620 cells had no EGFR expression, but were CAR positive; T24 cells were negative for CAR, but had relatively high levels of EGFR. These observations agree with published data (http://www.atcc.org/). T24 and SW620 cells were labelled with Cetuximab or biotinylated EGF-polymer, with appropriate isotype antibody or biotinylated polymer controls, to assess whether binding of Cetuximab or EGF-polymer correlated with cellular EGFR status (see sections 2.1.6 and 2.1.8). Figure 5-4 demonstrates that, compared to their respective controls, Cetuximab and biotinylated EGF-polymer bound to EGFR-positive T24 cells, but not to EGFR-negative SW620 cells, indicating that binding was EGF-dependent and specific. It is possible that the biphasic response observed with EGF-polymer binding, in the T24 cells may be due to the lower concentration of EGF-polymer relative to Cetuximab; some cells are not labelled due to limited availability of EGF-polymer.

AdCMV-Luc$_{\Delta E1}$ was coated with polymer and retargeted with Cetuximab, as described in section 5.2.1. A luciferase transgene expression assay (see section 2.2.8) was used to assess the level of transduction achieved with Cetuximab retargeting. An excess of Cetuximab was used to pre-incubate with cells to determine whether the infection was mediated by Cetuximab. Cetuximab was used, rather than an alternative EGFR-binding antibody, to ensure that the blocking antibody was competing for the identical EGFR epitopes. Use of an alternative EGFR-blocking antibody may not have been sufficient to prevent Cetuximab-binding, just as some monoclonal antibodies are able to selectively block EGFR-ligand binding (Winkler *et al.* 1989). Figure 5-5 demonstrates that Cetuximab retargeted adenovirus was able to successfully infect

EGFR-positive A431 and T24 cells, but that there was no significant difference between polymer coated and Cetuximab retargeted adenovirus reporter transgene expression in the EGFR-negative, CAR-positive SW620 cells. Further evidence for the specificity of Cetuximab retargeted adenovirus infection is shown in Figure 5-6. Pre-incubation with high levels of Cetuximab (final concentration during virus incubation of 10 μg/ml) for 40 min inhibited Cetuximab retargeted polymer coated virus, but had no effect on unmodified adenovirus or non-retargeted polymer coated adenovirus reporter transgene expression.

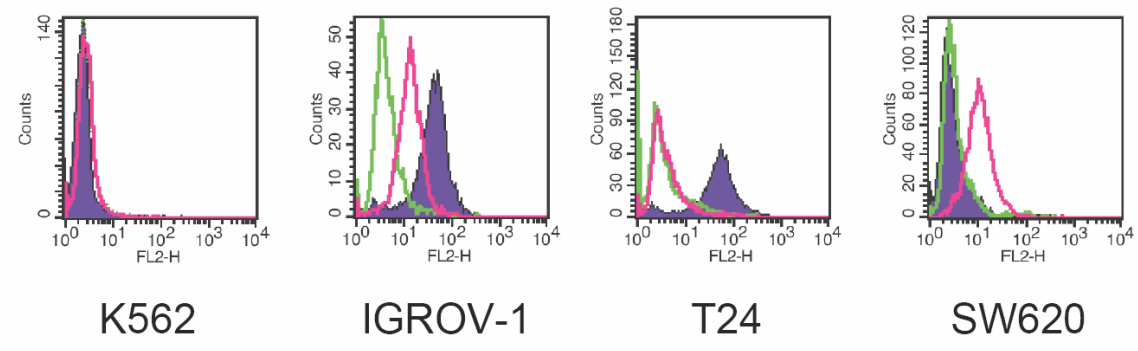


Figure 5-3 CAR and EGFR status of T24 and SW620 cell lines

Cells were grown in 25 cm^2 cell culture flasks until 90% confluent then scraped, pelleted and incubated in rotating polypropylene tubes with DMEM media containing HEPES at 37°C for 4 hours to allow EGFR recovery. Cells were washed and resuspended in 10% HINGS in 96 well v-bottomed plates. Cells were labelled with primary antibody at 4°C for 40 min, washed twice and labelled with secondary antibody for 40 min at 4°C. Cells were washed three times and fixed with 4% paraformaldehyde then analysed using a FACSCalibur machine for fluorescence at 585 nm. Isotype antibody labelled cells are represented with a green open histogram, anti-EGFR labelled cells with a purple filled histogram and CAR labelled cells with a pink open histogram.

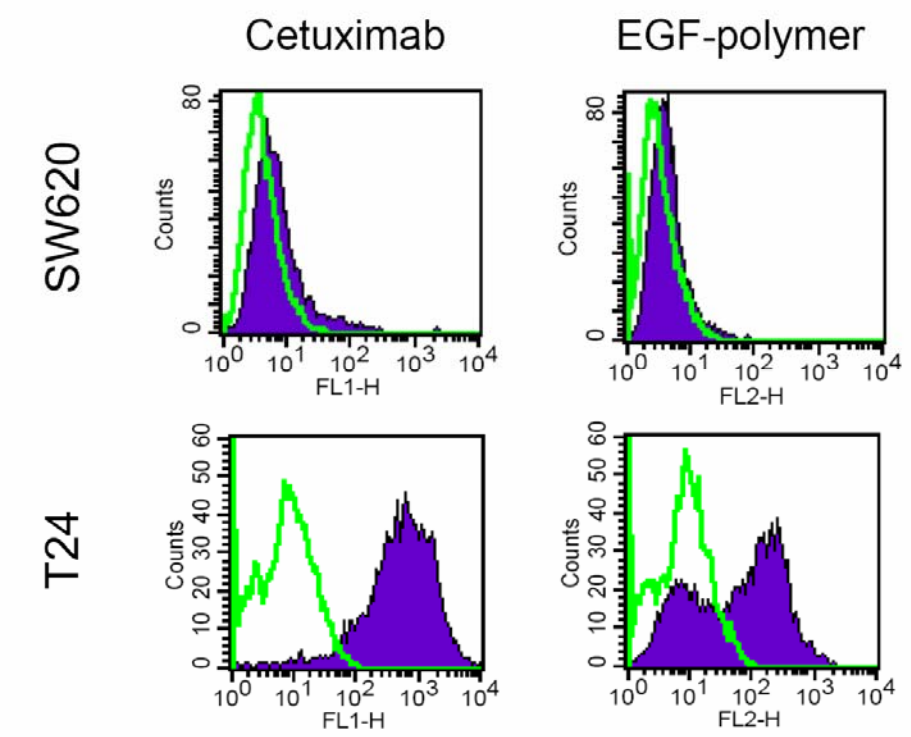
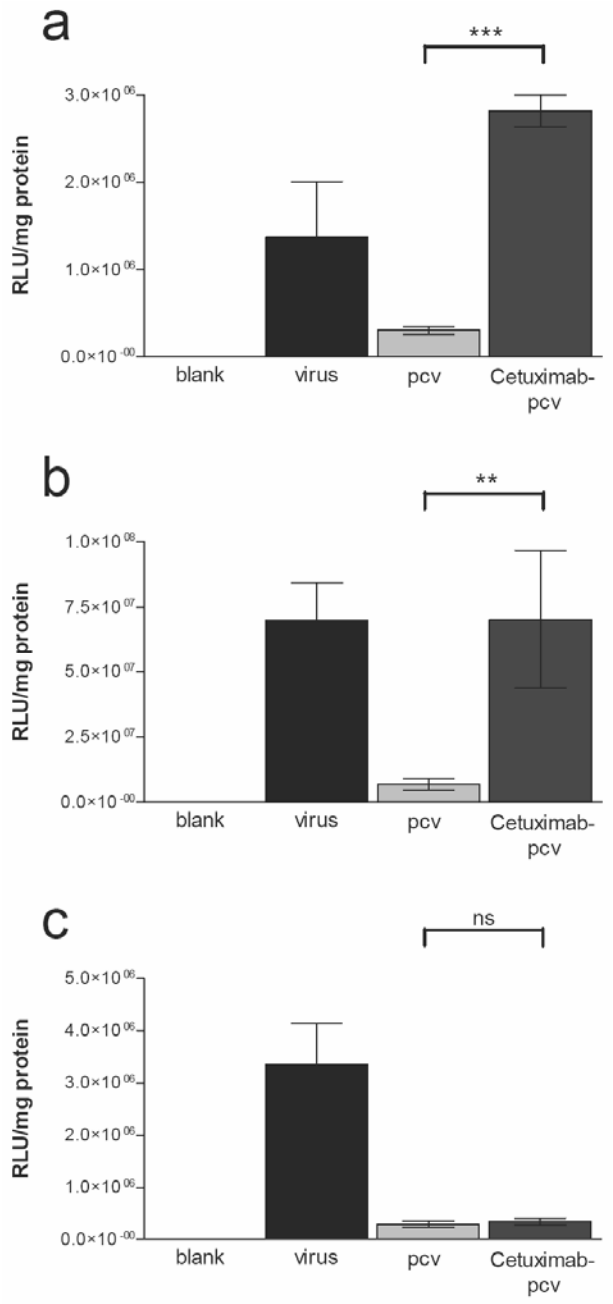


Figure 5-4 Cetuximab and EGF-polymer bind to T24 cells but not SW620 cells

EGFR-positive T24 cells and EGFR-negative SW620 cells were incubated with Cetuximab, an isotype control antibody, a biotinylated EGF-polymer, or a biotinylated-polymer control on ice for 40 min. Cells were washed and incubated with avidin-Texas red or an FITC-labelled secondary antibody for 40 min on ice. Cells were washed, fixed with 2% paraformaldehyde and analysed by flow cytometry at 530 nm or 585 nm. Green open histograms represent the polymer or antibody control; purple shaped histograms represent the biotinylated EGF-polymer or Cetuximab binding. 1 x 10^4 cells were counted per sample.



T24 cells
(EGFR +ve, CAR –ve)

A431 cells
(EGFR +ve, CAR +ve)

SW620 cells
(EGFR –ve, CAR +ve)

Figure 5-5 Cetuximab conjugation is able to retarget polymer-coated adenovirus to EGFR-positive cells

Cells (1 x 10^4/well) were seeded into 96 well plates for 24 hours. Virus was coated with 5 mg/ml of polymer overnight, purified on S400 spin columns, and particle number calculated from a PicoGreen analysis. Cells were pre-incubated with an EGF-blocking antibody or low serum media for 40 min. Either unmodified virus, polymer coated virus or Cetuximab-polymer coated virus at a MOI of 1,000 v.p./cell in low serum media was added without removing antibody and incubated for 90 min. Cells were then washed, normal growth media added and cells incubated for 48 hours. Cells were then lysed and assayed for luciferase transgene expression. Figures show values for media control pre-incubation in white bars, and EGF-blocking antibody in dark grey bars; (a) T24 cells, (b) A431 cells, and (c) SW620 cells. Results are representative of two independent experiments performed in triplicate. Error bars are +/- SEM and P values were calculated from log transformed data by ANOVA with Bonferroni's correction for multiple analyses. ns = not significant, ** = $P < 0.01$, *** = $P < 0.001$.

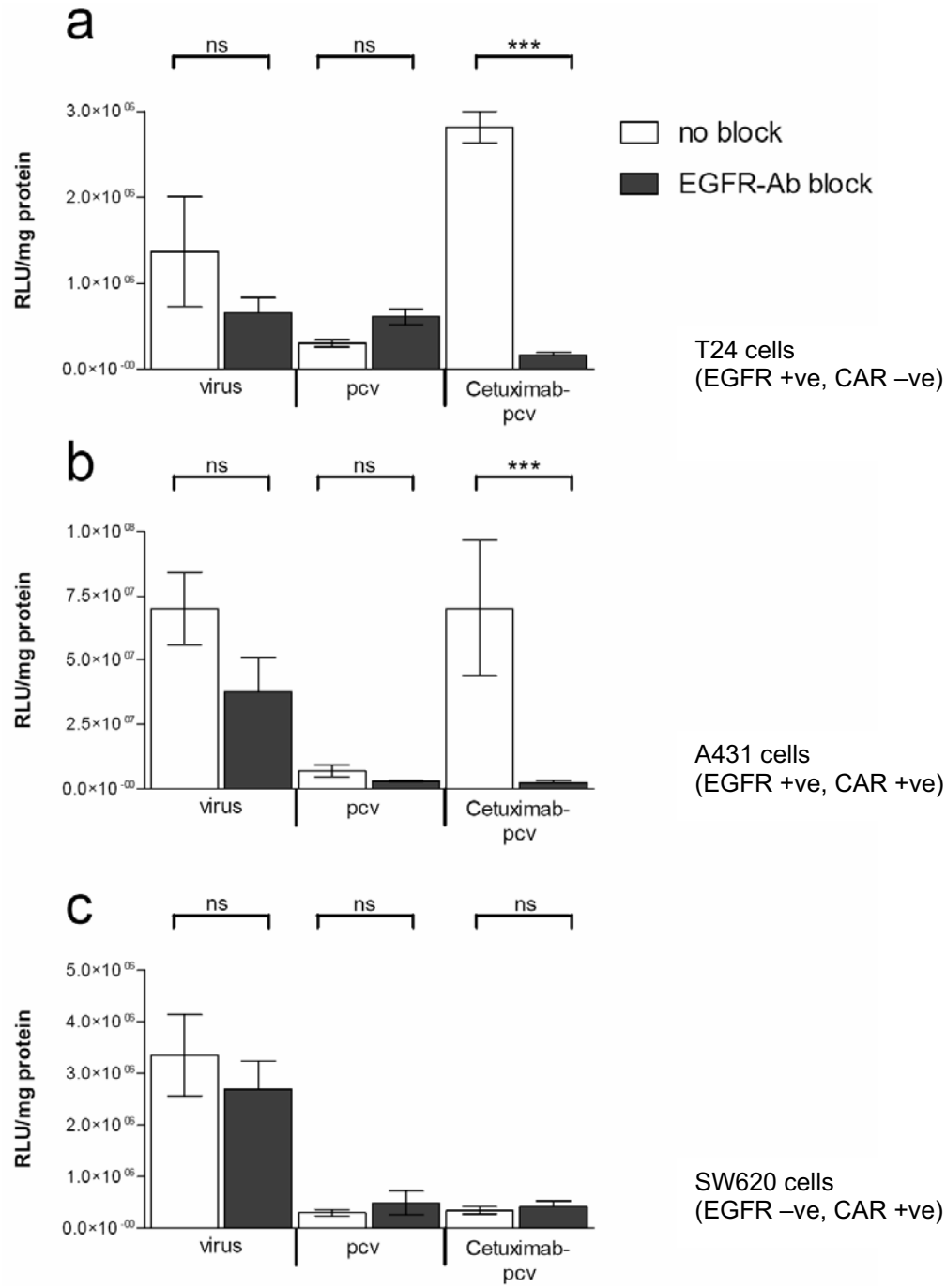


Figure 5-6 Blocking EGF-binding inhibits Cetuximab retargeted virus infection

Cells (1 x 10^4/well) were seeded into 96 well plates for 24 hours. Virus was coated with 20 mg/ml of polymer, purified on S400 spin columns, and retargeted overnight, purified on S400 spin columns, and particle number calculated from a PicoGreen analysis. Cells were pre-incubated with an EGF-blocking antibody (20 μg/ml) or low serum media for 40 min. Either unmodified virus, polymer coated virus or Cetuximab-polymer coated virus, at a MOI of 1,000 v.p./cell in low serum media, was added without removing antibody and incubated for 90 min. Cells were then washed, normal growth media added and cells incubated for 48 hours. Cells were then lysed and assayed for luciferase transgene expression. Figures show values for media control pre-incubation in white bars, and EGF-blocking antibody in dark grey bars; (a) T24 cells, (b) A431 cells, and (c) SW620 cells. Results are representative of two independent experiments performed in triplicate. Error bars are +/- SEM and P values were calculated from log transformed data by ANOVA with Bonferroni's correction for multiple analyses. ns = not significant, *** = $P < 0.001$.

However, the experiment was repeated with Cetuximab virus that had undergone a freeze-thaw cycle (Figure 5-7). Although the transgene expression levels achieved with Cetuximab-pcv in EGFR-positive cell lines was now lower than with unmodified virus, the activity could still be inhibited by pre-incubation with excess Cetuximab. There was no effect of pre-incubating with an isotype control antibody, indicating that the Cetuximab block was EGFR-specific. Furthermore, there was no significant difference in transgene expression between pcv and Cetuximab-pcv in EGFR-negative SW620 cells.

5.2.5 TGF-α polymer is able to retarget adenovirus transduction of EGFR positive cells

Engineered TGF-α (as described in section 5.1) was pre-conjugated to a reactive polymer based on pHPMA (polymer chemistry by Dr Simon Briggs). Reasons for using TGF-α are outlined in section 5.1. AdCMV-Luc $_{\Delta E1}$ was coated with TGF-α polymer overnight (as described in section 2.2.4), and PicoGreen analysis performed to assess virus particle numbers (see section 2.2.4). Unmodified, polymer coated, and TGF-α retargeted polymer coated adenovirus was then used in a luciferase reporter transgene assay to determine relative efficiencies of transduction (see section 2.2.8). TGF-α polymer coated adenovirus was able to successfully retarget A431 cells (EGFR positive) but not EGFR negative SW620 cells (Figure 5-8). TGF-α polymer coated adenovirus retargeting was blocked in A431 cells by pre-incubation for 40 min with an EGFR-blocking antibody (excess Cetuximab at a final concentration during virus incubation of 10 μg/ml). EGFR-blocking had no significant effect on TGF-α polymer coated adenovirus transduction of EGFR-negative SW620 cells.

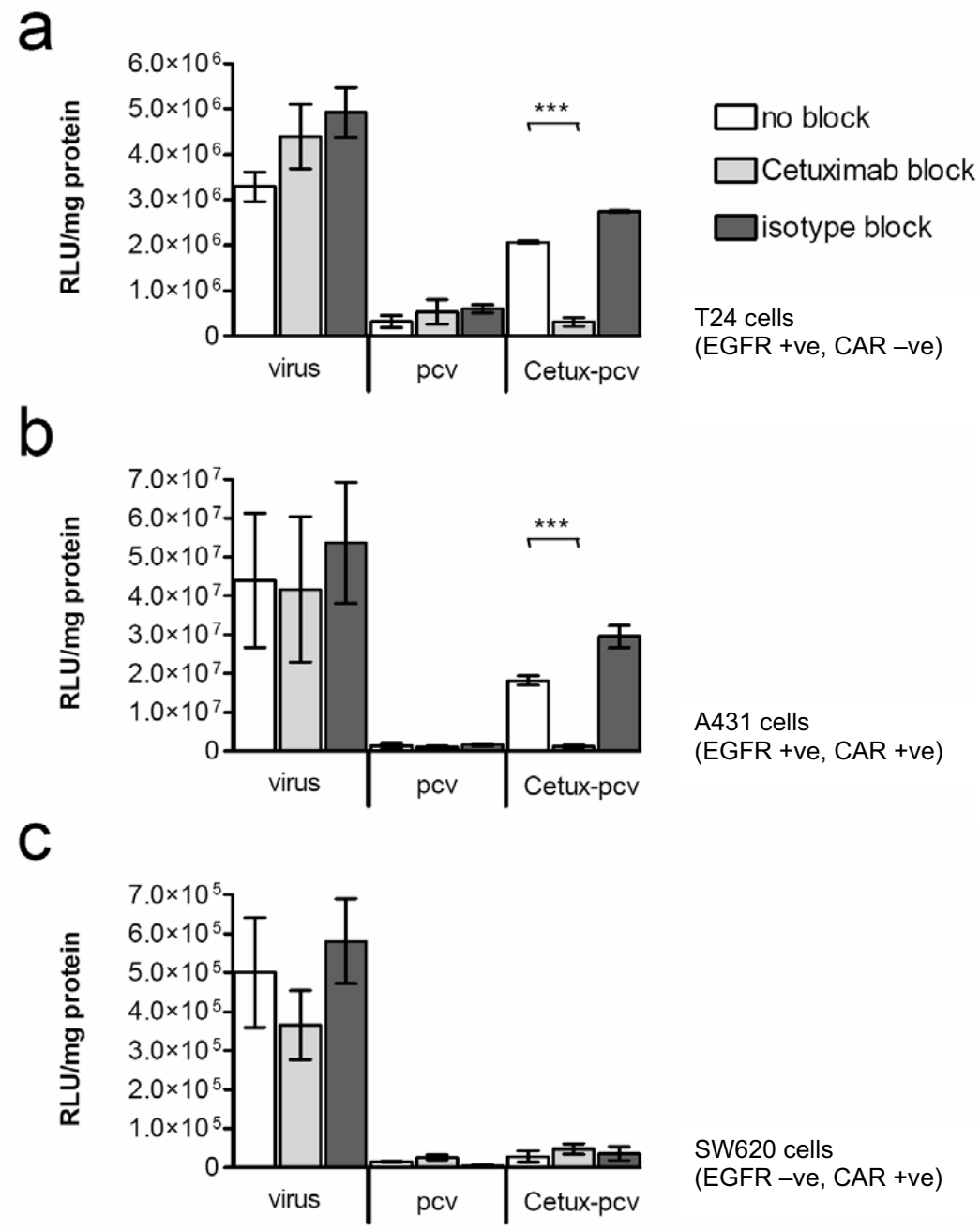


Figure 5-7 Cetuximab-pcv has reduced activity after a freeze-thaw cycle, but transduction remains EGFR specific

Cells (1 x 10^4/well) were seeded into 96 well plates for 24 hours. Virus was coated with 20 mg/ml of polymer, purified on S400 spin columns, and retargeted overnight, purified on S400 spin columns, and particle number calculated from a PicoGreen analysis. Virus was stored at −80°C for one month. Cells were pre-incubated with an EGF-blocking antibody (20 μg/ml) or an isotype control for 40 min. Either unmodified virus, polymer coated virus or Cetuximab-polymer coated virus, at a MOI of 1,000 v.p./cell in low serum media, was added without removing antibody and incubated for 90 min. Cells were then washed, normal growth media added and cells incubated for 48 hours. Cells were then lysed and assayed for luciferase transgene expression. Figures show values for media control pre-incubation in white bars, and EGF-blocking antibody in dark grey bars; (a) T24 cells, (b) A431 cells, and (c) SW620 cells. Results are representative of two independent experiments performed in triplicate. Error bars are +/- SEM and P values were calculated from log transformed data by ANOVA with Bonferroni's correction for multiple analyses. ns = not significant, *** = P < 0.001.

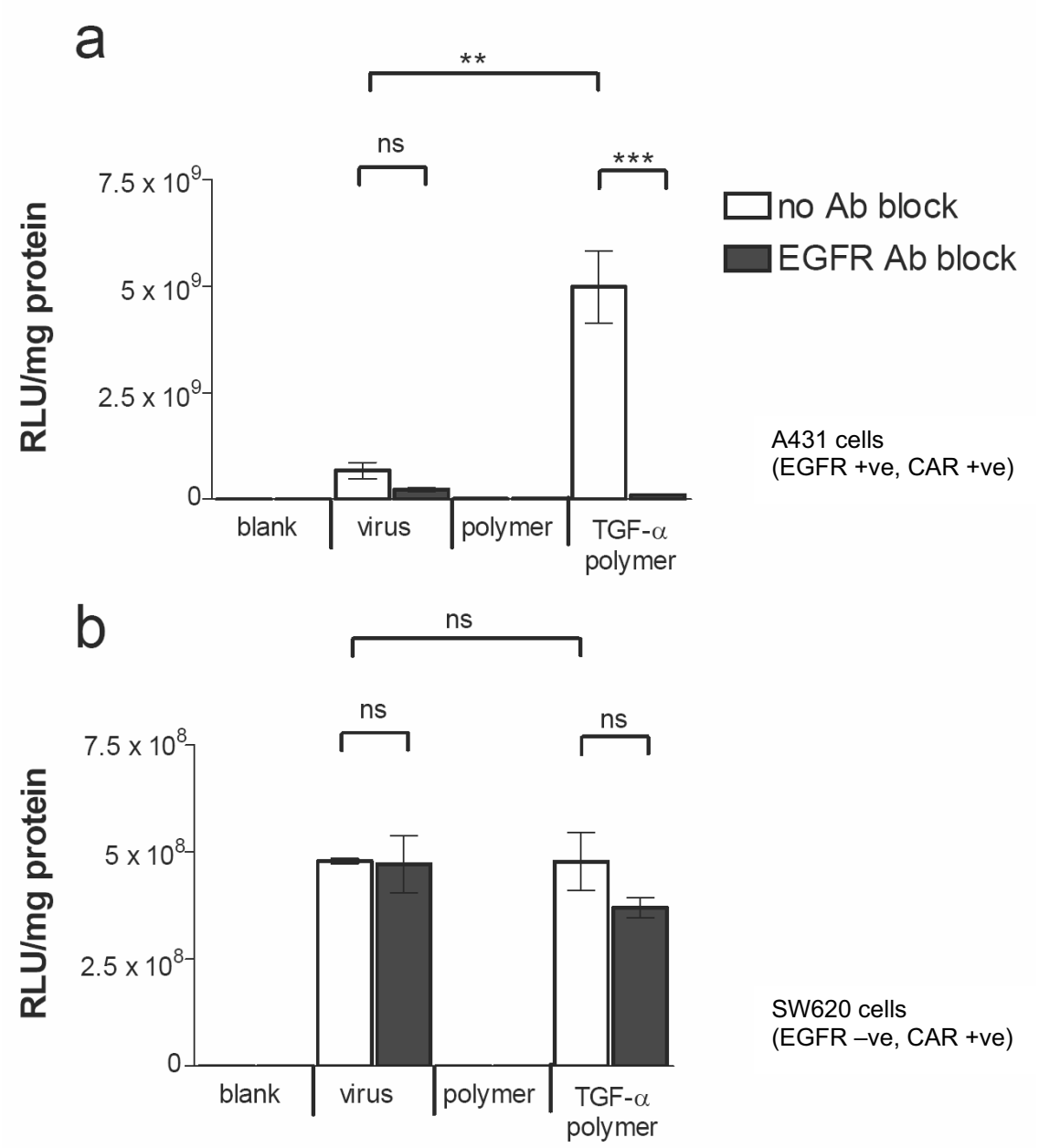


Figure 5-8 TGF-α polymer is able to retarget adenovirus infection via the EGFR

Cells (1 x 10^4/well) were seeded into 96 well plates for 24 hours. Virus was coated with 10 mg/ml of polymer for 40 min at room temperature and overnight at 4°C; virus particle number was calculated from a PicoGreen analysis. Cells were pre-incubated with either an EGF-blocking antibody (Cetuximab; final concentration 10 μg/ml) or low serum media for 40 min. Either unmodified virus, polymer coated virus or TGF-α-polymer coated virus, at a MOI of 1,000 v.p./cell in low serum media, was added without removing antibody and incubated for 90 min. Cells were then washed, normal growth media added and cells incubated for 24 hours. Cells were then lysed and assayed for luciferase transgene expression. Figures show values for media control pre-incubation in white bars, and EGF-blocking antibody in dark grey bars; (a) A431 cells, and (b) SW620 cells. Results are representative of two independent experiments performed in triplicate. Error bars are +/- SEM and P values were calculated from log transformed data by ANOVA with Bonferroni's correction for multiple analyses. ns = not significant; * = P <0.05; ** = P <0.01; *** = P <0.001.

5.2.6 Mitogenic activity of polymer coated viruses

It is possible that, even when using a therapeutic virus payload, polymer coating with growth factors, such as EGF and TGF-α may conversely have a mitogenic effect, especially if the specific activity of each virus particle was low. In order to determine the number of cells in each well, and so more accurately determine the mitogenic effect of EGF- and TGF-α-retargeted reporter adenovirus, a standard curve of MTS activity versus known cell number was produced. Cells were trypsinised to detach and resuspended so that there were between 500 and 5 x 10^5 cells per well in a 96 well plate in triplicate. Cells were incubated for 4 hours to recover in normal growth media (100 μl) and then 20 μl of MTS reagent was added per well and the optical density at 490 nm measured (see section 2.1.4). Standard curves were generated that confirmed the reliability of the method up to ~ 5 x 10^4 cells/well. At cell numbers greater than this the curve flattened off, presumably due to saturation of the reaction (see Figure 5-9). This then determined the number of cells plated out for the mitogenic assay, to avoid cell overgrowth and saturation of the assay.

T24 and A431 cells (2 x 10^3) were seeded into 96 well plates. After 24 hours, cells were washed with PBS and growth media replaced containing either 0.1% FCS, 10% FCS, or adenovirus at 1,000 v.p./cell (unmodified, polymer coated, Cetuximab-, EGF- and TGF-α–retargeted). Cells were incubated for 48 hours at 37°C in 5% CO_2 to allow for growth stimulation prior to assessment using the MTS assay. A standard curve for each cell line was generated as described in Figure 5-9. Cell numbers for experimental wells were extrapolated from standard curves using GraphPad Prism3 software. Results are demonstrated in Figure 5-10. Compared to background (0.1% FCS) only those cells in normal growth media (10% FCS) showed significant growth. There is a trend towards slightly higher cell numbers in the EGF and TGF-α polymer coated virus samples. However, the error bars overlap and so any effect is minimal. At 1,000 v.p./cell there is an approximate dose of 0.2 picograms of EGF in each well of a 96 well plate (see Equation 5-1). It is therefore not surprising that there is minimal mitogenic stimulus from the virus alone. However, in this experiment the EGF- and TGF-α- polymer coated virus had not been purified away from unconjugated EGF and TGF-α, and so there would have been approximately 1.2 μg of EGF in each experimental well, as EGF

on the virus would contribute approximately one sixth of the total EGF. This is still a relatively small mitogenic stimulus, compared with normal serum.

Equation 5-1 Calculation of dose of EGF on virus per experimental well

EGF molecules/polymer = 2

Polymer molecules/v.p. = 1,000

$\therefore$ EGF/virus = 2,000

v.p./well = $1 \times 10^4 \times 1{,}000 = 1 \times 10^7$

Avogadro's number = 6.02×10^{23}

MW EGF = 6,045

$\therefore$ mass EGF/well = 2×10^{-10} g

= 2×10^{-7} mg

Equation 5-2 Calculation of total EGF dose per experimental well

Coating concentration = 10 mg/ml polymer

EGF $\cong$ 10% polymer weight = 1 mg/ml

Volume of virus stock solution in each experimental well = 1×10^{-6} ml

$\therefore$ concentration of EGF = 1×10^{-6} mg + 2×10^{-7} mg (from virus)

=1.2×10^{-6} mg

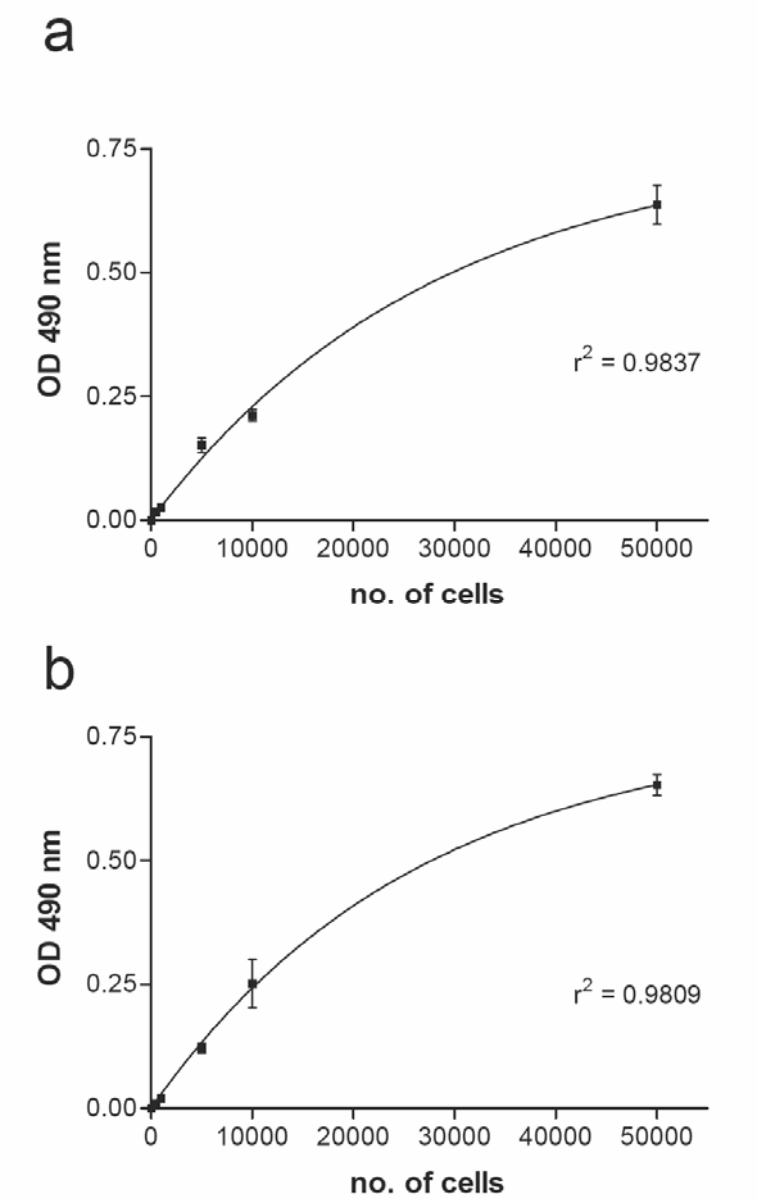


Figure 5-9 Cell standard curves for MTS assay

Cells were trypsinised, counted, a dilutional series generated in 100 μl of normal growth media and plated out in triplicate in 96 well plates. Cells were incubated for 4 hours at 37°C in 5% CO_2 to allow recovery. MTS reagent (20 μl) was added to each well and optical density readings taken at 490 nm over 0.1 sec following 15 and 30 min incubation. (a) A431 cells at 15 min; (b) T24 cells at 15 min.

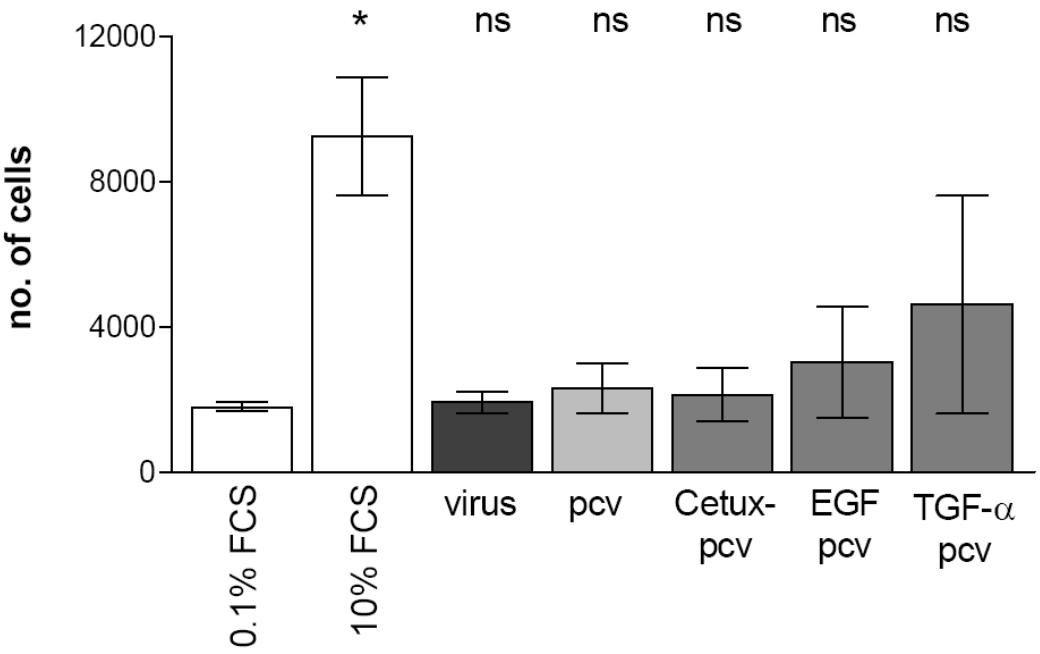


Figure 5-10 Mitogenic effect of adenoviruses coated with retargeted polymers

T24 and A431 cells (2 x 10^3) were seeded into 96 well plates. After 24 hours, cells were washed with PBS and growth media replaced containing 0.1% FCS, 10% FCS, or adenovirus at 1,000 v.p./cell. Cells were incubated for 48 hours at 37°C in 5% CO_2 to allow for growth stimulation. Cells were washed with PBS and normal growth media (100 μl) and MTS reagent (20 μl) was added to each well and optical density readings taken at 490 nm over 0.1 sec following 15 and 30 min incubation. A standard curve for each cell line was generated as described in Figure 5-9. Cell numbers for experimental wells were extrapolated from standard curves using Prism3 software. Error bars are +/- SEM and P values were calculated from log transformed data by ANOVA with Dunnett's correction for multiple analyses compared to the 0.1% FCS control. ns = not significant, * = $P < 0.05$. Data for T24 cells at 30 min incubation are demonstrated, but were representative of 2 independent experiments performed with both cell lines.

5.2.7 Stimulation of EGFR tyrosine kinase activity by EGFR retargeted adenovirus

No mitogenic effect of likely clinical significance was demonstrated *in vitro* with EGF- or TGF-α–retargeted adenovirus. Although it had previously been shown that EGF-polymer conjugate could stimulate EGFR autophosphorylation (see section 4.2.2), and that blocking EGFR could inhibit EGF and TGF-α polymer mediated transduction, the ability of EGFR retargeted polymer coated adenovirus to directly stimulate EGFR tyrosine kinase activity had not been demonstrated. EGF and TGF-α polymer coated adenovirus was therefore used to stimulate A431 cells and a western blot performed on cell lysate to detect phosphorylated EGFR (for methods see section 2.1.9). Unpurified EGF-and TGF-α- polymer coated adenovirus, as used in the mitogenic experiment described above at 10,000 v.p. per cell, were used to stimulate EGFR tyrosine kinase activity. EGFR autophosphorylation was readily detectable on a western blot as demonstrated in Figure 5-11. However, there would be a significant amount of free EGF or TGF-α polymer not conjugated to virus in this preparation; therefore, S400 spin column purified virus was used to stimulate A431 cells. Figure 5-12 demonstrates that purified EGF-polymer coated adenovirus is still able to stimulate a significant amount of EGFR autophosphorylation, as detected by western blot for pEGFR, at 500 v.p./cell. More significantly, this batch of adenovirus had been coated over 12 months previously and subsequently stored at −80°C. This would suggest that polymer coated retargeted adenovirus is able to retain biological activity over prolonged storage periods, which has important implications for clinical applications.

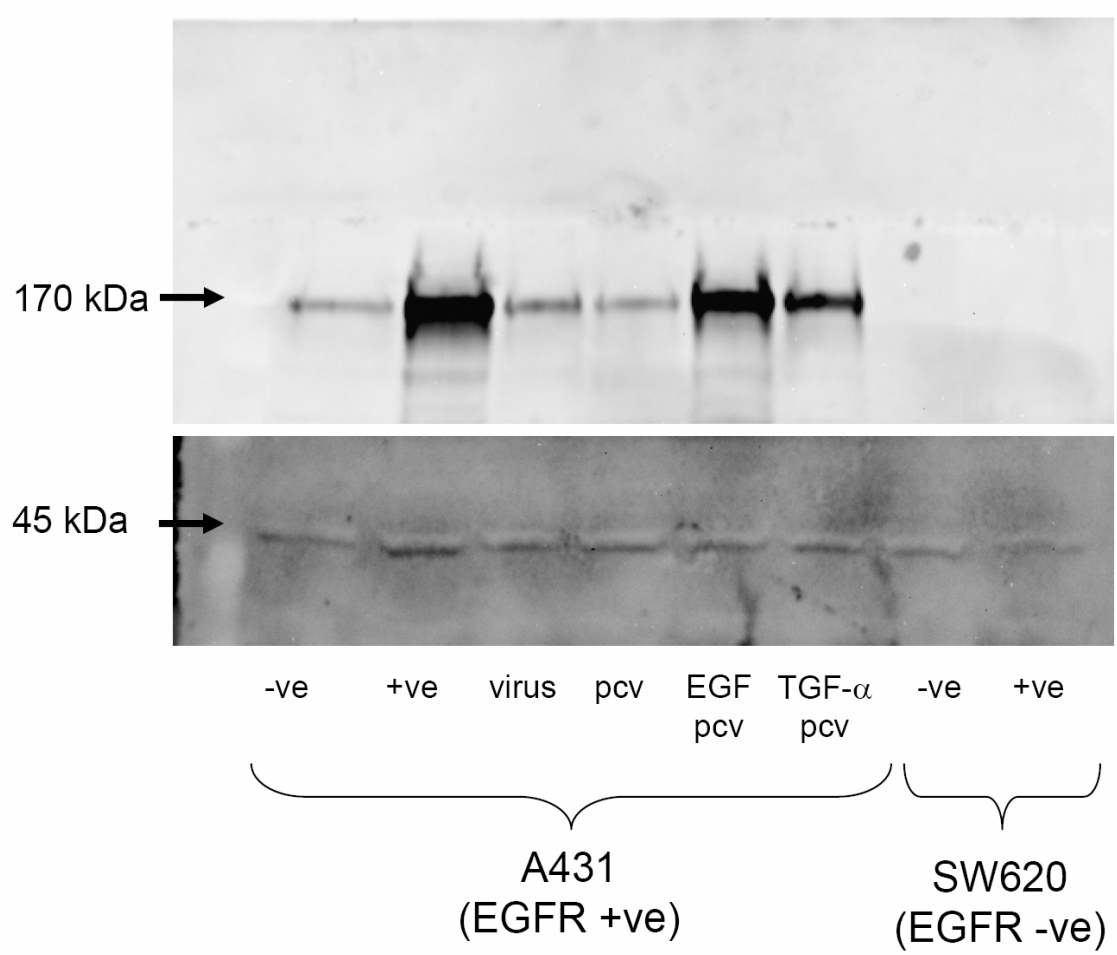


Figure 5-11 Stimulation of EGFR tyrosine kinase activity by EGF & TGF-α retargeted adenovirus

Cells (5 x 10^5) were plated out in 6 well plates and incubated overnight in normal growth media. They were then serum-starved for 6 hours prior to stimulation with EGF (200 nmol/l) or adenovirus (unmodified, polymer coated (pcv), EGF-polymer coated (EGF-pcv) or TGF-α polymer coated (TGF-α-pcv) at 10,000 v.p./cell, diluted in 0.1% BSA in DMEM for 30 min. Cells were lysed, a protein assay performed and equal amounts of protein (20 μg) loaded onto a 7.5% SDS gel. The gel was blotted onto nitrocellulose overnight, divided into two, and labelled with a goat anti-pEGFR primary antibody and an anti-goat-HRP conjugated secondary antibody (top panel), or rabbit anti-β-actin or anti-rabbit-HRP conjugated secondary antibody (bottom panel), and developed with Lumiglo®.

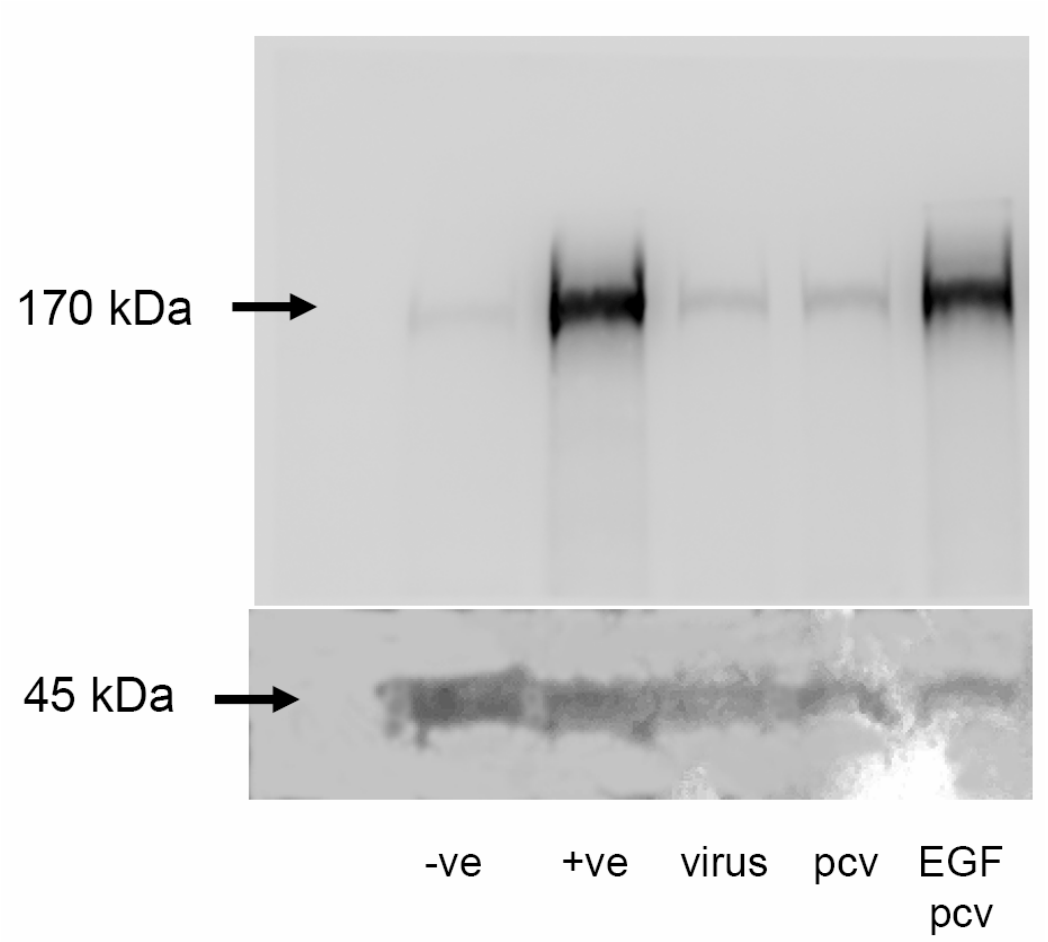


Figure 5-12 Stimulation of EGFR tyrosine kinase activity with purified EGF-pcv

A431 Cells (1 x 10^5) were plated out in 6 well plates and incubated for 72 hours in normal growth media. They were then serum-starved for 6 hours prior to stimulation with EGF (200 nmol/l) or S400 spin column purified adenovirus (unmodified, polymer coated (pcv) and EGF-polymer coated (EGF-pcv)) at 500 v.p./cell, diluted in 0.1% BSA in DMEM for 30 min. Cells were lysed, a protein assay performed and equal amounts of protein (20 μg) loaded onto a 7.5% SDS gel. The gel was blotted onto nitrocellulose overnight, divided into two, and labelled with a goat anti-pEGFR primary antibody and an anti-goat-HRP conjugated secondary antibody (top panel), or rabbit anti-β-actin or anti-rabbit-HRP conjugated secondary antibody (bottom panel), and developed with Lumiglo®.

5.3 Discussion

These data demonstrate that both Cetuximab and TGF-α are able to successfully retarget adenovirus via the EGFR. Furthermore, these data also indicate that EGFR tyrosine kinase activity is not necessary to stimulate adenovirus internalisation via the EGFR. However, since the pEGFR activity for Cetuximab alone was slightly above background levels, it may be that Cetuximab acts as a partial agonist on binding the EGFR, and so does not conclusively prove that some degree of EGFR tyrosine kinase activity is not necessary. In order to further

elucidate this, it would be necessary to use cell lines that had truncated or mutated EGFR that lacked tyrosine kinase activity, to determine whether EGF, TGF-α or Cetuximab polymers were still able to retarget adenovirus successfully.

Both EGF and TGF-α retargeted adenovirus, which had not been purified, were able to stimulate significant EGFR phosphorylation. It is not clear what proportion of this activity was due to EGF and TGF-α polymer conjugated to adenovirus or free polymer. However, S400 spin column purified EGF-polymer coated adenovirus was still able to stimulate EGFR autophosphorylation, as detected by western blot. Nevertheless, this quantity of polymer, whether free or virus conjugated, was not able to stimulate significant cell growth, when compared to media containing 10% serum. This would suggest that the mitotic effect of EGF and TGF-α polymer coated virus is negligible compared to normal levels of growth factors found *in vivo*. It would therefore be unlikely that EGF-polymer coated adenovirus would have an adverse effect *in vivo*, since cells stimulated by EGF-retargeted adenovirus would be those most likely to be killed, either by direct virus effects, in the case of replication competent viruses, or as the result of gene expression, if viruses were armed with suicide genes. Indeed, stimulating some mitotic activity may make cells more likely to respond to chemotherapy that non-specifically affects actively dividing cells, and could have a synergistic effect with conventional treatments.

Cetuximab was able to reliably retarget polymer coated adenovirus. Previous work using another anti-EGFR antibody (EMD-72000 (Vanhoefer *et al.* 2004)) had been unsuccessful (Dr S. Nicum, unpublished results). Unfortunately we do not have an amino acid sequence for either antibody, but it is likely that the differences in ability to retarget are dependent upon there being no reactive amino groups in or around the EGFR-binding site, which could sterically inhibit retargeting. Adenovirus has previously been retargeted with bispecific antibodies, and so we know that antibodies can mediate adenovirus uptake via alternative receptors. Since completion of these experiments, a study was published confirming that Cetuximab stimulates EGFR internalisation, even if EGFR tyrosine kinase activity is inhibited (Jaramillo *et al.* 2006). Cetuximab stimulated EGFR internalisation with a similar time course to EGF-induced EGFR

internalisation. However, pulse-chase experiments, using I^{125}-labelled antibody and I^{125}-labelled EGF, demonstrated that a greater percentage of internalised Cetuximab was recycled to the cell surface in an intact form, rather than routed to lysosomes for degradation (~ 60% vs. ~30% for EGF). The authors hypothesised that this was due to the binding of Cetuximab to EGFR being highly pH-dependent and demonstrated that at pH 6 no Cetuximab was bound to EGFR compared to 100% binding at pH 7.5. This is a likely explanation and mirrors the differential intracellular routing and fate of EGFR bound to either EGF, which is relatively stable at low pH and causes EGFR to be routed to and degraded within lysosomes, compared to TGF-α, which readily dissociates at low pH levels found in the early endosome and results in high levels of EGFR recycling (Maeda *et al.* 2002). However, although not directly comparable, due to differences in polymer conjugates, EGF, TGF-α and Cetuximab were all able to successfully mediate virus transduction, and similar ratios of reporter transgene expression from unmodified and retargeted adenovirus were observed in A431 cells. This is probably because adenovirus, once internalised, rapidly escapes from the early endosome, and so is not dependent upon eventual fate of the EGFR to which it has bound.

6 Therapeutic effect of EGF-polymer coating an oncolytic adenovirus in an animal model

6.1 Introduction

In the experiments described in Chapter 5 EGF-polymer coating was sufficient to successfully retarget adenovirus transduction via the EGFR *in vitro*. Previous work has shown that polymer coating improves circulation kinetics, reduces liver transduction, and decreases toxicity of adenovirus when given intravenously (Green *et al.* 2004). However, ovarian cancer remains largely confined to the peritoneal cavity, even at a late stage, and it is uncommon to find sites of distant metastasis. Accordingly, there is a clear rationale for treating confined regional disease with regional i.p. administration. This approach is supported by pharmacokinetic studies (DeGregorio *et al.* 1986), which showed 18-fold and 6-fold increases in carboplatin area under the curve (AUC) values within peritoneal fluid compared to plasma at 4 and 24 hours respectively. Indeed, data from clinical trials of conventional chemotherapy have suggested that this is the preferential route, generating improved efficacy and reducing side effects (Alberts *et al.* 1996). A recent randomized control trial of i.v. or i.p. cisplatin in addition to i.v. paclitaxel demonstrated improvements in progression free and overall survival for the i.p. cisplatin arm (49.7 versus 65.6 months overall survival P = 0.03) and has renewed enthusiasm for this route of administration (Armstrong *et al.* 2006). Although acute toxicity was higher in the i.p. arm, the quality of life at 12 months post treatment was similar between the groups.

It was noted in the early 20th Century that inoculation or infection with some live attenuated or wild type viruses coincided with the regression of certain cancers. As a result of this observation viruses were used experimentally to treat cancers, and therapeutic effects were reported (Higgins and Pack 1951; Pack 1950). Adenovirus has a lytic replication cycle and can have a direct anti-tumour effect. Adenovirus was first identified in 1953 and subsequently found to replicate very readily in epithelial cell lines, such as the cervical cancer derived cell line, HeLa. Wild type adenovirus administered intra-tumourally or intra-arterially was used to treat

cervical cancer patients who had recurrent disease following radiotherapy (Georgiades *et al.* 1959; Smith *et al.* 1956).

In the 30 patients with cervical cancer in the early studies by by Smith *et al*, there were dramatic responses in those treated with wild type adenovirus serotype 5 cultured on HeLa cells, but no responses were generated with heat-inactivated virus. Despite, in some cases, significant tumour necrosis and regression, residual tumour remained and the cancer eventually relapsed. Necrosis was seen only in tumour tissue, not in normal tissues, and tumour responses were inversely proportional to the amount of neutralising activity of individual patient sera prior to treatment. In the series from Poland (Georgiades *et al.* 1959; Smith *et al.* 1956), 10 women with advanced cervical cancer (FIGO stage III and IV) were treated with wild type adenovirus. This adenovirus had undergone multiple passages in cervical cancer cell lines (HeLa and Detroit-6) and virulence of anti-cancer activity increased with virus that had undergone high number of passages (range of 30-112), an early recognition of the benefit of *in vitro* selection of oncolytic viruses. Virus was administered both intra-tumourally and intravenously. Side effects were minimal, largely consisting of pyrexia, shivering and joint pains, which occurred on days 1-3 after inoculation and was more pronounced in patients who were given adrenocorticotropic hormone (ACTH) prior to virus inoculation. ACTH was given with the intention of reducing the inflammatory response to adenovirus in order to increase the oncolytic effect and duration. Seven of the 10 patients subsequently received radiotherapy following virus treatment; it was noted that in six of the seven patients 'the tumour showed considerable susceptibility to X-rays'. Virotherapy became unfashionable with the development of chemotherapeutic agents. However, with the emergence of gene therapy and the recognition that replication incompetent viruses were unlikely to spread effectively throughout a large tumour mass, oncolytic viruses have regained favour.

Researchers have made a range of genetic modifications to adenovirus to enhance its selectivity for cancer cells, creating what have become known as conditionally replicating adenoviruses or CRAds. During a normal replication cycle, adenovirus needs to activate the cellular machinery that controls DNA synthesis in order to achieve replication of the adenovirus

DNA genome. Several gene products expressed in the early phase of infection interact with and cause the inactivation of cellular proteins that are central to the control of the cell cycle (see Table 6-1). Thus, cancer cells, which are already actively cycling and have low levels of cell cycle regulatory proteins, are intrinsically more permissive to virus infection than normal quiescent/non-cycling cells. Gene products of the adenovirus E1A and E1B regions bind to and inactivate retinoblastoma gene product (pRb) and p53 respectively, which are central to the cell cycle and control the G1-S phase check point (Wang *et al.* 1991; Whyte *et al.* 1989; Yew and Berk 1992). Adenoviruses with deletions in these genes have been engineered to replicate selectively within cells that lack wild type p53 and pRb pathways. Another mechanism to confer conditional replication is to remove viral promoters of key gene products and replace them with tumour or tissue specific promoters, e.g. the α–fetoprotein (AFP) gene (up-regulated in hepatocellular carcinoma) (Hallenbeck *et al.* 1999); or the prostate specific antigen (PSA) promoter (up-regulated in prostate cancer) (Rodriguez *et al.* 1997).

Table 6-1 Interaction of adenovirus proteins with cell cycle control proteins

Virus gene product	*Cellular protein interaction*	*Reference*
E1B-55 kDa	Binds and inactivates p53	(Bischoff *et al.* 1996)
E4-34 kDa	Binds and promotes p53 degradation	(Corbin-Lickfett and Bridge 2003)
E1A	Binds and inactivates pRb	(Wang *et al.* 1991)

In developing an *in vivo* model to measure the therapeutic effect of EGF-polymer coating, it was decided to use a directly oncolytic adenovirus. In an immune incompetent nude mouse model of ovarian cancer, anti-tumour responses would be due to the oncolytic effect of the virus, rather than a bystander effect, as seen with VDEPT approaches, or an anti-viral, anti-transgene or anti-tumour adaptive immune response.

The aims of the experiments in this chapter were to:

- Determine the distribution and toxicity profiles of EGF-polymer coated adenovirus compared with polymer coated and unmodified virus in an animal model following i.p. delivery.
- Optimise the concentration of polymer used to coat adenovirus prior to the investigation of the therapeutic effect of EGF-polymer coated adenovirus in a nude mouse model of human ovarian cancer
- Identify a suitable oncolytic adenovirus (from the selection outlined in Table 6-2) and to use it as a therapeutic agent in a pre-clinical trial comparing unmodified adenovirus with EGF-polymer and Cetuximab-polymer coated adenovirus in a nude mouse model of human ovarian cancer.

Unfortunately, due to the limited supply of modified TGF-α, there was insufficient TGF-α polymer available to test the efficacy of TGF-α-polymer coating *in vivo* and so the following chapter will concentrate on EGF- and cetuximab- retargeting.

6.2 Methods and results

6.2.1 Effect of EGF-polymer on adenovirus organ transduction

Female nude mice aged 6-9 weeks were housed and cared for according to Home Office regulations (see section 2.3). SKOV-3 cells (1×10^7) were implanted by i.p. injection and animals were monitored for 5 weeks until abdominal tumours were just palpable and a small amount of ascites (~1 ml) had been produced. Animals (3 per group) were then injected i.p. with unmodified, polymer-coated or EGF-polymer coated (coating concentration 10 mg/ml) adenovirus (AdCMV-Luc$_{\Delta E1}$ 5×10^{10} v.p.) encoding the luciferase transgene. After 24 hours mice were sacrificed using a Schedule 1 approved method. A post-mortem dissection was performed and organ samples obtained for analysis of luciferase expression (see section 2.3.4). At harvesting, blood was taken by cardiac puncture and analysed for alanine transaminase (ALT) and aspartate transaminase (AST) levels (see section 2.3.6) to assess liver toxicity of virus treatment.

There were no significant increases in liver transaminase levels above background at 24 hours (Figure 6-1), suggesting that i.p. administration resulted in little acute hepatic toxicity. In accordance with the biochemical data, no adverse clinical signs were observed following i.p. virus injection at this virus dose in any individual. Administration of polymer coated virus and EGF-polymer coated virus resulted in no increases in transaminase levels. It has been reported that the i.v. delivery of 5 x 10^{10} v.p. adenovirus causes severe liver toxicity (Green *et al.* 2004). These experiments therefore indicate a benefit of i.p. delivery over i.v. delivery for an intraperitoneal tumour.

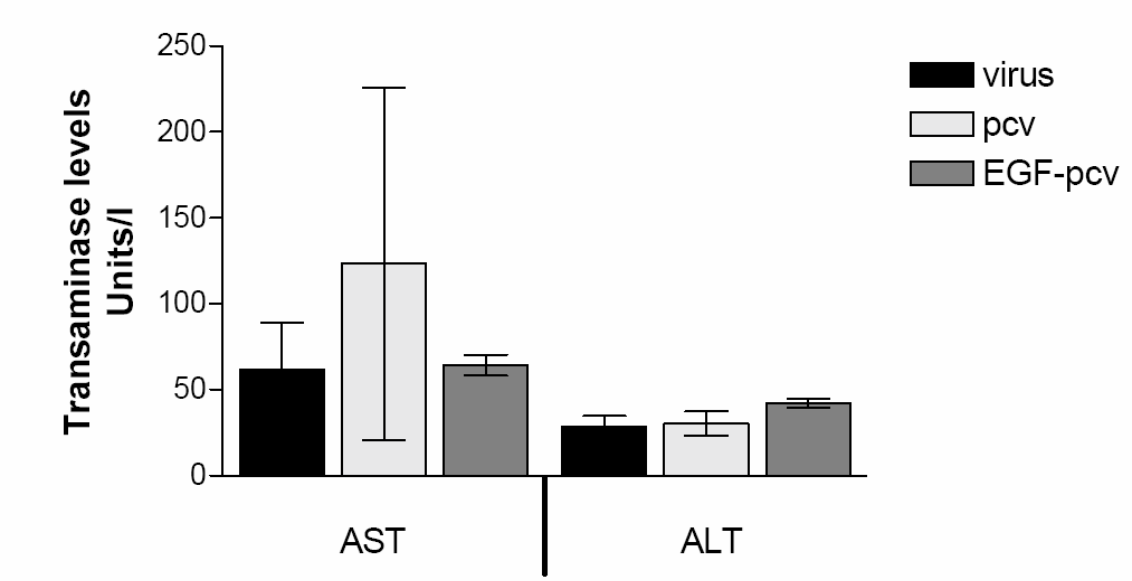


Figure 6-1 Transaminase levels at 24 hours in mice injected with adenovirus i.p.

Female nude mice (n = 3 per group) were injected i.p. with SKOV-3 cells (1 x 10^7) and tumours allowed to develop (~5 weeks). Mice were then injected i.p. with adenovirus (AdCMV-Luc $_{\Delta E1}$ 5 x 10^{10} v.p.) which was either unmodified or coated with polymer or EGF-polymer (10 mg/ml coating concentration). 24 hours after virus injection, mice were sacrificed and blood taken by cardiac puncture. Serum samples were assayed for AST and ALT activity (see section 2.3.6). Mean data from 3 individuals are shown; error bars are +/- SD. There were no significant differences between the different treatment groups.

Unexpectedly, only very small tumours developed in these mice, and in several animals no visible tumours were established. The study was therefore underpowered; group sizes were too small for there to be statistically significant differences in transduction levels between the groups. However, there was reduced liver transduction in all polymer coated virus groups, except for the 10 mg/ml EGF-polymer coated virus group, suggesting that this level of coating *in vivo* may not be adequate to detarget liver transduction (data not shown).

This experiment was repeated and polymer coating concentrations of 10 mg/ml and 20 mg/ml were used. Organs were analysed for luciferase gene expression and virus content by quantitative PCR. However, again there were problems with tumour formation in some mice, so that tumour:liver ratios could not be compared. Data from liver transduction levels (Figure 6-2) suggest that a coating concentration higher than 10 mg/ml is necessary to reduce liver transduction, although this study was underpowered to show any significant effect, even at the higher coating concentration of 20 mg/ml.

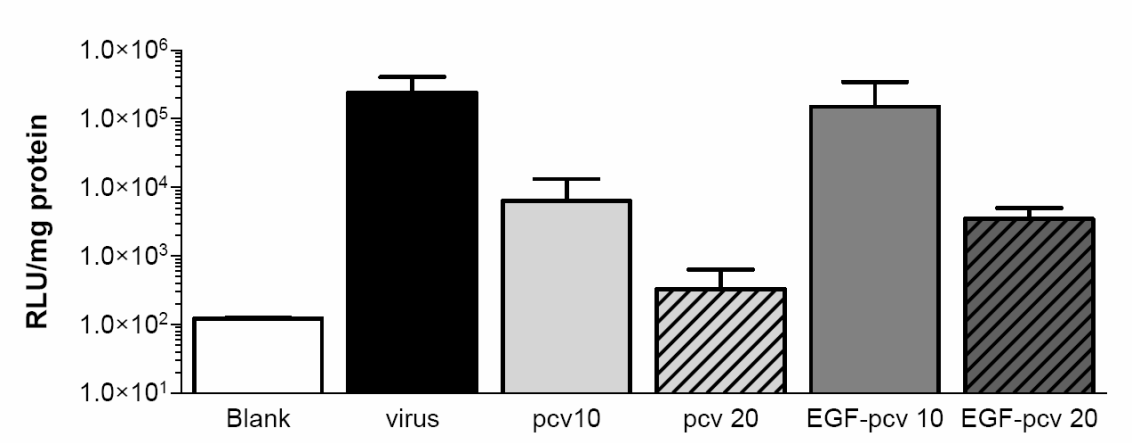


Figure 6-2 Luciferase expression *in vivo* at different polymer coating concentrations

Female nude mice (n = 3 per group) were implanted i.p. with SKOV-3 cells (1 x 10^7) and tumours allowed to establish for six weeks. Mice were injected i.p. with adenovirus (AdCMV-Luc $_{\Delta E1}$ 5 x 10^{10} v.p.) which was either unmodified or coated with polymer or EGF-polymer at 10 mg/ml and 20 mg/ml coating concentration. 24 hours after virus injection, mice were sacrificed and livers assayed for luciferase activity. Bars represent mean group values; error bars represent SD.

Previous data from intravenous administration and pharmacokinetic studies demonstrated that a polymer coating concentration of 20 mg/ml improved virus pharmacokinetics and reduced the very rapid hepatic uptake rates observed with unmodified virus (Green *et al.* 2004). The data presented here have low statistical power, due to problems with reduced *in vivo* tumour proliferation and low numbers in each group. This may be due to using older animals for these experiments (>10 weeks of age), which were due to problems with supply of nude mice at the time these experiments were performed. In addition, the cell line used was SKOV-3 cells, not SKOV-3-ip cells (which have better *in vivo* proliferation), as I was unable to obtain the SKOV-3-ip cell line. I therefore decided not to persist with obtaining surrogate end-points for efficacy of polymer coating *in vivo* and instead to proceed with a model which would investigate whether polymer coating and retargeting had any therapeutic benefit.

6.2.2 Potency of oncolytic adenoviruses on a panel of ovarian tumour cell lines

A panel of ovarian cancer cell lines was used in a cell survival study, utilising the MTS assay (see section 2.1.4) to determine the oncolytic effect of a range of conditionally replication competent adenoviruses (CRAds)(see section 2.2.1 and Table 6-2). Figure 6-3 demonstrates the results. IGROV-1 cells were highly sensitive to all of the adenoviruses, with no significant survival at 0.01 pfu/cell (see section 2.2.5.1 for method). This was likely due to IGROV-1 cells having relatively high CAR expression levels (see Figure 4-7). However, SKOV-3 cells were highly resistant to CRAds and even showed a level of resistance to wild type adenovirus. The multiplicity of infection of adenovirus required to kill 50% of the cells (IC_{50}) was calculated from the combined results of three independent experiments (Figure 6-4). However, as the IC_{50} was not achieved in every experiment for some cell lines, not all of these calculations could be made from triplicates. For all cell types the most potent oncolytic virus was wild type adenovirus. ONYX 017 and *dl*922-947 were the most effective conditionally oncolytic adenoviruses in this panel of ovarian cancer cell lines.

Table 6-2 Oncolytic viruses and their genetic modifications

CRAd	*Genetic modifications*	*Source/reference*
Wild type Adenovirus type 5 (Ad5WT)	nil	(Rowe *et al.* 1953)
ONYX-015	Deletion in E1B-55 kDa region and E3 deletion	(Heise *et al.* 1997)
ONYX-017	Deletion in E1B-55 kDa region (Δ1520)	(Jounaidi and Waxman 2004)
*dl*922-947	E1A pRb binding site mutation and E3B deletion (intact intact E3A region with E3 11.6, the adenovirus death protein)	(Heise *et al.* 2000)
EHE2F	E1A and E1B under control of oestrogen and hypoxia response elements. E2F-1 promoter in E4	(Hernandez-Alcoceba *et al.* 2002)

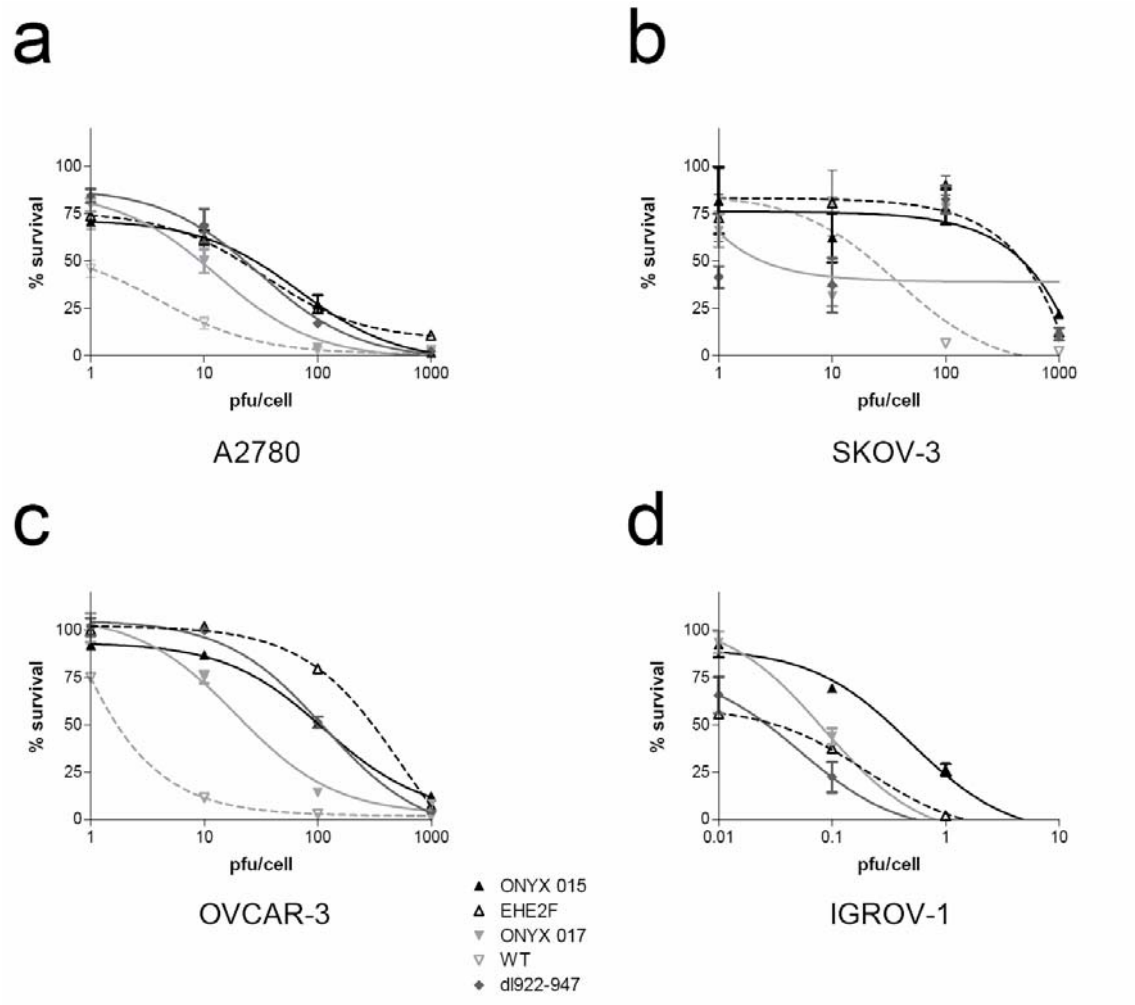


Figure 6-3 Oncolytic effect of conditionally replicating adenovirus

Cells (1 x 10^4) were seeded into 96 well plates and infected 24 hours later with different MOI (pfu) of conditionally replicating adenoviruses (see section 2.2.5.1). Cells were maintained in 2% FCS DMEM and fed with additional media at 48 hour intervals. An MTS assay was performed 6 days following infection to determine percentage cell survival. Experiments were performed in triplicate; error bars are +/- SEM. The results are representative of at least three independent experiments. (a) A2780 cells; (b) SKOV-3 cells; (c) OVCAR-3 cells; and (d) IGROV-1 cells.

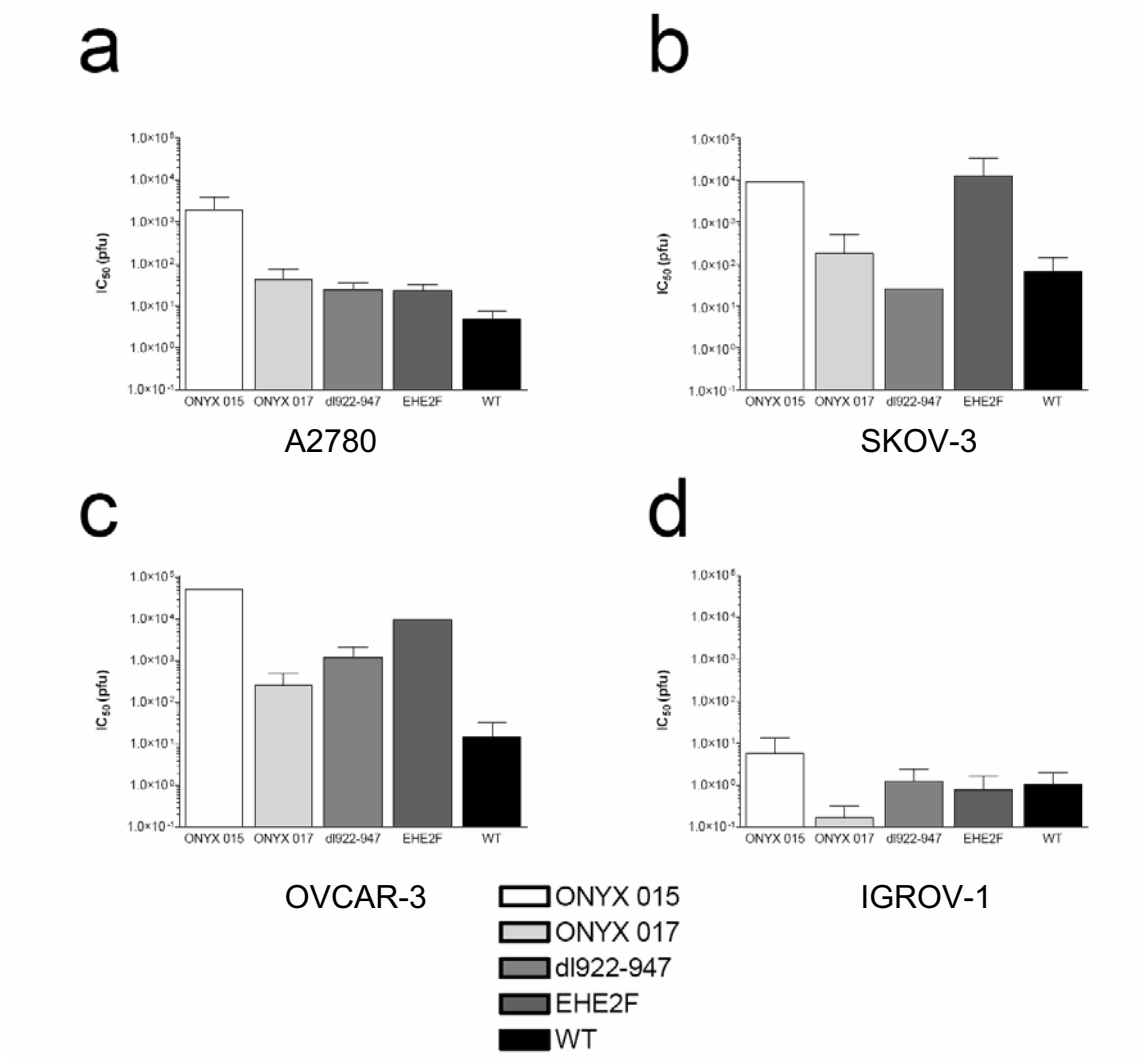


Figure 6-4 IC_{50} of conditionally replicating adenoviruses in ovarian cancer cells

Sigmoidal dose response curves (as shown in Figure 6-3) were used to generate IC_{50} data for different adenoviruses in the four different ovarian cell lines using Prism 4 software. Mean IC_{50} were generated from at least three independent experiments performed in triplicate for each different virus; error bars represent SD where at least three IC_{50} values were available (virus concentrations differed in the experiments to try and achieve ranges which covered 50% survival in order to generate IC_{50} values. However, in some experiments IC_{50} could not be generated, since the curve did not cross 50% survival, hence why there are not error bars for all viruses in every cell line). (a) A2780 cells; (b) SKOV-3 cells; (c) OVCAR-3 cells; and (d) IGROV-1 cells.

6.2.3 Effect of coating with EGF-polymer on oncolytic effect of wild type adenovirus (Ad5WT)

Previous data had shown that EGF-pcv was successfully retargeted to EGFR positive cell lines, as demonstrated by reporter transgene expression. Ad5WT was the most potent oncolytic virus when tested against a panel of CRAds. The next step was therefore to determine whether EGF-polymer coating of Ad5WT was able to successfully retarget a therapeutic effect, which requires not just transgene expression but a productive virus infection. Ad5WT was coated with polymer or EGF-polymer at 10 mg/ml. A panel of ovarian carcinoma cell lines were infected with unmodified virus, pcv and EGF-pcv and a cell survival assay performed, with assessment for viability performed 6 days after infection using the MTS assay. Figure 6-5 demonstrates that in SKOV-3 cells there was a slight increase in sensitivity to EGF-pcv compared to unmodified Ad5WT. Minimal cell kill was observed in A2780 cells following incubation with pcv, although EGF-pcv had similar activity to unmodified virus. No increased cell killing was seen with EGF-pcv compared with pcv in OVCAR-3 cells. IGROV-1 cells, as demonstrated in Figure 6-4, were exquisitely sensitive to Ad5WT, probably due to their high CAR expression, and there was little effect of polymer coating. This may be because polymer coating, although having a significant knock-down, does not completely prevent CAR-mediated infection of the polymer coated adenovirus, thus some cells would be infected by a few virus particles and support a lytic replication cycle, releasing non-coated adenovirus particles, which were then able to efficiently infect and kill any cells not infected by the initial inoculation with polymer-coated virus.

In summary, these data suggest that in some cell lines (SKOV-3 and OVCAR-3) EGF-polymer coating Ad5WT did enable it to produce an oncolytic effect, presumably by supporting a replication cycle, although in order to be certain about virus replication, this would need to be proven directly, e.g. by measuring burst size of virus or virus genome content by QPCR.

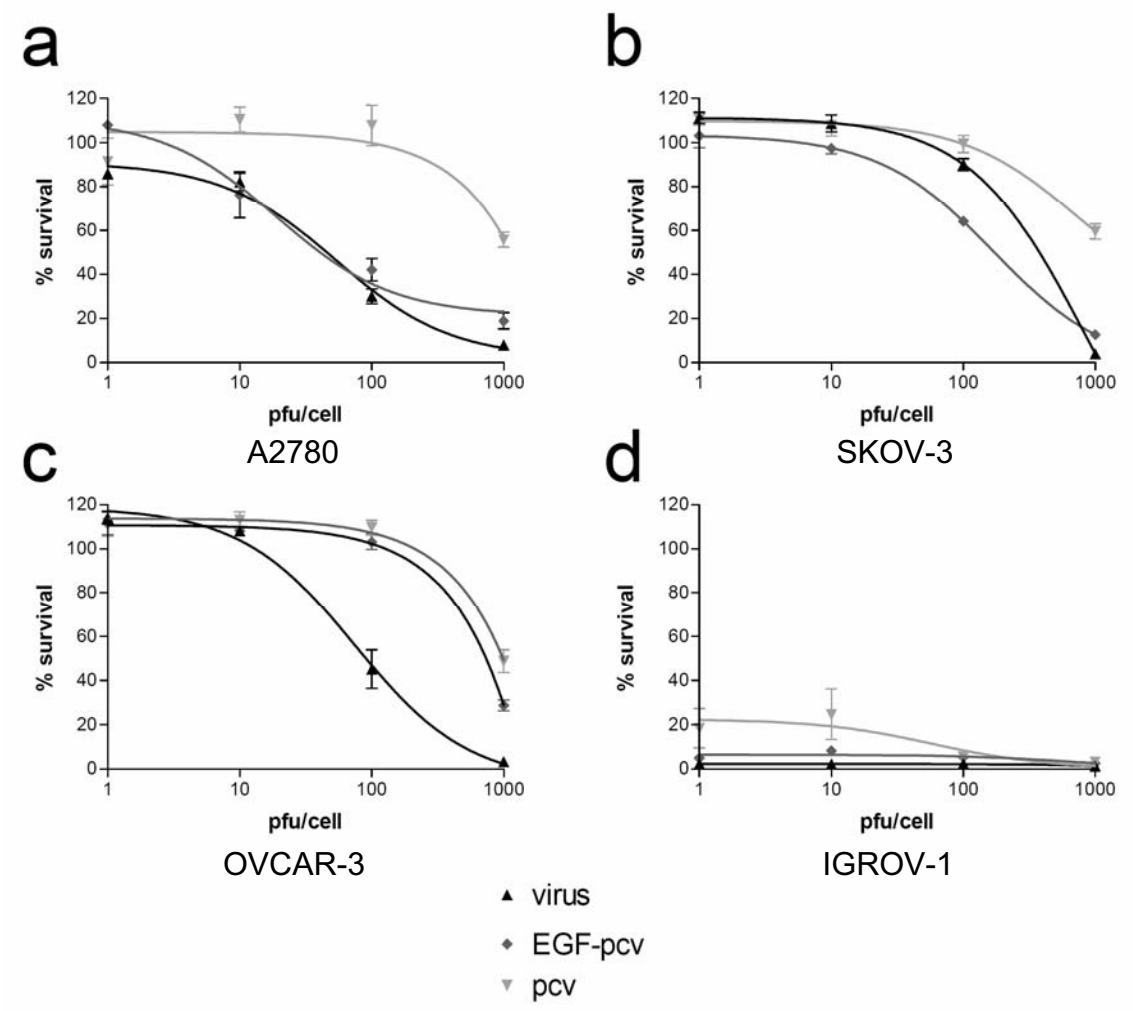


Figure 6-5 Effect of EGF-polymer coating on oncolytic potential of wild type Ad5

Four different ovarian cancer cell lines (5 x 10^3/well) were infected with wild type Ad5 at a variety of pfu/cell. Survival was assessed using the MTS assay to determine cell viability 6 days post infection. Unmodified Ad5WT (black triangles); Polymer coated (10 mg/ml) Ad5WT (light grey inverted triangles); and EGF-polymer coated (10 mg/ml) Ad5WT (dark grey diamonds). Graphs are representative of the effect of Ad5WT on: (a) A2780; (b) SKOV-3; (c) OVCAR-3; and (d) IGROV-1 cell lines. Data are representative of at least two independent experiments; data points represent mean values and error bars SEM.

6.2.4 Effect of adenovirus coating and re-targeting on anti-tumour activity

Wild-type adenovirus serotype 5 (Ad5WT) was selected as the therapeutic oncolytic virus, as this had shown maximum activity *in vitro* (see Figure 6-4). However, ubiquitous CAR expression by normal cells and low levels of CAR expression by ovarian tumour cells suggests that using unmodified wild type adenovirus *in vivo* would lack tumour selectivity and may reduce the therapeutic ratio, unlike the conditionally replication competent adenoviruses. However, I hypothesized that EGF-polymer coating would introduce selectivity at the transductional level and therefore permit the use of an inherently less selective, but more powerful Ad5WT.

Previous studies had suggested that icodextrin, an α, 1-4 linked glucose polymer developed for peritoneal dialysis, improved the efficiency of intraperitoneal virus transduction (Engler *et al.* 2003). Furthermore, icodextrin has been shown to reduce adhesion formation in animal models of surgery and peritonitis following conventional chemotherapy (Conroy *et al.* 2003; Verco *et al.* 2000), in addition to improving pharmacokinetics of intraperitoneal drug administration and reducing adhesion formation following surgery in clinical trials (diZerega *et al.* 2002; Kerr *et al.* 1996).

A two-by-two factorial pilot study was performed to assess the therapeutic effect of both the carrier fluid in which the virus was administered and the virus coating. This study design was chosen as it minimised the number of mice required. Groups of three mice were implanted with 1×10^7 SKOV cells i.p. After 48 hours, mice were treated with virus samples delivered in either phosphate buffered saline (PBS) or icodextrin. Treatments and carrier solutions were blinded and randomized by an independent person. A total of six mice received each treatment; either PBS control or 5×10^{10} viral particles of Ad5WT which was unmodified Ad5WT (virus), polymer coated Ad5WT (pcv) (20 mg/ml coating concentration), or EGF-polymer coated Ad5WT (EGF-pcv) (20 mg/ml coating concentration). A coating concentration of 20 mg/ml was chosen based on previous data demonstrating decreased liver transduction at this concentration (see section 6.2.1). Treatments were repeated twice at 48 hour intervals, so mice received a total of three

doses of virus. Mice were observed until the first mouse required sacrificing for tumour load (pre-determined humane end point). At this point all mice were sacrificed, tumours meticulously dissected and weighed and abdominal cavities scored for adhesions, using a four point scoring system (Table 6-3). Treatment groups were unblinded after post-mortem examination and dissection.

Table 6-3 Adhesion scoring system

Findings	***Adhesion score***
No adhesions	None
Mild filmy adhesions	Mild
Denser adhesions throughout abdominal cavity, still able to dissect out loops of bowel	Moderate
Dense adhesions causing bowel matting, dilatation or evidence of subacute bowel obstruction. Unable to dissect out loops of bowel.	Severe

6.2.4.1 Effect on tumour load

Analysis by two-way ANOVA demonstrated that there was no significant effect on tumour load by type of carrier solution ($P = 0.1636$), but that virus treatment group did have a significant effect on tumour load ($P = 0.0032$). There was no significant interaction between virus treatment and carrier ($P = 0.2849$). Data were therefore analysed by virus treatment group, combining mice in both PBS and icodextrin carrier groups (combined $n = 6$).

Compared with PBS control, treatment with Ad5WT significantly decreased the tumour load ($P < 0.01$). Although there appeared to be less tumour in the EGF-pcv treated group than the PBS group, the difference did not reach significance, probably due to the study being under powered (type 2 error). In addition, virus in both the pcv and EGF-pcv groups was coated at 20 mg/ml and at this coating concentration virus may be over coated and less able to replicate effectively (see section 6.2.1), which may explain why the therapeutic effect of EGF-pcv was not similar to that of unmodified virus. A coating concentration of 20 mg/ml of polymer was chosen because this concentration had been shown to improve virus pharmacokinetics following i.v.

administration *in vivo* (Green *et al.* 2004) and reduce liver transduction when administered i.p., as discussed in section 6.2.1.

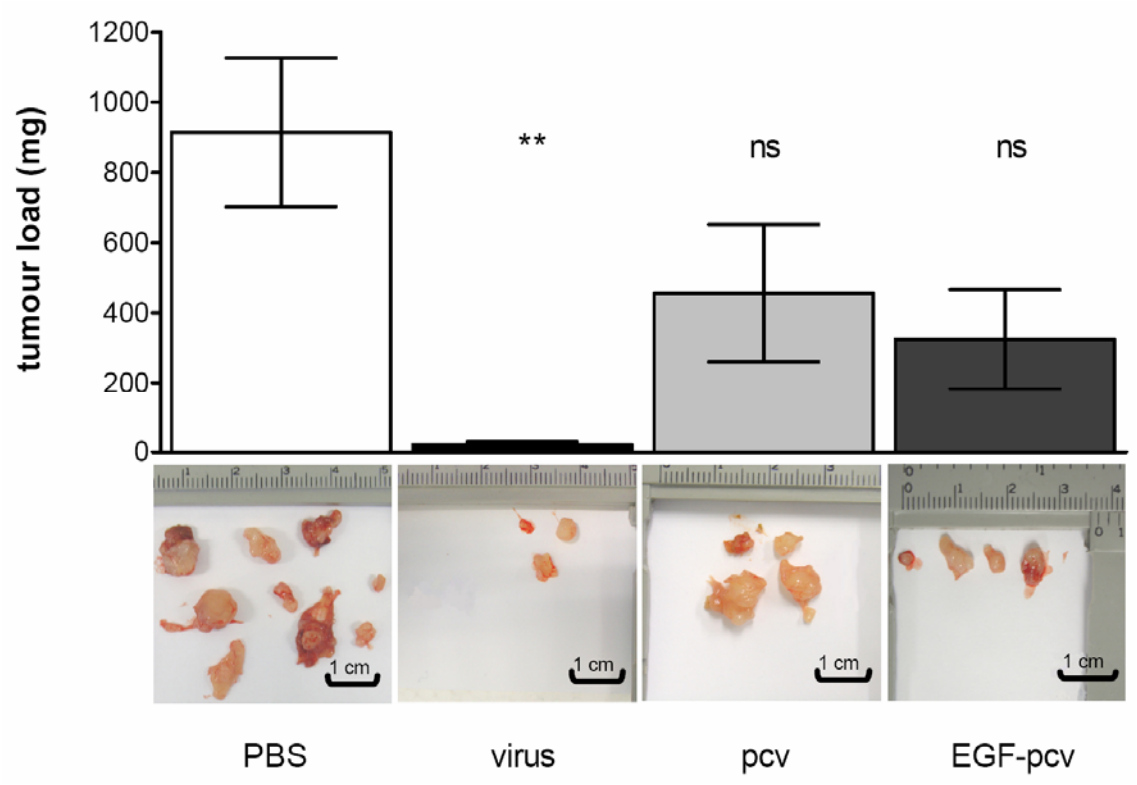


Figure 6-6 Therapeutic effect of polymer coating and re-targeting wild type adenovirus

Nude mice (aged 6-8 weeks) were injected with 1 x 10^7 SKOV cells i.p. After 48 hours mice were treated with either PBS control, Ad5WT, polymer coated virus or EGF-polymer retargeted adenovirus at 5 x 10^{10} v.p. Treatment was repeated at 96 hours and 164 hours post tumour cell implantation. All treatments and mouse groups were randomized (numbers picked out of bag) and investigators involved in the experiment were blinded to the treatment allocations (carriers and treatment groups labelled A & B and 1-4 respectively by an independent person, allocations kept in sealed envelope until after animals were harvested). Mean tumour masses are demonstrated; error bars represent SEM. Groups were analysed by the Kruskal-Wallis method with Dunn's correction for multiple comparisons. There was significantly less tumour in the group treated with Ad5WT than PBS control ($P < 0.01$). Although there was less tumour in the EGF-pcv group compared with PBS control, this difference did not reach significance. The bottom panel shows representative tumours dissected from mice in each group.

6.2.4.2 Effect on toxicity

Although EGF-pcv did not produce a significant reduction in tumour load compared to PBS control, unlike unmodified Ad5WT, there was a clinically marked effect of polymer coating virus on development of adhesions (see Figure 6-7). Adhesion scores were compared by Chi-squared analysis; there was a significant reduction in the tumour score in mice treated with EGF-pcv compared with unmodified Ad5WT ($P = 0.034$). Mice treated with unmodified Ad5WT frequently developed dense adhesions, with tethering of the bowel. In some cases the adhesions were so dense that the animal developed signs of bowel obstruction (weight loss, distended abdomen with visible loops of bowel) which required early sacrifice, prior to the humane tumour load end point. Adhesion formation may have confounded the amount of tumour recorded in these mice in two important ways: first, early sacrifice meant that tumours had less time to grow; second, due to the dense nature of the adhesions made dissection difficult and possibly not complete, meaning that all tumour deposits may not have been identified and tumour load in the unmodified virus group may have been under-estimated.

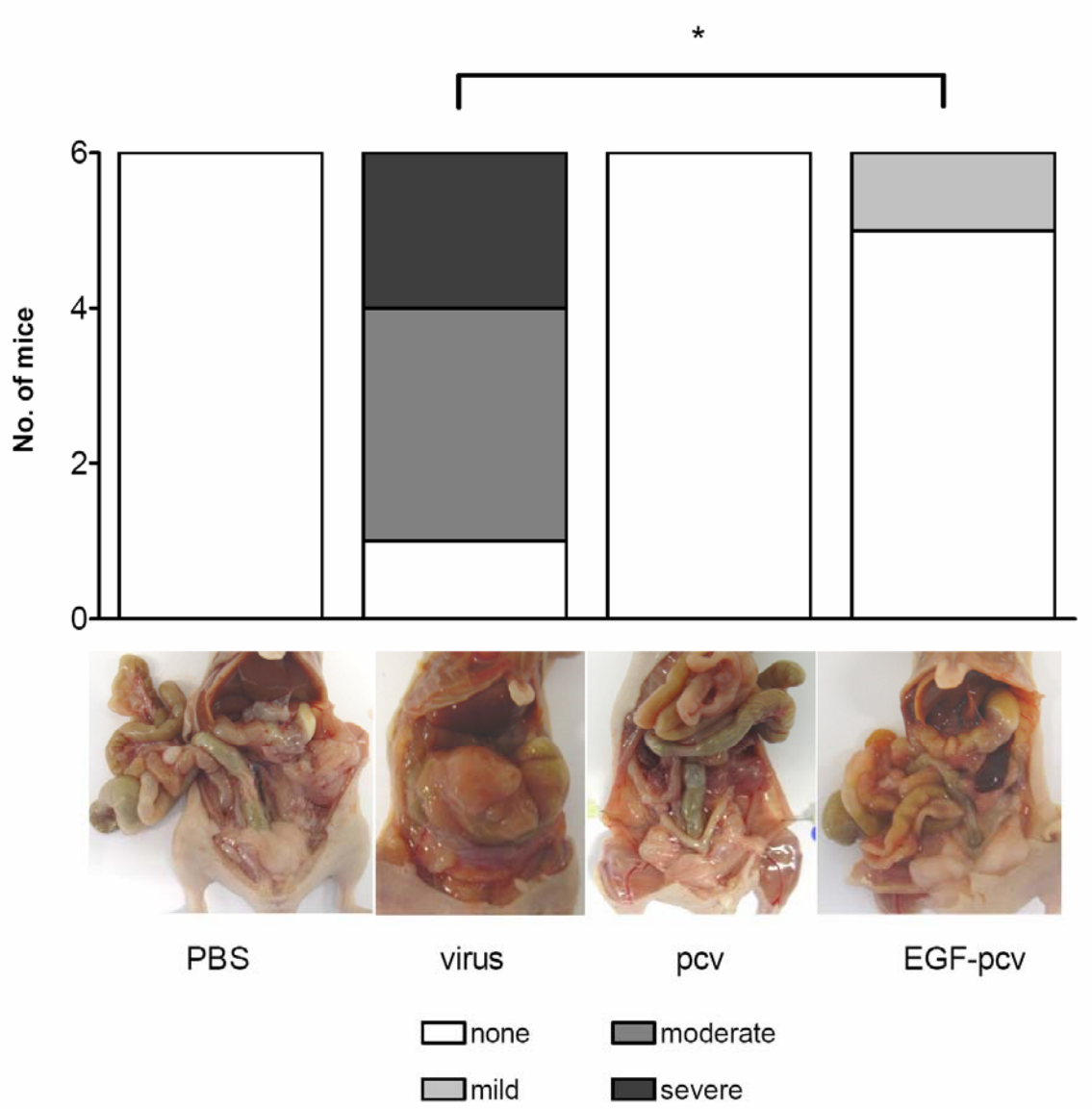


Figure 6-7 Adhesion score by i.p. adenovirus treatment groups

Mice sacrificed in the experiment described in 6.2.4 underwent a post-mortem examination and dissection to remove all visible tumour samples for analysis prior to unblinding of treatment allocations. Adhesions were scored according to a 4-point scale (0 = no visible adhesions; 1 = minimal adhesions; 2 = moderate adhesions throughout abdominal cavity; 3 = severe adhesions causing bowel obstruction/dilatation). Data analysed by Chi-square analysis, * P = 0.034. The bottom panel shows photographs of representative mouse abdominal cavities at time of post-mortem examination.

6.2.5 Calculation of tumour load by Q-PCR for human β-actin

Tumours contain both cancerous cells and non-malignant stromal cells. In a mouse xenograft model, any tumour is therefore a combination of mouse stromal and human cancer cells. In order to get a more accurate estimate of human tumour load, which excluded any normal mouse tissue that would otherwise be included if tumour load were assessed on mass of dissected tumour alone, Q-PCR primers were designed for the human β-actin promoter (see section 2.2.9). A standard curve for estimation of human β-actin copy number was generated using known concentrations of human β-actin promoter, which was generated from a plasmid encoding this sequence (pDRIVE-hβ-Actin-RU5'). Plasmid copy number to cell number was calculated using a standard curve of SKOV-3 cells spiked into mouse tissue lysate (Figure 6-8a). Tumours from mice were homogenised in lysis buffer at 300 mg/ml, DNA extracted from 200 μl aliquots, and 5 μl samples of DNA used for human β-actin copy number assessment by Q-PCR. Values of plasmid per mouse were calculated and shown in Figure 6-8b.

Only mice in the unmodified virus treated group demonstrated a significantly reduced amount of human DNA, as determined by Q-PCR, compared to the PBS treated group, in keeping with the gross tumour mass results. However, as there was not a linear relationship between human β-actin copy number and number of SKOV-3 cells, these data are unlikely to be reliable. Indeed, this was why the plasmid was used to create a standard curve, rather than known numbers of SKOV-3 cells. There was a problem with extracting DNA from SKOV-3 cells; using genomic DNA miniprep columns the tissue lysate with larger numbers of SKOV-3 cells became viscous and probably interfered with the efficiency of DNA extraction. I concluded that this was an unsatisfactory way of determining tumour cell load, especially if high cell numbers were expected, and that simply weighing the dissected tumours was more informative. Furthermore, I estimated that even if tumours only contained 50% human cells, in a tumour weighing 1g, there would be approximately 1-2 x 10^7 cells (assuming cubic cell of 30 μm width and cell density equivalent to that of water), and so the Q-PCR for β-actin was probably under-estimating cells by at least 10-fold.

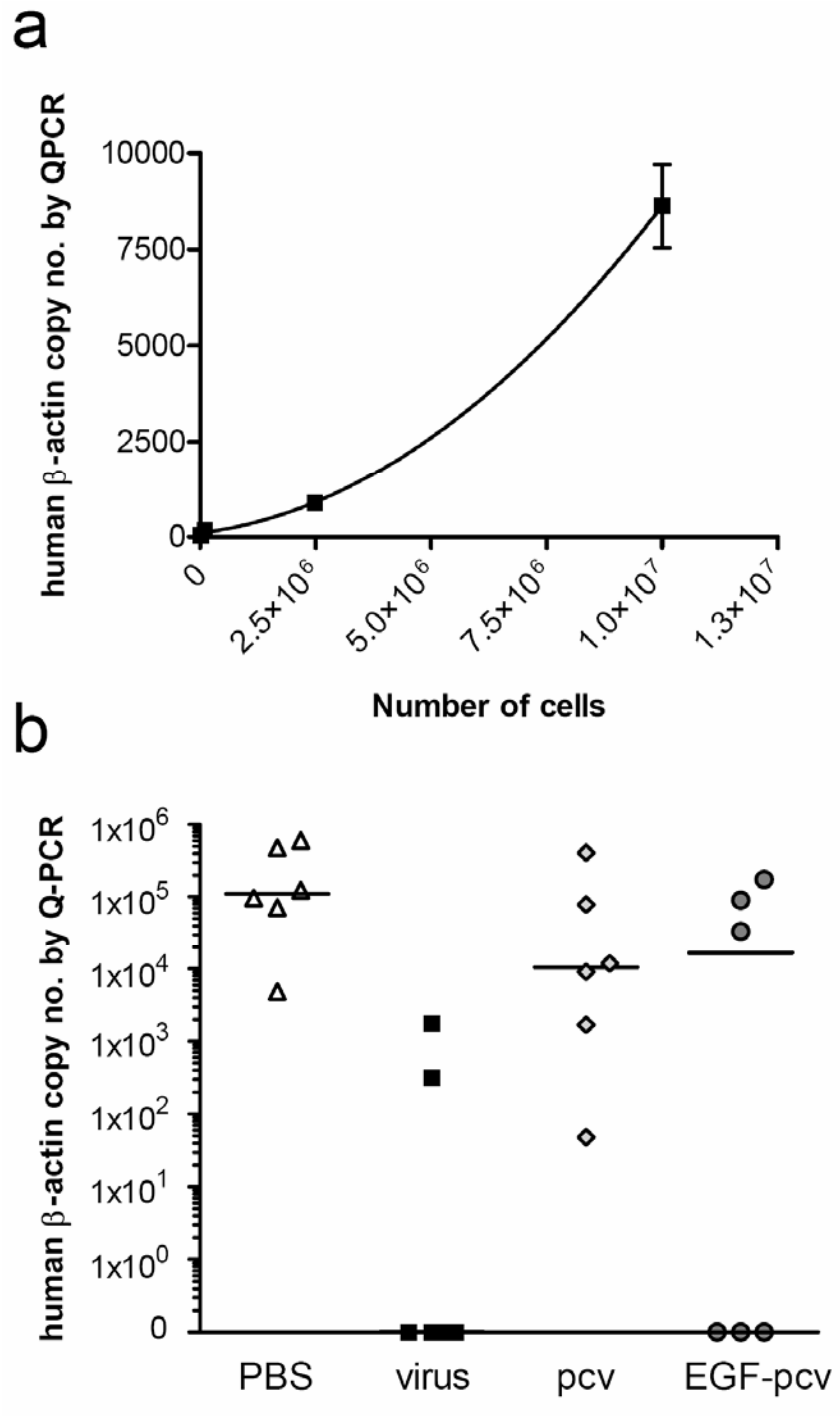


Figure 6-8 Standard curve of plasmid copy no. by Q-PCR vs. cell number

Tumours dissected from mice were homogenised in lysis buffer at a concentration of 300 mg/ml and DNA extracted from 200 μl aliquots. Mouse (non-tumour) tissue lysate (200 μl at 300 mg/ml) was spiked with known numbers of SKOV-3 cells to form a standard curve (a). DNA was analysed by Q-PCR for human β-actin copies and corrected for total number per mouse (b). Points demonstrate values for individual animals and the bars represent median values. Data were analysed by the Kruskal-Wallis test with Dunn's test for multiple analyses. Only the unmodified virus treated group was significantly different to PBS treated mice ($P < 0.001$).

6.2.6 Development of a bioluminescent i.p. tumour model to monitor tumour load *in vivo*

In the previous experiment an attempt was made to quantify the tumour load due to human SKOV-3 cells using Q-PCR against the human β-actin promoter. However, as described above, this was not considered to be a reliable method. In addition, it has the disadvantage of requiring sacrifice of the mouse, and therefore cannot provide an on-going estimate of tumour burden. Bioluminescence is a technique that uses a highly sensitive camera, which can image anaesthetised animals. Using either tumours or viruses that express the luciferase reporter gene, repeated measurements can be made in living mice. An i.p. model of human ovarian cancer using IGROV-1 cells expressing luciferase (Lockley *et al.* 2006) had previously been developed. However, IGROV-1 cells have unusually high CAR levels compared with other ovarian tumour cell lines and primary ovarian tumours (see Figure 4-7) and would therefore not provide a suitable model for adenovirus retargeting. SKOV-3-ip cells, which have lower CAR levels and are therefore more similar to primary ovarian cancer cell lines, stably expressing firefly luciferase (SKOV-luc) were kindly donated by Dr Iain McNeish.

The first step was to determine whether overall luminescence *in vitro* was proportional to cell number. Known numbers of SKOV-luc cells were lysed and analysed for luminescence after addition of luciferin (see section 2.2.8.1). SKOV-luc cell number was directly proportional to luminescence levels across a wide range (Figure 6-9).

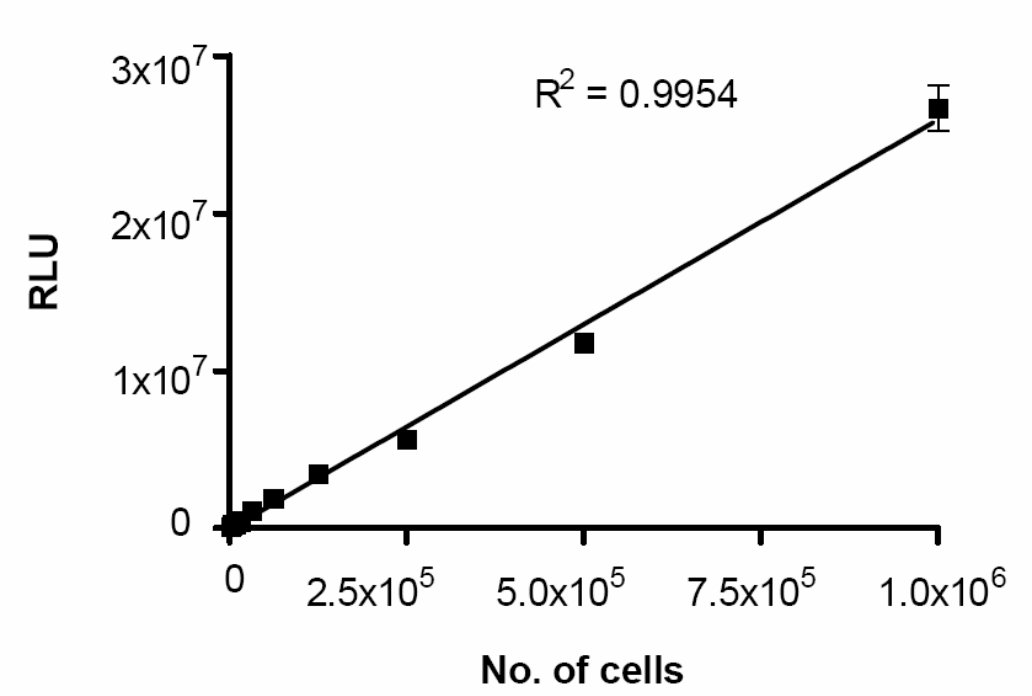


Figure 6-9 SKOV-luc cell luminescence is directly proportional to cell number

SKOV-luc cells were grown in DMEM supplemented with 20% FCS and 500 μg/ml G418. Cells were counted and plated out in a v-bottomed plate in a 2-fold dilution series. Cells were resuspended in 100 μl lysis buffer (Promega) and analysed for luminescence (see section 2.2.8.1). There was a direct linear relationship between number of cells and luminescence.

A pilot experiment was performed to determine whether bioluminescence levels were relatively stable during the time required for mouse manipulation and imaging, and which time period should be used to measure bioluminescence in the planned survival study. Three MF1 nude mice (8-9 weeks old) mice were implanted i.p. with SKOV-luc cells and tumours allowed to develop over 3-4 weeks. Mice were anaesthetised by isofluorane inhalation and injected i.p. with 100 μl of 50 mmol/l luciferin (potassium salt, Xenogen) in PBS. Mice were kept under a light anaesthetic for 4 minutes and were sequentially imaged at 2 minute intervals (2 sec exposure, medium binning F/stop 1) for up to 16 minutes from initial luciferin injection using an IVIS 100 imaging system (Xenogen). Light units emitted were calculated as flux using the Living Image® 2.50.1 software (Wavemetrics, Inc, USA) so that data could be compared between images, as this calibrated light emission for the exposure time, aperture setting and binning. Over this time period there was no significant drop in flux (photons/sec) from each mouse (Figure 6-11). Therefore, using this protocol for imaging, even if initial readings of mice were over-saturated, repeated images could be taken without a significant drop in flux occurring.

To determine the change in bioluminescence with tumour growth, MF1 nude mice (n = 6; 6 weeks old) were implanted with 1 x 10^7 SKOV-luc cells. Mice were observed daily and weighed three times per week. Three days after tumour cell implantation, mice were imaged for luciferase expression, to estimate tumour burden, as described in section 6.2.6. All mice were initially imaged for 1 minute (F/stop 1, medium binning) in a supine position and exposure time reduced accordingly if images were saturated. Mice were imaged supine and prone, oval regions-of-interest applied as described above, and the sum of supine and prone luminescence, minus background mouse luminescence, calculated. Mean group flux is represented in Figure 6-12. Mean group flux increased exponentially over time (R^2 for mean values >0.99), with a doubling time of 6 days. After 33 days all mice required sacrifice for tumour burden.

Following imaging mice were sacrificed and post-mortem examination performed to assess tumour growth. Tumour nodules were found throughout the abdominal cavity, especially around the omentum, liver, diaphragm and spleen. There were small tumour nodules on the small bowel mesentery and some mice had developed blood-stained ascites. The pattern of growth was similar to that seen in many epithelial ovarian cancers in patients, and is therefore a reasonable model to use for investigating i.p. treatments for ovarian cancer.

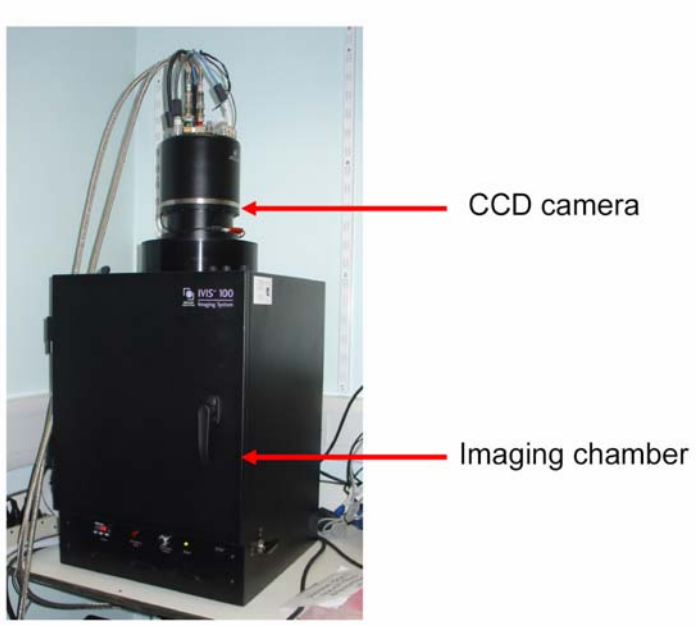


Figure 6-10 The IVIS 100 imaging system

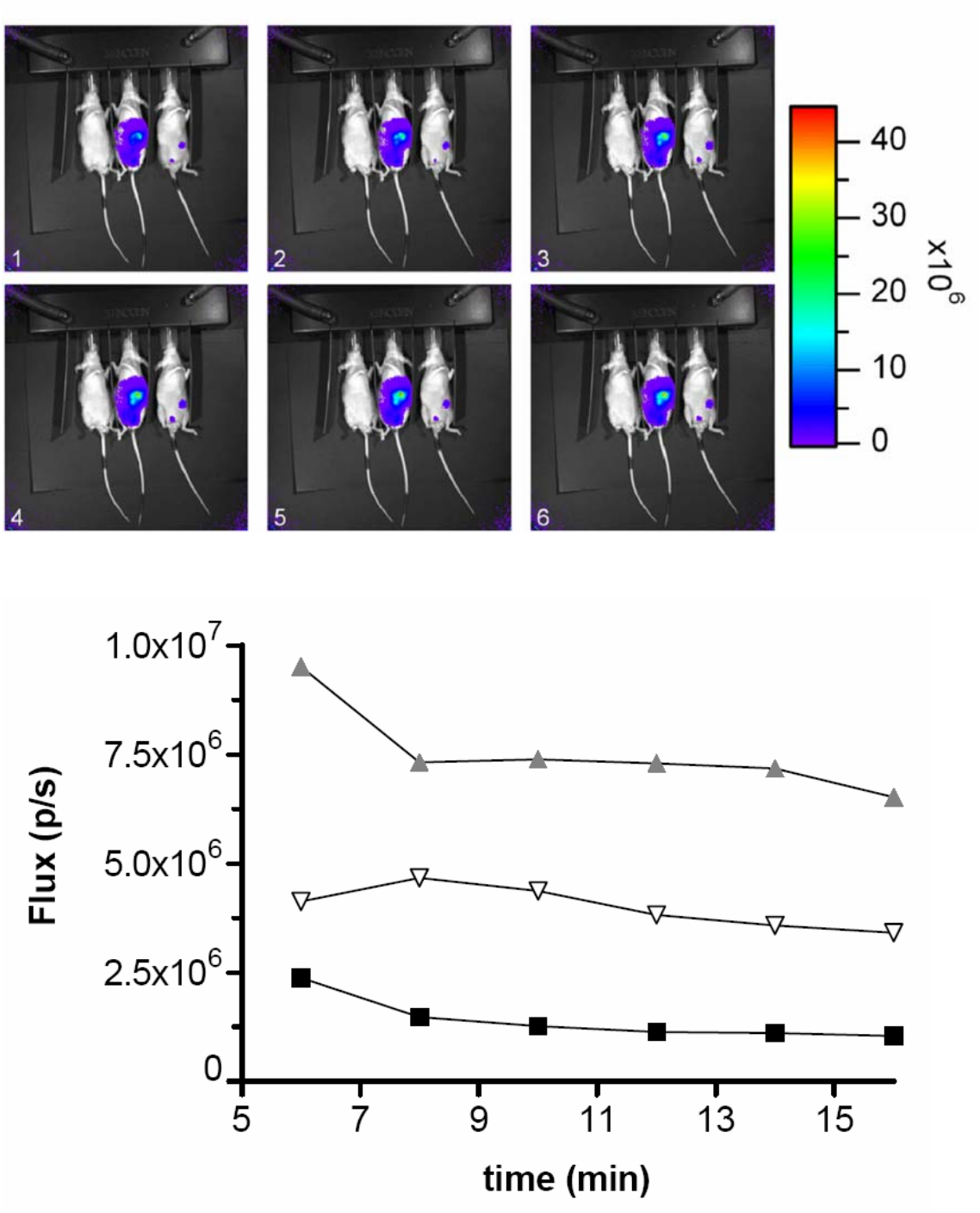


Figure 6-11 Flux measurements over time for individual mice

Nude mice were implanted with SKOV-luc cells and tumours allowed to establish over 3-4 weeks. Mice were injected i.p. with luciferin and imaged for emitted light at 6 time points over 16 minutes. Total flux was calculated (photons/second) for each mouse using Living Image software using an oval region-of-interest that included a mouse's entire abdomen. Background flux from a non-tumour bearing mouse was subtracted. Groups 1-6 are images taken at 2 minute intervals; 1 = 6 min from luciferin injection.

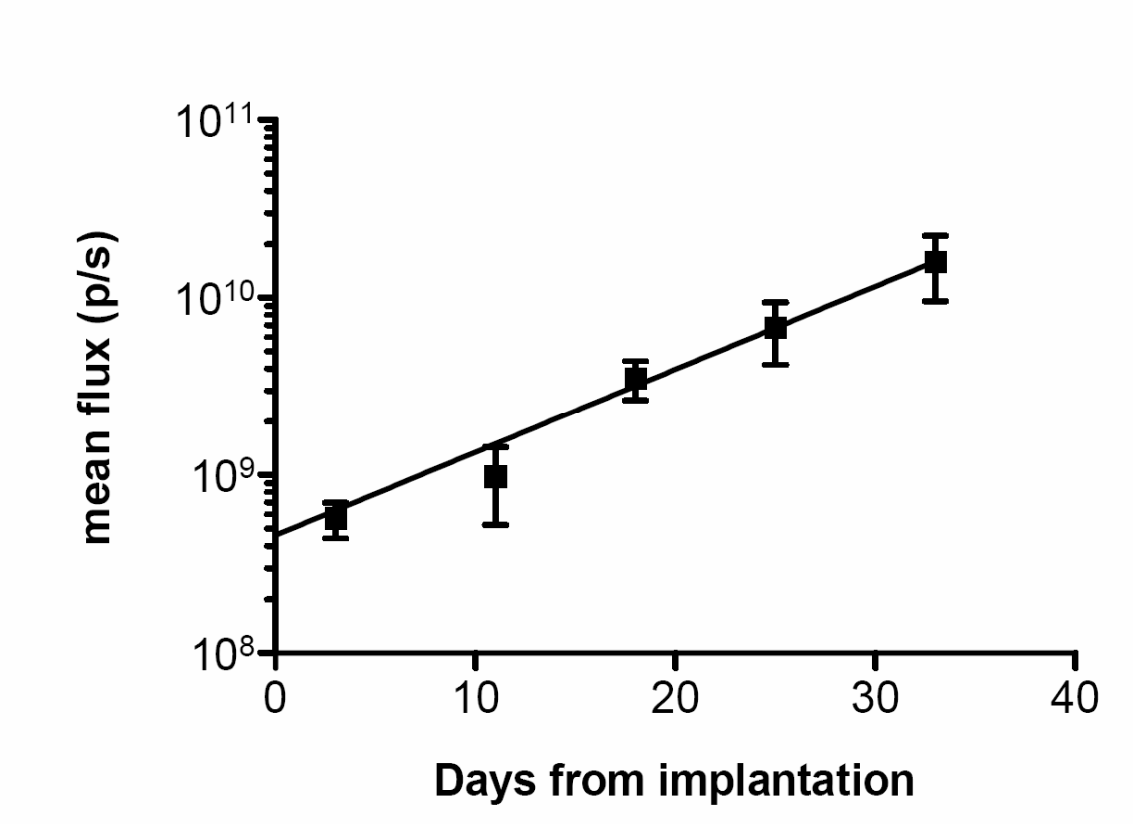


Figure 6-12 Exponential increase in total mouse flux over time in mice implanted with SKOV-luc cells

MF1 nude mice (n = 6) were implanted i.p. with 1 x 10^7 SKOV-luc cells and imaged, supine and prone, 3 days after implantation for total mouse bioluminescence and measurements repeated ~weekly. Each point represents mean group flux, after deduction of background; bars represent +/- SD. Flux is represented on a log scale and demonstrates exponential growth. N = 3 at 33 days post implantation, due to sacrifice of mice for excessive tumour load.

6.2.7 Determining the sample size required to adequately power a survival study of EGF-pcv Ad5WT

Data from the pilot study were entered into an *a priori* power calculation using the Gpower software (www.psycho.uni-duesseldorf.de/aap/projects/gpower) in order to calculate the number of mice required for an 80% probability of not missing a positive effect (α = 0.05, 1-β = 0.8). Entering details of the means of tumour loads from PBS control and EGF-pcv groups and the standard deviation of the data, gave a required minimum group size of 11 mice. Accordingly, twelve mice per group were used in the following survival experiment.

6.2.8 *In vivo* effect of EGF-polymer and Cetuximab-polymer coating of Ad5WT in a tumour load/survival experiment

Female MF1 nude mice (4-6 weeks) were implanted (n = 12 per group) with 1 x 10^7 SKOV-luc cells i.p. in 500 μl PBS (for schematic see Figure 6-13). After allowing 96 hours for implantation, mice were treated i.p. with 500 μl of PBS control or 5 x 10^{10} v.p. of Ad5WT, which was unmodified or coated overnight with polymer, EGF-polymer or Cetuximab-polymer, all at 20 mg/ml coating concentration. Treatment groups were randomized and coded as groups 1-5 by an independent person, so that investigators were blinded to treatment groups. Treatments were repeated twice at 72 hour intervals, so that a total of three doses of virus at 5 x 10^{10} v.p. were administered.

Mice were observed daily and weighed three times per week. Ten days after the third virus treatment, mice were imaged for luciferase expression, to estimate tumour burden, as described in section 6.2.6. All mice were initially imaged for 1 minute (F/stop 1, medium binning) in a supine position and exposure time reduced accordingly if images were saturated. Mice were imaged supine and prone, oval regions-of-interest applied as described above, and the sum of supine and prone luminescence, minus background mouse luminescence, calculated.

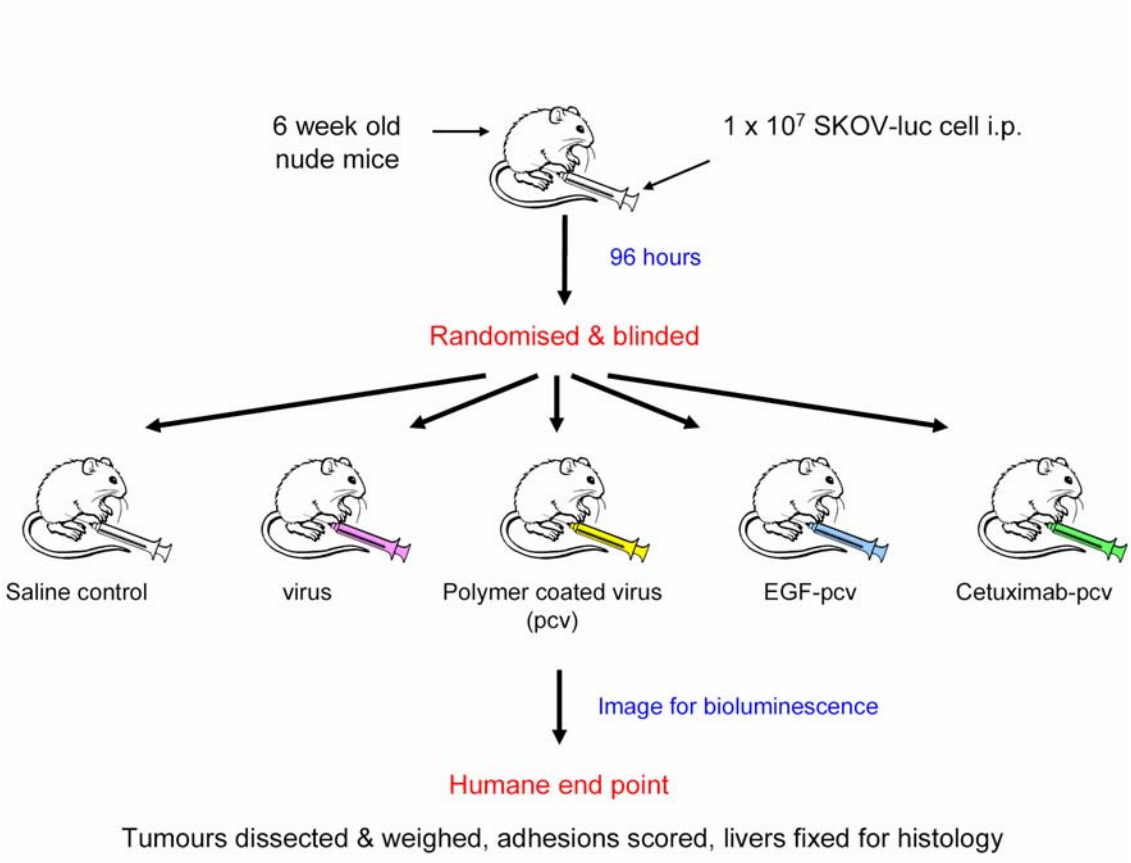


Figure 6-13 Schematic of survival experiment design

Imaging was repeated at weekly intervals over the course of a month. By this time there had been significant loss of mice in the greatest tumour load groups, and so further inter-group comparisons of luminescence would have been uninformative. In addition, there was a restriction on numbers of imaging sessions permitted per mouse according to the Home Office project licence.

Mice were monitored and sacrificed when they developed any of the following: (1) ascites; (2) evidence of bowel obstruction; (3) significant weight loss (>10% body mass); (4) reduced movement; (5) poor skin condition or hunched posture suggesting that they were unwell; (6) significant tumour visible on the abdominal wall. More subtle signs were recognised during the course of the experiment, allowing refinement of end-points and so keeping suffering to a minimum. Furthermore, use of bioluminescence to monitor tumour load, enabled identification of mice at risk, so that they could be closely monitored and sacrificed at an appropriate humane

end point. However, mice in some groups became unwell very rapidly with little warning and so daily checking was required over several weeks. This disease progression mimics the natural history of human ovarian epithelial carcinoma, which is often asymptomatic until very advanced and even then gives relatively little pain or discomfort. Following euthanasia by a schedule 1 method, mice were examined, adhesions scored, as per the previous scoring system, tumours dissected, livers excised and fixed in 4% formaldehyde in PBS and laparotomy findings recorded and photographed. Reasons for sacrificing and post-mortem findings are listed in appendix 9.4). At a pre-specified end-point 120 days following tumour implantation all remaining mice were imaged for bioluminescence and sacrificed. Mice with no evidence of SKOV-luc tumour development at any point were excluded from the subsequent analysis as 'tumour non-takes' (3 in PBS group, 2 in virus group, 2 in Cetuximab-pcv group and none in pcv or EGF-pcv groups) . Treatment groups were unblinded after all data had been recorded and analysed.

6.2.8.1 *In vivo* bioluminescence

Bioluminescence measurement at 10 days following the third virus treatment demonstrated no significant differences between mice treated with PBS or pcv. However, there were highly significant reductions in tumour load, as measured by bioluminescence between PBS treated mice and mice treated with unmodified Ad5WT, EGF-pcv and Cetuximab-pcv ($P < 0.001$ for all groups) (Figure 6-14 and Figure 6-15). This pattern of bioluminescence persisted over the next 4 weeks (Figure 6-16), although difference between the groups became less pronounced, as small numbers of tumour cell multiplied and mice with the greatest tumour burden required sacrificing.

6.2.8.2 Overall survival

Time from tumour implantation to sacrifice was recoded for each mouse, with 'tumour non-takes' excluded. Survival data were analysed by Kaplan-Meier analysis using GraphPad Prism4 software (Table 6-4, Figure 6-17) (median survival: PBS = 34 days; pcv = 46 days; virus = 58 days; Cetuximab-pcv = 63.5 days; EGF-pcv = 64.5 days). The survival curve for each treatment group was significantly different to the PBS control group, although the survival ratio of the pcv group was not significantly prolonged (95% CI for ratio of survival crosses 1). Both

EGF-pcv and Cetuximab-pcv treatment resulted in almost a doubling in survival time compared to PBS. Logrank test for trend in survival was also significant ($P < 0.0001$; PBS<pcv<virus<Cetuximab-pcv<EGF-pcv).

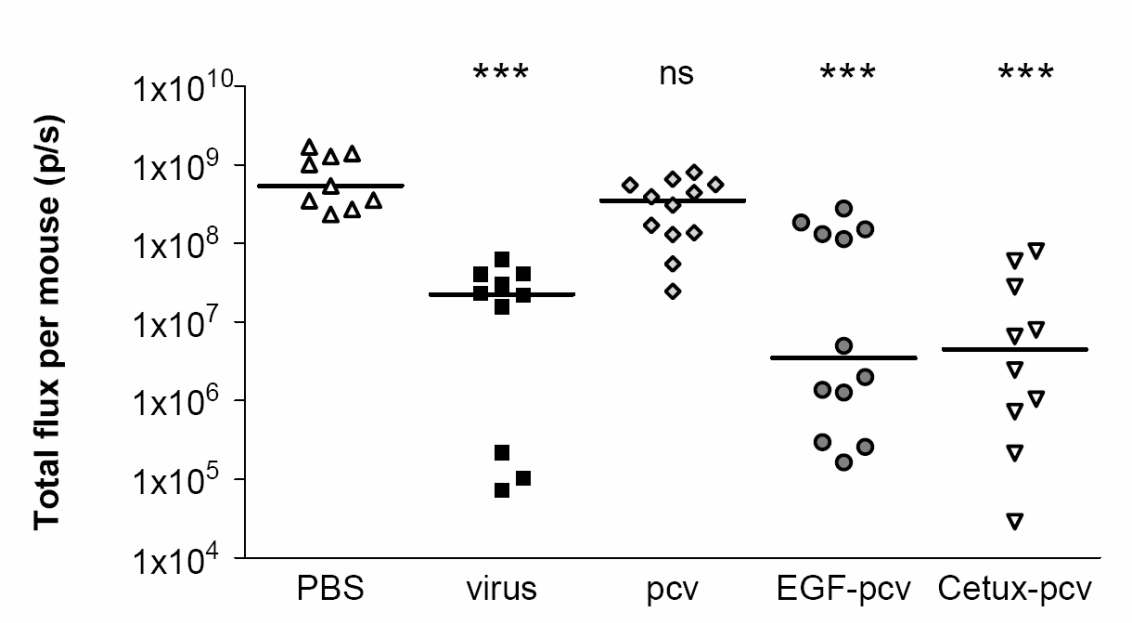


Figure 6-14 Bioluminescence by group at 10 days post treatment

MF1 nude mice implanted i.p. with 1 x 10^7 SKOV-luc cells, treated with three doses of 5 x 10^{10} v.p. of Ad5WT, unmodified, pcv, EGF-pcv, Cetuximab-pcv, or a non-virus PBS control, and imaged, supine and prone, 10 days after the final treatment dose for total mouse bioluminescence. 'Tumour non-take' mice were excluded and data were analysed by Kruskal-Wallis method with Dunn's multiple comparison correction. Each point represents an individual mouse; bars represent median values; ns = non-significant; *** = $P < 0.001$.

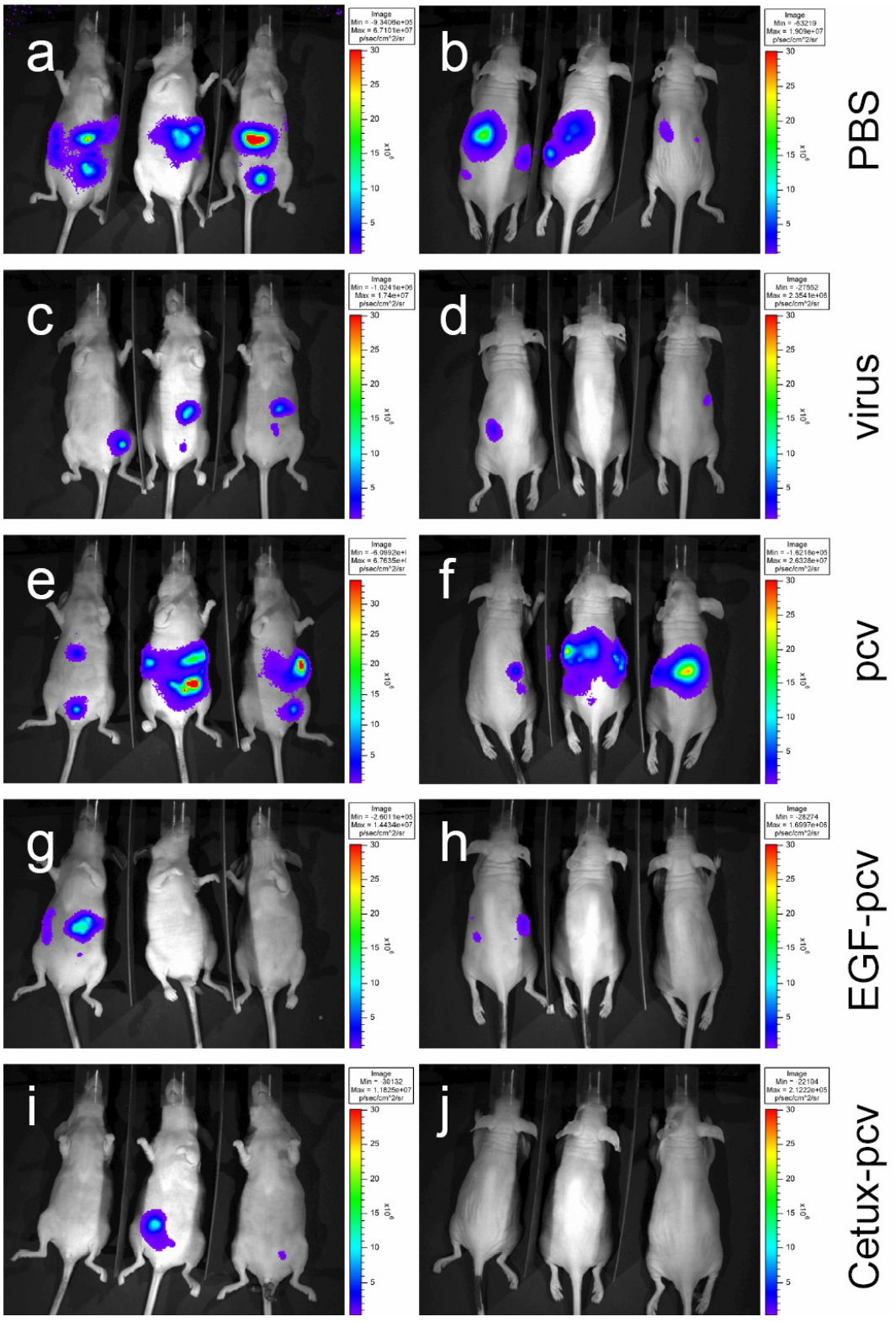


Figure 6-15 Composite bioluminescence images of mice 10 days post treatment

MF1 nude mice implanted i.p. with 1 x 10^7 SKOV-luc cells, treated with three doses of 5 x 10^{10} v.p. of Ad5WT, unmodified (c & d), pcv (e & f), EGF-pcv (g & h), Cetuximab-pcv (i & j), or a PBS control (a & b), and imaged, supine and prone, 10 days after the final treatment dose for total mouse bioluminescence. All images are displayed on the same false colour scale for easier comparison. Images shown are representative of the group and exclude 'tumour non-take' mice.

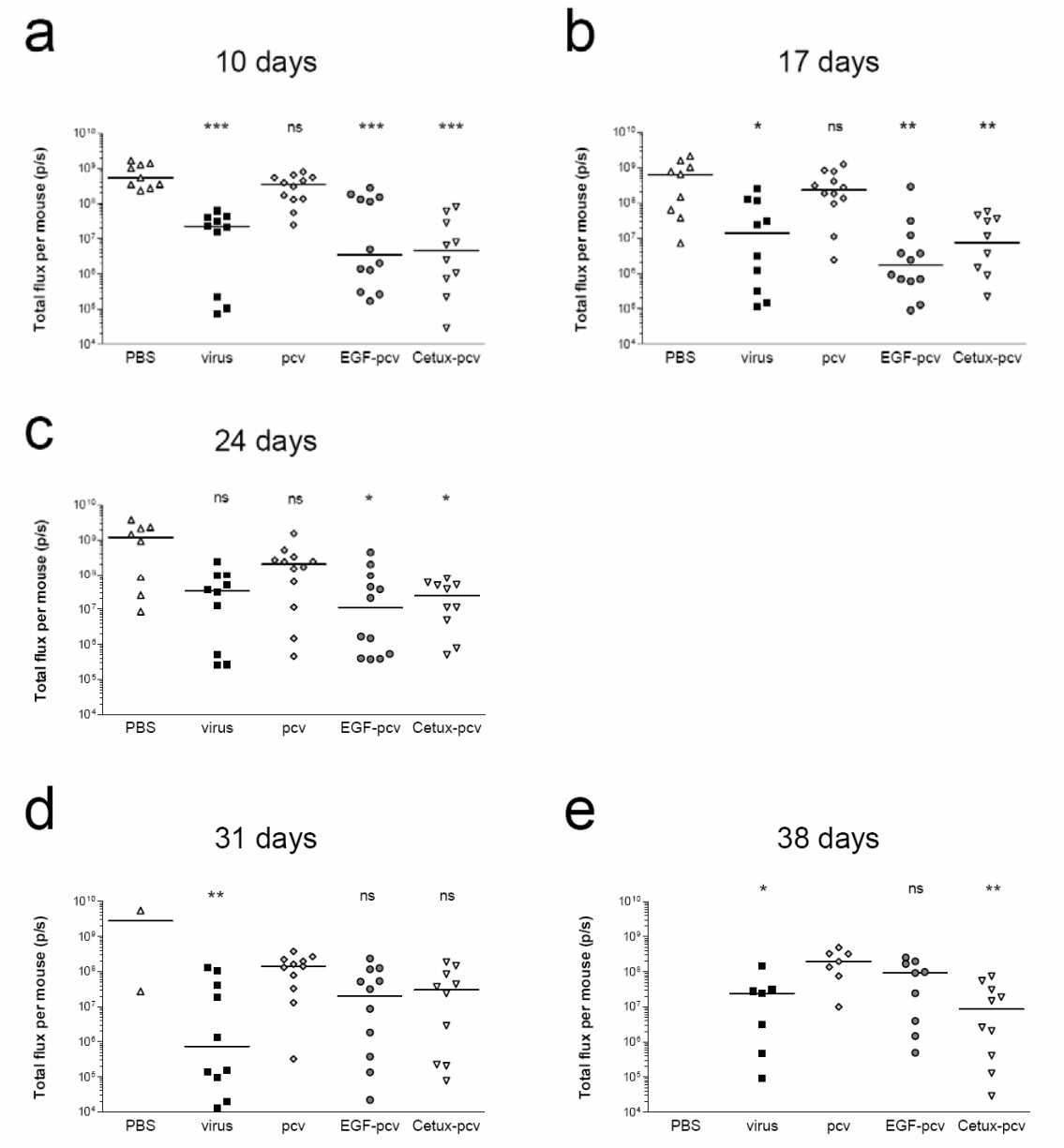


Figure 6-16 Bioluminescence by group at time intervals over 38 days post treatment

MF1 nude mice implanted i.p. with 1 x 10^7 SKOV-luc cells, treated with three doses of 5 x 10^{10} v.p. of Ad5WT, unmodified, pcv, EGF-pcv, Cetuximab-pcv, or a non-virus PBS control, and imaged, supine and prone, 10 days after the final treatment dose for total mouse bioluminescence, and repeated at weekly intervals. 'Tumour non-take' mice were excluded and data were analysed by Kruskal-Wallis method with Dunn's multiple comparison correction. Each point represents an individual mouse; bars represent median values; ns = non-significant; * = P <0.05; ** = P<0.01; *** = P < 0.001. In (a-c) values for each group are compared against the PBS control group. For (d) & (e) values are compared against the pcv treated group, since there were insufficient individuals still alive in the PBS group to allow for comparison.

Table 6-4 Analysis of survival curves

Treatment	*Median survival (days)*	*Logrank test P value (c.f. PBS)*	*Ratio (c.f. PBS)*	*95% CI of ratio*	*Hazard Ratio (c.f. PBS)*	*95% CI of HR*
PBS	34	-	-	-	-	-
Unmodified Ad5WT	58	0.0014	1.71	1.31 to 2.10	0.31	0.03 to 0.44
pcv	46	0.0002	1.35	0.93 to 1.77	0.27	0.022 to 0.31
EGF-pcv	64.5	P < 0.0001	1.90	1.48 to 2.31	0.19	0.01 to 0.10
Cetuximab-pcv	63.5	P < 0.0001	1.87	1.47 to 2.27	020	0.01 to 0.14

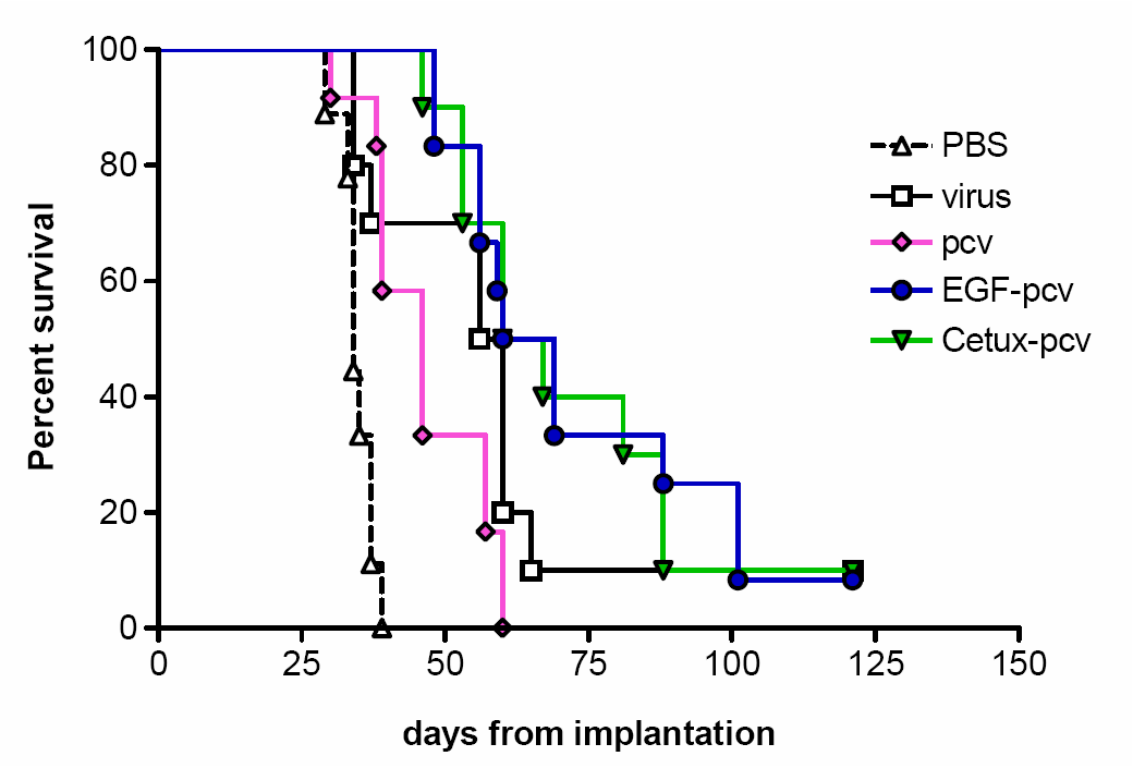


Figure 6-17 Survival curves for mice implanted with SKOV-luc

MF 1 nude mice (n = 12 per group) were implanted i.p. with 1 x 10^7 SKOV-luc cells and treated with three doses of 5 x 10^{10} v.p. of Ad5WT, unmodified, pcv, EGF-pcv, Cetuximab-pcv, or a non-virus PBS control. Kaplan-Meier analysis of percentage survival, following exclusion of 'tumour non-take' mice, was performed.

Interestingly, mice in the unmodified virus, EGF-pcv and Cetuximab-pcv treated groups survived significantly longer, but from careful observation they also appeared to have different patterns of tumour formation, compared with mice in the PBS and pcv groups (see appendix 9.4). Mice in the PBS group who developed tumours had widespread seedling metastases throughout the peritoneal compartment, which resulted in early bloody ascites formation. Mice in the pcv group had a similar pattern of disease. However, mice in the virus, EGF-pcv and Cetuximab-pcv groups tended to have either implantation site tumours, or masses around the stomach, spleen and liver, occasionally resulting in obstructive jaundice. These mice required sacrifice despite there being markedly less total tumour load compared to mice sacrificed in the PBS and pcv groups. It was only later in the course of their disease that mice in the unmodified virus, EGF-pcv and Cetuximab-pcv groups tended to develop widespread tumour seedlings throughout the peritoneum and small bowel mesentery, presumably as metastases from larger tumour nodules, rather than multiple implantation sites from the initial tumour inoculum.

6.2.8.3 Initial group bioluminescence and median group survival

In order to determine whether initial group fluorescence was a valid secondary end-point, the mean group flux, as recorded 10 days following the final virus dose, was plotted against median group survival. There was an inverse linear relationship between mean group flux and median survival (r^2=0.9717) (Figure 6-18). On an individual basis there was a relatively loose relationship between flux and survival, since some mice required sacrifice for adhesions or had relatively little tumour, but had complications caused by where the tumour had grown, e.g. small tumours blocked the bile duct and caused obstructive jaundice, or implantation site tumours at risk of ulceration. These data indicate that with adequate group sizes, levels of bioluminescence did give a good intermediate indication of subsequent *group* survival. Thus, bioluminescence is a valid secondary end-point for a survival study.

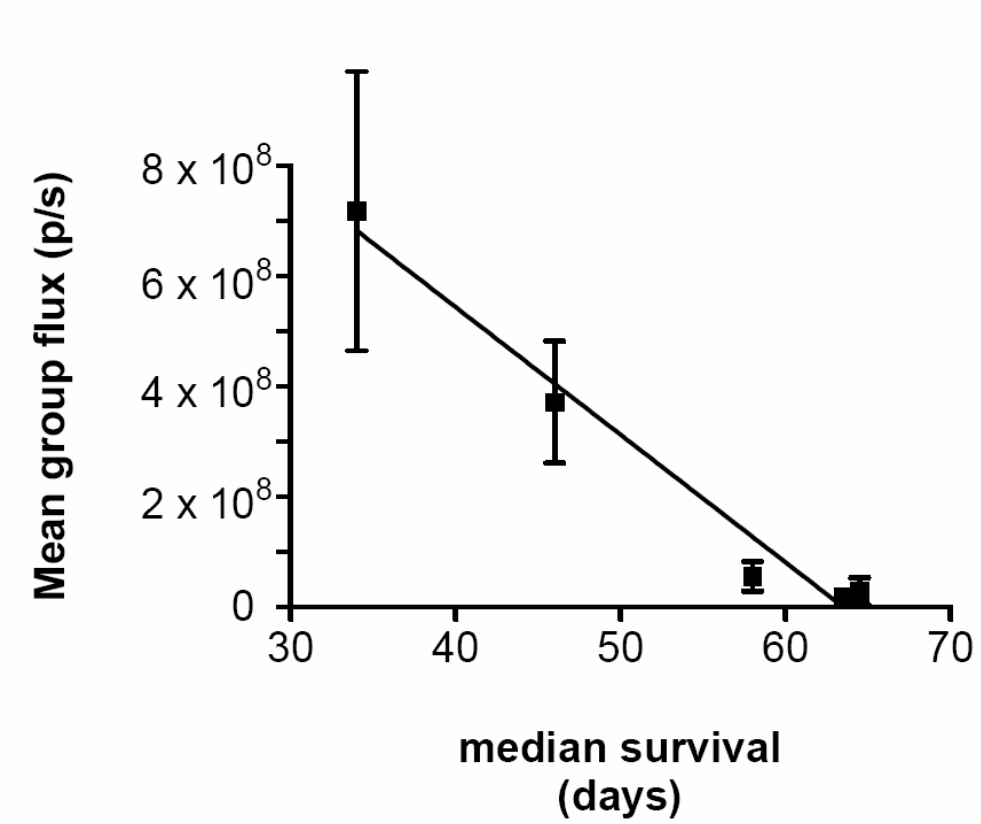


Figure 6-18 Relationship of mean group flux and median group survival

Bioluminescence data 10 days after treatments were plotted against group survival. There was an inverse linear relationship between initial mean group luminescence data and subsequent group survival ($r^2 = 0.9717$).

6.2.8.4 Tumour mass at sacrifice

At post-mortem tumours were dissected and stored at −20°C, prior to weighing and *in vitro* quantification of luminescence. If humane end-points were valid and all groups of mice were sacrificed at a similar point in their disease, then tumour weights across the groups should be similar. This analysis therefore checked for bias in time of sacrifice, but also would show inter-group differences if some groups required sacrifice for non-tumour end-points. Figure 6-19 demonstrates masses of tumour in each group. There was a trend for mice in the PBS group to have greater mass of tumour than those in other groups, although this was only significantly different to the virus group. Explanations for this could be that: (1) due to refinement of end-points and increased experience of disease progression during the experiment, mice were sacrificed with slightly less tumour than the control group; (2) mice in other groups developed tumours that had a different pattern of growth, e.g. implantation site tumours and blockage of

the bile duct, and so mice required sacrifice even though absolute tumour load was lower; (3) mice required sacrifice due to complications of treatment, i.e. adhesion formation, rather than a tumour end-point. Certainly, it is likely that some of the reduced tumour burden in the virus group was because some mice required early sacrifice for abdominal distension caused by complications from the treatment, and hence had less time for tumour to grow.

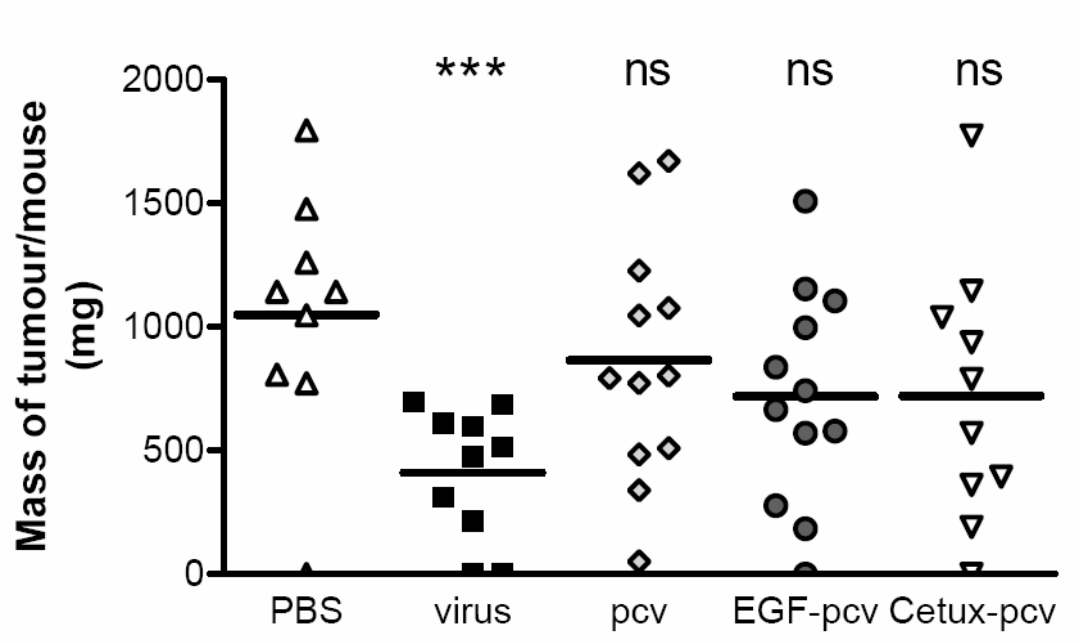


Figure 6-19 Mass of tumours removed at time of post-mortem examination

At post-mortem examination tumours were dissected and stored at −20°C. All tumours were then weighed. Points represent individual tumour load; bars represent median values. Data were analysed using the Kruskal-Wallis method with Dunn's multiple comparisons test to compare all groups to control. ns = not significant; *** = $P < 0.001$.

6.2.8.5 Tumour luciferase expression at sacrifice

All tumours were dissected and stored at −20°C, prior to weighing. Tumours were then homogenised in lysis buffer (Promega) at 300 mg/ml and luciferase activity of tumour analysed *in vitro* (see section 2.3.4). Mean relative light units per mg of tumour and total light units per mouse were calculated, to check that luciferase levels were not significantly different between groups (Figure 6-20). No group had significantly different luciferase expression compared to the PBS group, either per mg of tumour, or per mouse. There was a suggestion that there was a slight drop in tumour luciferase expression levels over time, as levels for the mice sacrificed later tended to be somewhat lower, although this was not a significant trend. This may be

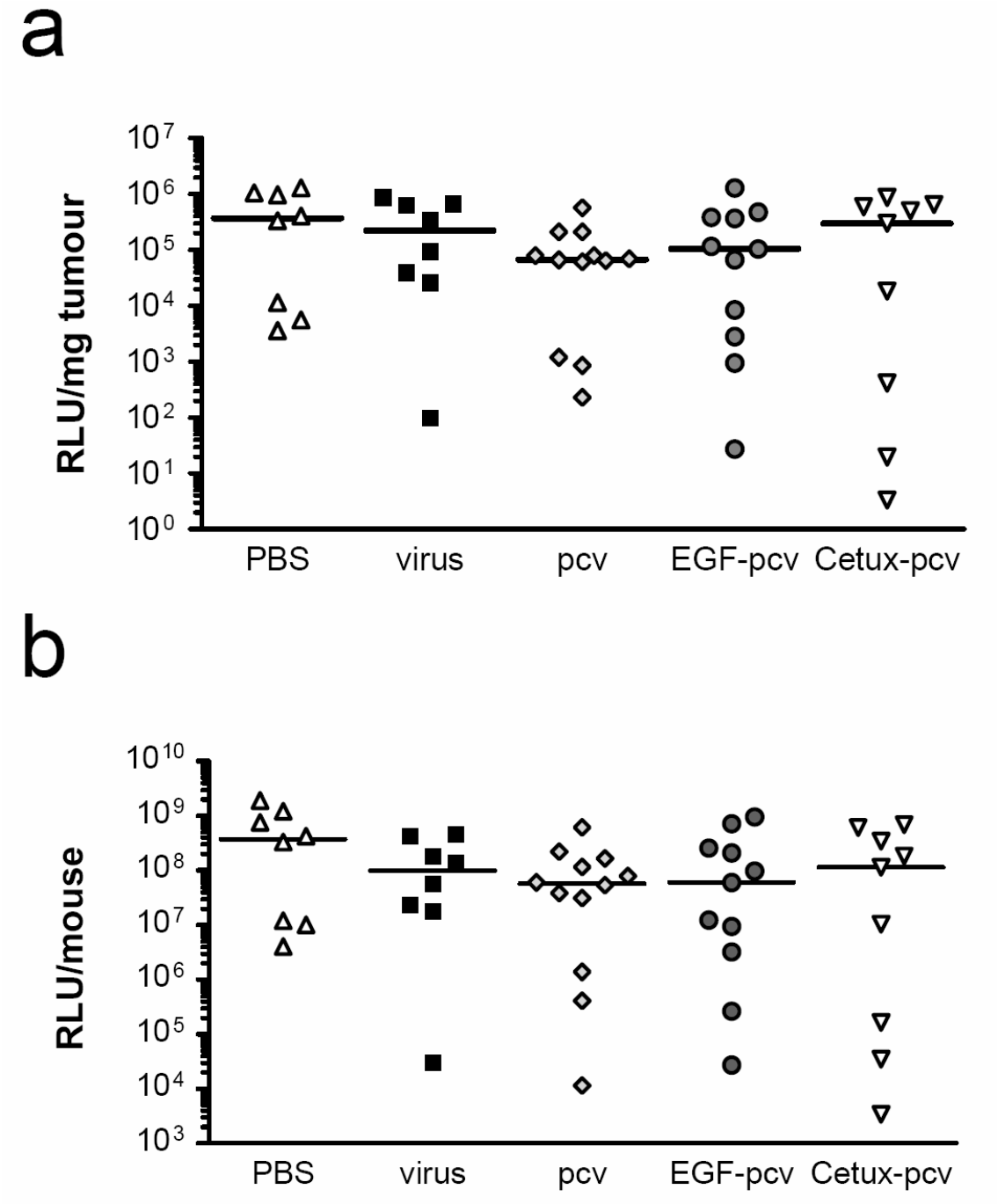


Figure 6-20 ***In vivo*** **bioluminescence of homogenised SKOV-luc tumours**

At post-mortem examination tumours were dissected and stored at −20°C. All tumours were then weighed and homogenised in lysis buffer at 300 mg/ml. Aliquots were assayed for luciferase expression (in triplicate). Points represent the mean of these values for each mouse; bars are median values. Data analysed by Kruskal-Wallis method with Dunn's multiple comparisons test to compare all groups to control. No group was significantly different to the PBS control.

because: either the tumours did reduce specific expression of luciferase over time, as antibiotic selection used *in vitro* could not be continued *in vivo*, due to toxicity; or the tissue harvested later had a greater mouse stromal component; or contained normal mouse tissue which had been mistaken for tumour. Unfortunately, due to a freezer malfunction, four tumour samples were excluded from the data, as they had defrosted over a weekend and their luciferase activity became degraded.

6.2.8.6 Effect of polymer coating Ad5WT on adhesion formation

At time of sacrifice (prior to unblinding), mice were examined and scored for adhesion formation, using a four-point scale (see Table 6-3). Representative post-mortem laparotomy images are shown in Figure 6-21. Mice treated with unmodified Ad5WT developed significantly more severe adhesions compared with polymer coated virus groups and PBS control (Figure 6-21), as determined by χ^2 analysis (Figure 6-22). Two mice in the unmodified virus group required sacrifice due to adhesion formation; neither of these mice had visible tumour present at time of sacrifice. No mice in any other group developed moderate or severe adhesions. These data were consistent with those seen in the pilot study and observations in clinical trials (phase I and phase II/III) of adenovirus p53 replacement, where adhesion formation occurred in women treated with virus. The virus used in that study was genetically modified adenovirus serotype 5 and was replication incompetent.

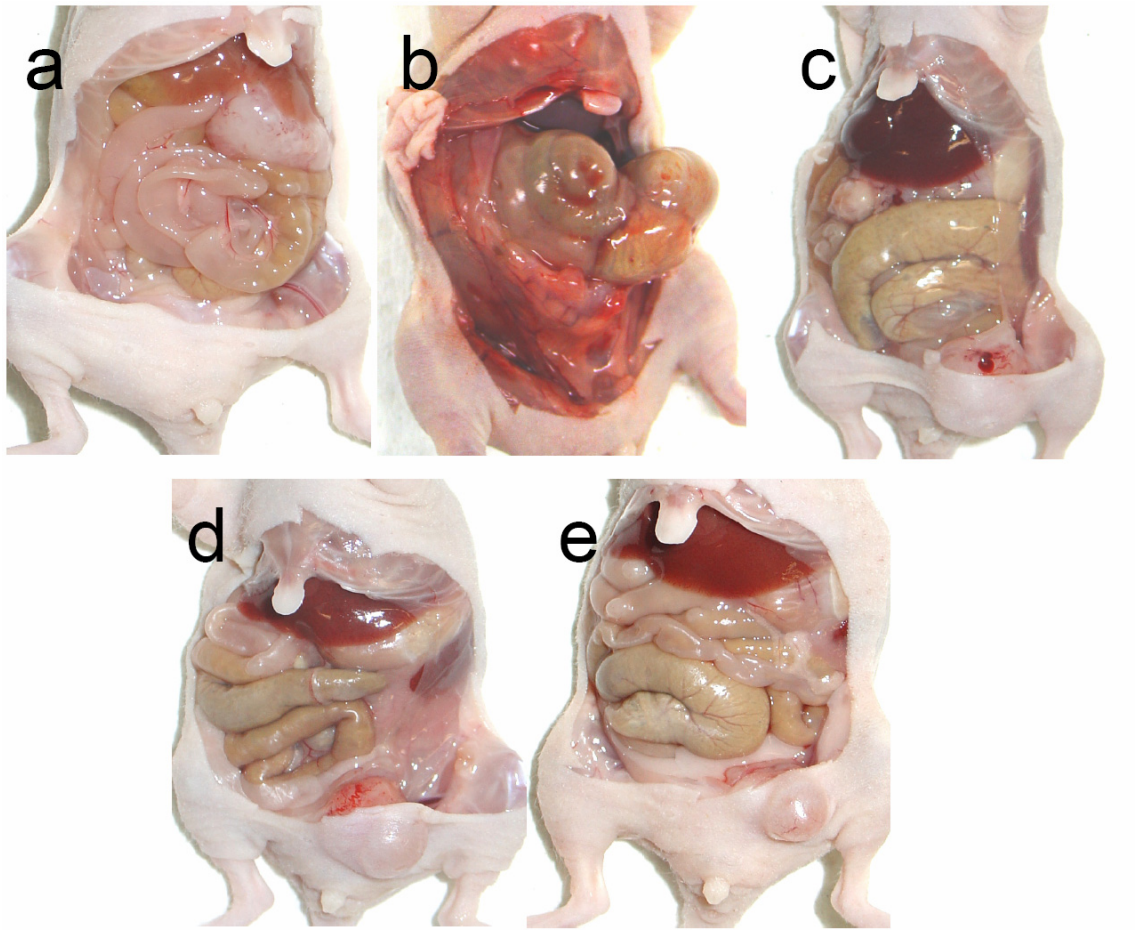


Figure 6-21 Post-mortem laparotomy images

Mice were carefully dissected at post-mortem examination and scored for adhesion formation. All tumours were meticulously dissected and weighed. Mice developed tumours in a similar pattern to human ovarian epithelial tumours: masses in the omentum and around the liver, stomach, diaphragm and small bowel mesentery. Mice shown are representative of their groups. Mice were treated with: (a) PBS; (b) unmodified Ad5WT; (c) pcv; (d) EGF-pcv; and (e) Cetuximab-pcv. In the individuals treated with unmodified Ad5WT, some developed abdominal distension, which was found to be due to adhesions causing bowel matting and dilatation of bowel loops. In addition, there were liver abnormalities, with reduced size and changes to the gross architecture.

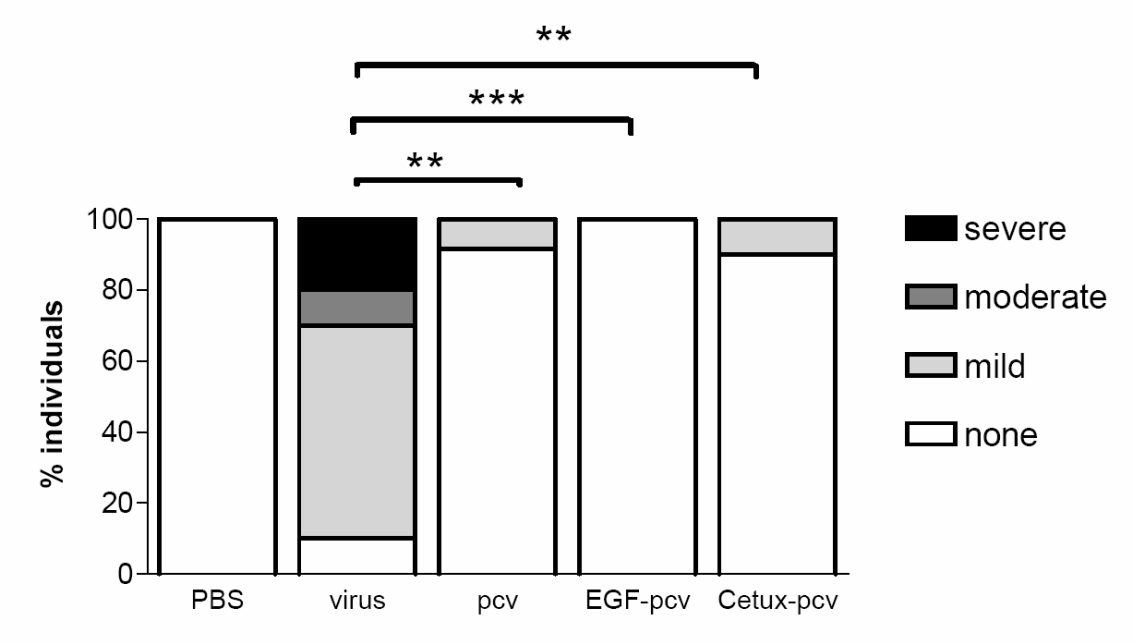


Figure 6-22 Adhesion scores for the survival study

MF1 nude mice implanted i.p. with 1 x 10^7 SKOV-luc cells, treated with three doses of 5 x 10^{10} v.p. of Ad5WT, unmodified, pcv, EGF-pcv, Cetuximab-pcv, or a non-virus PBS control, were sacrificed at human end points. At post-mortem examination, mice were scored for severity of adhesion formation within the peritoneal cavity. Contingency tables were generated from the group scores and analysed by χ^2 analysis. Overall significance across all groups P = 0.0002. Differences between virus and individual groups *** = P < 0.01; *** = P < 0.001.

6.2.8.7 Hepatic toxicity and effect of polymer coating

In addition to recording tumour mass (Figure 6-19) and scoring adhesions (Figure 6-22) at post mortem, the livers of mice from the survival study were examined microscopically. Livers were removed and immediately fixed in 4% formaldehyde/PBS solution. They were then dehydrated, mounted in paraffin and sectioned prior to staining with haematoxylin and eosin (see section 2.3.7). Paraffin-embedded sectionswere examined and scored for degree of liver pathology by an independent histopathologist (Dr S. Survana), who was blinded to the treatment groups and the nature of the experiment.

Figure 6-23 demonstrates the degree of hepatic inflammation (a) and necrosis (b) recorded. There were no statistically significant differences between the groups as determined by χ^2 analysis (hepatic inflammation P = 0.29; hepatic necrosis P = 0.11).

As high background levels of inflammation and necrosis were even recorded in the PBS treated group, it is suggested that much of this toxicity may be secondary to tumour development and not a treatment effect. However, it is surprising that no microscopic differences in liver pathology were observed, as clear macroscopic changes were seen in three mice in the group treated with unmodified adenovirus, which were not recorded in any other group (see appendix 9.4). Interestingly, these macroscopic changes did correspond with two cases where there was evidence of sub- and peri-capsular inflammation, which was not observed in any of the other groups. These abnormalities were not included in the hepatic pathology scoring system devised by the independent histopathologist, but included as a comment. Importantly, the histopathologist had not seen the un-fixed gross specimens, which may have provided additional information.

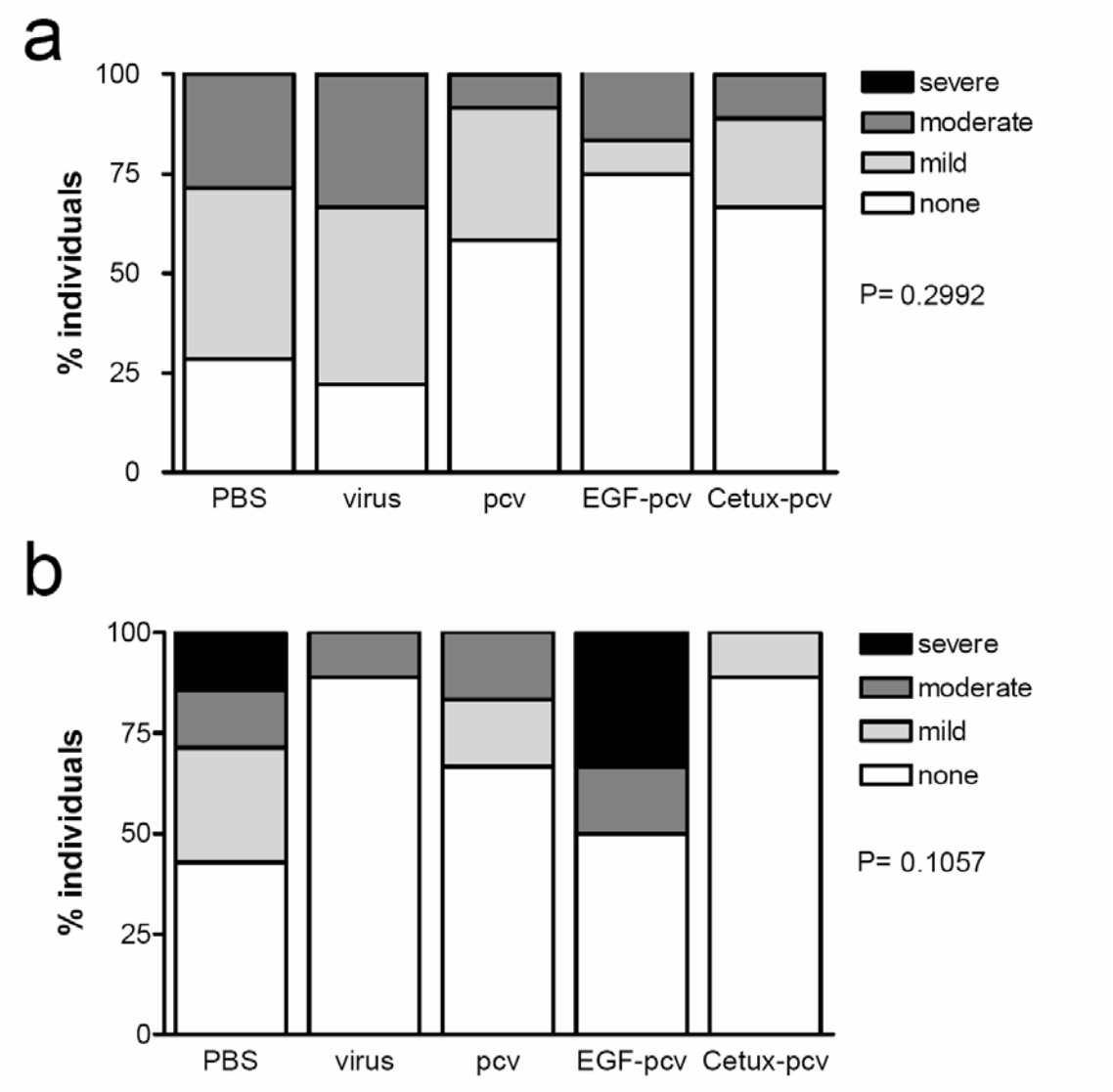


Figure 6-23 Hepatic histology findings

MF1 nude mice implanted i.p. with 1 x 10^7 SKOV-luc cells, treated with three doses of 5 x 10^{10} v.p. of Ad5WT, unmodified, pcv, EGF-pcv, Cetuximab-pcv, or a non-virus PBS control, were sacrificed at humane end points. At post-mortem examination livers were resected and immediately fixed in 4% formaldehyde/PBS solution. Livers were embedded in paraffin, sectioned, de-parafinized, re-hydrated, stained with haematoxylin and eosin, dehydrated and mounted in DPX (see section 2.3.7). Sections were examined by an independent histopathologist who was blinded to treatments and groups. Degree of necrosis and inflammation was scored on a four-point scale (none, mild, moderate and severe). Results are shown as percentage of the group. (a) hepatic inflammation; (b) hepatic necrosis. Contingency tables were generated from the group scores and analysed by χ^2 analysis. Overall significance across all groups; P = 0.3 and P = 0.11 for inflammation and necrosis respectively.

6.3 Discussion

6.3.1 Use of EGF-polymer coating to improve therapeutic index

Ad5WT has a significant oncolytic effect and, in this study, was more powerful *in vitro* than a panel of conditionally replicating adenoviruses based on Ad5 (ONYX-015, ONYX-017, *dl*922-947 and EHE2F). In all anti-cancer treatments a careful balance is required between a sufficiently aggressive treatment to cure the cancer and toxic side-effects caused by the treatment. This therapeutic index is narrow for many anti-cancer agents and limits the drug dose that can be delivered to the patient, hence compromising the clinical benefit and allowing tumour cells with increased resistance to treatment to survive and multiply. Although Ad5WT was effective as an anti-cancer agent *in vitro*, this benefit was limited *in vivo* by the development of adhesions: two mice developed significant adhesions and evidence of bowel obstruction resulting in early, non-tumour related sacrifice. Thus, EGF-polymer coating of Ad5WT improved the therapeutic index and could allow administration of increased amounts of virus compared with the unmodified virus. Indeed, no dose limiting toxicity (DLT) was observed in the EGF- or Cetuximab-pcv groups. As DLT was the major reason for halting the recent stage II/III clinical trial of adenovirus-delivered wild type p53 replacement at interim analysis (Dr S. Chang and Dr J. Horowitz – personal communication), the data from this experiment suggest that polymer coating and retargeting Ad5 may be a useful strategy for a variety of applications, particularly for treatment of intraperitoneal disease, such as ovarian cancer.

6.3.2 Use of bioluminescence to refine animal studies

Bioluminescence was investigated to determine whether it could be used as a surrogate end-point for survival experiments. These data demonstrated that initial flux levels indeed were inversely proportional to survival. Use of bioluminescence to measure efficacy of anti-cancer treatments is attractive as an alternative to survival end points for several reasons. First, intraperitoneal tumour load cannot be directly measured by conventional means, which limits the data that can be collected in i.p. tumour experiments. Second, ovarian cancer, both in this mouse model and in patients, often presents with few symptoms or signs until relatively late in the disease. This means that it is difficult to determine humane end-points as mice must be

examined daily for subtle signs to reduce the severity of the experiment to acceptable levels. Thus, being able to estimate the tumour load by bioluminescence enables humane surrogate survival end-points to be determined (e.g. when an individual mouse has flux levels greater than 1×10^9 photons/sec). Third, since flux levels were inversely proportional to median survival in this mouse model, it would be valid to use early flux measurements instead of continuing to survival end-points, which would greatly reduce the severity limit of the experiment, although this approach may miss non-tumour related survival end-points.

Previous work with a nude mouse model of ovarian cancer of IGROV-1, which stably express luciferin, demonstrated that there was an exponential increase in flux levels that correlated to tumour load (Lockley *et al.* 2006). A similar pattern was demonstrated for SKOV-luc cells at early time points performed during a preliminary experiment to the tumour load/survival experiment (Figure 6-12). However, this was not reliably shown during the tumour load/survival experiment, probably due to this tumour model developing bloody ascites at more advanced stages. Haemoglobin is effective at absorbing light and there would be less light to transilluminate through the abdominal wall to be detected by the camera system. In the Lockley study, mice were imaged nine times and imaging started much sooner after initial cell implantation. The project licence for our group permitted a maximum of seven bioluminescence measurements. In order not to exhaust this allocation too early, a decision was made not to image until 10 days after final treatment. In retrospect it would have been better to start measurements earlier, as once individuals required sacrifice for tumour load, it was then difficult to compare between groups. Finally, the IGROV-1 tumour model was a much more aggressive tumour than SKOV-luc, as the median survival following i.p. implantation of 3×10^6 cells was 19 days, compared with 34 days following implantation with 1×10^7 SKOV-luc cells. It may be, therefore, that the slower growing tumour is more difficult to monitor longitudinally using bioluminescence. Nevertheless, one of the key findings of these experiments was that early mean flux levels were inversely proportional to survival. Accordingly, bioluminescence is a valid secondary end point for the SKOV-luc tumour model.

In the Lockley study 20% icodextrin as an intraperitoneal carrier fluid had a positive effect on survival compared with PBS. It is possible that this may not be a direct anti-tumour effect, but may be due to amelioration of harmful side-effect of the adenovirus, as no comment was made about adhesion formation, nor were there data comparing tumour weights from these different groups. However, the virus used in the Lockley study (*dl*922-947) had less hepatotoxicity than Ad5WT so it may be that *dl*922-947 also induces less adhesion formation, although we have demonstrated that several Ad5-based viruses, both replication incompetent and conditionally replication competent (ONYX-015) do induce severe adhesions (Dr N. Green - unpublished data). Nevertheless, it is possible that icodextrin may have a directly beneficial effect on response to tumour. One study demonstrated that wild type p53 replacement therapy delivered with a replication incompetent Ad5 vector did not give a survival advantage when delivered in PBS, whereas a significant prolongation of survival did occur when the same dose of vector was delivered in 20% icodextrin (Engler *et al.* 2003). Indeed, greater reporter transgene expression was demonstrated using icodextrin as a carrier solution in this same study. It is known that icodextrin is able to improve pharmacokinetics of small molecules delivered i.p. (Hosie *et al.* 2003; Kerr *et al.* 1996) and so it is possible that it could indeed have a positive effect on virus delivered gene therapy. Certainly icodextrin would be likely to improve the adhesion formation demonstrated in response to Ad5, although a larger study would be required to confirm this hypothesis. It is most probable that the absence of positive effect on tumour load demonstrated in these experiments was due to the pilot study not being adequately powered.

6.3.3 Effect of polymer coating concentration on level of anti-tumour activity

In vitro transduction studies demonstrated that levels of transgene expression following infection with EGF-pcv or Cetuximab-pcv in EGFR positive cell lines exceeded that obtained with unmodified adenovirus. However, *in vivo* the effect on survival was similar. This may be due to using an increased concentration of polymer for virus coating in the *in vivo* studies; the *in vitro* studies used adenovirus coated at 5 or 10 mg/ml, whereas the survival studies used virus coated at 20 mg/ml. The reason for this was because previous *in vivo* work had demonstrated that coating adenovirus at 20 mg/ml reduced toxicity when delivered i.v. (Green *et al.* 2004) and

this had also been the coating concentration that reduced liver transduction in section 6.2.1. However, data from *in vitro* transgene expression studies in Chapter 4 did demonstrate that coating at this concentration reduced the specific activity of adenovirus, hence explaining why the therapeutic effect of retargeted adenovirus was not greater than unmodified virus. Coating at 20 mg/ml may over-modify the virus capsid, shielding it not only from interactions with cellular receptors and the immune system, but also modifying critical hexon residues required for nuclear uptake. There is therefore a compromise with this current polymer coating technology between coating sufficiently to shield the adenovirus prior to cellular uptake and allowing adenovirus to function once internalised. Work is continuing to develop polymers that optimise coating/protection of virus in the delivery phase whilst permitting activity within target cells.

The data in this chapter demonstrate that EGF-pcv and Cetuximab-pcv have improved therapeutic ratios compared to unmodified adenovirus and offer therapeutic potential. This work forms the basis for a paper submitted for publication, which can be found in the appendix section of this thesis.

7 General discussion and conclusions

Gene therapy using E1-deleted Group C adenoviruses has been used to deliver therapeutic transgenes encoding tumour suppressors (Buller *et al.* 2002; Wolf *et al.* 2004), immunostimulatory proteins (Green *et al.* 2003) or prodrug-activating enzymes (Palmer *et al.* 2004). However, clinical success with these agents has not fulfilled early promise. Recently the concept of 'virotherapy' has revitalised interest in this field; in this strategy lytic viruses replicate selectively within tumour cells and lyse them, before spreading to adjacent tumour cells and repeating the process (Ganly *et al.* 2000; Vasey *et al.* 2002). This approach enables amplification of the therapeutic agent (a 'conditionally replicating' virus) as it spreads through the cancer, minimising side effects and promising a high therapeutic index.

Conditionally-replicating serotype 5 adenoviruses (Ad5) have been developed to achieve selective replication by exploiting tumour-associated mutations, notably mutations in tumour suppressor genes such as p53 (Onyx-015) (Ganly *et al.* 2000; Vasey *et al.* 2002) and Rb (*dl*922-947) (Heise *et al.* 2000). These agents are doubly attractive for therapy since they may become more virulent as tumours accumulate mutations, for example in aggressive and drug resistant disease. In addition, this should provide good synergies with chemotherapy (Ganly *et al.* 2001).

However, although therapeutic adenoviruses show promise in pre-clinical studies, their efficacy in clinical trials has been limited due to neutralisation by pre-existing anti-adenovirus antibodies and poor target cell transduction, reflecting low cellular levels of CAR. In addition, Ad5 vectors have been found to cause toxicity, leading to early termination of a multicentre phase II/III clinical trial using an Ad5 vector delivered i.p. to treat ovarian cancer, due to the formation of adhesions (Zeimet and Marth 2003). Accordingly, the focus of this thesis was to address the major limitations of i.p. adenovirus delivery, enabling deployment of the virotherapy approach for clinical treatment of ovarian cancer.

7.1 Principal findings

7.1.1 Retargeting adenovirus with EGF-pHPMA *in vitro*

The primary aim was to determine whether the infection of EGF-pHPMA coated adenovirus could be retargeted to the EGFR, since this receptor is up-regulated in ovarian cancer and internalises though a pathway similar to that of adenovirus (for references see section 1.1.7.4). To determine whether infection was specific to the EGFR, I generated EGFR-positive, CAR-negative cell lines, based on stable transfection of murine A9 cells, which stably expressed EGFR for more than 6 months. These cell lines express low levels of EGFR compared with ovarian cancer cell lines, which over-express EGFR. Nevertheless, my experiments suggest that these EGFR are able to internalise on stimulation with EGF, although the assays employed to demonstrate EGFR phosphorylation were inadequately sensitive.

Using the polymer-coating technology, increased transgene expression was demonstrated in EGF-pcv infected cells compared with unmodified virus. In A9-EGFR cell lines, which lack CAR expression, levels of transduction were increased approximately 2.5-fold above that achieved with unmodified adenovirus. In A9-EGFR cell lines, EGF-pcv transgene expression was increased markedly compared with non-retargeted pcv (9-300x transduction; $P < 0.05$). Polymer coating was able to knock down transgene expression in CAR-negative cell lines, since adenovirus is able to infect via receptors other than CAR, e.g. heparan-sulphate and integrins. Polymer-coating of adenovirus detargets these uptake mechanisms in addition to CAR-mediated infection. Previous work in our group has demonstrated that retargeted uptake of pcv was independent of integrin-binding and not blocked by anti-integrin antibodies (Dr S. Hale, D.Phil. thesis, University of Oxford). EGF-polymer coated adenovirus mediated gene expression was inhibited by an anti-EGFR antibody, which is known to block EGF-binding. Anti-EGFR antibody did not block transgene expression in A9-CAR cells, nor did it inhibit non-EGF retargeted adenovirus transgene expression. Anti-CAR antibody was able to inhibit uncoated virus transgene mediated expression, but had no inhibiting effect on EGF-polymer coated adenovirus mediated transgene expression. These data therefore provide proof that the

infectious route of EGF-polymer coated Ad is both specific to the EGFR and independent of CAR.

EGF-polymer coating was able to retarget adenovirus to EGFR-positive cancer cell lines. Indeed, in some cell lines levels of gene expression with EGF-pcv were higher than for unmodified virus (2- to 35- fold increases). Further evidence that infection with EGF-pcv is EGFR-mediated comes from results in EGFR-positive cancer cell lines; levels of EGF-pcv transgene expression were directly proportional to cellular EGFR expression. Specific activity (transgene expression per virus genome internalised) of EGF-pcv coated at 10 mg/ml was similar to that of unmodified virus (~10 RLU/v.p.), suggesting that this level of covalent modification did not significantly reduce virus activity.

Retargeting of adenovirus gene therapy has previously been achieved using bispecific single chain antibodies, with dual specificity for adenoviral fibre knob and EGFR (Grill *et al.* 2001), or a secretory fusion molecule comprised of the CAR extracellular domain and EGF (Hemminki *et al.* 2001). These studies have shown that retargeting of adenovirus infection via the EGFR is possible and can produce high levels of transgene expression; using a bispecific antibody for adenovirus fibre knob-EGFR, transgene expression was increased around ten-fold in head and neck squamous cell carcinomas that had little CAR expression (Blackwell *et al.* 1999). Retargeted-transduction could be blocked by anti-EGFR antibodies, but not anti-CAR antibodies. Other studies have demonstrated that a fusion protein comprised of the soluble form of truncated CAR and EGF was able to retarget transgene expression of a luciferase-expressing adenovirus (Dmitriev *et al.* 2000). In pancreatic carcinoma cell lines transgene expression from retargeted adenovirus was up to five times that of non-retargeted virus; these cell lines have very low CAR levels (Wesseling *et al.* 2001). These data concur with the findings presented in this thesis and suggest that adenovirus infection can be successfully mediated via alternative receptors, although specific activity of virus (number of particles:luciferase expression) was not demonstrated in those published studies.

However, use of bispecific antibodies does not adequately protect adenovirus from neutralising antibodies. Previous work using pHPMA to coat adenovirus with bFGF retargeting demonstrated a ten-fold reduction in neutralisation of adenovirus encoding a green fluorescence protein (GFP) transgene (Fisher *et al.* 2001). Studies of human sera have demonstrated that the majority of neutralising antibodies to adenovirus are anti-hexon antibodies and bind to residues which are involved with uptake through the nuclear pore complex, rather than at the level of cell uptake (Sumida *et al.* 2005; Varghese *et al.* 2004). Thus, modification of the fibre protein alone is unlikely to have a major protective effect. Another limitation of using bispecific antibodies for retargeting adenovirus infection is that antibodies bind by electrostatic charge, not by covalent interaction, and so have 'off rates' of binding, which may limit their activity *in vivo*.

Modification of the fibre knob alone, whether with antibodies or genetically, does not adequately detarget adenovirus infection, since heparin-sulphate and integrin binding is not inhibited. Genetically retargeting adenovirus by modification of the fibre knob alone resulted in high transduction of hepatocytes in a murine model of adenovirus gene delivery (Einfeld *et al.* 2001) and double modification of both fibre and penton-base deletions were required to reduce liver transduction and prolong circulation time in the blood when delivered i.v. (Akiyama *et al.* 2004). However, another group found that double ablation was not sufficient to significantly reduce liver transduction (Martin *et al.* 2003) and deletion of all three uptake mechanisms was required for adequate detargeting in a murine model (Koizumi *et al.* 2006). The triple-detargeted vector demonstrated reduced toxicity compared with unmodified adenovirus, although no specific receptor retargeting had been achieved in this system. Importantly, some groups have demonstrated reduced efficiency of cellular uptake and endosomal escape in virus detargeted by penton-base deletions (Shayakhmetov *et al.* 2005a). One of the major benefits of the EGF-polymer-coated system is that it efficiently detargets adenovirus from the normal uptake mechanisms, whilst allowing efficient retargeting and infection (similar specific activity to wild type virus).

7.1.2 Retargeting adenovirus to EGFR with Cetuximab and TGF-α

In this study ligands other than EGF were shown to be capable of retargeting pcv to the EGFR. Although murine EGF is able to retarget adenovirus there remains the possibility of antibody development against murine EGF, if used in a clinical setting. Thus there are theoretical advantages to the use of human TGF-α and Cetuximab as targeting ligands. Another potential concern with EGF is that it would stimulate cell growth and thus have a positive mitogenic effect. This was investigated with replication incompetent AdCMV-Luc $_{\Delta E1}$. There was no significant stimulation of growth in EGFR-positive cancer cells incubated with EGF-pcv and TGF-α-pcv compared to unmodified virus, Cetuximab-pcv, pcv or a non-infected control in an *in vitro* growth mitogenic assay. This was despite both EGF-pcv and TGF-α-pcv stimulating significant EGFR tyrosine kinase activity. However, the dose of growth factors present on virus is small compared to that present either in sera or within tumours, especially as there is an autocrine production of EGF in many epithelial tumours. In the clinical setting, where the retargeted adenovirus would be delivering a therapeutic transgene, given that 40% of adenovirus that binds to a cell has its DNA transferred to the nucleus (Greber *et al.* 1997), it is likely that cells which do bind to either EGF-pcv or TGF-α-pcv would be successfully transduced and killed, as data demonstrated a similar specific activity for EGF-polymer coated adenovirus to unmodified adenovirus. Indeed, oncolytic adenoviruses stimulate cells to enter S phase (Heise *et al.* 2000; Lockley *et al.* 2006), and so stimulation of mitotic activity in the cell may actually aid virus transduction and replication, accelerating cell death.

7.1.3 *In vivo* effects of retargeting adenovirus to the EGFR

In a murine model of human ovarian cancer using a luciferase reporter virus administered i.p. to study virus pharmacodynamics, EGF-pcv showed a trend to improved liver:tumour ratio of transgene expression compared to unmodified virus. This finding was not demonstrated to be statistically significant, due to problems with lack of tumour development in some mice. However, there was a reduction in liver luciferase transgene expression following EGF-pcv delivery i.p. compared to unmodified adenovirus. These data indicated that there may be an improved therapeutic index if an anti-tumour adenovirus was coated with EGF-polymer.

A panel of ovarian cancer cell lines was tested for the oncolytic effect of a selection of conditionally replication competent adenoviruses. Of the cell lines tested, IGROV-1 was the most sensitive to all of the adenoviruses (based on Ad5), probably as a result of its relatively high level of CAR expression. However, since primary ovarian cancers have been found to have low CAR expression, IGROV-1 was not chosen as the xenograft for the murine model of therapeutic effect. The SKOV-3 cell line has been widely used as a murine model for ovarian cancer in nude mice, has EGFR and CAR levels representative of many ovarian cancer cell lines and primary tumours and grows in a pattern similar to that seen in patients with ovarian cancer, SKOV-3 was therefore chosen as the model in these studies.

From the oncolytic adenoviruses tested, Ad5WT had the greatest oncolytic activity in all ovarian cell lines tested and was chosen as the therapeutic virus for the survival/tumour load studies. Previous work demonstrated improved oncolytic effect *in vitro* with *dl*922-947 compared to Ad5WT (Heise *et al.* 2000; Lockley *et al.* 2006) in a number of cell lines. However, with the exception of IGROV-1, which was highly sensitive to all of the oncolytic Ad5, the cell lines tested here were not published in the Heise and Lockley studies, and so it is not clear whether these data are contrary to those previously published. Another reason for choosing Ad5WT was to determine whether there was any therapeutic effect of EGF-pcv. Lockley *et al* had demonstrated that *dl*922-947 induced reduced liver toxicity compared with Ad5WT.

A two-by-two factorial designed *in vivo* pilot study was initially performed to assess the effect of polymer coating Ad5WT and whether icodextrin improved therapeutic effect of Ad5WT. This experimental design enabled reduction in the number of animals and, as tumour burden was the end-point, rather than a survival study, it also enabled refinement of the experiment, as most animals were sacrificed prior to developing significant illness, thereby limiting severity. Data obtained was used in an *a priori* power calculation for the survival study. This study also provided the first evidence that polymer coating ameliorated formation of adhesions (Figure 6-7**).**

In vitro bioluminescence of SKOV-luc cells was demonstrated to be proportional to cell number. A pilot study was performed to identify a suitable time point over which measurements could be performed *in vivo*. This also gave the opportunity to develop a protocol for measuring bioluminescence prior to an experiment involving 60 animals. Bioluminescence measurements at early time points were found to be inversely proportional to eventual group survival. Later measurements were not as reliable, often due to reduced luminescence in animals that had developed bloody ascites. Haemoglobin is effective at absorbing light and presence of blood in the abdominal cavity is a major impediment to laparoscopic surgery. These problems were not encountered in a study using IGROV cells expressing luciferase (Lockley *et al.* 2006) where flux levels increased exponentially over 50 days. However, in this study *ex vivo* flux of SKOV-luc tumours harvested at different times did not differ significantly, suggesting that flux levels of tumours did not fall significantly over time.

Formation of adhesions and development of bowel obstruction was one of the primary reasons that a phase II/III clinical trial of i.p. Ad5 p53 replacement was halted at interim analysis (personal communication). Previously this complication had not been reported in pre-clinical trials of Ad5 vectors. However, it has been frequently observed in our research group with different Ad5 vectors, whether replication incompetent, competent or conditionally replicating (ONYX 015) (Dr N. Green, unpublished data). In the experiments presented here polymer coating of adenovirus prevented the development of adhesions. These results were demonstrated both in the pilot tumour load study and in an appropriately powered (n = 12 per group) survival study (Figure 6-21 and Figure 6-22). It should be noted that the investigator was blinded to treatment groups for the duration of the experiment. Unblinding occurred at the end of the experiment following final post-mortem examination and dissection of tumours in the surviving animals. Although many pre-clinical studies are not randomized and blinded, this is the gold standard for phase III clinical trials comparing different treatments, where both participants and researchers are blinded to treatments in order to avoid confounding factors influencing the outcome. In this study it was considered important that treatment groups should be randomized and blinded in order to avoid potential bias, either in adhesion scoring or dissection of tumours and thus increasing the confidence in the findings of this study. The

demonstration that EGF-polymer coating of Ad5WT can ameliorate the sometimes lethal complications of adhesion formation caused by Ad5WT, without compromising the anti-tumour activity (thereby improving the therapeutic index) is important for clinical therapeutics.

Fully characterising the mechanisms for the decreased toxicity of EGF-pcv will require further study. However, it has been previously reported that pHPMA polymer coating has a major effect on the kinetics of adenovirus when administered i.v. and mediated reduced hepatotoxicity (Green *et al.* 2004). This i.v. study measured liver enzymes for acute toxicity, rather than examining longer term effects of adenovirus on the liver. In addition, virus used in this study was a non-therapeutic replication incompetent reporter adenovirus. Another recent study demonstrated that PEGylation of adenovirus can substantially inhibit the innate immune response to adenovirus when injected intravenously (De Geest *et al.* 2005). It was reported that adenovirus conjugated with PEG polymers elicited reduced IL-6 responses, as determined by ELISA and RT-PCR compared with unmodified adenovirus. Cytokine responses were reduced to baseline in mice pre-dosed with methylprednisolone, a corticosteroid that has potent anti-inflammatory activity. Down-stream effects were a reduction in neutrophil and T-cell infiltration of the liver and prevention of thrombocytopaenia, which normally occurs due to unmodified adenovirus inducing disseminated intravascular coagulation (DIC) when delivered i.v. Similar results have been reported by other groups and are thought to be because PEGylation modifies critical residues on the adenovirus fibre that are involved with macrophage uptake/stimulation (Croyle *et al.* 2005; Mok *et al.* 2005). Indeed, it has been shown that macrophages can be triggered by ultraviolet light-inactivated adenovirus and by empty virus capsids to a similar levels as intact adenovirus (Higginbotham *et al.* 2002; Liu and Muruve 2003). This demonstration that the response is instigated by the capsid and not the expression of viral genes strengthens the rationale for the surface modification of adenovirus.

It is noteworthy that hepatitis B virus (HBV) stimulates macrophages to produce cytokines via interaction with its capsid and the macrophage toll-like receptor 2 (TLR2) (Cooper *et al.* 2005). This cytokine response was inhibited by excess of heparin or loss of arginine rich areas on the HBV capsid, which interact with heparin sulphate proteoglycans on the macrophage, and was

due to a specific heparin-ligand interaction, rather than a non-specific charge effect. The effect was shown to be mediated through TLR2 and assisted by CD14, a co-receptor for TLR2 and involved signalling through NF-κB. Adenovirus fibres also have a heparin sulphate binding area; it is possible that this may be involved in activation of the innate immune response to adenovirus in a similar manner to HBV. Indeed, these residues are modified by PEGylation and fibre-deleted adenovirus capsids do not induce such a strong inflammatory response (Smith *et al.* 2003).

7.2 Limitations

Levels of EGFR expression in isolated transfected A9 colonies were relatively low (at approximately 1,000 – 3,000 EGFR per cell), making assessment of EGFR function extremely difficult, especially as many of the methods for assessment of EGFR function are normally performed in cell lines with high EGFR expression levels. Comparisons that attempted to demonstrate EGFR activity were not significant and it was not possible to explore whether this was due to lack of EGFR functionality or alternatively because assays were below the level of detection. It may be that using protein A beads for immunoprecipitation or dot blot would concentrate EGFR sufficiently to allow detection by western blotting. Additionally, use of flow cytometry to select the cells expressing EGFR at the highest level may have improved the overall EGFR expression levels. As an alternative strategy for production of a stably expressing cell line, a retrovirus expressing a human EGFR could have been used to transduce the A9 parental cells, as this is often a more efficient method, and may have negated the need for extensive tissue culture and screening of potential EGFR-expressing A9 clones However, a suitable retrovirus was not available, and, since the EGFR receptor levels were high enough to allow analysis of EGF-polymer coated adenovirus mediated transduction and the major focus of the thesis was not examination of transfected EGFR activity, this was not pursued further.

Another major problem encountered was that of inefficient tumour establishment with the SKOV-3 cells in the nude mouse model. SKOV-3-ip cells are available, which have been selected by passage in vivo to grow more reliably. However, despite several attempts, I was

unable to obtain approval to use these cells, which are not commercially available. It may be that using much younger animals (6 weeks and under) would improve the efficiency of intraperitoneal tumour establishment, although difficulties with supply of nude mice for some time during the course of these experiments, necessitated the use of animals that had previously been ordered by another investigator; hence these animals were somewhat older than normally used.

Polymer coating at 20 mg/ml was used in the *in vivo* studies to assess the effect of EGF-polymer coating of adenovirus on anti-tumour activity. At this concentration of coating, there is reduced activity of adenovirus, probably due to modification of critical residues involved with uptake at the nuclear pore complex. This would explain why the anti-tumour effect with EGF-pcv was not greater than unmodified adenovirus, as might have been expected from the results of *in vitro* transduction experiments. This level of polymer coating was used *in vivo* as it had been shown that more highly modified adenovirus had improved pharmacokinetics. However, it may be that a lower polymer coating concentration would be adequate, as the polymer used in the i.v. pharmacokinetic studies was a previous generation of reactive pHPMA polymer and the polymer used in this study gives more efficient knockdown of transduction. Nevertheless, an improved therapeutic ratio was demonstrated for polymer coated retargeted adenovirus, which gives the potential to use higher numbers of virus particles, so increasing the anti-tumour effect without increasing the adverse side effects seen with unmodified virus.

7.3 Future work

Data presented in this thesis demonstrated that there was significant adhesion development following i.p. delivery of unmodified Ad5WT and that this toxicity was abrogated by covalent capsid modification with a reactive polymer. This is of great potential benefit in a clinical setting, as development of adhesions following repeated administration of adenovirus i.p. was one of the major limiting factors that lead to the curtailment of the i.p. adenovirus p53 replacement trial in ovarian cancer (Zeimet and Marth 2003). The effects of reducing toxicity of i.p. delivered adenovirus presented here were seen in a nude mouse model of ovarian cancer previously

naïve to adenovirus. Nude mice are athymic and lack an adaptive T-cell response. Adhesion formation in these mice is therefore likely to be caused by activation of the innate immune system, although little is currently known about the i.p. inflammatory response to adenovirus. Innate immune responses were also implicated in the death of Jesse Gelsinger, who died following i.v. administration of an adenovirus vector (Raper *et al.* 2003). Accordingly, reducing the inflammatory response to adenovirus would have major clinical implications, both for regional i.p. delivery and systemic i.v. delivery for a variety of diseases. Further work will therefore aim to elucidate mechanisms by which adenovirus causes intraperitoneal adhesions and how this may be modified by polymer coating of the adenovirus capsid. Work will concentrate on examining the innate immune response following exposure to adenovirus in an *in vitro* macrophage model system and by examination of cytokine responses in *in vivo* models.

It has been widely reported that adenovirus particles are able to stimulate an innate immune response and virus capsids localise to Kupffer cells, resident liver macrophages, and splenic macrophages when administered i.v. (Schnell *et al.* 2001) leading to the release of inflammatory cytokines. Chemokines of the CC class, such as RANTES, macrophage inflammatory protein 1β (MIP-1β), MIP-2 and MCP-1 bind to receptors on monocytes, recruiting and activating them to become tissue macrophages, in addition to T cell stimulatory functions. MIP-2 has neutrophil recruiting properties and is one of the first chemokines to be produced in an inflammatory response, inducing the sequential release of MIP-1α and tumour necrosis factor-α (TNF-α) (Ramos *et al.* 2006). TNF-α stimulates neutrophil activation, in addition to aiding neutrophil recruitment, by stimulating endothelial cells to express adhesion molecules. Thus, the initial stimulus triggers a co-ordinated cytokine cascade, which orchestrates the immediate innate immune response to the pathogen.

However, cytokines also have deleterious consequences. Local production of reactive oxygen species and release of neutrophil lysosomal contents can cause local tissue destruction. Fibrin formation within the peritoneal cavity initiates the production of adhesions. Fibrin, produced by inflammatory stimulation of the clotting cascade, is broken down by the protease, plasmin. An altered fibrin/plasmin ratio and apposition of peritoneal surfaces, e.g. small bowel visceral

peritoneum and abdominal parietal peritoneum, leads to the formation of adhesions (Sulaiman *et al.* 2002). In the acute stage, these are filmy fibrinous sheets, but can become dense and organised over time. The mesothelial and endothelial cells of the peritoneum have fibrinolytic activity (Myrhe-Jensen *et al.* 1969). Plasmin is produced by proteolytic activation of plasminogen; the adhesive phenotype is associated with an increase in peritoneal plasminogen inhibitor (Hellebrekers *et al.* 2005). In the peritoneal compartment macrophages, through the production of TNF-α, have a role in adhesion formation (Echtenacher *et al.* 2001). Fibrin formation reduced death from bacterial peritonitis, probably by blocking escape of bacteria through peritoneal stomata. This was inhibited by treatment with heparin (which prevents fibrin formation), urokinase (which increases plasmin production) and anti-TNF-α antibodies. It would therefore appear that acute adhesion formation is beneficial in containing peritoneal infection, but that an abnormal balance in fibrin/plasmin, or reduced plasmin production following the acute inflammatory stage, is responsible for development of permanent adhesions.

I will therefore investigate the innate immune response to i.p. administration of adenoviruses, comparing unmodified adenovirus and EGF-pcv. Inflammatory responses will be assessed in serum and peritoneal washings by measuring cytokine levels using a bead multiplex system, which allows simultaneous assessment of multiple cytokines, and peritoneal influx of immune cells by immunohistochemistry. These experiments will be performed using immunocompetent Balb/C mice and nude mice bearing human ovarian cancers. These studies will be reinforced by assays using murine peritoneal macrophages (isolated following administration of Biogel beads to promote macrophage recruitment into the peritoneal compartment). Cytokine responses will be assessed using the multiplex system to probe the effects of polymer coating the viruses on the macrophage activity they provoke.

Another area for future study is refinement of the pHPMA polymer to allow improved protection from neutralising antibodies, which currently is only partial (Fisher *et al.* 2001). *In vitro* data presented here demonstrate that increasing the degree of polymer coating decreases the specific activity of adenovirus. Preliminary data suggest that the level of inhibition is intracellular; it is likely that this is due to over-modification of critical residues on the hexon

protein that are necessary for uptake at the nuclear pore complex. Current polymer coating technology means that there is a compromise between coating sufficiently to allow protection from liver uptake and antibody neutralisation and over-modification of critical residues on the capsid, which inactivates the virus. We are investigating the use of reducible polymers that are degraded in the low pH reducing environment of the endosome, so allowing uncoating of the virus capsid. Other areas of investigation include development of self-assembling polymers, which form on the virus capsid, allowing production of large dendrimer structures, which would offer improved steric protection of critical residues on the virus capsid without over-modification and cross-linking of the capsid.

Further work will therefore initially focus on the following areas:

- The response of macrophages to adenovirus *in vitro* and the effect of polymer coating on the production of cytokines.
- The time course of cytokine and cellular response to intraperitoneal injection of adenovirus to determine suitable points at which to assess the effect of polymer coating.
- The effect of polymer coating on cytokine and acute inflammatory cell response to adenovirus in immune competent mice and immune incompetent tumour bearing mice.

The ultimate aim of this work is to optimise the polymer coating and retargeting technology so that it may be taken forward to clinical trials to improve outcome for women with advanced ovarian cancer. These data already suggest that EGF-polymer coating provides benefit *in vivo* and work will concentrate on improving the polymer coating and understanding adenovirus toxicity when delivered intraperitoneally. I aim to establish whether polymer coating and retargeting improves the therapeutic ratio of an i.p. delivered oncolytic adenovirus in a dose limiting toxicity experiment in a mouse model prior to phase I clinical trials.

7.4 Conclusions

Current clinical applications of adenovirus gene therapy have been limited by adenovirus neutralisation and poor target cell transduction. Development of an efficient gene delivery system to avoid these major hurdles is crucial to the success of any gene therapy approach. Retargeting adenovirus using reactive polymers based on pHPMA is possible using a variety of ligands that bind to the EGFR. Transduction efficiency in EGFR positive cells is maintained or improved, dependent on the level of cellular EGFR expression. *In vivo* this reduced toxicity, thereby improving the therapeutic index of adenovirus treatments.

Chemical retargeting of adenovirus is an attractive approach to improve adenovirus-delivered anti-cancer therapy. Although this thesis demonstrates that polymer coated adenovirus may be retargeted via the EGFR, this is a proof of principle study and potentially many other cancer-specific or up-regulated ligands could be used for retargeting. In addition, this polymer coating technology can be used to deliver a variety of adenovirus 'payloads', thereby removing the necessity for genetic retargeting of different therapeutic viruses. These data demonstrate that toxic side effects of adenovirus, presumably caused by an inflammatory response to the virus capsid, can be ameliorated; a problem that is currently a major limiting factor for gene therapy. Further work is required to understand how these effects are mediated and to improve the polymer coating technology to provide significant protection from neutralising antibodies.

8 References

Akiyama, M., Thorne, S., Kirn, D.*, et al.* (2004) Ablating CAR and integrin binding in adenovirus vectors reduces nontarget organ transduction and permits sustained bloodstream persistence following intraperitoneal administration. *Mol Ther* 9, 218-230.

Alberts, D.S., Liu, P.Y., Hannigan, E.V.*, et al.* (1996) Intraperitoneal cisplatin plus intravenous cyclophosphamide versus intravenous cisplatin plus intravenous cyclophosphamide for stage III ovarian cancer. *N. Engl. J. Med.* 335, 1950-1955.

Allen, T.M. (1994) Long-circulating (sterically stabilized) liposomes for targeted drug delivery. *Trends Pharmacol. Sci.* 15, 215-220.

Alper, O., Bergmann-Leitner, E.S., Bennett, T.A., Hacker, N.F., Stromberg, K. & Stetler-Stevenson, W.G. (2001) Epidermal growth factor receptor signaling and the invasive phenotype of ovarian carcinoma cells. *J. Natl. Cancer Inst.* 93, 1375-1384.

Alvarez, R.D., Gomez-Navarro, J., Wang, M.*, et al.* (2000) Adenoviral-mediated suicide gene therapy for ovarian cancer. *Mol Ther* 2, 524-530.

Amalfitano, A., Hauser, M.A., Hu, H., Serra, D., Begy, C.R. & Chamberlain, J.S. (1998) Production and characterization of improved adenovirus vectors with the E1, E2b, and E3 genes deleted. *J. Virol.* 72, 926-933.

Armstrong, D.K., Bundy, B., Wenzel, L.*, et al.* (2006) Intraperitoneal cisplatin and paclitaxel in ovarian cancer. *N. Engl. J. Med.* 354, 34-43.

Assessment of adenoviral vector safety and toxicity: report of the National Institutes of Health Recombinant DNA Advisory Committee. (2002) *Hum. Gene Ther.* 13, 3-13.

Bache, K.G., Slagsvold, T. & Stenmark, H. (2004) Defective downregulation of receptor tyrosine kinases in cancer. *EMBO J.* 23, 2707-2712.

Bailey, C.J., Crystal, R.G. & Leopold, P.L. (2003) Association of adenovirus with the microtubule organizing center. *J. Virol.* 77, 13275-13287.

Balague, C., Zhou, J., Dai, Y.*, et al.* (2000) Sustained high-level expression of full-length human factor VIII and restoration of clotting activity in hemophilic mice using a minimal adenovirus vector. *Blood* 95, 820-828.

Bandera, C.A., Tsui, H.W., Mok, S.C. & Tsui, F.W. (2003) Expression of cytokines and receptors in normal, immortalized, and malignant ovarian epithelial cell lines. *Anticancer Res.* 23, 3151-3157.

Bartlett, J.M., Langdon, S.P., Simpson, B.J*., et al.* (1996) The prognostic value of epidermal growth factor receptor mRNA expression in primary ovarian cancer. *Br. J. Cancer* 73, 301-306.

Baselga, J., Albanell, J., Molina, M.A. & Arribas, J. (2001) Mechanism of action of trastuzumab and scientific update. *Semin. Oncol.* 28, 4-11.

Baselga, J., Rischin, D., Ranson, M*., et al.* (2002) Phase I safety, pharmacokinetic, and pharmacodynamic trial of ZD1839, a selective oral epidermal growth factor receptor tyrosine kinase inhibitor, in patients with five selected solid tumor types. *J. Clin. Oncol.* 20, 4292-4302.

Bell, J., Brady, M.F., Young, R.C*., et al.* (2006) Randomized phase III trial of three versus six cycles of adjuvant carboplatin and paclitaxel in early stage epithelial ovarian carcinoma: a Gynecologic Oncology Group study. *Gynecol. Oncol.* 102, 432-439.

Benard, J., Da Silva, J., De Blois, M.C*., et al.* (1985) Characterization of a human ovarian adenocarcinoma line, IGROV1, in tissue culture and in nude mice. *Cancer Res.* 45, 4970-4979.

Bergelson, J.M., Cunningham, J.A., Droguett, G*., et al.* (1997) Isolation of a common receptor for Coxsackie B viruses and adenoviruses 2 and 5. *Science* 275, 1320-1323.

Bingham, C., Roberts, D. & Hamilton, T.C. (2001) The role of molecular biology in understanding ovarian cancer initiation and progression. *Int J Gynecol Cancer* 11 Suppl 1, 7-11.

Bischoff, J.R., Kirn, D.H., Williams, A*., et al.* (1996) An adenovirus mutant that replicates selectively in p53-deficient human tumor cells. *Science* 274, 373-376.

Blackwell, J.L., Miller, C.R., Douglas, J.T*., et al.* (1999) Retargeting to EGFR enhances adenovirus infection efficiency of squamous cell carcinoma. *Arch. Otolaryngol. Head Neck Surg.* 125, 856-863.

Block, A., Freund, C.T., Chen, S.H*., et al.* (2000) Gene therapy of metastatic colon carcinoma: regression of multiple hepatic metastases by adenoviral expression of bacterial cytosine deaminase. *Cancer Gene Ther.* 7, 438-445.

Blomer, U., Naldini, L., Kafri, T., Trono, D., Verma, I.M. & Gage, F.H. (1997) Highly efficient and sustained gene transfer in adult neurons with a lentivirus vector. *J. Virol.* 71, 6641-6649.

Blume-Jensen, P. & Hunter, T. (2001) Oncogenic kinase signalling. *Nature* 411, 355-365.

Bookman, M.A. (2006) *GOG0182-ICON5: 5-arm phase III randomized trial of paclitaxel (P) and carboplatin (C) vs combinations with gemcitabine (G), PEG-lipososomal doxorubicin (D), or topotecan (T) in patients (pts) with advanced-stage epithelial ovarian (EOC) or primary peritoneal (PPC) carcinoma.* Paper presented at: 2006 ASCO Annual Meeting Proceedings Journal of Clinical Oncology.

Bookman, M.A., Darcy, K.M., Clarke-Pearson, D., Boothby, R.A. & Horowitz, I.R. (2003) Evaluation of monoclonal humanized anti-HER2 antibody, trastuzumab, in patients with recurrent or refractory ovarian or primary peritoneal carcinoma with overexpression of HER2: a phase II trial of the Gynecologic Oncology Group. *J. Clin. Oncol.* 21, 283-290.

Brown, P.M., Debanne, M.T., Grothe, S.*, et al.* (1994) The extracellular domain of the epidermal growth factor receptor. Studies on the affinity and stoichiometry of binding, receptor dimerization and a binding-domain mutant. *Eur. J. Biochem.* 225, 223-233.

Buller, R.E., Runnebaum, I.B., Karlan, B.Y.*, et al.* (2002) A phase I/II trial of rAd/p53 (SCH 58500) gene replacement in recurrent ovarian cancer. *Cancer Gene Ther.* 9, 553-566.

Buttitta, F., Marchetti, A., Gadducci, A.*, et al.* (1997) p53 alterations are predictive of chemoresistance and aggressiveness in ovarian carcinomas: a molecular and immunohistochemical study. *Br. J. Cancer* 75, 230-235.

Carter, R.E. & Sorkin, A. (1998) Endocytosis of functional epidermal growth factor receptor-green fluorescent protein chimera. *J. Biol. Chem.* 273, 35000-35007.

Cavazzana-Calvo, M., Hacein-Bey, S., de Saint Basile, G.*, et al.* (2000) Gene therapy of human severe combined immunodeficiency (SCID)-X1 disease. *Science* 288, 669-672.

Chemotherapy in advanced ovarian cancer: an overview of randomised clinical trials. Advanced Ovarian Cancer Trialists Group. (1991) *BMJ* 303, 884-893.

Chen, L., Yu, L.J. & Waxman, D.J. (1997) Potentiation of cytochrome P450/cyclophosphamide-based cancer gene therapy by coexpression of the P450 reductase gene. *Cancer Res.* 57, 4830-4837.

Chen, X. & Wang, Z. (2001) Regulation of epidermal growth factor receptor endocytosis by wortmannin through activation of Rab5 rather than inhibition of phosphatidylinositol 3-kinase. *EMBO Rep* 2, 842-849.

Chillon, M., Lee, J.H., Fasbender, A. & Welsh, M.J. (1998) Adenovirus complexed with polyethylene glycol and cationic lipid is shielded from neutralizing antibodies in vitro. *Gene Ther.* 5, 995-1002.

Chirmule, N., Propert, K., Magosin, S., Qian, Y., Qian, R. & Wilson, J. (1999) Immune responses to adenovirus and adeno-associated virus in humans. *Gene Ther.* 6, 1574-1583.

Ciardiello, F., Bianco, R., Damiano, V.*, et al.* (1999) Antitumor activity of sequential treatment with topotecan and anti-epidermal growth factor receptor monoclonal antibody C225. *Clin. Cancer Res.* 5, 909-916.

Connolly, J.M. & Rose, D.P. (1987) Quantitative differences in the effects of mouse and human epidermal growth factors on A431 human tumor cells. *Cancer Lett.* 37, 241-249.

Conroy, S.E., Baines, L., Rodgers, K., Deviren, F. & Verco, S.J. (2003) Prevention of chemotherapy-induced intraperitoneal adhesion formation in rats by icodextrin at a range of concentrations. *Gynecol. Oncol.* 88, 304-308.

Cooley, S., Burns, L.J., Repka, T. & Miller, J.S. (1999) Natural killer cell cytotoxicity of breast cancer targets is enhanced by two distinct mechanisms of antibody-dependent cellular cytotoxicity against LFA-3 and HER2/neu. *Exp. Hematol.* 27, 1533-1541.

Cooper, A., Tal, G., Lider, O. & Shaul, Y. (2005) Cytokine induction by the hepatitis B virus capsid in macrophages is facilitated by membrane heparan sulfate and involves TLR2. *J. Immunol.* 175, 3165-3176.

Corbin-Lickfett, K.A. & Bridge, E. (2003) Adenovirus E4-34kDa requires active proteasomes to promote late gene expression. *Virology* 315, 234-244.

Cristiano, R.J. & Roth, J.A. (1996) Epidermal growth factor mediated DNA delivery into lung cancer cells via the epidermal growth factor receptor. *Cancer Gene Ther.* 3, 4-10.

Croyle, M.A., Chirmule, N., Zhang, Y. & Wilson, J.M. (2001) "Stealth" adenoviruses blunt cell-mediated and humoral immune responses against the virus and allow for significant gene expression upon readministration in the lung. *J. Virol.* 75, 4792-4801.

Croyle, M.A., Le, H.T., Linse, K.D.*, et al.* (2005) PEGylated helper-dependent adenoviral vectors: highly efficient vectors with an enhanced safety profile. *Gene Ther.* 12, 579-587.

D'Agostino, G., Ferrandina, G., Ludovisi, M.*, et al.* (2003) Phase II study of liposomal doxorubicin and gemcitabine in the salvage treatment of ovarian cancer. *Br. J. Cancer* 89, 1180-1184.

De, B.K., Misono, K.S., Lukas, T.J., Mroczkowski, B. & Cohen, S. (1986) A calcium-dependent 35-kilodalton substrate for epidermal growth factor receptor/kinase isolated from normal tissue. *J. Biol. Chem.* 261, 13784-13792.

De Geest, B., Snoeys, J., Van Linthout, S., Lievens, J. & Collen, D. (2005) Elimination of innate immune responses and liver inflammation by PEGylation of adenoviral vectors and methylprednisolone. *Hum. Gene Ther.* 16, 1439-1451.

DeGregorio, M.W., Lum, B.L., Holleran, W.M., Wilbur, B.J. & Sikic, B.I. (1986) Preliminary observations of intraperitoneal carboplatin pharmacokinetics during a phase I study of the Northern California Oncology Group. *Cancer Chemother. Pharmacol.* 18, 235-238.

Denning, C. & Pitts, J.D. (1997) Bystander effects of different enzyme-prodrug systems for cancer gene therapy depend on different pathways for intercellular transfer of toxic metabolites, a factor that will govern clinical choice of appropriate regimes. *Hum. Gene Ther.* 8, 1825-1835.

Descamps, V., Duffour, M.T., Mathieu, M.C.*, et al.* (1996) Strategies for cancer gene therapy using adenoviral vectors. *J. Mol. Med.* 74, 183-189.

Deshpande, D., Toledo-Velasquez, D., Thakkar, D., Liang, W. & Rojanasakul, Y. (1996) Enhanced cellular uptake of oligonucleotides by EGF receptor-mediated endocytosis in A549 cells. *Pharm. Res.* 13, 57-61.

diZerega, G.S., Verco, S.J., Young, P.*, et al.* (2002) A randomized, controlled pilot study of the safety and efficacy of 4% icodextrin solution in the reduction of adhesions following laparoscopic gynaecological surgery. *Hum. Reprod.* 17, 1031-1038.

Djeha, A.H., Hulme, A., Dexter, M.T.*, et al.* (2000) Expression of Escherichia coli B nitroreductase in established human tumor xenografts in mice results in potent antitumoral and bystander effects upon systemic administration of the prodrug CB1954. *Cancer Gene Ther.* 7, 721-731.

Dmitriev, I., Kashentseva, E., Rogers, B.E., Krasnykh, V. & Curiel, D.T. (2000) Ectodomain of coxsackievirus and adenovirus receptor genetically fused to epidermal growth factor mediates adenovirus targeting to epidermal growth factor receptor-positive cells. *J. Virol.* 74, 6875-6884.

Dmitriev, I., Krasnykh, V., Miller, C.R.*, et al.* (1998) An adenovirus vector with genetically modified fibers demonstrates expanded tropism via utilization of a coxsackievirus and adenovirus receptor-independent cell entry mechanism. *J. Virol.* 72, 9706-9713.

Downward, J., Parker, P. & Waterfield, M.D. (1984) Autophosphorylation sites on the epidermal growth factor receptor. *Nature* 311, 483-485.

Dutheil, N., Shi, F., Dupressoir, T. & Linden, R.M. (2000) Adeno-associated virus site-specifically integrates into a muscle-specific DNA region. *Proc. Natl. Acad. Sci. U. S. A.* 97, 4862-4866.

Dvorin, J.D. & Malim, M.H. (2003) Intracellular trafficking of HIV-1 cores: journey to the center of the cell. *Curr. Top. Microbiol. Immunol.* 281, 179-208.

Ebner, R. & Derynck, R. (1991) Epidermal growth factor and transforming growth factor-alpha: differential intracellular routing and processing of ligand-receptor complexes. *Cell Regul.* 2, 599-612.

Echtenacher, B., Weigl, K., Lehn, N. & Mannel, D.N. (2001) Tumor necrosis factor-dependent adhesions as a major protective mechanism early in septic peritonitis in mice. *Infect. Immun.* 69, 3550-3555.

Einfeld, D.A., Schroeder, R., Roelvink, P.W.*, et al.* (2001) Reducing the native tropism of adenovirus vectors requires removal of both CAR and integrin interactions. *J. Virol.* 75, 11284-11291.

Ekstrand, A.J., Sugawa, N., James, C.D. & Collins, V.P. (1992) Amplified and rearranged epidermal growth factor receptor genes in human glioblastomas reveal deletions of sequences encoding portions of the N- and/or C-terminal tails. *Proc. Natl. Acad. Sci. U. S. A.* 89, 4309-4313.

Engler, H., Machemer, T.R., Schluep, T.*, et al.* (2003) Development of a formulation that enhances gene expression and efficacy following intraperitoneal administration in rabbits and mice. *Mol Ther* 7, 558-564.

Farquhar, D., Pan, B.F., Sakurai, M., Ghosh, A., Mullen, C.A. & Nelson, J.A. (2002) Suicide gene therapy using E. coli beta-galactosidase. *Cancer Chemother. Pharmacol.* 50, 65-70.

Fava, R. & Cohen, S. (1984) Isolation of a calcium-dependent 35-kilodalton substrate for the epidermal growth factor receptor/kinase from A-431 cells. *J. Biol. Chem.* 259, 2636-2645.

Fisher, K.D., Stallwood, Y., Green, N.K., Ulbrich, K., Mautner, V. & Seymour, L.W. (2001) Polymer-coated adenovirus permits efficient retargeting and evades neutralising antibodies. *Gene Ther.* 8, 341-348.

Fisher, K.J., Jooss, K., Alston, J.*, et al.* (1997) Recombinant adeno-associated virus for muscle directed gene therapy. *Nat. Med.* 3, 306-312.

Fogh, J. (1975) Human tumour cells in vitro. *Plenum Press*, 115-159.

Fogh, J., Fogh, J.M. & Orfeo, T. (1977) One hundred and twenty-seven cultured human tumor cell lines producing tumors in nude mice. *J. Natl. Cancer Inst.* 59, 221-226.

Fujiwara, T., Grimm, E.A., Mukhopadhyay, T., Zhang, W.W., Owen-Schaub, L.B. & Roth, J.A. (1994) Induction of chemosensitivity in human lung cancer cells in vivo by adenovirus-mediated transfer of the wild-type p53 gene. *Cancer Res.* 54, 2287-2291.

Ganly, I., Kim, Y.T., Hann, B., Balmain, A. & Brown, R. (2001) Replication and cytolysis of an E1B-attenuated adenovirus in drug-resistant ovarian tumour cells is associated with reduced apoptosis. *Gene Ther.* 8, 369-375.

Ganly, I., Kirn, D., Eckhardt, G.*, et al.* (2000) A phase I study of Onyx-015, an E1B attenuated adenovirus, administered intratumorally to patients with recurrent head and neck cancer. *Clin. Cancer Res.* 6, 798-806.

Garrett, T.P., McKern, N.M., Lou, M.*, et al.* (2003) The crystal structure of a truncated ErbB2 ectodomain reveals an active conformation, poised to interact with other ErbB receptors. *Mol. Cell* 11, 495-505.

Gaspar, H.B., Parsley, K.L., Howe, S.*, et al.* (2004) Gene therapy of X-linked severe combined immunodeficiency by use of a pseudotyped gammaretroviral vector. *Lancet* 364, 2181-2187.

Georgiades, J., Zielinski, T., Cicholska, A. & Jordan, E. (1959) Research on the oncolytic effect of APC viruses in cancer of the cervix uteri; preliminary report. *Biul. Inst. Med. Morsk. Gdansk.* 10, 49-57.

Giannakakou, P., Nakano, M., Nicolaou, K.C.*, et al.* (2002) Enhanced microtubule-dependent trafficking and p53 nuclear accumulation by suppression of microtubule dynamics. *Proc. Natl. Acad. Sci. U. S. A.* 99, 10855-10860.

Giard, D.J., Aaronson, S.A., Todaro, G.J.*, et al.* (1973) In vitro cultivation of human tumors: establishment of cell lines derived from a series of solid tumors. *J. Natl. Cancer Inst.* 51, 1417-1423.

Goldstein, N.I., Prewett, M., Zuklys, K., Rockwell, P. & Mendelsohn, J. (1995) Biological efficacy of a chimeric antibody to the epidermal growth factor receptor in a human tumor xenograft model. *Clin. Cancer Res.* 1, 1311-1318.

Gordon, A.N., Finkler, N., Edwards, R.P.*, et al.* (2005) Efficacy and safety of erlotinib HCl, an epidermal growth factor receptor (HER1/EGFR) tyrosine kinase inhibitor, in patients with advanced ovarian carcinoma: results from a phase II multicenter study. *Int J Gynecol Cancer* 15, 785-792.

Graham, F.L., Smiley, J., Russell, W.C. & Nairn, R. (1977) Characteristics of a human cell line transformed by DNA from human adenovirus type 5. *J. Gen. Virol.* 36, 59-74.

Gram, G.J., Nielsen, S.D. & Hansen, J.E. (1998) Spontaneous silencing of humanized green fluorescent protein (hGFP) gene expression from a retroviral vector by DNA methylation. *J. Hematother.* 7, 333-341.

Greber, U.F., Suomalainen, M., Stidwill, R.P., Boucke, K., Ebersold, M.W. & Helenius, A. (1997) The role of the nuclear pore complex in adenovirus DNA entry. *EMBO J.* 16, 5998-6007.

Greber, U.F., Willetts, M., Webster, P. & Helenius, A. (1993) Stepwise dismantling of adenovirus 2 during entry into cells. *Cell* 75, 477-486.

Green, N.K., Herbert, C.W., Hale, S.J.*, et al.* (2004) Extended plasma circulation time and decreased toxicity of polymer-coated adenovirus. *Gene Ther.* 11, 1256-1263.

Green, N.K., McNeish, I.A., Doshi, R., Searle, P.F., Kerr, D.J. & Young, L.S. (2003) Immune enhancement of nitroreductase-induced cytotoxicity: studies using a bicistronic adenovirus vector. *Int. J. Cancer* 104, 104-112.

Griffiths, C.T. (1975) Surgical resection of tumor bulk in the primary treatment of ovarian carcinoma. *Natl. Cancer Inst. Monogr.* 42, 101-104.

Griffiths, C.T. & Fuller, A.F. (1978) Intensive surgical and chemotherapeutic management of advanced ovarian cancer. *Surg. Clin. North Am.* 58, 131-142.

Grill, J., Van Beusechem, V.W., Van Der Valk, P.*, et al.* (2001) Combined targeting of adenoviruses to integrins and epidermal growth factor receptors increases gene transfer into primary glioma cells and spheroids. *Clin. Cancer Res.* 7, 641-650.

Hacein-Bey-Abina, S., Von Kalle, C., Schmidt, M.*, et al.* (2003) LMO2-associated clonal T cell proliferation in two patients after gene therapy for SCID-X1. *Science* 302, 415-419.

Haigler, H., Ash, J.F., Singer, S.J. & Cohen, S. (1978) Visualization by fluorescence of the binding and internalization of epidermal growth factor in human carcinoma cells A-431. *Proc. Natl. Acad. Sci. U. S. A.* 75, 3317-3321.

Hallenbeck, P.L., Chang, Y.N., Hay, C.*, et al.* (1999) A novel tumor-specific replication-restricted adenoviral vector for gene therapy of hepatocellular carcinoma. *Hum. Gene Ther.* 10, 1721-1733.

Hamilton, T.C., Young, R.C., McKoy, W.M.*, et al.* (1983) Characterization of a human ovarian carcinoma cell line (NIH:OVCAR-3) with androgen and estrogen receptors. *Cancer Res.* 43, 5379-5389.

Hamilton, T.C., Young, R.C. & Ozols, R.F. (1984) Experimental model systems of ovarian cancer: applications to the design and evaluation of new treatment approaches. *Semin. Oncol.* 11, 285-298.

Hamstra, D.A. & Rehemtulla, A. (1999) Toward an enzyme/prodrug strategy for cancer gene therapy: endogenous activation of carboxypeptidase A mutants by the PACE/Furin family of propeptidases. *Hum. Gene Ther.* 10, 235-248.

Hauswirth, W.W., Lewin, A.S., Zolotukhin, S. & Muzyczka, N. (2000) Production and purification of recombinant adeno-associated virus. *Methods Enzymol.* 316, 743-761.

Heise, C., Hermiston, T., Johnson, L.*, et al.* (2000) An adenovirus E1A mutant that demonstrates potent and selective systemic anti-tumoral efficacy. *Nat. Med.* 6, 1134-1139.

Heise, C., Sampson-Johannes, A., Williams, A., McCormick, F., Von Hoff, D.D. & Kirn, D.H. (1997) ONYX-015, an E1B gene-attenuated adenovirus, causes tumor-specific cytolysis and antitumoral efficacy that can be augmented by standard chemotherapeutic agents. *Nat. Med.* 3, 639-645.

Hellebrekers, B.W., Emeis, J.J., Kooistra, T.*, et al.* (2005) A role for the fibrinolytic system in postsurgical adhesion formation. *Fertil. Steril.* 83, 122-129.

Hemminki, A., Dmitriev, I., Liu, B., Desmond, R.A., Alemany, R. & Curiel, D.T. (2001) Targeting oncolytic adenoviral agents to the epidermal growth factor pathway with a secretory fusion molecule. *Cancer Res.* 61, 6377-6381.

Hemminki, A., Wang, M., Hakkarainen, T., Desmond, R.A., Wahlfors, J. & Curiel, D.T. (2003) Production of an EGFR targeting molecule from a conditionally replicating adenovirus impairs its oncolytic potential. *Cancer Gene Ther.* 10, 583-588.

Herbst, J.J., Opresko, L.K., Walsh, B.J., Lauffenburger, D.A. & Wiley, H.S. (1994) Regulation of postendocytic trafficking of the epidermal growth factor receptor through endosomal retention. *J. Biol. Chem.* 269, 12865-12873.

Hernandez-Alcoceba, R., Pihalja, M., Qian, D. & Clarke, M.F. (2002) New oncolytic adenoviruses with hypoxia- and estrogen receptor-regulated replication. *Hum. Gene Ther.* 13, 1737-1750.

Higginbotham, J.N., Seth, P., Blaese, R.M. & Ramsey, W.J. (2002) The release of inflammatory cytokines from human peripheral blood mononuclear cells in vitro following exposure to adenovirus variants and capsid. *Hum. Gene Ther.* 13, 129-141.

Higgins, G.K. & Pack, G.T. (1951) Virus therapy in the treatment of tumors. *Bull. Hosp. Joint Dis.* 12, 379-382.

Hosie, K.B., Kerr, D.J., Gilbert, J.A.*, et al.* (2003) A pilot study of adjuvant intraperitoneal 5-fluorouracil using 4% icodextrin as a novel carrier solution. *Eur. J. Surg. Oncol.* 29, 254-260.

Huang, H.S., Nagane, M., Klingbeil, C.K.*, et al.* (1997) The enhanced tumorigenic activity of a mutant epidermal growth factor receptor common in human cancers is mediated by threshold levels of constitutive tyrosine phosphorylation and unattenuated signaling. *J. Biol. Chem.* 272, 2927-2935.

Huber, B.E., Richards, C.A. & Krenitsky, T.A. (1991) Retroviral-mediated gene therapy for the treatment of hepatocellular carcinoma: an innovative approach for cancer therapy. *Proc. Natl. Acad. Sci. U. S. A.* 88, 8039-8043.

Jacobs, I., Oram, D., Fairbanks, J., Turner, J., Frost, C. & Grudzinskas, J.G. (1990) A risk of malignancy index incorporating CA 125, ultrasound and menopausal status for the accurate preoperative diagnosis of ovarian cancer. *Br. J. Obstet. Gynaecol.* 97, 922-929.

Jaramillo, M.L., Leon, Z., Grothe, S., Paul-Roc, B., Abulrob, A. & O'Connor McCourt, M. (2006) Effect of the anti-receptor ligand-blocking 225 monoclonal antibody on EGF receptor endocytosis and sorting. *Exp. Cell Res.* 312, 2778-2790.

Jooss, K., Yang, Y., Fisher, K.J. & Wilson, J.M. (1998) Transduction of dendritic cells by DNA viral vectors directs the immune response to transgene products in muscle fibers. *J. Virol.* 72, 4212-4223.

Jounaidi, Y. & Waxman, D.J. (2004) Use of replication-conditional adenovirus as a helper system to enhance delivery of P450 prodrug-activation genes for cancer therapy. *Cancer Res.* 64, 292-303.

Kawamoto, T., Sato, J.D., Le, A., Polikoff, J., Sato, G.H. & Mendelsohn, J. (1983) Growth stimulation of A431 cells by epidermal growth factor: identification of high-affinity receptors for epidermal growth factor by an anti-receptor monoclonal antibody. *Proc. Natl. Acad. Sci. U. S. A.* 80, 1337-1341.

Kehoe, S., Powell, J., Wilson, S. & Woodman, C. (1994) The influence of the operating surgeon's specialisation on patient survival in ovarian carcinoma. *Br. J. Cancer* 70, 1014-1017.

Kehoe, S. & Wheeler, S. (2003) CHORUS (Chemotherapy or Upfront Surgery). A randomised feasibility trial to determine the impact of timing of surgery and chemotherapy in newly diagnosed patients with advanced epithelial ovarian, primary peritoneal or fallopian tube carcinoma. London: Royal College of Obstetricians and Gynaecologists.

Kerr, D.E., Li, Z., Siemers, N.O., Senter, P.D. & Vrudhula, V.M. (1998) Development and activities of a new melphalan prodrug designed for tumor-selective activation. *Bioconjug. Chem.* 9, 255-259.

Kerr, D.J., Young, A.M., Neoptolemos, J.P.*, et al.* (1996) Prolonged intraperitoneal infusion of 5-fluorouracil using a novel carrier solution. *Br. J. Cancer* 74, 2032-2035.

Khuu, H., Conner, M., Vanderkwaak, T.J.*, et al.* (1999) Detection of Coxsackie-Adenovirus Receptor (CAR) Immunoreactivity in Ovarian Tumors of Epithelial Derivation. *Appl Immunohistochem Mol Morphol* 7, 266-270.

Kohn, K.W., Aladjem, M.I., Kim, S., Weinstein, J.N. & Pommier, Y. (2006) Depicting combinatorial complexity with the molecular interaction map notation. *Mol Syst Biol* 2, 51.

Koizumi, N., Kawabata, K., Sakurai, F., Watanabe, Y., Hayakawa, T. & Mizuguchi, H. (2006) Modified adenoviral vectors ablated for coxsackievirus-adenovirus receptor, alphav integrin, and heparan sulfate binding reduce in vivo tissue transduction and toxicity. *Hum. Gene Ther.* 17, 264-279.

Kwok, Y.C. & Yip, C.C. (1987) Tyrosine phosphorylation of two cytosolic proteins of 50 kDa and 35 kDa in rat liver by insulin-receptor kinase in vitro. *Biochem. J.* 248, 27-33.

Lambert, H.E., Gregory, W.M., Nelstrop, A.E. & Rustin, G.J. (2004) Long-term survival in 463 women treated with platinum analogs for advanced epithelial carcinoma of the ovary: life expectancy compared to women of an age-matched normal population. *Int J Gynecol Cancer* 14, 772-778.

Lax, I., Johnson, A., Howk, R.*, et al.* (1988) Chicken epidermal growth factor (EGF) receptor: cDNA cloning, expression in mouse cells, and differential binding of EGF and transforming growth factor alpha. *Mol. Cell. Biol.* 8, 1970-1978.

Lenferink, A.E., De Roos, A.D., Van Vugt, M.J., Van de Poll, M.L. & Van Zoelen, E.J. (1998) The linear C-terminal regions of epidermal growth factor (EGF) and transforming growth factor-alpha bind to different epitopes on the human EGF receptor. *Biochem. J.* 336 (Pt 1), 147-151.

Li, S., Schmitz, K.R., Jeffrey, P.D., Wiltzius, J.J., Kussie, P. & Ferguson, K.M. (2005) Structural basis for inhibition of the epidermal growth factor receptor by cetuximab. *Cancer Cell* 7, 301-311.

Liu, Q. & Muruve, D.A. (2003) Molecular basis of the inflammatory response to adenovirus vectors. *Gene Ther.* 10, 935-940.

Liu, X.L., Clark, K.R. & Johnson, P.R. (1999) Production of recombinant adeno-associated virus vectors using a packaging cell line and a hybrid recombinant adenovirus. *Gene Ther.* 6, 293-299.

Lockley, M., Fernandez, M., Wang, Y.*, et al.* (2006) Activity of the adenoviral E1A deletion mutant dl922-947 in ovarian cancer: comparison with E1A wild-type viruses, bioluminescence monitoring, and intraperitoneal delivery in icodextrin. *Cancer Res.* 66, 989-998.

Lusky, M., Christ, M., Rittner, K.*, et al.* (1998) In vitro and in vivo biology of recombinant adenovirus vectors with E1, E1/E2A, or E1/E4 deleted. *J. Virol.* 72, 2022-2032.

Lyons, M., Onion, D., Green, N.K.*, et al.* (2006) Adenovirus type 5 interactions with human blood cells may compromise systemic delivery. *Mol Ther* 14, 118-128.

Maeda, K., Kato, Y. & Sugiyama, Y. (2002) pH-dependent receptor/ligand dissociation as a determining factor for intracellular sorting of ligands for epidermal growth factor receptors in rat hepatocytes. *J Control Release* 82, 71-82.

Manome, Y., Wen, P.Y., Dong, Y*., et al.* (1996) Viral vector transduction of the human deoxycytidine kinase cDNA sensitizes glioma cells to the cytotoxic effects of cytosine arabinoside in vitro and in vivo. *Nat. Med.* 2, 567-573.

Marme, A., Strauss, G., Bastert, G., Grischke, E.M. & Moldenhauer, G. (2002) Intraperitoneal bispecific antibody (HEA125xOKT3) therapy inhibits malignant ascites production in advanced ovarian carcinoma. *Int. J. Cancer* 101, 183-189.

Martin-Fernandez, M., Longshaw, S.V., Kirby, I*., et al.* (2004) Adenovirus type-5 entry and disassembly followed in living cells by FRET, fluorescence anisotropy, and FLIM. *Biophys. J.* 87, 1316-1327.

Martin, K., Brie, A., Saulnier, P., Perricaudet, M., Yeh, P. & Vigne, E. (2003) Simultaneous CAR- and alpha V integrin-binding ablation fails to reduce Ad5 liver tropism. *Mol Ther* 8, 485-494.

Martinez-Arca, S., Bech-Serra, J.J., Hurtado-Kuttner, M., Borroto, A. & Arribas, J. (2005) Recycling of cell surface pro-transforming growth factor-{alpha} regulates epidermal growth factor receptor activation. *J. Biol. Chem.* 280, 36970-36977.

Massague, J. (1983) Epidermal growth factor-like transforming growth factor. II. Interaction with epidermal growth factor receptors in human placenta membranes and A431 cells. *J. Biol. Chem.* 258, 13614-13620.

Massoglia, S., Gray, A., Dull, T.J*., et al.* (1990) Epidermal growth factor receptor cytoplasmic domain mutations trigger ligand-independent transformation. *Mol. Cell. Biol.* 10, 3048-3055.

Mayr, G.A. & Freimuth, P. (1997) A single locus on human chromosome 21 directs the expression of a receptor for adenovirus type 2 in mouse A9 cells. *J. Virol.* 71, 412-418.

McGuire, W.P., Hoskins, W.J., Brady, M.F*., et al.* (1996) Cyclophosphamide and cisplatin compared with paclitaxel and cisplatin in patients with stage III and stage IV ovarian cancer. *N. Engl. J. Med.* 334, 1-6.

McNeish, I.A., Green, N.K., Gilligan, M.G*., et al.* (1998) Virus directed enzyme prodrug therapy for ovarian and pancreatic cancer using retrovirally delivered E. coli nitroreductase and CB1954. *Gene Ther.* 5, 1061-1069.

Medina-Kauwe, L.K., Maguire, M., Kasahara, N. & Kedes, L. (2001) Nonviral gene delivery to human breast cancer cells by targeted Ad5 penton proteins. *Gene Ther.* 8, 1753-1761.

Meier, O., Boucke, K., Hammer, S.V.*, et al.* (2002) Adenovirus triggers macropinocytosis and endosomal leakage together with its clathrin-mediated uptake. *J. Cell Biol.* 158, 1119-1131.

Meier, O. & Greber, U.F. (2004) Adenovirus endocytosis. *J Gene Med* 6 Suppl 1, S152-163.

Misra, V., Klamut, H.J. & Rauth, A.M. (2002) Expression of the prodrug-activating enzyme DT-diaphorase via Ad5 delivery to human colon carcinoma cells in vitro. *Cancer Gene Ther.* 9, 209-217.

Mittereder, N., March, K.L. & Trapnell, B.C. (1996) Evaluation of the concentration and bioactivity of adenovirus vectors for gene therapy. *J. Virol.* 70, 7498-7509.

Mohr, L., Rainov, N.G., Mohr, U.G. & Wands, J.R. (2000) Rabbit cytochrome P450 4B1: A novel prodrug activating gene for pharmacogene therapy of hepatocellular carcinoma. *Cancer Gene Ther.* 7, 1008-1014.

Mok, H., Palmer, D.J., Ng, P. & Barry, M.A. (2005) Evaluation of polyethylene glycol modification of first-generation and helper-dependent adenoviral vectors to reduce innate immune responses. *Mol Ther* 11, 66-79.

Mollenhauer, H.H., Morre, D.J. & Rowe, L.D. (1990) Alteration of intracellular traffic by monensin; mechanism, specificity and relationship to toxicity. *Biochim. Biophys. Acta* 1031, 225-246.

Montelione, G.T., Winkler, M.E., Burton, L.E., Rinderknecht, E., Sporn, M.B. & Wagner, G. (1989) Sequence-specific 1H-NMR assignments and identification of two small antiparallel beta-sheets in the solution structure of recombinant human transforming growth factor alpha. *Proc. Natl. Acad. Sci. U. S. A.* 86, 1519-1523.

Moolten, F.L. & Wells, J.M. (1990) Curability of tumors bearing herpes thymidine kinase genes transferred by retroviral vectors. *J. Natl. Cancer Inst.* 82, 297-300.

Morishige, K., Kurachi, H., Amemiya, K.*, et al.* (1991) Involvement of transforming growth factor alpha/epidermal growth factor receptor autocrine growth mechanism in an ovarian cancer cell line in vitro. *Cancer Res.* 51, 5951-5955.

Moscatello, D.K., Holgado-Madruga, M., Godwin, A.K.*, et al.* (1995) Frequent expression of a mutant epidermal growth factor receptor in multiple human tumors. *Cancer Res.* 55, 5536-5539.

Moulder, S.L., Yakes, F.M., Muthuswamy, S.K., Bianco, R., Simpson, J.F. & Arteaga, C.L. (2001) Epidermal growth factor receptor (HER1) tyrosine kinase inhibitor ZD1839 (Iressa) inhibits HER2/neu (erbB2)-overexpressing breast cancer cells in vitro and in vivo. *Cancer Res.* 61, 8887-8895.

Muggia, F.M., Braly, P.S., Brady, M.F., *et al.* (2000) Phase III randomized study of cisplatin versus paclitaxel versus cisplatin and paclitaxel in patients with suboptimal stage III or IV ovarian cancer: a gynecologic oncology group study. *J. Clin. Oncol.* 18, 106-115.

Myrhe-Jensen, O., Larsen, S.B. & Astrup, T. (1969) Fibrinolytic activity in serosal and synovial membranes. Rats, guinea pigs, and rabbits. *Arch. Pathol.* 88, 623-630.

Nakano, M.Y., Boucke, K., Suomalainen, M., Stidwill, R.P. & Greber, U.F. (2000) The first step of adenovirus type 2 disassembly occurs at the cell surface, independently of endocytosis and escape to the cytosol. *J. Virol.* 74, 7085-7095.

Nicholson, R.I., Gee, J.M. & Harper, M.E. (2001) EGFR and cancer prognosis. *Eur. J. Cancer* 37 Suppl 4, S9-15.

Nicklin, S.A., Wu, E., Nemerow, G.R. & Baker, A.H. (2005) The influence of adenovirus fiber structure and function on vector development for gene therapy. *Mol Ther* 12, 384-393.

O'Neal, W.K., Zhou, H., Morral, N., *et al.* (1998) Toxicological comparison of E2a-deleted and first-generation adenoviral vectors expressing alpha1-antitrypsin after systemic delivery. *Hum. Gene Ther.* 9, 1587-1598.

O'Riordan, C.R., Lachapelle, A., Delgado, C., *et al.* (1999) PEGylation of adenovirus with retention of infectivity and protection from neutralizing antibody in vitro and in vivo. *Hum. Gene Ther.* 10, 1349-1358.

O'Shea, C.C., Johnson, L., Bagus, B., *et al.* (2004) Late viral RNA export, rather than p53 inactivation, determines ONYX-015 tumor selectivity. *Cancer Cell* 6, 611-623.

O'Toole, C., Perlmann, P., Unsgaard, B., Moberger, G. & Edsmyr, F. (1972) Cellular immunity to human urinary bladder carcinoma. I. Correlation to clinical stage and radiotherapy. *Int. J. Cancer* 10, 77-91.

Oda, K., Matsuoka, Y., Funahashi, A. & Kitano, H. (2005) A comprehensive pathway map of epidermal growth factor receptor signaling. *Mol Syst Biol* 1, 2005 0010.

Ogiso, H., Ishitani, R., Nureki, O., *et al.* (2002) Crystal structure of the complex of human epidermal growth factor and receptor extracellular domains. *Cell* 110, 775-787.

Pack, G.T. (1950) Note on the experimental use of rabies vaccine for melanomatosis. *Geburtshilfe Frauenheilkd.* 62, 694-695.

Paclitaxel plus carboplatin versus standard chemotherapy with either single-agent carboplatin or cyclophosphamide, doxorubicin, and cisplatin in women with ovarian cancer: the ICON3 randomised trial. (2002) *Lancet* 360, 505-515.

Palmer, D.H., Mautner, V., Mirza, D.*, et al.* (2004) Virus-directed enzyme prodrug therapy: intratumoral administration of a replication-deficient adenovirus encoding nitroreductase to patients with resectable liver cancer. *J. Clin. Oncol.* 22, 1546-1552.

Palmer, J.A., Branston, R.H., Lilley, C.E.*, et al.* (2000) Development and optimization of herpes simplex virus vectors for multiple long-term gene delivery to the peripheral nervous system. *J. Virol.* 74, 5604-5618.

Parker, A.L., Waddington, S.N., Nicol, C.G.*, et al.* (2006) Multiple vitamin K-dependent coagulation zymogens promote adenovirus-mediated gene delivery to hepatocytes. *Blood* 108, 2554-2561.

Parker, W.B., King, S.A., Allan, P.W.*, et al.* (1997) In vivo gene therapy of cancer with E. coli purine nucleoside phosphorylase. *Hum. Gene Ther.* 8, 1637-1644.

Piccart, M.J., Bertelsen, K., Stuart, G.*, et al.* (2003) Long-term follow-up confirms a survival advantage of the paclitaxel-cisplatin regimen over the cyclophosphamide-cisplatin combination in advanced ovarian cancer. *Int J Gynecol Cancer* 13 Suppl 2, 144-148.

Quinn, M., Babb, B., Brock, A. & Jones, J. (2001) Cancer Trends in England and Wales, London, The Stationery Office.

Raben, D., Helfrich, B., Chan, D.C.*, et al.* (2005) The effects of cetuximab alone and in combination with radiation and/or chemotherapy in lung cancer. *Clin. Cancer Res.* 11, 795-805.

Ramos, C.D., Fernandes, K.S., Canetti, C., Teixeira, M.M., Silva, J.S. & Cunha, F.Q. (2006) Neutrophil recruitment in immunized mice depends on MIP-2 inducing the sequential release of MIP-1alpha, TNF-alpha and LTB(4). *Eur. J. Immunol.*

Raper, S.E., Chirmule, N., Lee, F.S.*, et al.* (2003) Fatal systemic inflammatory response syndrome in a ornithine transcarbamylase deficient patient following adenoviral gene transfer. *Mol. Genet. Metab.* 80, 148-158.

Rodriguez, R., Schuur, E.R., Lim, H.Y., Henderson, G.A., Simons, J.W. & Henderson, D.R. (1997) Prostate attenuated replication competent adenovirus (ARCA) CN706: a selective cytotoxic for prostate-specific antigen-positive prostate cancer cells. *Cancer Res.* 57, 2559-2563.

Romanczuk, H., Galer, C.E., Zabner, J., Barsomian, G., Wadsworth, S.C. & O'Riordan, C.R. (1999) Modification of an adenoviral vector with biologically selected peptides: a novel strategy for gene delivery to cells of choice. *Hum. Gene Ther.* 10, 2615-2626.

Rose, P.G., Nerenstone, S., Brady, M.F.*, et al.* (2004) Secondary surgical cytoreduction for advanced ovarian carcinoma. *N. Engl. J. Med.* 351, 2489-2497.

Rowe, W.P., Huebner, R.J., Gilmore, L.K., Parrott, R.H. & Ward, T.G. (1953) Isolation of a cytopathogenic agent from human adenoids undergoing spontaneous degeneration in tissue culture. *Proc. Soc. Exp. Biol. Med.* 84, 570-573.

Samaniego, L.A., Neiderhiser, L. & DeLuca, N.A. (1998) Persistence and expression of the herpes simplex virus genome in the absence of immediate-early proteins. *J. Virol.* 72, 3307-3320.

Sandercock, J., Parmar, M.K., Torri, V. & Qian, W. (2002) First-line treatment for advanced ovarian cancer: paclitaxel, platinum and the evidence. *Br. J. Cancer* 87, 815-824.

Schlessinger, J. & Ullrich, A. (1992) Growth factor signaling by receptor tyrosine kinases. *Neuron* 9, 383-391.

Schnell, M.A., Zhang, Y., Tazelaar, J.*, et al.* (2001) Activation of innate immunity in nonhuman primates following intraportal administration of adenoviral vectors. *Mol Ther* 3, 708-722.

Shayakhmetov, D.M., Eberly, A.M., Li, Z.Y. & Lieber, A. (2005a) Deletion of penton RGD motifs affects the efficiency of both the internalization and the endosome escape of viral particles containing adenovirus serotype 5 or 35 fiber knobs. *J. Virol.* 79, 1053-1061.

Shayakhmetov, D.M., Gaggar, A., Ni, S., Li, Z.Y. & Lieber, A. (2005b) Adenovirus binding to blood factors results in liver cell infection and hepatotoxicity. *J. Virol.* 79, 7478-7491.

Shepherd, J.H. (1989) Revised FIGO staging for gynaecological cancer. *Br. J. Obstet. Gynaecol.* 96, 889-892.

Singer, V.L., Jones, L.J., Yue, S.T. & Haugland, R.P. (1997) Characterization of PicoGreen reagent and development of a fluorescence-based solution assay for double-stranded DNA quantitation. *Anal. Biochem.* 249, 228-238.

Sirena, D., Lilienfeld, B., Eisenhut, M.*, et al.* (2004) The human membrane cofactor CD46 is a receptor for species B adenovirus serotype 3. *J. Virol.* 78, 4454-4462.

Slamon, D.J., Godolphin, W., Jones, L.A.*, et al.* (1989) Studies of the HER-2/neu proto-oncogene in human breast and ovarian cancer. *Science* 244, 707-712.

Smith, R.R., Huebner, R.J., Rowe, W.P., Schatten, W.E. & Thomas, L.B. (1956) Studies on the use of viruses in the treatment of carcinoma of the cervix. *Cancer* 9, 1211-1218.

Smith, T.A., Idamakanti, N., Marshall-Neff, J.*, et al.* (2003) Receptor interactions involved in adenoviral-mediated gene delivery after systemic administration in non-human primates. *Hum. Gene Ther.* 14, 1595-1604.

Soric, J. & Gordon, J. (1986) Calcium-dependent isolation of the 36-kilodalton substrate of pp60src- kinase. Fractionation of the phosphorylated and unphosphorylated species. *J. Biol. Chem.* 261, 14490-14495.

Stallwood, Y., Fisher, K.D., Gallimore, P.H. & Mautner, V. (2000) Neutralisation of adenovirus infectivity by ascitic fluid from ovarian cancer patients. *Gene Ther.* 7, 637-643.

Stegman, L.D., Zheng, H., Neal, E.R.*, et al.* (1998) Induction of cytotoxic oxidative stress by D-alanine in brain tumor cells expressing Rhodotorula gracilis D-amino acid oxidase: a cancer gene therapy strategy. *Hum. Gene Ther.* 9, 185-193.

Stribbling, S.M., Friedlos, F., Martin, J.*, et al.* (2000) Regressions of established breast carcinoma xenografts by carboxypeptidase G2 suicide gene therapy and the prodrug CMDA are due to a bystander effect. *Hum. Gene Ther.* 11, 285-292.

Sulaiman, H., Dawson, L., Laurent, G.J., Bellingan, G.J. & Herrick, S.E. (2002) Role of plasminogen activators in peritoneal adhesion formation. *Biochem. Soc. Trans.* 30, 126-131.

Sumida, S.M., Truitt, D.M., Lemckert, A.A.*, et al.* (2005) Neutralizing antibodies to adenovirus serotype 5 vaccine vectors are directed primarily against the adenovirus hexon protein. *J. Immunol.* 174, 7179-7185.

Suomalainen, M., Nakano, M.Y., Keller, S., Boucke, K., Stidwill, R.P. & Greber, U.F. (1999) Microtubule-dependent plus- and minus end-directed motilities are competing processes for nuclear targeting of adenovirus. *J. Cell Biol.* 144, 657-672.

Swart, A.M. & Parmar, M.K. (2005) Observations on the interpretation of clinical trials in early ovarian cancer. *J. Clin. Oncol.* 23, 927; author reply 937-928.

Thomson, A.H., Vasey, P.A., Murray, L.S.*, et al.* (1999) Population pharmacokinetics in phase I drug development: a phase I study of PK1 in patients with solid tumours. *Br. J. Cancer* 81, 99-107.

Trimbos, J.B., Parmar, M., Vergote, I.*, et al.* (2003) International Collaborative Ovarian Neoplasm trial 1 and Adjuvant ChemoTherapy In Ovarian Neoplasm trial: two parallel randomized phase III trials of adjuvant chemotherapy in patients with early-stage ovarian carcinoma. *J. Natl. Cancer Inst.* 95, 105-112.

Trotman, L.C., Mosberger, N., Fornerod, M., Stidwill, R.P. & Greber, U.F. (2001) Import of adenovirus DNA involves the nuclear pore complex receptor CAN/Nup214 and histone H1. *Nat Cell Biol* 3, 1092-1100.

van der Burg, M.E., van Lent, M., Buyse, M.*, et al.* (1995) The effect of debulking surgery after induction chemotherapy on the prognosis in advanced epithelial ovarian cancer. Gynecological

Cancer Cooperative Group of the European Organization for Research and Treatment of Cancer. *N. Engl. J. Med.* 332, 629-634.

Vanhoefer, U., Tewes, M., Rojo, F.*, et al.* (2004) Phase I study of the humanized antiepidermal growth factor receptor monoclonal antibody EMD72000 in patients with advanced solid tumors that express the epidermal growth factor receptor. *J. Clin. Oncol.* 22, 175-184.

Varghese, R., Mikyas, Y., Stewart, P.L. & Ralston, R. (2004) Postentry neutralization of adenovirus type 5 by an antihexon antibody. *J. Virol.* 78, 12320-12332.

Vasey, P.A., Shulman, L.N., Campos, S.*, et al.* (2002) Phase I trial of intraperitoneal injection of the E1B-55-kd-gene-deleted adenovirus ONYX-015 (dl1520) given on days 1 through 5 every 3 weeks in patients with recurrent/refractory epithelial ovarian cancer. *J. Clin. Oncol.* 20, 1562-1569.

Verco, S.J., Peers, E.M., Brown, C.B., Rodgers, K.E., Roda, N. & diZerega, G. (2000) Development of a novel glucose polymer solution (icodextrin) for adhesion prevention: pre-clinical studies. *Hum. Reprod.* 15, 1764-1772.

Vine, M.F., Calingaert, B., Berchuck, A. & Schildkraut, J.M. (2003) Characterization of prediagnostic symptoms among primary epithelial ovarian cancer cases and controls. *Gynecol. Oncol.* 90, 75-82.

Vrudhula, V.M., Svensson, H.P., Kennedy, K.A., Senter, P.D. & Wallace, P.M. (1993) Antitumor activities of a cephalosporin prodrug in combination with monoclonal antibody-beta-lactamase conjugates. *Bioconjug. Chem.* 4, 334-340.

Wada, I., Lai, W.H., Posner, B.I. & Bergeron, J.J. (1992) Association of the tyrosine phosphorylated epidermal growth factor receptor with a 55-kD tyrosine phosphorylated protein at the cell surface and in endosomes. *J. Cell Biol.* 116, 321-330.

Wang, H.G., Draetta, G. & Moran, E. (1991) E1A induces phosphorylation of the retinoblastoma protein independently of direct physical association between the E1A and retinoblastoma products. *Mol. Cell. Biol.* 11, 4253-4265.

Wang, X. & Bergelson, J.M. (1999) Coxsackievirus and adenovirus receptor cytoplasmic and transmembrane domains are not essential for coxsackievirus and adenovirus infection. *J. Virol.* 73, 2559-2562.

Watkins, S.J., Mesyanzhinov, V.V., Kurochkina, L.P. & Hawkins, R.E. (1997) The 'adenobody' approach to viral targeting: specific and enhanced adenoviral gene delivery. *Gene Ther.* 4, 1004-1012.

Wen, X., Wu, Q.P., Lu, Y.*, et al.* (2001) Poly(ethylene glycol)-conjugated anti-EGF receptor antibody C225 with radiometal chelator attached to the termini of polymer chains. *Bioconjug. Chem.* 12, 545-553.

Wesseling, J.G., Bosma, P.J., Krasnykh, V.*, et al.* (2001) Improved gene transfer efficiency to primary and established human pancreatic carcinoma target cells via epidermal growth factor receptor and integrin-targeted adenoviral vectors. *Gene Ther.* 8, 969-976.

Weyel, D., Sedlacek, H.H., Muller, R. & Brusselbach, S. (2000) Secreted human beta-glucuronidase: a novel tool for gene-directed enzyme prodrug therapy. *Gene Ther.* 7, 224-231.

Whyte, P., Williamson, N.M. & Harlow, E. (1989) Cellular targets for transformation by the adenovirus E1A proteins. *Cell* 56, 67-75.

Wickham, T.J., Mathias, P., Cheresh, D.A. & Nemerow, G.R. (1993) Integrins alpha v beta 3 and alpha v beta 5 promote adenovirus internalization but not virus attachment. *Cell* 73, 309-319.

Wierdl, M., Morton, C.L., Weeks, J.K., Danks, M.K., Harris, L.C. & Potter, P.M. (2001) Sensitization of human tumor cells to CPT-11 via adenoviral-mediated delivery of a rabbit liver carboxylesterase. *Cancer Res.* 61, 5078-5082.

Wiethoff, C.M., Wodrich, H., Gerace, L. & Nemerow, G.R. (2005) Adenovirus protein VI mediates membrane disruption following capsid disassembly. *J. Virol.* 79, 1992-2000.

Winkler, M.E., Bringman, T. & Marks, B.J. (1986) The purification of fully active recombinant transforming growth factor alpha produced in Escherichia coli. *J. Biol. Chem.* 261, 13838-13843.

Winkler, M.E., O'Connor, L., Winget, M. & Fendly, B. (1989) Epidermal growth factor and transforming growth factor alpha bind differently to the epidermal growth factor receptor. *Biochemistry (Mosc).* 28, 6373-6378.

Wolf, J.K., Bodurka, D.C., Gano, J.B.*, et al.* (2004) A phase I study of Adp53 (INGN 201; ADVEXIN) for patients with platinum- and paclitaxel-resistant epithelial ovarian cancer. *Gynecol. Oncol.* 94, 442-448.

Working, P.K., Newman, M.S., Sullivan, T. & Yarrington, J. (1999) Reduction of the cardiotoxicity of doxorubicin in rabbits and dogs by encapsulation in long-circulating, pegylated liposomes. *J. Pharmacol. Exp. Ther.* 289, 1128-1133.

Worthylake, R., Opresko, L.K. & Wiley, H.S. (1999) ErbB-2 amplification inhibits down-regulation and induces constitutive activation of both ErbB-2 and epidermal growth factor receptors. *J. Biol. Chem.* 274, 8865-8874.

Yamashiro, D.J. & Maxfield, F.R. (1987) Acidification of morphologically distinct endosomes in mutant and wild-type Chinese hamster ovary cells. *J. Cell Biol.* 105, 2723-2733.

Yan, Z., Zhang, Y., Duan, D. & Engelhardt, J.F. (2000) Trans-splicing vectors expand the utility of adeno-associated virus for gene therapy. *Proc. Natl. Acad. Sci. U. S. A.* 97, 6716-6721.

Yew, P.R. & Berk, A.J. (1992) Inhibition of p53 transactivation required for transformation by adenovirus early 1B protein. *Nature* 357, 82-85.

Yoon, S.S., Carroll, N.M., Chiocca, E.A. & Tanabe, K.K. (1998) Cancer gene therapy using a replication-competent herpes simplex virus type 1 vector. *Ann. Surg.* 228, 366-374.

Young, R.C., Walton, L.A., Ellenberg, S.S.*, et al.* (1990) Adjuvant therapy in stage I and stage II epithelial ovarian cancer. Results of two prospective randomized trials. *N. Engl. J. Med.* 322, 1021-1027.

Zeimet, A.G. & Marth, C. (2003) Why did p53 gene therapy fail in ovarian cancer? *Lancet Oncol* 4, 415-422.

Zeimet, A.G., Muller-Holzner, E., Schuler, A.*, et al.* (2002) Determination of molecules regulating gene delivery using adenoviral vectors in ovarian carcinomas. *Gene Ther.* 9, 1093-1100.

Zerial, M. & McBride, H. (2001) Rab proteins as membrane organizers. *Nat Rev Mol Cell Biol* 2, 107-117.

Zhu, H.J., Iaria, J., Orchard, S., Walker, F. & Burgess, A.W. (2003) Epidermal growth factor receptor: association of extracellular domain negatively regulates intracellular kinase activation in the absence of ligand. *Growth Factors* 21, 15-30.

9 Appendix

9.1 Unmodified human TGF-α protein sequence

VVSHFNDCPD SHTQFCFHGT CRFLVQEDKP ACVCHSGYVG ARCEHADLLA

Val-Val-Ser-His-Phe-Asn-Asp-Cys-Pro-Asp-Ser-His-Thr-Gln-Phe-Cys-Phe-His-Gly-Thr-Cys-Arg-Phe-Leu-Val-Gln-Glu-Asp-**Lys**-Pro-Ala-Cys-Val-Cys-His-Ser-Gly-Tyr-Val-Gly-Ala-Arg-Cys-Glu-His-Ala-Asp-Leu-Leu-Ala

9.2 Human EGF protein sequence

NSDSECPLSH DGYCLHDGVC MYIEALDKYA CNCVVGYIGE RCQYRDLKWW ELR

Asn-Ser-Asp-Ser-Glu-Cys-Pro-Leu-Ser-His-Asp-Gly-Tyr-Cys-Leu-His-Asp-Gly-Val-Cys-Met-Tyr-Ile-Glu-Ala-Leu-Asp-**Lys**-Tyr-Ala-Cys-Asn-Cys-Val-Val-Gly-Tyr-Ile-Gly-Glu-Arg-Cys-Gln-Tyr-Arg-Asp-Leu-**Lys**-Trp-Trp-Glu-Leu-Arg

9.3 Murine EGF protein sequence

NSYPGCPSSY DGYCLNGGVC MHIESLDSYT CNCVIGYSGD RCQTRDLRWW ELR

Asn-Ser-Tyr-Pro-Gly-Cys-Pro-Ser-Ser-Tyr-Asp-Gly-Tyr-Cys-Leu-Asn-Gly-Gly-Val-Cys-Met-His-Ile-Glu-Ser-Leu-Asp-Ser-Tyr-Thr-Cys-Asn-Cys-Val-Ile-Gly-Tyr-Ser-Gly-Asp-Arg-Cys-Gln-Thr-Arg-Asp-Leu-Arg-Trp-Trp-Glu-Leu-Arg

9.4 Post-mortem findings from survival experiment

At time of sacrifice all mice were dissected, tumours removed and frozen and livers fixed with 4% formaldehyde in PBS prior to paraffin embedding and sectioning. Details of findings at post mortem examination were recorded and are listed below in tables. The animal handlers and those performing the experiment were blinded to treatment groups, and these had been coded 1-5 by an independent person, not involved with the experiment, and the codes kept in a sealed envelope. Treatment groups were unblinded at the end of the experiment.

Treatment group	*Treatment*
1	Unmodified Ad5 WT
2	PBS control
3	Cetuximab-pcv Ad5WT
4	pcv Ad5 WT
5	EGF-pcv Ad5WT

Treatment	Cage	Mouse	Date implanted	Date sacrificed	Days survival	Adhesion score (1-4)	Why sacrificed	Findings at laparotomy
1	a	i	20/03/2006	15/05/2006	56	1	jaundiced wt loss	Tumour obstructing gall bladder/bile duct. Dilated gall bladder. Tumour under liver and around stomach. Implantation site tumour. Mild adhesions from liver to bowel.
1	a	ii	20/03/2006	26/04/2006	37	1	injection site tumour at risk of eroding. Wt loss	Mild adhesions on bowel and liver. Injection site tumour. Liver shrivelled and misshapen. Injection site tumour. Small tumour deposits on bowel mesentery.
1	a	iii	20/03/2006	23/04/2006	34	4	Very distended abdomen. Loops of bowel visible.	Abnormal small ?cirrhotic liver. Very dense adhesions from liver to peritoneum and diaphragm. Very difficult to dissect off. Bowel one matt of adhesions with distended loops. Probable partial small bowel obstruction. Unable to find any tumour, but bowel very difficult to dissect from mesentery, other loops or peritoneum.
1	a	iv	20/03/2006	19/07/2006	121	1	end of expt	Mild filmy adhesions of liver to stomach. Blunted edges to liver. No tumour.
1	a	v	20/03/2006	19/07/2006	121	1	end of expt	Tumour on abdominal wall ? Implantation site. One lobe of liver adherent to upper pole of kidney. No other tumour or adhesions.
1	a	vi	20/03/2006	19/05/2006	60	2	Implantation tumour & wt loss	multiple adhesions throughout abdominal cavity, especially of liver to bowel. Abnormal liver - ? Cirrhotic. Trace clear ascites. Bowel not obstructed. Implantation site tumour. Small nodules under stomach and larger nodule under liver.
1	b	i	20/03/2006	19/05/2006	60	1	implantation site tumour & wt loss	Mild filmy adhesions. Liver grossly normal. Implantation site tumour and moderate nodule from omentum.
1	b	ii	20/03/2006	19/07/2006	121	0	end of expt	No adhesions, no tumour.
1	b	iii	20/03/2006	26/04/2006	34	4	very distended abdominal. Loops of bowel visible.	Severe adhesions with matt of small bowel and dilated bowel loops. No visible tumour, even when bowel loops dissected.
1	b	iv	20/03/2006	24/05/2006	65	1	anaemic, implantation tumour, wt loss	Implantation tumour. Small omental tumour. Implant in porta hepatis. Grossly abnormal liver architecture. Adhesions on liver surface. Small seedlings on small bowel mesentery (few). Clinically anaemic.
1	b	v	20/03/2006	19/05/2006	60	1	implantation tumour	Implantation tumour. Small omental tumour and another under spleen. Fine filmy adhesions in pelvis and thickening of peritoneum. Liver grossly normal.
1	b	vi	20/03/2006	15/05/2006	56	0	implantation site tumour & wt loss	Implantation site tumour. Further tumour seedlings on peritoneum and tumour in omentum and nodules under liver. No gross adhesions or liver abnormality.

Treatment	Cage	Mouse	Date implanted	Date sacrificed	Days survival	Adhesion score (1-4)	Why sacrificed	Findings at laparotomy
2	a	i	20/03/2006	23/04/2006	34	0	obvious ascites and some reduced movement/activity.	1ml of bloody ascites. large masses of tumour under and above stomach. Seedlings along whole bowel mesentery and on ovaries.
2	a	ii	20/03/2006	19/07/2006	121	0	end of expt	Nil of note
2	a	iii	20/03/2006	22/04/2006	33	?	Died over night. Developing mild ascites day before	?
2	a	iv	20/03/2006	23/04/2006	34	0	obvious ascites and some reduced movement/activity.	3.5 ml bloody ascites. Large tumour masses on greater and lesser curvatures of stomach and on spleen. Large tumour seedlings throughout bowel mesentery.
2	a	v	20/03/2006	18/04/2006	29	0	obvious ascites and some reduced movement/activity. Although weight gain, looking quite thin in body	3ml bloody ascites. Large mass of tumour around transverse colon, lesser curvature of stomach, spleen and under liver. SB mesentery a curtain of small tumour nodules. More small nodules on retroperitoneum and down onto ovaries.
2	a	vi	20/03/2006	19/07/2006	121	0	end of expt	Nil of note
2	b	i	20/03/2006	26/04/2006	37	0	ascites & reduced movement, anaemia	3ml bloody ascites. Tumour on greater and lesser curvatures of stomach, around spleen, under liver and on bowel mesentery.
2	b	ii	20/03/2006	23/04/2006	34	0	ascites and some reduced movement/activity. Anaemic.	2ml bloody ascites. Large tumour masses on greater and lesser curvatures of stomach and on spleen. Large tumour seedlings throughout bowel mesentery.
2	b	iii	20/03/2006	28/04/2006	39	0	wt loss. Lumps of tumour visible in abdominal.	Large tumour under stomach. Tumour around stomach, under liver and around spleen. Some retroperitoneal tumour and mass on bladder. No ascites.
2	b	iv	20/03/2006	26/04/2006	37	0	wt loss. Lumps of tumour visible in abdominal.	Tumour in omentum and under liver. Minimal seedlings in bowel mesentery. Jaundiced and dehydrated.
2	b	v	20/03/2006	24/04/2006	35	0	ascites recent rapid wt gain due to ascites	0.5ml bloody ascites. Injection site tumour on parietal peritoneum. Tumour on lesser and greater curvatures of stomach, under liver, spleen and diaphragm. Little on bowel mesentery.
2	b	vi	20/03/2006	19/07/2006	121	0	end of expt	Nil of note

Treatment	Cage	Mouse	Date implanted	Date sacrificed	Days survival	Adhesion score (1-4)	Why sacrificed	Findings at laparotomy
3	a	i	20/03/2006	19/07/2006	121	0	end of expt	Nil of note
3	a	ii	20/03/2006	16/06/2006	88	0	wt loss, thin poor movement	Large tumour mass behind bladder, stuck to sacrum. Another large tumour on lesser curvature of stomach.
3	a	iii	20/03/2006	12/05/2006	53	0	implantation site tumour at risk of erosion	Nil else abnormal. No other tumour. Liver normal. No ascites.
3	a	iv	20/03/2006	19/05/2006	60	0	implantation site tumour & some wt loss	Implantation site tumour. Nil else abnormal.
3	a	v	20/03/2006	16/06/2006	88	0	Poor movement and weight loss	One large tumour attached to the rectum. Tumour between liver and stomach and stomach and spleen. Nodules on diaphragm and tiny nodules on small bowel mesentery.
3	a	vi	20/03/2006	06/09/2006	81	0	visible peritoneal deposits. Slightly hunched	Peritoneal deposits (not implantation site) tumour on surface of liver and subdiaphragmatic. Small seedlings on stomach. Trace of straw coloured ascites (0.5 ml).
3	b	i	20/03/2006	26/07/2006	67	1	anaemia and bloody ascites. Sudden wt gain.	2 ml bloody ascites. Large omental tumour and sub hepatic tumour. Sub-diaphragmatic deposits and multiple small deposits on parietal peritoneum and on small bowel mesentery.
3	b	ii	20/03/2006	05/05/2006	60	0	implantation site tumour	Implantation site tumour. Further nodule on omentum and under liver. Tiny seedlings around left ureter.
3	b	iii	20/03/2006	19/05/2007	46	0	implantation site tumour at risk of erosion. Otherwise really well.	Implantation site tumour. No other tumour visible. Liver normal. No adhesions. No splenomegaly. No ascites.
3	b	iv	20/03/2006	19/07/2006	121	0	end of expt	Nil of note
3	b	v	20/03/2006	19/07/2006	121	0	end of expt	Large omental tumour, one small i.p. wall nodule. Normal liver, no adhesions
3	b	vi	20/03/2006	12/05/2006	53	0	wt loss. Poor condition of skin.	Tiny implantation site tumour. Single tumour nodule on omentum. Nil else abnormal. No obvious cause for wt loss seen.

Treatment	Cage	Mouse	Date implanted	Date sacrificed	Days survival	Adhesion score (1-4)	Why sacrificed	Findings at laparotomy
4	a	i	20/03/2006	19/04/2006	30	0	obvious ascites and some reduced movement/activity.	3ml bloody ascites. Large mass of tumour around transverse colon, lesser curvature of stomach, spleen and under liver. Small bowel mesentery a curtain of small tumour nodules. More small nodules on retro peritoneum and down onto ovaries.
4	a	ii	20/03/2006	28/04/2006	39	1	wt loss	Filmy adhesions of liver to diaphragm. Splenomegaly. Large tumour nodule under stomach. Some nodules in mesentery.
4	a	iii	20/03/2006	16/05/2006	57	0	wt loss & poor condition of coat	Large tumour mass in bowel mesentery near iliocaecal junction. Another mass below stomach. Large nodule on left upper liver (diaphragmatic surface) and small nodules around porta hepatis
4	a	iv	20/03/2006	28/04/2006	39	0	skin lesions getting worse. Wt loss	Small tumour deposits under stomach and liver
4	a	v	20/03/2006	05/05/2006	46	0	wt loss. Poor movement due to implantation site tumour.	Large nodule under stomach and further tumour nodules under liver and next to spleen. Couple of small nodules on bowel. No adhesions. Liver grossly normal. Implantation site tumour.
4	a	vi	20/03/2006	05/05/2006	46	0	wt loss. Poor movement due to implantation site tumour.	Large implantation site tumour approx 7mm diameter. Tumour on greater and lesser curvatures of stomach and around spleen and under diaphragm. Few nodules on bowel mesentery. Grossly normal liver. No adhesions.
4	b	i	20/03/2006	28/04/2006	39	0	wt loss	Mass of tumour all around stomach in omentum. Slight splenomegaly. Tumour under liver.
4	b	ii	20/03/2006	16/05/2006	57	0	wt loss & poor condition of skin, tinge of jaundice	Large tumour mass in omentum and further tumour under liver, around spleen. Small nodules on ovaries and small bowel mesentery Small implantation site tumour.
4	b	iii	20/03/2006	19/05/2006	60	0	wt loss & implantation tumour - subdued	Large implantation tumour. Further tumour on bladder. Large masses in SB mesentery, under liver, and up under spleen. Grossly normal liver.
4	b	iv	20/03/2006	28/04/2006	46	0	moribund	Small implantation site tumour. Small amount of tumour around stomach and under liver and couple of small nodules on small bowe mesentery.
4	b	v	20/03/2006	19/05/2006	60	0	wt loss - subdued	Large mass of tumour in liver hilum and post to liver displacing it into abdominal. Moderate nodule from omentum and small implantation site tumour.
4	b	vi	20/03/2006	27/04/2006	38	0	signs of ascites developing	Implantation site tumour. Large tumour masses from greater and lesser curvatures of stomach, spleen and subdiaphragmatic. Multiple small nodules along length of small bowel mesentery. Small deposit on bladder. Nodules on diaphragm and on post abdominal wall. 2ml ascites - bloody.

Treatment	Cage	Mouse	Date implanted	Date sacrificed	Days survival	Adhesion score (1-4)	Why sacrificed	Findings at laparotomy
5	a	i	20/03/2006	18/05/2006	59	0	wt loss visible lumps in abdominal	Large tumour on omentum, beside spleen, lesser curvature of stomach, post peritoneum under liver and around left renal hilum, obstructing left renal vein. Further tumour on bladder, seedlings on peritoneum and nodule on liver.
5	a	ii	20/03/2006	05/07/2006	48	0	implantation site tumour at risk of erosion	Extraperitoneal implantation site tumour. One tiny tumour on omentum. Nil else. No ascites, adhesions, liver grossly normal.
5	a	iii	20/03/2006	29/06/2006	101	0	obvious ascites, prominent backbone, weight gain	Large tumour on ovary, lots of tiny nodules attached to gut mesentery and another tumour attached to small intestine. Large tumour in/on liver. Small nodules round stomach. Whole diaphragm taken as quite large nodules of tumour covering it. Approximately 2.5mls bloody ascites.
5	a	iv	20/03/2006	19/05/2006	60	0	implantation site tumour	Implantation site tumour. Tumour on omentum, nodule next to caecum.
5	a	v	20/03/2006	28/05/2006	69	0	wt loss, hunched and some reduced movement	Small parietal peritoneal tumour. Large subdiaphragmatic mass displacing liver caudally and eroding into liver and diaphragm.
5	a	vi	20/03/2006	28/05/2006	69	0	ascites, anaemia, hunched, reduced movement	omental tumour, small nodules on small bowel mesentery, parietal peritoneal implant. Large mass of tumour subdiaphragmatic eroding into upper liver.
5	b	i	20/03/2006	15/05/2006	56	0	wt loss implantation site tumour	Implantation site tumour. Small omental tumour and tumour under liver. Liver grossly normal. No ascites, no adhesions.
5	b	ii	20/03/2006	15/05/2006	56	0	Jaundice, wt loss	Large tumour in omentum and sub diaphragmatic between liver and duodenum obstructing bile duct. Tumour around spleen and lesser curvature of the stomach.
5	b	iii	20/03/2006	29/06/2006	101	0	Wt. loss, poor skin condition, looked hunched	Spleen very enlarged. Please see photos as never seem this before! One liver lobe attached to diaphragm, very red and clotted. One side looked white and could be tumour but not sure. This lump as a whole had been put in tube and frozen. No other tumour found.
5	b	iv	20/03/2006	05/07/2006	48	0	jaundice and weight loss	Tiny extraperitoneal implantation site tumour. Tumour nodule on omentum. Tiny tumour nodule on duodenum blocking bile duct. Dilated bile duct. Obstructive jaundice. Tiny spots of tumour on peritoneum of abdominal wall
5	b	v	20/03/2006	16/06/2006	88	0	ascites	Large tumour mass under diaphragm and under liver. Small nodules on SB mesentery. More tumour in omentum and on surface of liver. 1.5 ml bloody ascites.
5	b	vi	20/03/2006	19/07/2006	121	0	end of expt	Tumour attached to stomach and liver (8mm diameter). No adhesions, normal liver.

9.5 Publications arising from this work

The following papers have been or are due to be presented or published as a result of work carried out during this thesis. Also appended is a publication that has been submitted for publication (see section 9.5.4).

9.5.1 Publications in peer-reviewed journals

Kehoe S, and Morrison J. (2005) Current management of ovarian carcinoma. *Therapy*, **2**(2): 275-286

Morrison, J. (2005) Advances in the understanding and treatment of ovarian cancer. *J Br Menopause Soc* 11, 66-71.

Morrison, J. & Kehoe, S. (2006) Key clinical trials in gynaecological oncology. *Eur. J. Surg. Oncol*. 32, 887-891.

9.5.2 Book chapters

Morrison, J., and MacKenzie, I.Z. Uterine fibroids. In: *The Abnormal Menstrual Cycle*. Editors: Rees M, Hope S and Ravnikar V. Taylor and Francis. 2005: p 81-95

Morrison J, and Kerr D. Virus-directed suicide gene therapy. In: *Cancer Therapy: Molecular Targets in Tumor-Host Interactions*. Editor: Weber G. Horizon Scientific Press 2005: p363-390

Morrison, J., and Kehoe, S. Gynaecological Cancer. In: *Women over 70; when normative treatment plans do not apply.* Editor: Rees, M. Informa Healthcare. (In press)

9.5.3 Abstracts presented at scientific conferences

9.5.3.1 Oral

Morrison, J., Briggs, S.S., Hale, A., Green, N., Herbert, C., Fisher, K.D., Kehoe, S. and Seymour, L.W. Retargeting adenovirus gene therapy via the epidermal growth factor receptor. British Society of Gynaecological Oncology, Nov, 2005

Morrison, J., Briggs, S.S., Hale, A., Green, N., Herbert, C., Fisher, K.D., Kehoe, S. and Seymour, L.W. Retargeting adenovirus gene therapy via the epidermal growth factor receptor. Blair-Bell Competition Meeting, Royal College of Obstetricians and Gynaecologists, Nov, 2005

9.5.3.2 Poster

Morrison, J., Stevenson, M., Briggs, S.S., Hale, A., Bazan-Peregrino, M., Fisher, K.D., Kehoe, S. and Seymour, L.W. Development of EGFR-positive, Coxsackie-adenovirus receptor negative cell lines to investigate retargeting of adenoviral gene therapy. British Society for Gene Therapy Annual Meeting, Manchester 2005.

Briggs, S.S., Morrison, J., Phipps, S., Ulbrich, K., Subr, V., Fisher, K.D., Seymour, L.W. Synthesis and characterization of EGF modified poly[N-(2-hydroxypropyl) methacrylamide] copolymers for retargeting adenoviral vectors. British Society for Gene Therapy Annual Meeting, Manchester 2005.

Morrison, J., Briggs, S.S., Hale, A., Green, N., Herbert, C., Fisher, K.D., Kehoe, S. and Seymour, L.W. Retargeting adenovirus gene therapy via the epidermal growth factor receptor. European Society of Gene Therapy, Prague, Oct 2005.

Morrison, J., Briggs, S.S., Hale, A., Green, N., Phipps, S.L., Fisher, K.D., Kehoe, S. and Seymour, L.W. Retargeting adenovirus gene therapy via the epidermal growth factor receptor. British Society for Gene Therapy, London, Mar 2006.

9.5.4 Paper submitted for publication

Improving virotherapy for ovarian cancer using adenovirus cloaked with polymers and retargeted to the epidermal growth factor receptor

Jo Morrison[1], Simon Briggs[2], Nicola Green[3], Kerry Fisher[2], Karel Ulbrich[4], Sean Kehoe[1] & Leonard Seymour[2]

[1]Nuffield Department of Obstetrics and Gynaecology, John Radcliffe Hospital, Headington, Oxford, OX3 9DU
[2]Department of Clinical Pharmacology, Radcliffe Infirmary, Oxford, OX2 6HE
[3]Hybrid Systems Ltd, Cherwell Innovation Centre, Heyford Park, Upper Heyford, Oxfordshire, OX25 5HD
[4]Institute of Macromolecular Chemistry, Academy of Sciences of the Czech Republic, Prague 6, 16206, Czech Republic

Correspondence should be addressed to Jo Morrison (jo.morrison@obs-gyn.ox.ac.uk)

Adenovirus gene therapy for intraperitoneal cancer is limited in clinical trials by low tumor cell transduction efficiency and development of adhesions. We have shown previously that normal virus tropism can be ablated by coating the virus with multivalent reactive polymers based on poly[N-(2-hydroxypropyl)methacrylamide] (pHPMA)[1]. Here, murine epidermal growth factor (mEGF) was pre-conjugated to pHPMA and the resulting mEGF-polymer coated adenovirus (mEGF-pc-virus) lost its normal tropism and selectively transduced cells bearing the EGF receptor (EGFR). Receptor-specificity was shown by EGFR blockade. In a peritoneal xenograft model of human ovarian cancer, the oncolytic activity of wild type adenovirus type 5 (Ad5) was retained following mEGF polymer coating and retargeting, and adhesion formation was decreased compared with unmodified virus. Thus, mEGF-pc-virus may improve adenoviral cancer gene therapy by targeting transduction to cancer cells and enabling use of higher doses by decreasing toxicity, two areas critical to the success of this approach.

Intraperitoneal therapy for ovarian cancer provides the opportunity to treat tumor cells with high levels of therapeutic agents whilst minimizing systemic exposure. The concept is particularly attractive for gene therapy, whereby viruses may be applied regionally to infect cancer cells efficiently and selectively. However, promising pre-clinical trials of intraperitoneal adenovirus gene therapy have not been replicated in patients. A recent multicentre phase II/III clinical trial of adenovirus mediated p53 gene supplementation was halted at interim analysis due to inadequate therapeutic benefit and complications in the treatment arm[2]. There are several factors that may be responsible for this poor clinical response, notably intraperitoneal toxicities such as bowel adhesions and obstruction that were also noted in the phase I clinical trial[3]. In addition the Coxsackie-adenovirus receptor (CAR) is expressed at only low levels in many epithelial ovarian tumors, potentially limiting effective transduction by Ad5[4]. We therefore set out to develop an adenovirus delivery system capable of more efficient infection of tumor cells, coupled with decreased unwanted toxicities arising through indiscriminate infection of non-target cells.

Soluble polymers based on N-(2-hydroxypropyl)methacrylamide (pHPMA) have been used to deliver doxorubicin in clinical trials[6]. Amino-reactive co-polymers of pHPMA have now been developed that are able to covalently coat the adenovirus capsid, shielding receptor-binding epitopes and providing steric protection from cell and antibody binding. Normal infection is thereby inhibited, although novel tropisms can be introduced by subsequent covalent linkage of specific ligands, e.g. bFGF[1]. Polymer coated adenovirus (pc-virus) displays improved pharmacokinetics and reduces hepatotoxicity when administered intravenously[7]; pc-virus may also give partial protection from neutralizing antibodies, which are found at similar levels in peritoneal fluid as in serum[8]. It is therefore feasible to consider using this technology to retarget pc-virus to infect cells via the epidermal growth factor receptor (EGFR), which is over-expressed by

many ovarian carcinomas[5]. Tumor-selective retargeting of pc-virus has not been attempted before, and efficacy in *in vivo* cancer models has not previously been demonstrated.

Murine EGF was dissolved in DMSO and pre-conjugated to pHPMA bearing reactive thiazolidone groups (pHPMA-TT) under anhydrous conditions via the N-terminal α-amino group (**Supplementary Fig. 1**). Amino acid analysis demonstrated that an average of 1.8 EGFR molecules were incorporated into each polymer, thereby accounting for 10% of the weight of mEGF-pHPMA . The resulting mEGF-pHPMA-TT retained 6.4 mol% of amino-reactive TT groups.

mEGF-pHPMA-TT and pHPMA-TT control were modified using biotin ethylenediamine to permit flow cytometric evaluation of the ability of conjugated mEGF to bind to cell surface EGFR. The polymer conjugates were incubated with EGFR-positive and -negative cells, and binding was detected with extravidin-R-phycoerythrin (PE). A significant shift in fluorescence was demonstrated in EGFR-positive, but not EGFR-negative cells using mEGF-pHPMA-biotin, while the mEGF-free control conjugate failed to bind either cell type. This indicates that mEGF still retains EGFR-binding ability following conjugation to pHPMA (**Fig. 1a**).

To determine whether pHPMA-conjugated mEGF retained the ability to stimulate EGFR tyrosine kinase activity; EGFR positive cells were stimulated for 30 min and analyzed by SDS-PAGE and western blotting for EGFR phosphotyrosine residues (**Fig. 1b**). mEGF-pHPMA and mEGF mediated equivalent EGFR phosphorylation , suggesting that polymer-conjugated mEGF retained its receptor-stimulating activity.

Following stimulation by its ligand, EGFR normally internalizes into endosomes in a process that can be visualized by immunocytochemistry and confocal microscopy. To assess whether polymer-conjugated mEGF retained the ability to promote internalization, EGFR distribution was evaluated during exposure of cells to mEGF and mEGF-pHPMA. After 60 min of exposure, EGFR had moved from the cell surface into perinuclear areas of the cells following incubation with both mEGF and mEGF-pHPMA-biotin (**Fig. 1c**). mEGF-pHPMA-biotin was visualized by labeling with Avidin-Texas red, and co-localization of EGFR and mEGF-pHPMA-biotin was demonstrated in peri-nuclear areas. Taken together these data suggest that mEGF-pHPMA is able to bind specifically to EGFR-positive cells; can stimulate EGFR tyrosine kinase activity and internalization; and remains in the same endosomal compartment as EGFR once inside the cell.

To assess whether EGFR retargeting supported a permissive infection of adenovirus, EGFR-negative, CAR-negative cells based on the murine fibroblast cell line A9 were stably transduced with the human EGFR (**Supplementary Fig. 2**). Transduction activity using tropism-ablated pc-virus was reduced compared to the unmodified virus control in both parental A9 cells and EGFR-expressing A9 cells (A9-EGFR). In contrast coating virus with mEGF-pHPMA significantly enhanced transduction of A9-EGFR cells, but not the parental EGFR-negative A9 cells (**Fig. 2a**). Pre-incubation with an antibody known to block EGF binding could inhibit mEGF-pc-virus transduction of A9-EGFR cells (**Fig. 2b**). Using an A9-based cell line stably transfected with human chromosome 21, which expresses CAR (A9-CAR) as a control, the same EGF-blocking antibody had no significant effect on A9-CAR cell transduction with either virus or mEGF-pc-virus (**Fig. 2b**). These data demonstrate the EGFR-specificity of transduction using mEGF-pc-virus. In a range of EGFR positive cell lines, mainly of ovarian origin, pc-virus achieved only low levels of transduction (using a luciferase reporter), whereas mEGF-pc-virus transduction levels were high, in some cases above that of unmodified virus (**Fig 2c**). Cellular EGFR levels were measured using a commercial ELISA (**Supplementary Fig. 3a**) and luciferase expression levels were directly proportional to cellular EGFR levels for mEGF-pcv, but not unmodified AdCMV-Luc $_{\Delta E1}$ (**Supplementary Fig. 3b**). IGROV-1 cells had a slightly higher than expected level of luciferase activity following transduction with mEGF-pc-virus than would be predicted from their EGFR level, possibly reflecting its unusually high CAR levels (**Supplementary Fig. 4**). Thus, transduction of IGROV-1 cells probably represents a mixture of EGFR-mediated uptake and some residual CAR mediated uptake, which was 90-95% abrogated using these coating conditions. Inhibition of CAR-mediated uptake with an anti-CAR antibody or excess free Ad5 fiber protein (xs knob) was able to significantly reduce luciferase expression of unmodified virus in A431 cells. However, CAR blockade had no significant inhibitory effect on mEGF-pc-virus transduction (**Fig. 2d**). Taken together all of these data indicate that mEGF-pHPMA is able to successfully retarget adenovirus via the EGFR in vitro and that the majority of CAR-mediated uptake is inhibited. Importantly, measuring virus

uptake by quantitative PCR (QPCR), the specific activity of each virus particle was similar for adenovirus coated with mEGF-pc-virus compared with unmodified virus (**Supplementary Fig. 5**).

Adenovirus can be used in cancer therapy either to deliver a therapeutic transgene, as in the case of p53 replacement or suicide gene therapy, or as a directly oncolytic replication competent virus, during the lytic replication cycle. Adenoviruses have been genetically engineered to exploit mutations in cancer cells, for example, dl922-947 which replicates efficiently within cells lacking a functional retinoblastoma pathway[9]. However, wild type adenovirus is able to replicate more efficiently in cancer cells and has historically been used as an oncolytic virotherapy for cervical cancer [10, 11].

Wild type adenovirus (Ad5WT) was therefore used intraperitoneally (i.p.) as an oncolytic virotherapy in a murine xenograft model of human ovarian cancer. In a randomized and blinded pilot study MF1 nude mice (n=6) were implanted with SKOV-3 cells, and treated with three doses of 5 x 10^{10} viral particles (vp) of unmodified virus, pc-virus, mEGF-pc-virus and a phosphate buffered saline (PBS) control. Mice were all sacrificed at the same time (identified beforehand as the day when the first mouse required humane sacrifice due to tumor load). Tumors were meticulously dissected, weighed and level of adhesions scored using a 4 point scoring system. mEGF-pc-virus reduced tumor load compared with pc-virus and a PBS control. However, differences in tumor load did not reach statistical significance (**Supplementary Fig. 6a**). In an attempt to objectively quantify tumor load due to SKOV-3 cells, a method of quantitative polymerase chain reaction using primers to the human β-actin promoter sequence was developed. However, although these gave an indication of relative cell numbers (**Supplementary Fig. 6b**), the approach was limited by inefficient extraction of DNA from SKOV-3 tumor. Although numbers were small, it was noted that mice treated with unmodified Ad5WT had marked development of adhesions, evidence of sub-acute bowel obstruction and gross liver abnormalities. In contrast mice treated with mEGF-pc-virus had very few adhesions, no bowel obstructions and no obvious liver abnormalities.

Pilot data were used in an *a priori* power calculation for a survival experiment (see methods). A randomized and blinded survival study using 12 mice per group was performed. Mice were implanted with SKOV cells which stably expressed luciferase (a generous gift of Dr I. McNeish). Four days following implantation mice were treated with 5 x 10^{10} vp of Ad5WT, either unmodified, coated with pHPMA or mEGF-pHPMA, or a PBS control, and treatment repeated twice at 72 hour intervals. Accordingly the activity of unmodified virus and EGF-pc-virus were compared at equal numbers of virus particles, not equitoxic doses. *In vivo* bioluminescence was then measured weekly for five weeks to monitor tumor load. Importantly, *in vivo* bioluminescence enabled refinement of humane end-points, in addition to providing an on-going estimate of tumor burden. Mice were sacrificed and post-mortem examination performed; adhesions were scored and tumors dissected. Only mice which had shown evidence of initial tumor establishment were included in the analysis.

The primary end-point was survival (**Fig. 3b**). mEGF-pc-virus mediated a significantly longer median survival compared with pc-virus or PBS control (64.5 vs. 34 days for PBS; $P < 0.0001$; hazard ratio 0.1876; 95% confidence interval 0.004809 to 0.1007). It is noteworthy that some animals treated with mEGF-pc-virus and pc-virus were sacrificed because of subcutaneous tumor growth at the site of injection, and were free of macroscopic peritoneal disease at the time of death. Bioluminescence at 16 days post implantation demonstrated a significantly lower tumor load for unmodified virus and mEGF-pc-virus compared with either pc-virus or PBS control treatments (**Fig. 3a**) (150-fold lower median flux for mEGF-pc-virus vs. PBS) ($P < 0.001$). However, mice treated with unmodified virus were at increased risk of developing adhesions and evidence of sub-acute bowel obstruction, sufficient to require early sacrifice in 3 cases (**Supplementary Fig. 7**). The adhesion score in mice treated with unmodified Ad5WT was significantly increased compared with PBS control or mEGF-pcv, as determined by Chi-squared analysis (virus vs. mEGF-pcv; $P = 0.00039$) (**Fig. 3c**).

There was a linear inverse relationship between mean group flux levels at 16 days post implantation and median survival, indicating that bioluminescence, in this model, is a useful surrogate end-point (**Supplementary Fig. 8**).

We have therefore demonstrated that, by conjugation with mEGF-pHPMA, adenovirus can be significantly detargeted by shielding normal receptor-binding epitopes and that transduction can be retargeted to the

EGFR. *In vivo*, shielding normal adenovirus ligands and retargeting improves survival and tumor load, whilst offering significant amelioration of the toxic effects of unmodified adenovirus that have been observed in this *in vivo* study and in previous clinical trials. This should permit the use of higher doses of mEGF-pc-virus, further increasing efficacy without necessarily inducing toxicity.

Others have developed strategies to retarget adenovirus via the EGFR. Strategies for retargeting have included pre-incubation with adapter molecules, such as bifunctional antibodies[12, 13]and production of an adenovirus that secrets its own fiber-EGFR adapter molecule[14]. However, neither of these approaches efficiently detargets normal adenovirus tropism *in vivo*, offers protection from neutralizing antibodies or significantly reduces the innate immune response to the adenovirus capsid. In contrast the complete detargeting achieved by this approach[7], coupled with evidence that covalent capsid modification using polymers such as polyethylene glycol, may reduce the innate immune response to adenovirus, should lead to the development of a clinically valuable strategy[15].

Improving the efficacy of gene delivery and avoiding the toxic side effects caused by delivery vectors is critical to the future success of gene therapy. Chemically shielding and retargeting adenovirus using this polymer technology offers a widely applicable method for improving adenovirus gene delivery. Although EGFR is highly expressed on many cancer cells and is a target for other anti-cancer therapies, such as tyrosine kinase inhibitors[16] and monoclonal antibodies[17], this technology offers the potential to retarget to a variety of cancer-associated receptors. Furthermore, unlike genetically retargeted viruses, this polymer-based retargeting strategy avoids safety concerns arising from introducing new, heritable, virus tropisms and allows retargeting of any adenovirus payload without lengthy cloning strategies.

METHODS

Chemicals
All chemicals were purchased from either Arcos Organics (Leicester, UK) or Aldrich (Poole, UK) and used as received unless otherwise stated. Anhydrous methyl sulfoxide (DMSO) was purchased containing molecular sieves, acetone and ether were dried over anhydrous $MgSO_4$ and anhydrous dimethylformamide was redistilled from ninhydrin under vacuum.

Analysis
Standard ^{1}H NMR spectra were recorded on a Bruker AC300 (300 MHz) spectrometer using deuterated solvents and the residual solvent as the lock. Deuterated solvents were purchased from Sigma Aldrich. Standard ^{13}C NMR were recorded on a Bruker AV300 (75.5 MHz) spectrometer using the PENDANT sequence and the residual solvent used as the lock. Multiplicities abbreviated as follows: s = singlet, d = doublet, dd = doublet of doublets, t = triplet, q = quartet, m = multiplet, b = broad. Electrospray ionisation mass Spectrometry (ESI-MS) was performed on a VG ProSpec. Molecular weight characterization was carried out using a Shimadzu HPLC, (LC10-AD*VP* x 2, DGU-14A, SPD-10AV*VP*, SIL-10AD*VP*, SCL-10A*VP*) and a Superpose 6 GPC column, analyzed using LC Solutions software, and run using Dulbecco's phosphate buffered saline (PAA, Austria) at 0.5 mLmin^{-1}. Standards were kindly provided by Prof. Karel Ulbrich, Prague, and used to calibrate the column. Mw stated is relative to the N-(2-hydroxy)propylmethacrylamide standards used whose Mw was determined using multi-angle light scattering. Amino acid analysis was also performed on the Shimadzu HPLC by OPT derivitisation of conjugate hydrolysates and run using a water/acetonitrile gradient on a Phenomenex Luna C18(2) column. Standard concentration samples were prepared and used to generate standard curves for the individual amino acids. UV spectra were colleted using a Shimadzu UV-1601PC double beam UV spectrometer using quartz cuvettes.

Synthesis of N-(2-hydroxy)propylmethacrylamide (HPMA)
HPMA was synthesized as previously described [1]. Anhydrous $NaHCO_3$(11.2 g, 0.11 mol) was suspended in a solution of 1-aminopropan-2-ol (7.63 g, 0.1 mol) and a catalytic amount of catechol in DCM (30 mL). The suspension was cooled to 0° and a solution of methacryloyl chloride (10.6 g, 0.1 mmol) in DCM (15 mL) was added drop wise with vigorous stirring and maintaining the temperature of 0°C over a period of 30 minutes. The reaction was then stirred for a further 90 minutes at room temperature, Anhydrous Na_2SO_4 (5 g) was added to dry the solution. The reaction mixture was then filtered to remove the solid and the filtrate was reduced *in vacuo* by 50 %. The solution was then cooled to -20°C which induced crystallization. The solid white crystals were isolated and recrystalized from acetone, yielding a white crystalline solid. Yield 9.2 g, (65 %), m.p. 68 – 69°C. δ_H (300MHz) $CDCl_3$ 6.37 ppm (1H, b), 5.70 ppm (1H, s), 5.33 ppm (1H, t), 3.95 ppm (1H, m), 3.52 ppm (1H, dt), 3.17 ppm (1H, m) 2.91 ppm (1H, b), 2.00 ppm (3H, s), 1.20 ppm (3H, d) δ_C (125MHz) 123, 73, 55, 20, 19 m/z (ESI MS), 165 (M + Na).

Synthesis of [2-(2-methyl-acryloylamino)-acetylamino]-acetic acid (Ma-GG-OH)
To a solution of glycylglycine (5 g, 38 mmol) in 1M NaOH (40 mL) was added drop wise a solution of methacryloyl chloride (3.96 g, 37.8 mmol) in dioxane (10 mL) with a catalytic amount of octylpyrocatechol, with vigorous stirring and cooled to -10°C. The reaction was stirred for a further 90 minutes at room temperature. The solution was then acidified to pH 1 resulting in a white precipitate. The white precipitate was isolated and recrystalized from 50/50 EtOH and water. Yield 5.62 g (74%) δ_H (300MHz, $CDCl_3$) 5.73 (s, 1H), 5.47 (t, 1H), 3.97 (d, 4H), 1.88 (s, 3H) δ_C (100MHz, $CDCl_3$) 171.32, 169.85, 162.89, 140.26, 119.57, 51.24, 48.26, 20.19 m/z (ESI MS) 223 (M + Na).

Synthesis of Ma-GG-TT
Ma-GG-OH (4.00 g, 10 mmol) and 2-mercaptothiazoline (1.25 g, 10.5 mmol) were dissolved in 30 mL of freshly distilled DMF and the solution kept at –15 °C for 1 h. DCC (2.5 g, 12 mmol) was dissolved in 10 mL of DMF and the solution was cooled down to –15 °C for 1 h. Afterwards, both solutions were mixed, DMAP (~50 mg) was added and the mixture was kept at 0-5 °C for 24 h. The mixture was stirred 1 h at room temperature, acetic acid (50 µL) was added followed by stirring for further 1 h. DCU was filtered off, and the crude product was concentrated *in vacuo*. The crude product was dissolved in 40 mL of dry acetone and stirred at room temperature for 1 h. The residue of DCU was filtered off. Dry diethyl ether (40 mL) was added to the filtrate and the resulting solution was kept at 0-5 °C for crystallization. Ma-GG-TT was obtained as yellow crystals after recrystallization from ethyl acetate. Yield: 1.8 g (60 %). ^{1}H NMR (300 MHz, D_6DMSO): δ 1.87 (s, 3H), 3.44 (t, 2H), 3.78 d, 2H (Gly); 4.50(t, 2H) , 4.65 (d, 2H) , 5.37 (s, 1H) , 5.73 (s, 1H) , 8.14 (t, 1H), 8.20 (t, 1H).

Synthesis of pHPMA -TT
A degassed solution of Ma-GG-TT monomer (1.08 g, 3.6 mM), HPMA (3.58g, 25.2 mM) and AIBN (43.8 mg, 0.27 mM) in anhydrous DMSO (35 mL) was sealed in an Ace Tube and heated at 60 ºC for 6 hours. The polymer was isolated by precipitation in an anhydrous acetone: ether mixture (3:1). The solid was isolated by filtration and dried under high vacuum. Mw = 114,000 and content of reactive monomer was 8.68 mol% as determined by UV spectroscopy (ε = 10280, λ = 305nm).

Conjugation of mEGF to pHPMA-TT
5 mg mEGF was dissolved in 250 µL 18.2 MΩ water and added to 20 mg MeOPEG-OH (2000 Da) (250 µL 18.2 MΩ water). The sample was then lyophilized in 100 µL aliquots and stored at 4 °C. Polymer modification was carried out in polypropylene tubes at a concentration of 50 mg/mL polymer in anhydrous DMSO, to which was added the mEGF/PEG mixture in DMSO (500 µL DMSO for 5 mg mEGF). A catalytic amount of triethylamine or DMAP was also used. The reaction tube sealed and mixed on a blood wheel for 2 hours. The polymer conjugate was isolated by precipitation in 20 vol. acetone:ether (1:1). mEGF was incorporated at an efficiency of approximately 65% over 2 hours i.e. a ratio of mEGF:polymer = 3, an incorporation of 1.8 – 2 mEGF per polymer was achieved as determined by amino acid analysis of the purified conjugate.

Modification of pHPMA-TT polymers with biotin ethylenediamine
To a solution pHPMA -TT based polymer (5 mg/mL, 100 mM HEPES, pH 7.8) was added a 10 fold excess of biotin etheylenediamine to amino reactive groups and agitated over night. The solution was then purified on a PD10 Column (GE Healthcare) and lyophilized.

mEGF-pHPMA cell binding, internalization and EGFR stimulation
For assessment of mEGF-pHPMA cell binding, cells were incubated with biotinylated polymer then extravidin-R-PE (Sigma) for 40 min at 4ºC with appropriate PBS washes, fixed with 4% paraformaldehyde in PBS and analyzed by flow cytometry (FACSCalibur, BD Biosciences). Internalization of EGFR and mEGF-pHPMA was determined by stimulating serum starved cells on chamber slides with either 100nmol/L mEGF (Serotec, UK) or mEGF-pPHMA for 2-60 min. Cells were fixed, permeablised and labeled with mouse anti-EGFR (Santa Cruz) and anti-mouse-FITC (Vector, UK). Cells were mounted with Vectashied and nuclei counterstained with TO-PRO-3 (Molecular Probes) prior to confocal microscopy. EGFR phosphorylation was assayed by western blotting. Cells were stimulated with300ng/mL mEGF or a dilutional series of mEGF-pHPMA for 30 min and lysed (1x RIPA lysis buffer (Sigma) and Complete tablets (protease inhibitor cocktail, Roche Diagnostics)). Protein content of supernatant was determined using the Advanced protein assay reagent (Cytoskeleton). Equal amounts of protein (20 µg) were loaded onto a 7.5% SDS/PAGE gel for electrophoresis, blotted onto nitrocellulose paper, blocked with 5% non-fat milk in PBS, and developed with antibodies (goat anti-pEGFR (Santa Cruz); anti-goat-HRP (Vector, UK); rabbit anti-β actin (Sigma); anti-rabbit-HRP (Abcam)) and Lumiglo (Insight Biotechnologies, UK).

Coating adenovirus with pHPMA-TT
Polymers based on pHPMA-TT were dissolved in 18.2 MΩ water at 100 mg/mL and diluted with 18.2 MΩ water to give final polymer concentrations of 20 mg/mL or 5 mg/mL when added to virus. Virus stock in 40 µL storage buffer (50 mmol/L HEPES, pH 7.8, 0.1 g/L Ca and $MgCl_2$, 10% Glycerol)[1] was added to 10 µL polymer and incubated at room temperature for 40 min. Virus was then transferred onto ice and incubated at 4°C overnight.

Virus transduction

Adenovirus infection and expression was determined using a luciferase reporter virus (AdCMV-Luc$_{\Delta E1}$). Cells (were plated out 24 hours prior to transduction in DMEM (PAA) with 10% FBS (PAA). Cells were washed with PBS and AdCMV-Luc$_{\Delta E1}$ at 1,000 virus particles per cell added in DMEM supplemented with 2% FBS and incubated for 90 min, at which time virus was removed, cells washed, and DMEM with 10% FBS added to wells. All experiments were performed in triplicate. At 48 hours post transduction media was removed, cells washed and lysed with lysis buffer (Promega). Luciferin (Promega) was added to cell lysate and luminescence measured (Berthold luminometer).

***In vivo* model and bioluminescence**

All procedures were performed humanely under license according to Home Office regulations using appropriate analgesia and anesthesia. Nude mice (6-8 weeks old), house in environmentally enriched, individually ventilated cages, were implanted by intraperitoneal (ip) injection with 1 x 10^7 SKOV-ip-luc cells (courtesy of Dr Iain McNeish) in 500 µl PBS. After 96 hours mice were treated with $5e^{10}$ vp Ad5WT (unmodified, pcv, mEGF-pcv) and a PBS control by ip injection (in 500 µl PBS) and treatments repeated twice at 72 hour intervals. Treatment vials were randomized and blinded independently, so that experimenters were blinded to treatment groups. Mice were imaged weekly five times using a Xenogen IVIS imaging system. Under isoflurane general anesthetic, mice were injected ip with 50 mmol/L luciferin (100 µL), transferred to the imaging cabinet (37°C) for 4 min, and imaged supine and prone for 1 min (f/stop 1, medium binning). Exposure times for saturated images were reduced accordingly. Flux levels were measured and analyzed with Living Image Software. At post-mortem examination, mice were scored for adhesion formation: none; mild (few filmy adhesions); moderate (more extensive adhesions); severe (extensive adhesions with evidence of bowel matting, distension and sub-acute obstruction).

Statistical analysis

Virus transduction data were log transformed where appropriate and analyzed by ANOVA using GraphPad Prism4 software, with Bonferroni and Dunnet corrections for multiple analyses as required. Non-parametric data was analyzed by Kruskal-Wallis analysis with Dunn's multiple comparison test. Kaplan-Meier survival analysis was performed for the survival study using GraphPad Prism4 software. Chi-square analysis was used to compare adhesion scores using Excel software (Microsoft, USA).

ACKNOWLEGDEMENTS

This work was supported by the Oxfordshire Health Services Research Council, WellBeing of Women and Cancer Research UK JM was also supported by Macmillan Cancer Relief. We are very grateful to Dr Iain McNeish for the generous donation of the SKOV-luc cell line, Prof. Newbold for the A9-CAR cell line, and Dr Vivien Mautner for the AdCMV-Luc$_{\Delta E1}$ and anti-CAR antibody. We also thank Dr Shibani Nicum who performed preliminary work on EGF-polymer conjugates.

COMPETING INTERESTS STATEMENT

Leonard Seymour and Kerry Fisher are directors of Hybrid Systems Ltd, which owns intellectual property on the pHPMA virus coating technology. The other authors have no competing financial interests.

Figure 1

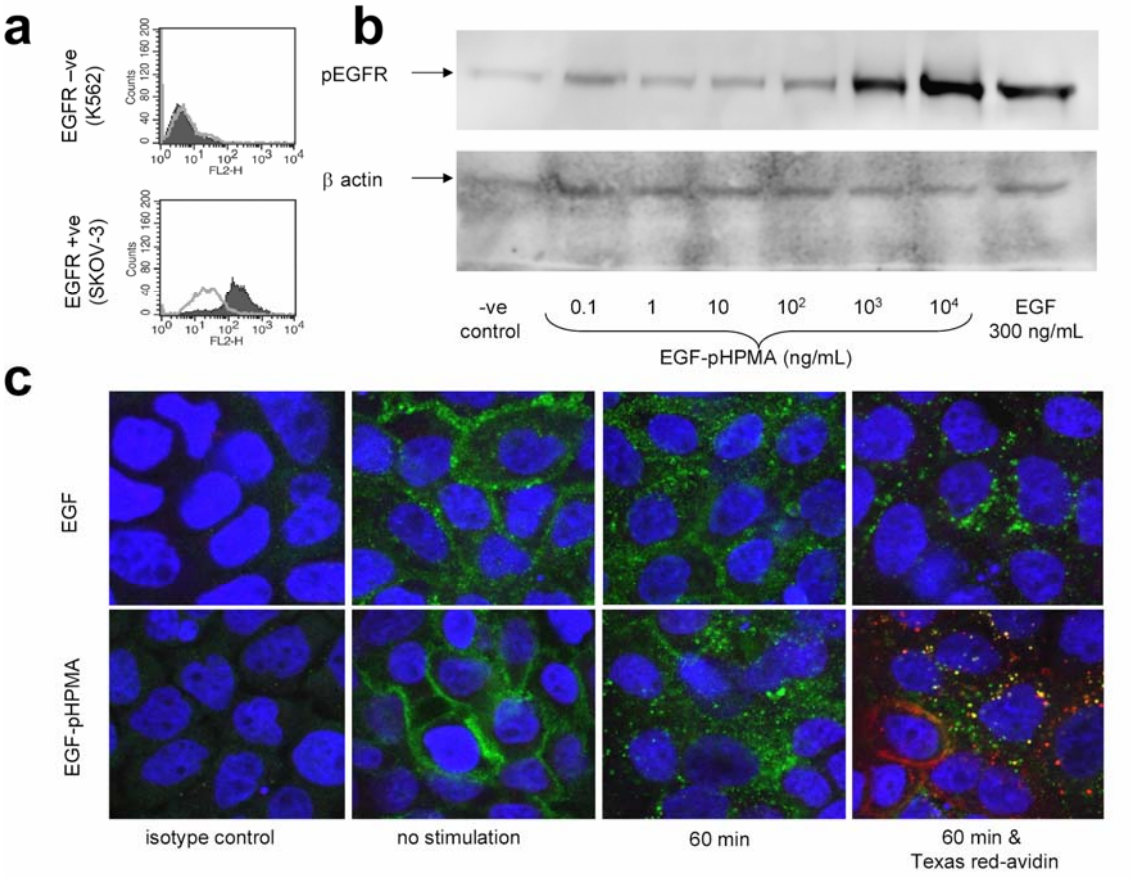


Figure 2

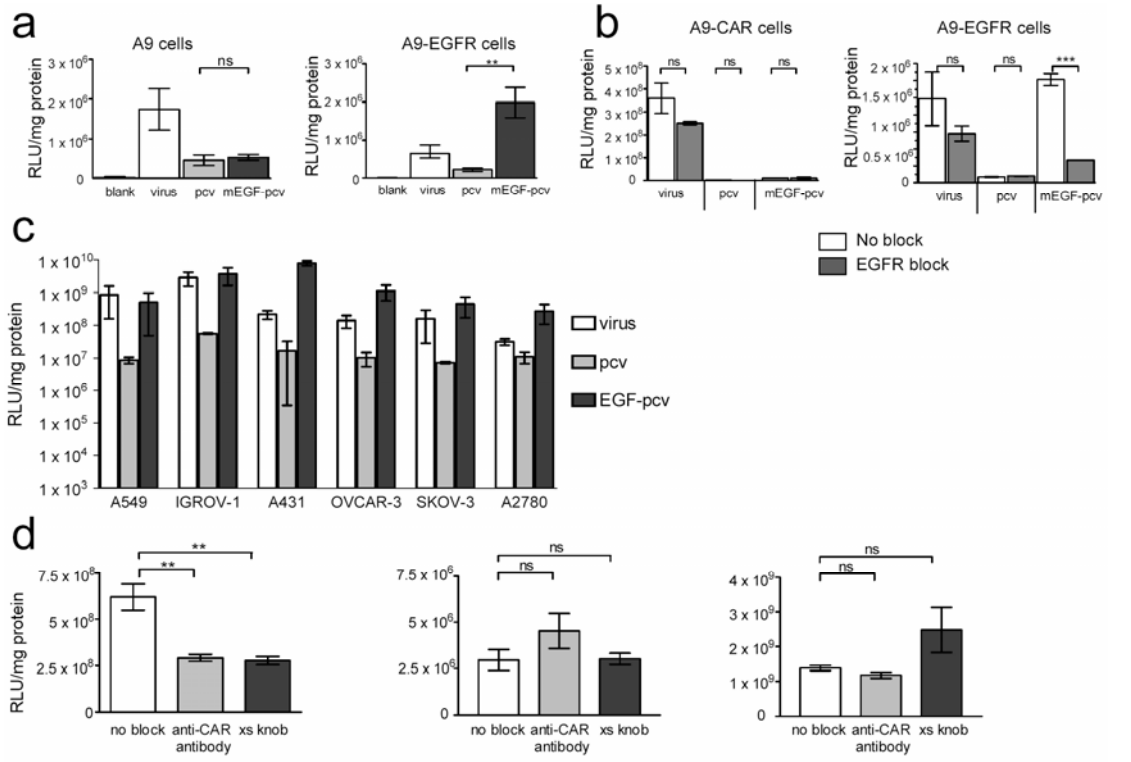
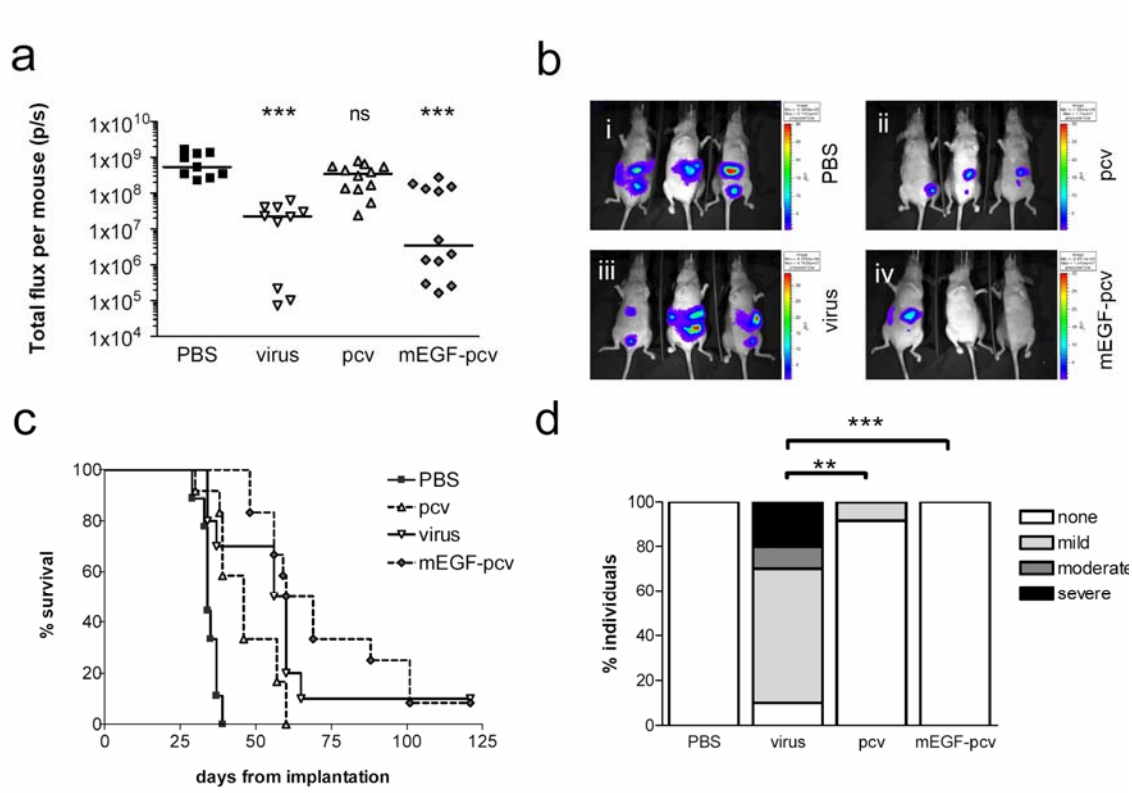
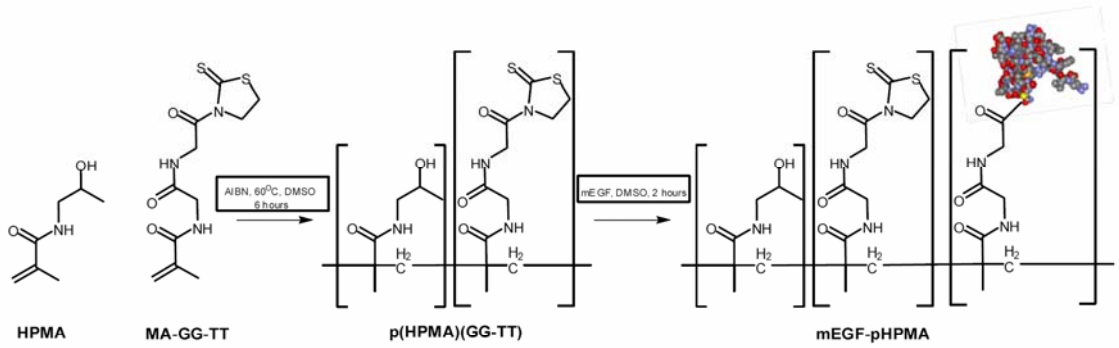
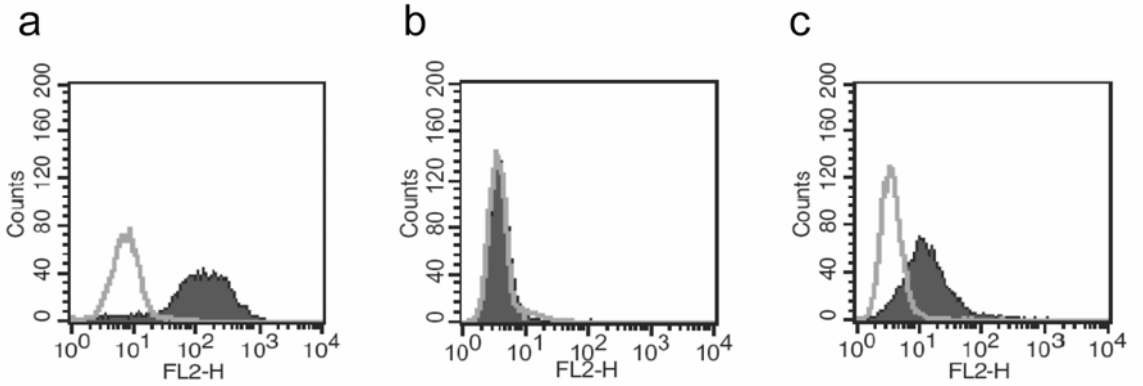


Figure 3

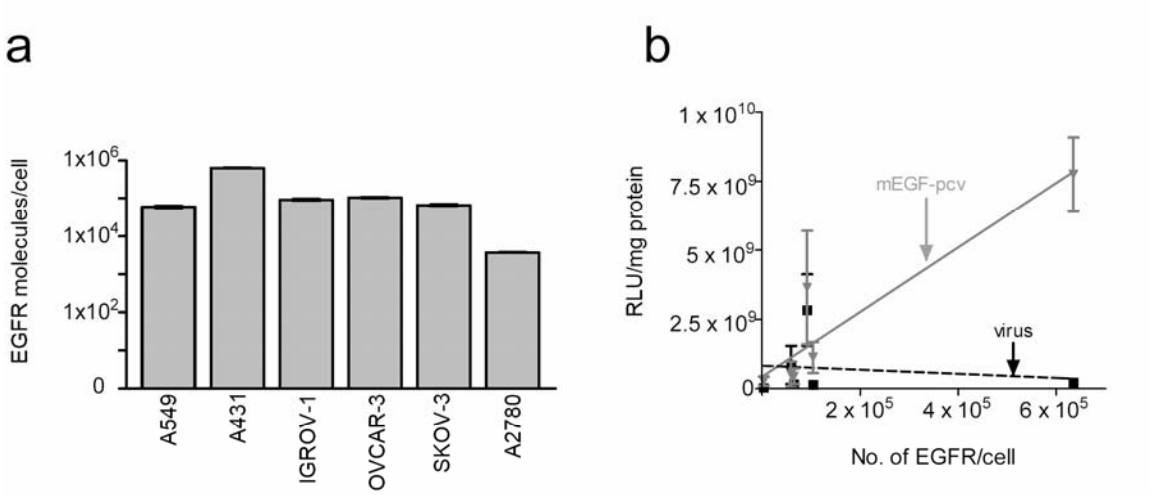

a
Total flux per mouse (p/s)
1x10^10
1x10^9
1x10^8
1x10^7
1x10^6
1x10^5
1x10^4
***
ns
***
PBS
virus
pcv
mEGF-pcv
b
i
ii
iii
iv
PBS
pcv
virus
mEGF-pcv
c
% survival
100
80
60
40
20
0
0
25
50
75
100
125
days from implantation
PBS
pcv
virus
mEGF-pcv
d
***
**
% individuals
100
80
60
40
20
0
PBS
virus
pcv
mEGF-pcv
none
mild
moderate
severe



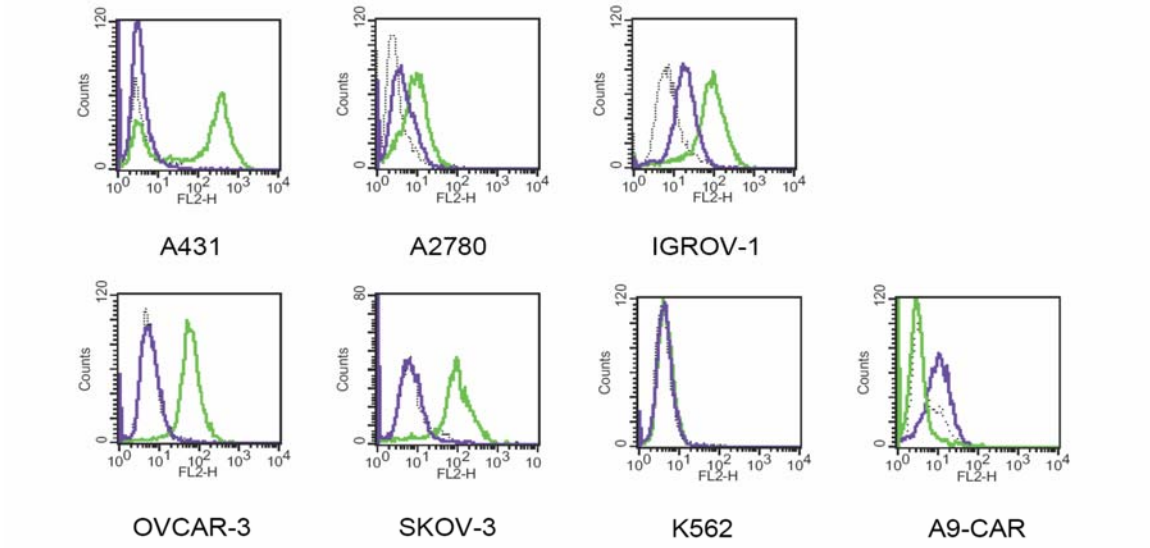
Supplementary Fig. 1
Synthesis of mEGF-pHPMA. For details see methods section.



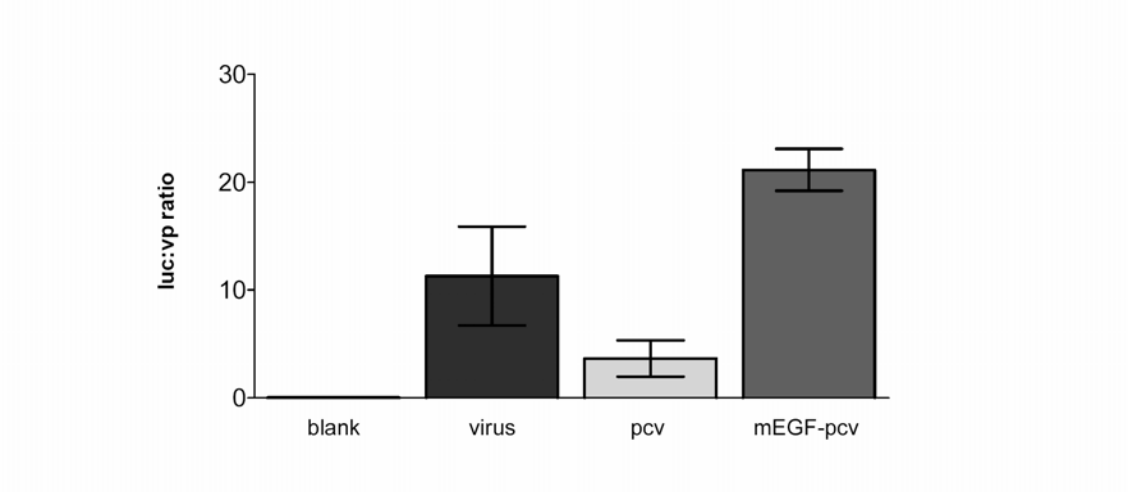
Supplementary Fig. 2
Murine fibroblast cell line A9 was transfected with pUSEamp-EGFR (Upstate, USA) which encodes the human epidermal growth factor receptor (EGFR). Successfully transfected cells were selected with G418 (800 μg/mL), positive colonies picked, passaged and screened by flow cytometry. Cells were labelled with mouse anti-EGFR antibody and goat anti-mouse-R-PE. Histograms demonstrate isotype control antibody in open peaks and EGFR in solid peaks: **(a)** A549 cells (positive control); **(b)** A9 cells; **(c)** A9-EGFR cells.



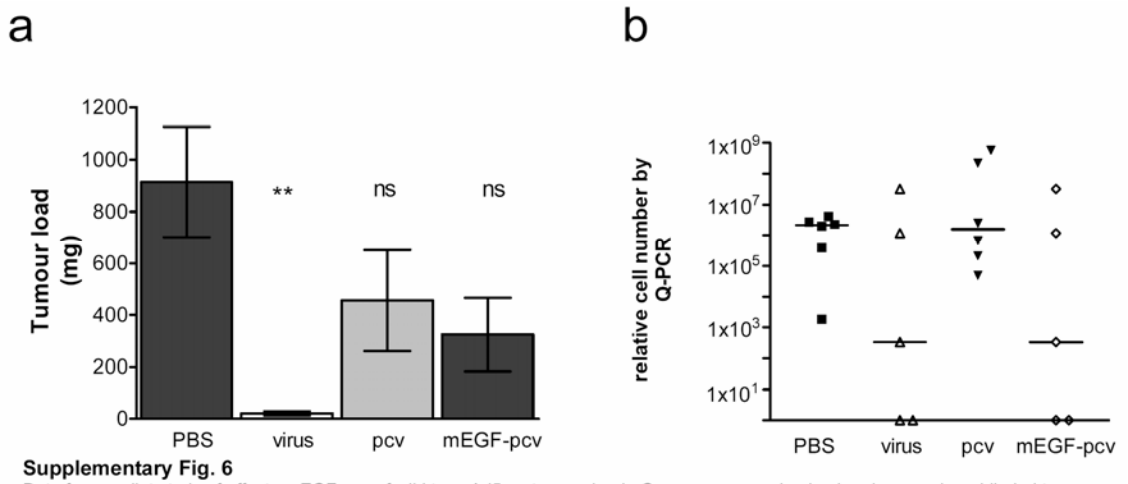
Supplementary Fig. 3
(**a**) The average number of EGFR per cell for a range of human carcinoma cells lines (mainly ovarian) was determined using a comercial ELISA (Dako). (**b**) When plotted against the level of reporter transgene expression, that for mEGF-pcv (grey triangles), but not virus (black squares), was directly proportional to cellular EGFR levels.



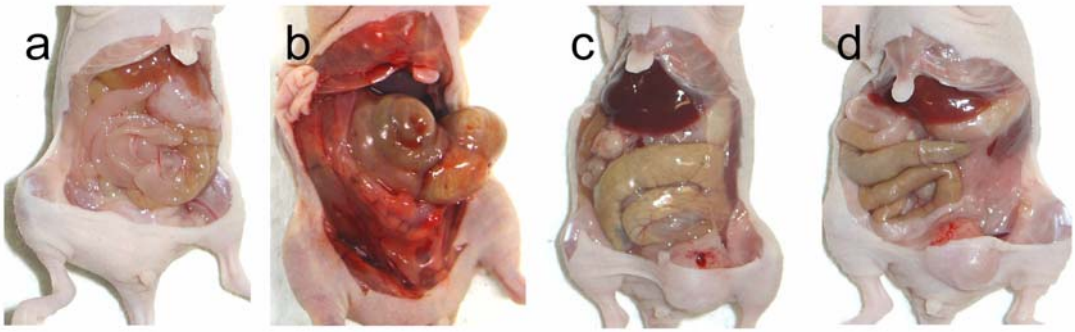
Supplementary Fig. 4
EGFR and CAR levels were assessed in a range of cell lines. The histograms demonstrate EGFR signal as green peaks, CAR as purple peaks and isotype controls as black dotted peaks.



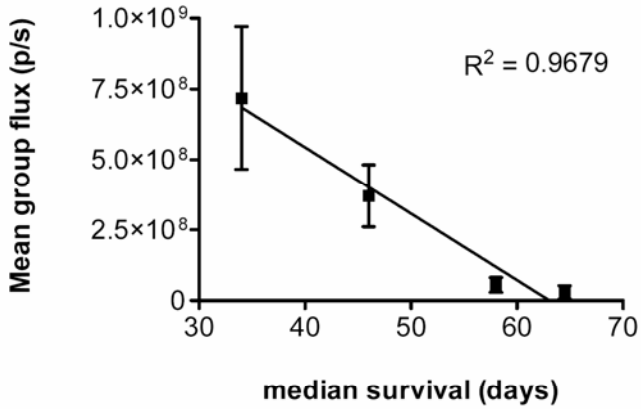
Supplementary Fig. 5
A431 cells were transduced with AdCMV-Luc$_{\Delta E1}$ (unmodified or coated at 10 mg/ml with pHPMA or mEGF-pHPMA) at 1000 v.p. per cell for 90 min, then cells washed to remove non-bound virus. After 24 hours cells were lysed and analysed for luciferase activity and cell associated virus particles (by quantitative PCR). Specific activity of mEGF-pcv virus was similar to unmodified virus, suggesting that virus taken up via the EGFR entered into a pathway permissive for infection.



Supplementary Fig. 6
Data from a pilot study of effect on EGF-pcv of wild type Ad5 on tumour load. Groups were randomized and researchers blinded to treatments. Nude mice (n=6 per group) were implanted with 1 x 10^7 SKOV cells intraperitoneally. After 48 hours mice were treated with 5 x 10^{10} vp of wild type Ad5 (Ad5WT): unmodified (virus); polymer coated (pcv); EGF-polymer coated (EGF-pcv: or a non-virus PBS control. When the first mouse developed tumour requiring euthanasia, all mice were sacrificed, tumour dissected and weighed and analysed for human β-actin promoter by quantitative PCR (Q-PCR). Analysis by Kruskal-Wallis with Dunn's correction for multiple comparison found that only virus gave a statistically significant anti-tumour effect based on gross tumour weight (**a**). However, virus caused severe adhesions and some bowel obstruction, which was prevented by EGF-pcv. These data were used to power a larger survival study. Q-PCR data (**b**) mirrored gross tumour weight, although there were problems extracting SKOV DNA using DNA extraction columns, hence the relatively low relative cell numbers. This was one reason to change to tumour load estimation using bioluminescence. In addition, measurement of bioluminescence allowed refinement of experiments, by predicting when mice were likely to become unwell and sacrificing prior to this point wherever possible.



Supplementary Fig. 7
Mice were carefully dissected at post-mortem examination and scored for adhesion formation. All tumor was meticulously dissected and weighed. Mice developed tumor in a similar pattern to human ovarian epithelial tumors: masses in the omentum and around the liver, stomach, diaphragm and small bowel mesentery. Mice shown are representative of their groups. Mice treated with: (a) PBS; (b) unmodified Ad5WT; (c) polymer coated Ad5WT; and (d) mEGF-polymer coated Ad5WT. In the mice treated with unmodified Ad5WT, some mice developed abdominal distension, which was found to be due to adhesions causing bowel matting and dilation of bowel loops. In addition, there was commonly gross liver abnormalities, with reduced size and changes to the gross architecture.



Supplementary Fig. 8
There was a linear inverse relationship between mean luminescence at the first measurement (d16 post-implantation) and median survival. These data suggest that bioluminescence is a valid secondary endpoint and could be utilized as a surrogate humane endpoint to refine the experimental design and reduce the severity limit of the experiment.